AD NUMBER

AD863640

NEW LIMITATION CHANGE

TO

Approved for public release, distribution unlimited

FROM

Distribution authorized to U.S. Gov't. agencies and their contractors; Critical Technology; OCT 1969. Other requests shall be referred to Air Force Aero Propulsion Laboratory, Attn: APRT, Wright-Patterson AFB, OH 45433.

AUTHORITY

afapl ltr, 12 apr 1972

AFAPL-TR-69-98
Volume I

A SECOND-ORDER NUMERICAL METHOD OF CHARACTERISTICS FOR THREE-DIMENSIONAL SUPERSONIC FLOW

VOLUME I. THEORETICAL DEVELOPMENT AND RESULTS

Victor H. Ransom, Joe D. Hoffman, and H. Doyle Thompson

Jet Propulsion Center
Purdue University
Lafayette, Indiana 47907

TECHNICAL REPORT AFAPL-TR-69-98, VOLUME I

OCTOBER 1969

AIR FORCE AERO PROPULSION LABORATORY
AIR FORCE SYSTEMS COMMAND
WRIGHT-PATTERSON AIR FORCE BASE, OHIO

NOTICES

When Government drawings, specifications, or other data are used for any purpose other than in connection with a definitely related Government procurement operation, the United States Government thereby incurs no responsibility nor any obligation whatsoever, and the fact that the Government may have formulated, furnished, or in any way supplied the said drawings, specifications, or other data, is not to be regarded by implication or otherwise as in any manner licensing the holder or any other person or corporation, or conveying any rights or permission to manufacture, use, or sell any patented invention that may in any way be related thereto.

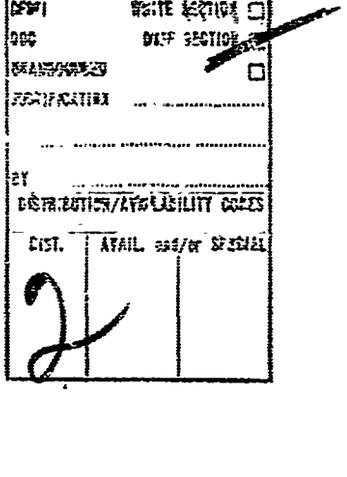

Copies of this report should not be returned unless return is required by security considerations, contractual obligations, or notice on a specific document.

AFAPL-TR-69-98
Volume I

A SECOND-ORDER NUMERICAL METHOD OF CHARACTERISTICS FOR THREE-DIMENSIONAL SUPERSONIC FLOW

VOLUME I. THEORETICAL DEVELOPMENT AND RESULTS

Victor H. Ransom, Joe D. Hoffman, and H. Doyle Thompson

Jet Propulsion Center
Purdue University

TECHNICAL REPORT AFAPL-TR-69-98, VOLUME I

OCTOBER 1969

Air Force Aero Propulsion Laboratory
Air Force Systems Command
Wright-Patterson Air Force Base, Ohio

Foreword

The present study is part of the program "An Analytical Study of the Exhaust Expansion System (Scramjet Scientific Technology)" being conducted by the Jet Propulsion Center, Purdue University, under United States Air Force Contract No. F33615-67-C-1068, BPSN 7(63 301206 6205214). The Air Force program monitor was Lt. Gary J. Jungwirth of the Air Force Aero Propulsion Laboratory. This report presents a second-order numerical method of characteristics for three-dimensional supersonic exhaust nozzle flow analysis.

Numerous discussions of the problem with Professor Ellis Cumberbatch of the Mathematical Sciences Division and Professor Czeslaw P. Kentzer of the School of Aeronautics, Astronautics and Engineering Sciences, Purdue University, are acknowledged and appreciated. The contributions of Robert Craigin and Stephen Kissick in the development of portions of the computer program and the plotting routines are also acknowledged.

This report was submitted by the authors on 31 August 1969.

Publication of this report does not constitute Air Force approval of the report's findings or conclusions. It is published only for the exchange and stimulation of ideas.

Gary J. Jungwirth
1st Lt., USAF
Project Engineer
Ramjet Technology Branch
Ramjet Engine Division
AF Aero Propulsion Laboratory

ABSTRACT

A new method of characteristics numerical scheme for three-dimensional steady flow has been developed which has second-order accuracy. Heretofore all such schemes for three-dimensional flow have had accuracies less than second-order. A complete numerical algorithm for computing internal supersonic flows of the type encountered in ramjet, scramjet, or rocket propulsion systems has been developed and programmed for both the IBM 7094 and CDC 6500 computers. The method has been tested for order of accuracy using the exact solution for source flow and Prandtl-Meyer flow. The results of these tests have verified the second-order accuracy of the scheme. Additional accuracy tests using existing methods for solution of two-dimensional axisymmetric flows have shown that the scheme produces accuracies comparable to that of the two-dimensional method of characteristics.

The computer program has been used to generate the flow field for several three-dimensional nozzle contours and for nonsymmetric flow into an axisymmetric nozzle. These results reveal the complex nature of three-dimensional flows and the general inadequacy of quasi-three-dimensional analyses which neglect crossflow.

An operationally convenient computer program was produced. The program has the capability to analyze nonisoenergetic and nonhomentropic flows of a calorically perfect gas or homentropic flows of a real gas in chemical equilibrium. The initial-value surface options include uniform flow, source flow or axisymmetric tabular data. The nozzle boundary options include conical nozzles, axisymmetric contoured nozzles and supercelliptical nozzles.

TABLE OF CONTENTS

LIST OF ILLUSTRATIONS

NOMENCLATURE

A	difference system amplification matrix
A_I	coefficients of the second-order least squares polynomial ($I=1,2,3,4,5,6$)
A_2, A_3	intercepts of super-elliptical equation
a	speed of sound
a_i	vector of directional differentiation
c	velocity of divergence of Mach conoid surface
E_2, E_3	exponents of super-elliptical equation
f	general functional or second-order interpolating polynomial function
h, H	enthalpy and stagnation enthalpy, respectively
I	frequency index or difference scheme point designation
L	characteristic length
M, N	frequency factors of Fourier components of solution
m, n	difference network indicies
N	total or half dimension of the logical array
n_i	components of unit normal
p, P	pressure and stagnation pressure, respectively
q	magnitude of the velocity
δq	heat transfer to the system
r_i	components of the radius vector
T	temperature
t	parameter in bicharacteristic parameterization or independent variable in directional derivative
$\bar{U}$	vector whose components are the dependent variables u_i and p
u_i	component of velocity
X	polynomial function
x, y, z	alternate designations for the x_i ($i=1,2,3$) coordinates
x_i	rectangular cartesian coordinate ($i=1,2,3$)

Greek Symbols

α_i	reference vector components
β_i	reference vector components
γ	angle between the streamline and the initial-value surface
δ_{ij}	Kronecker delta
λ_i	eigenvalues of system amplification matrix
θ	angular parameter of bicharacteristic parameterization
ρ	density

Subscripts

i,j,k	rectangular cartesian coordinate or component ranging from 1 to 3
$_I$	denotes the respective wave surface bicharacteristic, (1,2,3,4)

Superscripts

$\sim$	a small variation
-	mean value

Operators

$d_{\underline{a}}f$	directional differential along the direction a_i
$\Delta_{\underline{a}}f$	directional first difference along the direction a_i

SECTION I

INTRODUCTION

1. GENERAL REMARKS

The method of characteristics for two-dimensional axisymmetric, supersonic internal flow has been used for approximately twenty years in design of wind tunnel nozzles, rocket engine nozzles and air inlets for supersonic aircraft. The most sophisticated design techniques use the calculus of variations to establish the boundary conditions such that an optimum design for a particular set of constraints is produced. Subsequently the method of characteristics is used to establish the flow field and the nozzle or inlet wall shape. While these methods for two-dimensional problems have become highly developed, equivalent methods for three independent variables are in their infancy, roughly equivalent to the state of two-dimensional methods some twenty years ago.

The reasons that the development of the three-dimensional methods has lagged are three-fold: 1) the three-dimensional problem is fundamentally more difficult than the two-dimensional problem; 2) the required computer capacity for three-dimensional calculations has only been achieved in the present generation of digital computers; and 3) applications requiring three-dimensional supersonic internal flows were not frequently encountered. In fact, the need to calculate the external flow about supersonic vehicles flying at angles of attack has been the principal motivation for the existing three-dimensional work.

At present, however, there are several applications which require three-dimensional supersonic nozzle flow calculations. These include nonaxisymmetric flow into an axisymmetric nozzle, nonsymmetric disturbances in axisymmetric nozzles, three-dimensional nozzles for rocket engines having nonsymmetric exit area constraints, and three-dimensional nozzles for scramjet systems where a high degree of integration of engine and vehicle structure is desired. The scramjet nozzle application was

the motivation for this research.

The objective of the present research is the development of a practical and accurate numerical method and associated computer program, for analysis of three-dimensional supersonic exhaust nozzle flows. The chronological development of this work is documented in references (1) and (2), which are year-end progress reports for United States Air Force Contract No. F33615-67-C-1068.

2. THEORETICAL REMARKS

The equations of motion for a steady supersonic flow of an inviscid fluid in three independent space variables are well established. The equations can be classified as a system of quasi-linear, first order, symmetric, hyperbolic partial differential equations. The number of dependent variables will depend upon the assumed nature of the flow, i.e. number of chemical components, whether or not chemical equilibrium is assumed to exist, existence of vorticity, presence of condensed phases, etc. The mathematical character of the system does not depend upon the specific nature of these assumptions and, consequently, neither does the theoretical method of solution. However, the numerical algorithm and the associated computer program will depend upon the specific system of equations.

The finite difference integration schemes which have been proposed and/or used for the solution of systems of hyperbolic partial differential equations fall into two categories: 1) schemes based on characteristic directions and 2) schemes based on the coordinate directions. Variations of both approaches have been investigated both analytically and numerically; however, no one method has been shown to be superior for all problems. Numerical stability, accuracy, and time of computation are the factors of primary importance in evaluating a particular method. Secondary factors such as ease of programming and ease of incorporating boundary conditions are also important. In the subsequent text, the more pertinent efforts of investigators in this field are briefly discussed in an attempt to establish a "state of the art".

3. SURVEY OF THE LITERATURE

a. General. To a limited extent the numerical stability and accuracy of finite difference schemes can be investigated by theoretical methods. These methods provide certain necessary conditions which should be satisfied by any numerical scheme before proceeding with its numerical implementation.

Courant, Friedrichs and Lewy (3) have shown that a necessary condition for stability of numerical methods for solution of linear hyperbolic partial differential equations with constant coefficients is that the domain of dependence of the differential system must be contained within the convex hull of the difference system points in the initial-value surface. For three-dimensional supersonic flow the zone of dependence of the differential system consists of the area enclosed by the intersection of the Mach conoid, through the solution point, with the initial-value surface. The convex hull of the differencing scheme is the polygon formed by connecting the outermost points of the differencing scheme in the initial-value surface. Hahn (4) has shown that the CFL criterion is both a necessary and sufficient condition for stability of simplicial differencing schemes, i.e., schemes that use L + 1 points on an L dimensional initial-value surface to determine a new solution point. The von Neumann condition, Refs. (5) and (6), is a stronger stability criterion which requires that the eigenvalues of the amplification matrix be less than or equal to one in absolute value. The von Neumann condition is also a sufficient condition for analytic initial data. If the governing differential equations have variable coefficients and are nonlinear, then no exact test for stability exists. The usual approach is to require that the CFL condition be satisfied and to apply the von Neumann condition locally after linearization of the differential equations, Ref. (5). Experience to date has verified the soundness of this approach. Thus any numerical scheme which does not satisfy both the CFL and von Neumann conditions is regarded as unsatisfactory.

The absolute accuracy of a numerical scheme is difficult to establish without actually comparing numerical results with an exact solution. However, a desired order of accuracy, which governs how rapidly the solution

converges with reduction of the step size, can be achieved by using consistent approximations throughout the numerical scheme. For a particular scheme, the absolute accuracy will increase as the order of accuracy is increased. It is reasonable to expect that different schemes having the same order of accuracy will have comparable absolute accuracy, although there is no guarantee of this.

A more accurate scheme will permit the use of larger step sizes and thus fewer points need to be computed. In three independent variable problems, increasing the computing interval by a factor of two results in a reduction in the number of computed points by a factor of eight Thus, a more accurate but more complex scheme may actually require less total computer time.

b. Method of Characteristics. The concept of characteristic directions was first discussed by Massau (7) in 1899, and since that time the method has been widely applied to the solution of two-dimensional problems.* The method of characteristics has been very successful in two-dimensional problems because it provides a means by which a system of partial differential equations is reduced to a system of coupled ordinary differential equations along characteristic directions. The utility of the method of characteristics is weakened when three independent variables are considered because the system of equations can no longer be reduced to a system of ordinary differential equations. Instead, the equations can only be reduced to a system of partial differential equations in a space of one lower dimension, i.e., a characteristic surface, and any integration scheme necessarily includes numerical evaluation of derivatives ... at least two independent directions.

The characteristic surfaces for three-dimensional stationary flow are shown by Rusanov (8) to be surfaces tangent to the local Mach conoid, wave surfaces, and surfaces which are composed of the streamlines, stream surfaces. Thus, two infinite families of characteristic surfaces exist. The system of differential equations reduces to an interior operator, i.e., a characteristic compatibility relation on these surfaces.

*A review of the literature for the method of characteristics in two independent variables will not be given here as the volume of such literature is enormous and has only indirect bearing on the problem at hand.

Numerical integration along a system of such surfaces is theoretically less complex than integration along noncharacteristic surfaces where derivatives with respect to all three independent variables necessarily appear.

A number of investigators have proposed numerical schemes using the characteristic compatibility relations for three independent variable problems; however, only a few have developed complete numerical algorithms and obtained results. Good surveys of the various approaches which have been taken are given by Powell (9), Thompson (10), and Strom (11).

All schemes using the method of characteristics are based on the fact that the original system of hyperbolic partial differential equations can be replaced by an equivalent system of independent differential characteristic compatibility relations. Frequently, the question arises whether or not all the differential compatibility relations which are used in a particular approach are independent. Rusanov (8) has investigated both the number of independent characteristic compatibility relations which can exist at a point on a particular characteristic surface and the number of such independent relations considering all possible characteristic surfaces. Two infinite families of differential compatibility relations exist which correspond to the two families of characteristic surfaces. Thus, considerable freedom exists in the choice of differential systems.

The number of independent characteristic differential relations at a point cannot exceed the number of original differential equations which comprise the system. For a complete system this number will be just equal to the number of dependent variables. Rusanov found that a maximum of three differential wave surface compatibility relations are independent. In addition, he obtained the conditions under which the wave surface and stream surface differential compatibility relations are dependent. It is important for the discussion of the various numerical schemes to note that these criteria for independence apply only to differential relations at a point in the solution space. Specifically, they do not apply to the difference relations which are obtained when the derivatives are replaced by finite differences. This is so because the finite difference relations are approximate integrals of the equations and are all independent, at

least to within the order of approximation.

In the application of the method of characteristics to two independent variable problems, numerically stable schemes result and second-order accuracy is easily achieved. For three independent variable problems, stable schemes do not necessarily result and second-order accuracy is much more difficult to achieve. There is no way a priori to assure stability of a scheme, and the CFL and von Neumann stability criteria must be applied to each scheme which is devised. With the exception of the work by Butler (12), all schemes which have been proposed for applying the method of characteristics to three independent variable problems have had only first-order accuracy. Some of the schemes may be more accurate than others for a finite step size. However, all share the characteristic that the local error approaches zero with the square of step size, whereas with Butler's scheme, the local error approaches zero with the cube of step size.

If in forming a finite difference scheme, the differentials are simply replaced by finite differences and the coefficients and remaining terms in each equation are evaluated at one of the end points of the finite difference network, then the accuracy of the resulting scheme is first-order in step size, i.e., the equivalent of the Euler scheme for ordinary differential equations. The number of independent difference relationships required for schemes having first-order accuracy is equal to the number of independent variables of the system. Some investigators have used more than the minimum number of finite difference relations required for a determinate system. The additional relations are independent, and as a result, the system is overdetermined such that multiple solutions are possible. Such an overdetermined system was solved in the least squares sense by Chu, Niemann and Powers (13, 14). Multiple solutions were obtained and subsequently averaged by Strom (11) and Sauerwein (15).

If higher-order approximations are used for the differential relations, then additional unknowns will be introduced and a greater number of independent relations must be used. The additional unknowns will be in the form of higher-order coefficients in the power series expansions or equivalently, the derivatives of the dependent variables at the unknown point. Butler (12) has shown that only two additional independent relations

are necessary for a numerical scheme having second-order accuracy. Undoubtedly even higher-order schemes could be devised; however, the numerical complexity would probably increase greatly as the order of accuracy is increased.

It is important to note that the number of independent finite difference relations which must be used in a particular numerical scheme is not only a function of the number of dependent variables of the differential system, but is also dependent upon the order of accuracy of the scheme. This fact, as well as the importance of the domain of dependence for a point in the solution space to numerical stability, will help to clarify some of the differences between the various numerical schemes.

A variety of finite difference schemes having first-order accuracy have been proposed. Two schemes, the hexahedral network of bicharacteristics and the hexahedral network of general characteristic surfaces, were proposed by Thornhill (16) in 1948. The resulting networks for these two schemes are illustrated in Figure 1. These methods were developed for an irrotational flow, and in this case, only a single family of characteristic surfaces, the wave surfaces, are obtained in the analysis. The envelope of all such surfaces through a point is the Mach conoid, see Figure 1. Later numerical work by Sauerwein (17) with these schemes showed the first to be unstable and the second to be stable. The cause of the instability is now recognized as being due to the fact that the CFL stability criterion is violated, see Figure 1.

Moeckel (18) in 1949 described a method of characteristics scheme which was based on the work of Ferrari (19). This method consists of applying the characteristic compatibility conditions along the intersections of two characteristic surfaces with two reference planes and the intersection of the two characteristic surfaces with each other. This scheme is known as the network of intersections of reference planes and is illustrated in Figure 2a. The major objection to this scheme is that the CFL stability criterion is violated, Ref. (5). A further difficulty in applying this scheme is that additional boundary conditions are required on the end reference planes, such as a plane of symmetry, or iteration is required if the reference planes are chosen as radial planes through a fixed axis. The iteration is required to obtain closure of

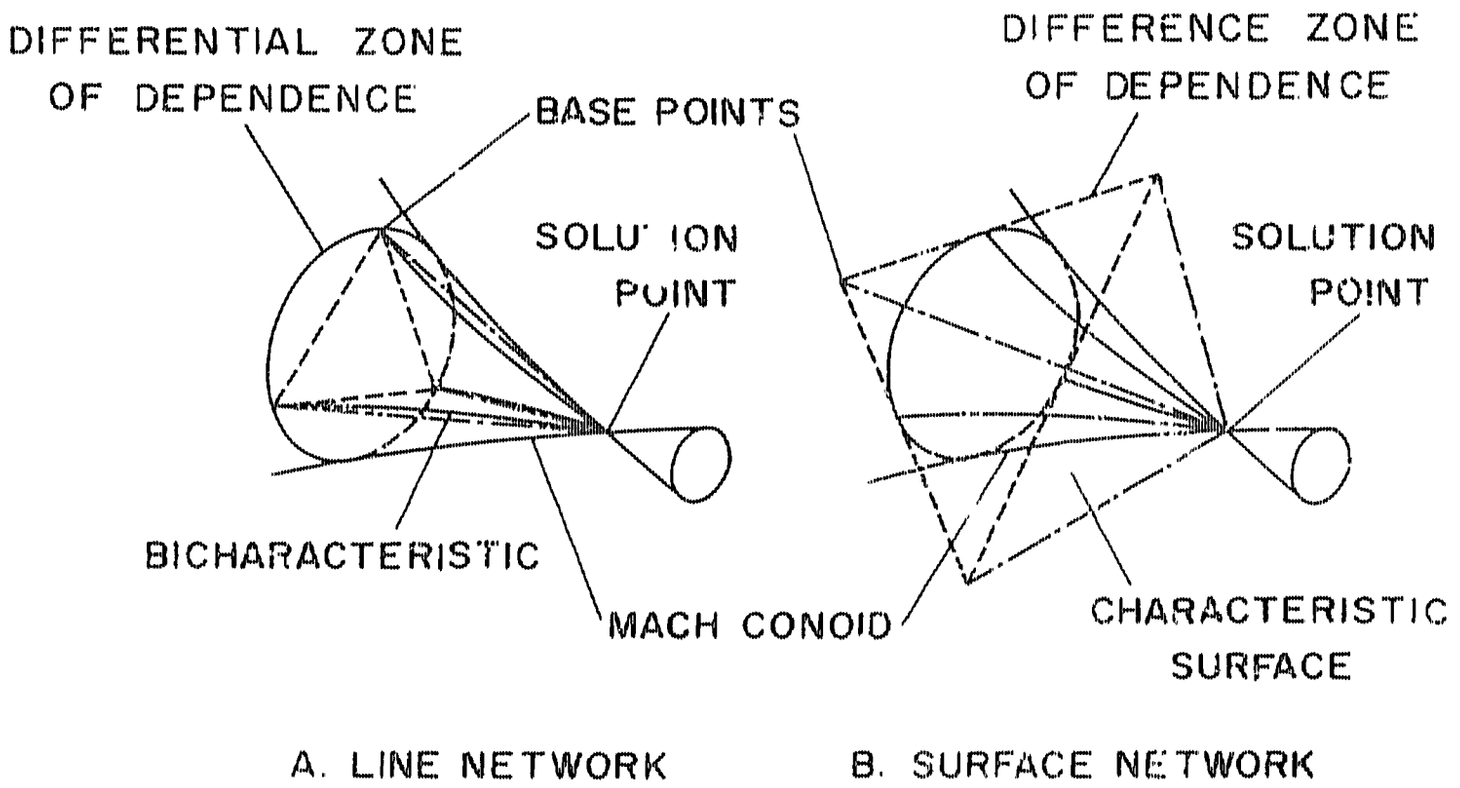

FIGURE I. HEXAHEDRAL CHARACTERISTIC NETWORKS

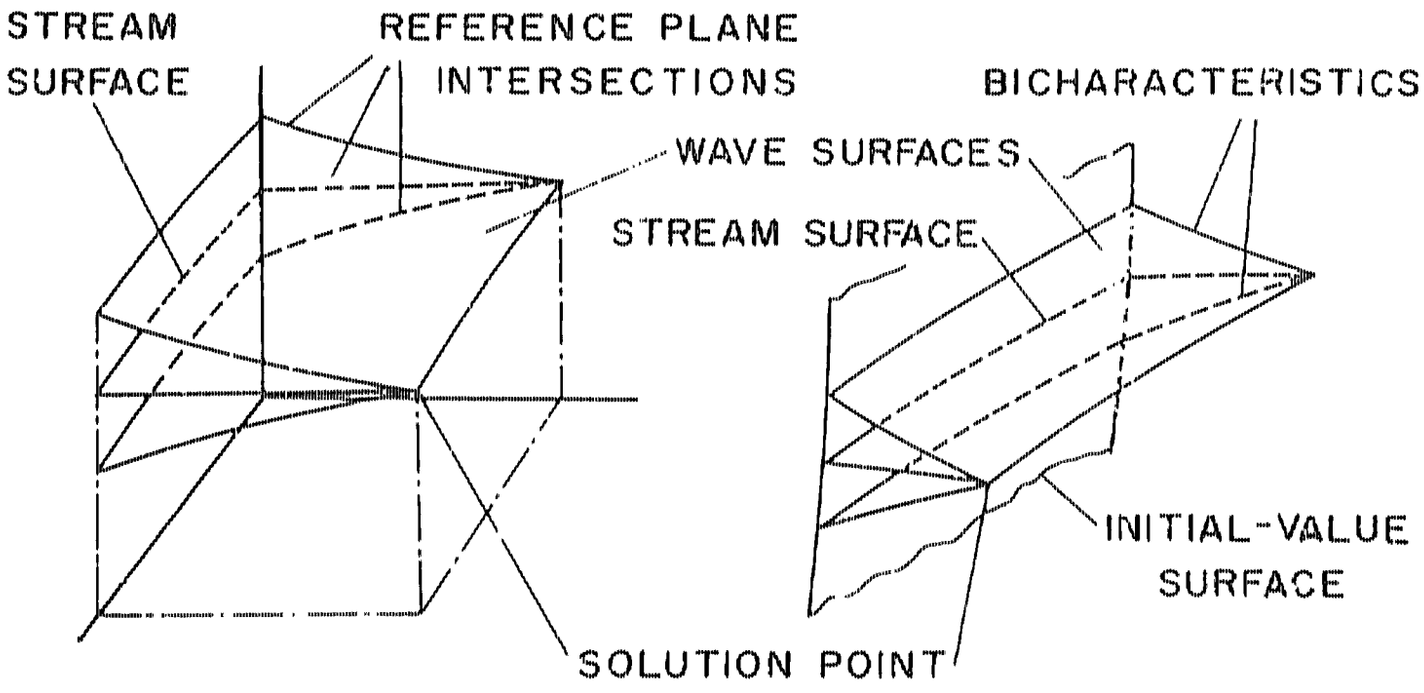

FIGURE 2. CHARACTERISTIC SURFACE NETWORKS

the finite difference solution between the first and last radial planes.

Based on the work of Titt (20) and Colburn and Dolph (21), Holt (22) has suggested a network that is formed by the intersection of two characteristic surfaces emanating from two lines in the initial-value surface. In this method the compatibility equations are applied along bicharacteristics within the two characteristic surfaces, see Figure 2b. It has been pointed out by Hale and Leigh (5, 6) that this scheme violates the CFL stability criterion, and they propose further modification of Holt's scheme to produce an "implicit prismatic characteristic surface network" which satisfies the CFL stability condition. Apparently no attempts to use either of these methods have been made.

Another serious shortcoming of the reference plane methods is that one of the finite difference relationships used in the solution for a point is applied along a direction which lies completely outside the zone of dependence of the unknown point. While this is desirable from a stability standpoint, it is undesirable for accuracy. Accuracy is greatest when the difference scheme zone of dependence just exceeds the differential system zone of dependence. Further, as pointed out by Butler (12), difficulties would be encountered at boundaries formed by shock waves, particularly when the principle direction of propagation of the shock is in the direction of the ordinary curve used in the integration scheme.

A method using intersections of characteristic surfaces with a single reference plane, called the method of near characteristics, was developed by Sauer (23, 24) and Holt (25, 26) and used for numerical computation by Moretti (27, 28) and Rakich (29, 30). This method appears to be the simplest first-order scheme which has been devised and the network is illustrated in Figure 3a. The method is very similar to other reference plane schemes except that the terms containing cross derivatives are evaluated in the initial-value surface, while the other methods use a finite difference approximation to these cross derivatives along an ordinary coordinate direction through the unknown point. Rakich (30) has used a version of this approach for the calculation of flow about yawed cones and the results agree well with experiment. This scheme is particularly well suited to flow about bodies of revolution where the

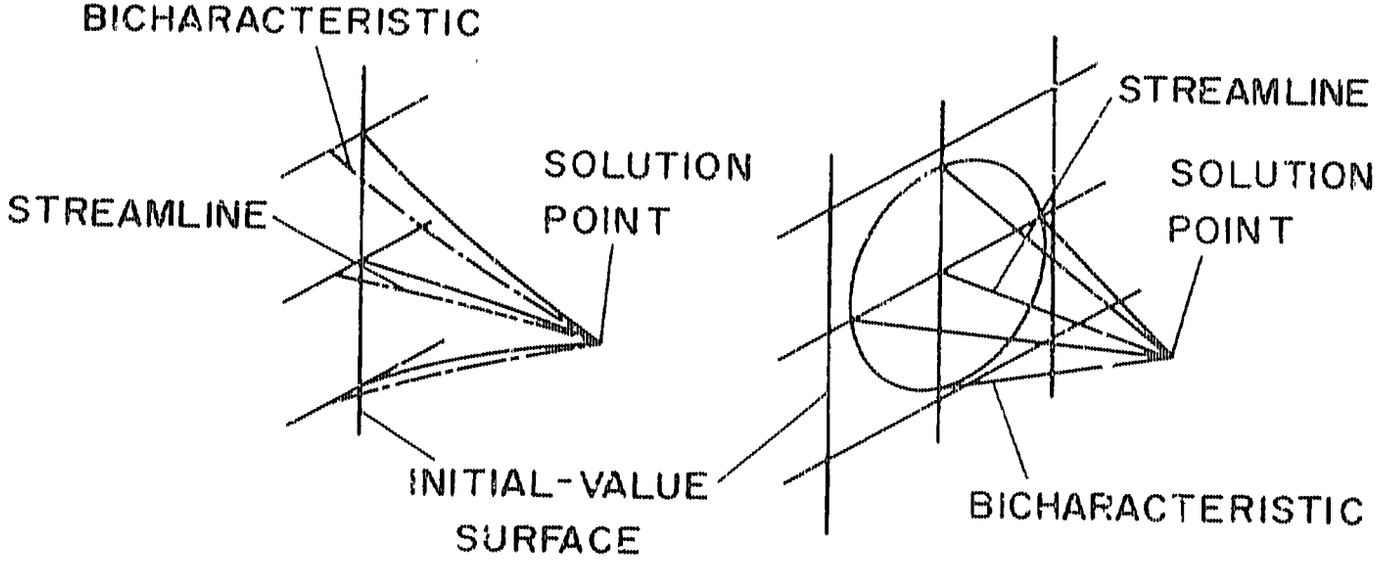

FIGURE 3. NEAR CHARACTERISTIC AND REDUNDANCY NETWORKS

reference planes can be taken as meridional planes through the body and the axis points do not enter the calculation. However, it is not clear that this method could be applied with equal success to more arbitrary three-dimensional flows.

The near characteristics scheme has two potential problem areas. The most significant is the fact that the near characteristics are in general outside the zone of dependence of the unknown point. Only when the reference plane contains the velocity vector will the near characteristics correspond to bicharacteristics and define the true zone of dependence of the new point. Rakich (30) has pointed out that this condition helps assure that the CFL stability criterion is satisfied. While this is true, it also results in a more rapid error growth due to the fact that the speed of propagation of numerical disturbances can be significantly greater than required for stability at high yaw angles. A second potential problem is the fact that the convex hull of the difference scheme will depend upon the manner by which the cross derivatives are evaluated in the initial-value surface, and thus, whether or not the CFL condition for stability is satisfied.

Powell (9) in 1951 applied the hexahedral method of bicharacteristics which was proposed by Thornhill (15), see Figure 1a. Only hand calculations were performed for a few points and the fact that the scheme is numerically unstable was not discovered. The unstable character of this scheme was discovered by Sauerwein (31, 32, 33) in his attempts to apply it to two-dimensional, unsteady flows. Sauerwein subsequently modified the scheme such that the CFL stability condition was satisfied and was able to obtain useful results.

Tsung (34) in 1961 used the hexahedral method of characteristic surfaces proposed by Thornhill (16). Figure 1b, which satisfies the CFL stability condition, for calculation of the irrotational flow over a conical boattail with elliptic cross-section and a delta wing at angle of attack. No numerical instabilities were encountered and results were obtained which agreed closely with experimental results. Reed (35, 36, 37) also has used the method of hexahedral characteristic surfaces for calculating rotational flow in nozzles. Numerical calculations were only made for axisymmetric flows for purposes of checking the program.

Pridmore Brown and Franks (38) in 1965 reported results of numerical stability studies using a redundant system of four bicharacteristics which were solved or satisfied in a least squares sense. The question of a preferred orientation for the difference network was investigated in which two of the bicharacteristics used lie in a plane defined by the velocity vector and the streamline normal. Chu, Niemann and Powers (13) in 1966 reported results which were obtained using the redundant characteristics scheme, see Figure 3b. Apparently, stability problems motivated the use of the redundancy method, as it is reported that the redundancy method showed marked stability improvement. The convex hull of the difference scheme does not satisfy the CFL stability condition if the points used are those from previous calculations. When it is necessary to interpolate in the initial-value surface, the convex hull of the difference scheme is increased and the CFL condition can be satisfied. Interpolation was used in the reported calculations, and it was apparently sufficient to stabilize the method.

All of the methods which have been discussed thus far produce a solution which is accurate to at least first-order in step size. The method developed by Butler (12) is unique in that second-order accuracy is clearly maintained. In addition, the method originally proposed by Butler does not involve integration along a finite number of directions. The numerical relations which result involve integrals over the convex hull of the Mach conoid and the intersection of the streamline with the initial-value surface. However, in practice the integrals are evaluated by weighted summation over four particular bicharacteristics. The network is illustrated in Figure 4. This scheme was programmed for two-dimensional unsteady flow by Elliott(39) and Richardson (40) and numerical results were obtained. The numerical results compared favorably with experimental values; however, no information is available on required computing time or relative step size used. Thus a comparison with results obtained using schemes having first-order accuracy cannot be made.

Butler's proposed approach for three-dimensional steady flow is analagous to the Hartree (41) scheme for two-dimensional flow. The numerical accuracy is the same order (i.e., second order), and the method for computing the location of new points by the intersection of streamlines with consecutive coordinate planes is the same. In contrast to the

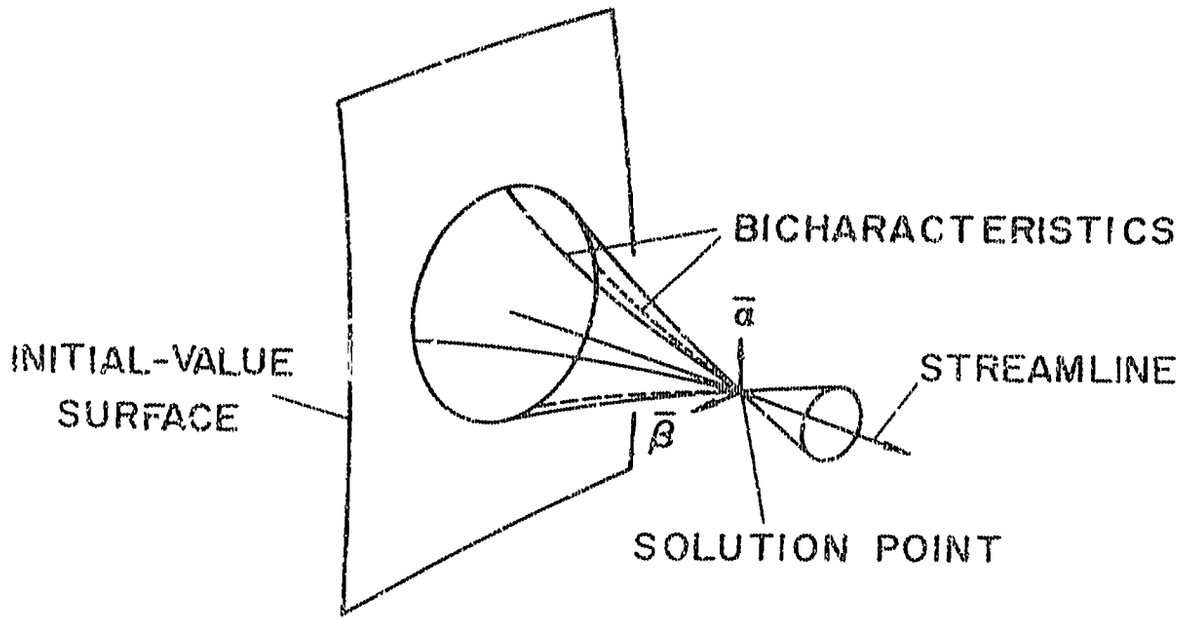

FIGURE 4. BUTLER'S PROPOSED BICHARACTERISTIC NETWORK

variety of first-order networks which have been proposed, the original second-order scheme proposed by Butler does not allow any freedom in the choice of network. The compatibility equation is integrated over all bicharacteristics passing through a point, i.e., the Mach cone, and in effect all bicharacteristics are utilized. When the integrals are replaced by summation over four particular bicharacteristics, one degree of freedom is possible in the choice of network orientation.

e. Finite Difference Methods. The use of ordinary finite difference methods for solution of the steady flow equations in three dimensions has also received considerable attention in the past several years. Since the advent of high speed digital computers, more and more attention has been given to numerical schemes for integration of systems of partial differential equations by simply replacing the derivatives by difference quotients. The books by Richtmeyer (42) and Forsyth and Wasow (43) treat the elements of this approach. The major problems which are encountered in applications of ordinary finite difference methods are numerical stability and accuracy. The most serious accuracy problems are encountered in devising means to satisfy boundary conditions on surfaces which do not correspond to coordinate planes, thus necessitating interpolation or extrapolation. Even when the boundaries correspond to coordinate planes, a loss of accuracy occurs because the derivatives at the boundaries can only be approximated by one-sided difference quotients.

Thomson, D'Attorre and Nowak (44, 45, 46) have recently completed programs for calculating the interaction region of multiple rocket engine exhausts using a Lax-Wendroff (47) type differencing scheme. As a check case, the flow field of an axisymmetric jet has been calculated and the results are in excellent agreement to those obtained by the two-dimensional method of characteristics. Bahenko (48) has also used a finite difference method for computing the three-dimensional flow over smooth bodies with apparent success.

4. THE GENERAL NUMERICAL METHOD

The objective of this research is the development of a numerical method for solution of a particular system of partial differential equations (i.e., the equations of motion for a steady supersonic flow).

However, the general method is applicable to any system of quasi-linear hyperbolic partial differential equations for which the characteristic equation consists of a quadratic factor and a repeated linear factor, see Appendix A, Eq. (A-17).

The numerical method is based on the work reported by Butler in Ref. (12), with the exception that an improvement is made to the original method which results in a considerable simplification of the final numerical scheme. The account of Butler's work contained in Ref. (12) is extremely brief and for this reason Appendix B is a redevelopment of the improved approach with the intermediate steps and theory included. This information as well as that in Appendix A is not essential to a general understanding of the numerical scheme for supersonic flow, but is intended for the researcher who may attempt modification or extension of the method to other systems.

SECTION II

GAS DYNAMIC MODEL

1. GOVERNING EQUATIONS

The supersonic motion of most compressible fluids encountered in propulsion systems can be accurately described by means of the governing equations for the motion of an ideal fluid. The major assumptions which constitute the gas dynamic model are: 1. continuum, 2. inviscid, 3. steady, 4. strictly adiabatic (i.e., each particle of fluid is considered to be an adiabatic system in addition to the overall system being adiabatic), 5. frozen or equilibrium chemical composition, and 6. smooth initial data and boundaries.

The governing equations for such a system are: the continuity equation*

$$u_i(\partial\rho/\partial x_i) + \rho(\partial u_i/\partial x_i) = 0 \qquad (1)$$

and the Euler momentum equations

$$\rho\, u_j(\partial u_i/\partial x_j) + \partial p/\partial x_i = 0, \qquad (i = 1, 2, 3) \qquad (2)$$

where the u_i are the velocity components, ρ is the density, p is the pressure and x_i is a system of rectangular cartesian coordinates. These equations, Eqs. (1) and (2), are a system of quasi-linear partial differential equations which govern the three-dimensional motion of an ideal fluid. However, they do not form a complete system since the number of dependent variables exceeds the number of equations.

A complete system for a compressible flow is obtained by expressing the derivatives of density in terms of derivatives of the velocity components and the pressure. This is accomplished through consideration of

*Repeated indicies imply summation over the range 1 to 3 unless stated otherwise.

the first law of thermodynamics for a particle of fluid having continuous property variations, i.e.,

$$de = \delta q - \delta w \tag{3}$$

where de is a differential change in internal energy, δq is the heat transfer to the particle and δw is the work done on the surroundings. As a result of the strictly adiabatic assumption, the heat transfer δq is identically zero. Further, as a result of the inviscid assumption no shear forces are present and the only form of work done by the particle is the volume displacement against the pressure of the surroundings, i.e.,

$$\delta w = pd(1/\rho) \tag{4}$$

Thus the first law for a particle yields the result

$$dh = (1/\rho)dp \tag{5}$$

where h is the particle enthalpy (i.e., $h = e + p/\rho$). The general thermodynamic equation for a particle of the fluid, with the composition either frozen or in chemical equilibrium, is shown in Appendix C to be

$$Tds = dh - (1/\rho)dp \tag{6}$$

where T is temperature and s is entropy. Using the first law result for the particle system, Eq. (5), the general thermodynamic equation reduces to

$$ds = 0 \tag{7}$$

which, when expressed in terms of spatial derivatives of the entropy, yields the result

$$u_i(\partial s/\partial x_i) = 0 \tag{8}$$

Thus the entropy is a constant along each streamline of the flow with the value determined by some initial condition.

The speed of propagation of an infinitesimal and isentropic disturbance (i.e., the sound speed) is given by

$$a^2 = (\partial p/\partial \rho)_{s,\ c_i \text{ or } e} \tag{9}$$

where the subscript c_i or e denotes either frozen composition, c_i, or chemical equilibrium, e. Since the entropy and atomic composition are constant for a particle of fluid, the partial derivative in Eq. (9) may be written as the ratio of property differentials for a particle, so that along any streamline

$$a^2 = dp/d\rho \tag{10}$$

or when the particle differentials are expressed in terms of spatial derivatives

$$u_i(\partial \rho/\partial x_i) = a^{-2}\, u_i(\partial p/\partial x_i) \tag{11}$$

Equation (11) is used to eliminate the spatial derivatives of density from the continuity equation, Eq. (1), and thus the number of dependent variables which appears in the system of equations, Eq. (1) and (2), is reduced by one. The resulting system of equations can be written in a convenient matrix notation using the Kronecker delta

$$\begin{bmatrix} \rho u_i & 0 & 0 & \delta_{1i} \\ 0 & \rho u_i & 0 & \delta_{2i} \\ 0 & 0 & \rho u_i & \delta_{3i} \\ \rho a^2 \delta_{1i} & \rho a^2 \delta_{2i} & \rho a^2 \delta_{3i} & u_i \end{bmatrix} \begin{Bmatrix} \dfrac{\partial u_1}{\partial x_i} \\ \dfrac{\partial u_2}{\partial x_i} \\ \dfrac{\partial u_3}{\partial x_i} \\ \dfrac{\partial p}{\partial x_i} \end{Bmatrix} = 0 \tag{12}$$

Although Eq. (12) is a determinate system of quasi-linear differential equations, the density and the speed of sound, which appear in the coefficient matrix, must be expressed in terms of the dependent variables before a solution can be attempted.

2. THERMODYNAMICS OF THE FLOW

The additional relationships required for solution of the governing equations are obtained by consideration of the thermodynamic properties of the fluid. The fluid is assumed to be produced by the combustion of an oxidizer and a fuel stream, each of which enters the combustor with uniform composition and stagnation enthalpy. In this case the stagnation enthalpy is a single valued function of the oxidizer to fuel ratio (the stagnation enthalpy of the individual streams includes the heat of formation). Generally spatial variations of the oxidizer to fuel ratio are present within the combustion chamber and thus corresponding variations in the composition and stagnation enthalpy of the combustion products will result. As a result of the inviscid and strictly adiabatic assumptions, the atomic composition and stagnation enthalpy are constant along streamlines so that

$$u_i(\partial H/\partial x_i) = 0 \tag{13}$$

where $H = h + q^2/2$ (see Appendix C).

In the general case, particularly in scramjet systems, the stagnation pressure after combustion will have spatial variations due to variations in pressure and velocity of the individual streams entering the combustor and in the local oxidizer to fuel ratio. However, in the absence of discontinuous property variations the stagnation pressure can also be shown, see Appendix C, to be constant along the streamlines of the flow, i.e.,

$$u_i(\partial P/\partial x_i) = 0 \tag{14}$$

The existence of shock waves within the flow has been implicitly excluded in the flow model as a result of the assumption of continuous property variations. When shock waves are included, Eq. (13) for conservation of stagnation enthalpy remains valid throughout the flow; however, stagnation pressure is not conserved and the shock must be treated as a discontinuity surface across which the Rankine-Hugoniot conditions apply.

The combustion products produced by combustion of uniform oxidizer and fuel streams form a simple system in the stagnation state. Thus specification of any two thermodynamic properties is sufficient to define the stagnation state. The stagnation enthalpy and stagnation pressure are the most convenient choices for independent variables to define the stagnation state. Since both of these properties are constant along streamlines of the continuous property flow, the remaining properties are one-dimensional functions and are uniquely determined by specification of the local pressure. Thus the global variation of density and the speed of sound can be functionally expressed in terms of the pressure, stagnation pressure and stagnation enthalpy, (see Appendix C), i.e.,

$$\rho = \rho(p,P,H) \tag{15}$$

and

$$a = a(p,P,H) \tag{16}$$

For a thermally and calorically perfect gas the relations for the density and speed of sound are analytic functions. For multicomponent systems, having either frozen or equilibrium chemical composition with real gas effects, the density and speed of sound must be obtained from thermochemical calculations. In this case the relations, Eqs. (15) and (16), are usually obtained as tabular functions.

The gas dynamic model consists of the equations for conservation of mass and momentum, Eq. (12), the equations for conservation of the stagnation pressure and enthalpy, Eqs. (13) and (14), and the functional relations for the density and speed of sound, Eqs. (15) and (16). The differential equations form a complete system of first-order, quasi-linear, partial differential equations.

SECTION III

CHARACTERISTIC RELATIONS

1. GENERAL

The governing equations for the steady flow of an ideal compressible fluid in three dimensions constitute a system of quasi-linear, first-order, partial differential equations. When the flow velocity exceeds the local velocity of sound the equations are classed as hyperbolic and within the solution space surfaces exist on which the system reduces to an interior operator. These surfaces are called characteristic surfaces and they have great significance with respect to determining the conditions for a well posed problem and devising numerical methods for solution. The theory of such systems and the conditions for a well posed problem are discussed in greater detail in Appendix A

In Appendix D it is shown that two infinite families of characteristic surfaces exist for three-dimensional supersonic flow; these are the stream surfaces and the wave surfaces. The family of stream surfaces consists of all surfaces made up of streamlines of the flow. The wave surfaces consist of all surfaces tangent to the local Mach conoid. The system of equations reduces to an interior operator on each surface of both families of characteristic surfaces (i.e., a linear combination of the equations can be found which involves only directions of differentiation which lie within the surface). The linear combinations of the equations which have the characteristic property are called compatibility relations. Data cannot be arbitrarily specified on characteristic surfaces since the compatibility relation must be satisfied.

The original system of equations can be replaced by an equivalent system of independent compatability relations. For systems having two independent variables a unique system of compatibility relations is obtained. However, with three independent variables not only is the system not unique, but an infinite variety of possible choices exist, see

Appendix D. Thus many different, but theoretically equivalent, systems of compatibility relations have been proposed and used as the basis for numerical schemes. Normally all such schemes are termed "method of characteristics" schemes.

The numerical scheme which is developed in a later section uses certain of these compatibility relations as well as one noncharacteristic relation.

2. CHARACTERISTIC SURFACES

The characteristic equation for the system of equations for three-dimensional flow, Eq. (D-4) of Appendix D, is

$$\rho^3(u_k n_k)^4[u_i u_j - a^2\delta_{ij}]n_i n_j = 0 \qquad (17)$$

where n_i is the unit normal vector to a characteristic surface. Note that the characteristic equation has the same general form as was assumed in the development of the general numerical scheme in Appendix B, i.e., a repeated linear factor times a quadratic factor.

The characteristic equation is satisfied if either of the factors vanish. The first factor yields the family of stream surfaces while the quadratic factor yields the family of surfaces which touch a quadratic cone the wave surfaces. The equation of the envelope formed by the wave surfaces is obtained by inversion of the quadratic factor, see Appendix A, to obtain the reciprocal conoid

$$[u_i u_j - (q^2 - a^2)\delta_{ij}]dx_i dx_j = 0 \qquad (18)$$

Note that the surface is real only if the quantity $(q^2 - a^2)$ is positive, i.e., $q \geq a$. Equation (18) is the equation for the Mach conoid of supersonic flows. The relation between the two families of characteristic surfaces, i.e., the stream surfaces and the wave surfaces, is illustrated in Figure 5.

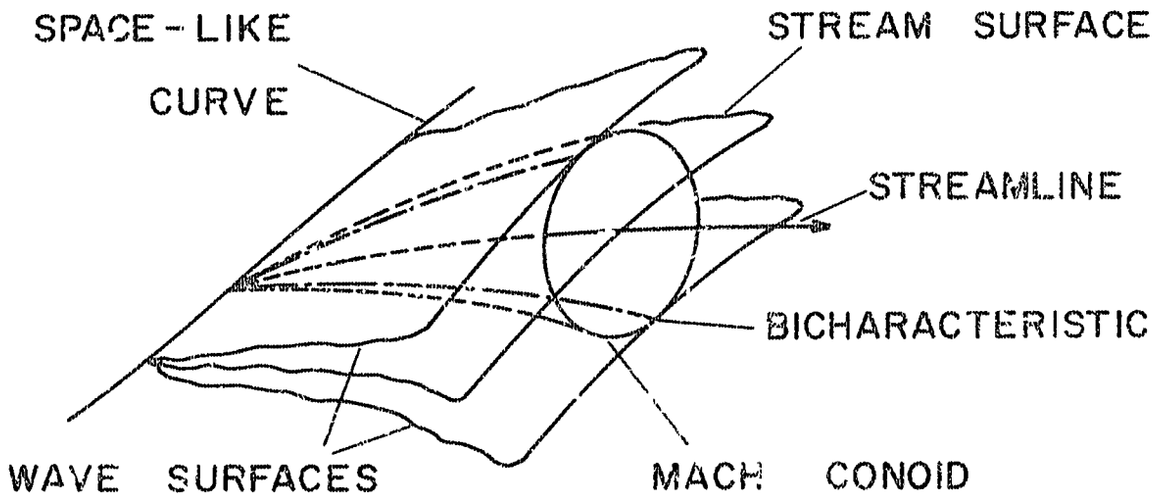

FIGURE 5. CHARACTERISTIC SURFACES

5. COMPATIBILITY RELATIONS

The general numerical method developed in Appendix B utilizes certain of the stream surface compatibility relations and the wave surface compatibility relation for systems of equations having more than three dependent variables. Three stream surface compatibility relations are required in the numerical scheme. The independent relations of interest are (see Eqs. (D-11), (D-12) and (D-13) of Appendix D)

$$u_i(\partial P/\partial x_i) = 0 \tag{19}$$

$$u_i(\partial H/\partial x_i) = 0 \tag{20}$$

and

$$\rho u_i u_j\,(\partial u_j/\partial x_i) + u_i(\partial p/\partial x_i) = 0 \tag{21}$$

Equations (19) and (20) are identical to the corresponding equations of the original system. This is a result of the fact that these equations have the characteristic property in their original form (i.e., differentiation in a space of lower dimension, a line in this case). The last equation, Eq. (21), is the differential form of Bernoulli's equation.

The single wave surface compatibility relation which exists for a particular wave surface designated by the unit normal n_i (see Appendix D, Eq. (D-15)) is

$$(u_i - an_i)(\partial p/\partial x_i) + \rho a(a\delta_{ij} - n_i u_j)(\partial u_i/\partial x_j) = 0 \tag{22}$$

The characteristic compatibility relations, Eqs. (19), (20), (21) and (22), along with one independent noncharacteristic relation, corresponding to Eq. (B-39) of Appendix B, form the basis for the numerical scheme.

SECTION IV

SECOND-ORDER INTEGRATION SCHEME

1. GENERAL

In the application of the method of characteristics to two-dimensional hyperbolic problems, second-order accuracy can be easily achieved by the use of any explicit second-order integration scheme, such as the modified Euler scheme. This is possible because the characteristic compatibility equations involve directional differentiation in a space of one lower dimension (i.e., a line). Therefore, the compatibility relations can be expressed in terms of directional differentials along this single direction such that the coefficients of the derivatives are functions only of the dependent variables.

In three-dimensional problems the situation is more complicated. Some of the compatibility relations contain two independent directions of directional differentiation. Thus when the compatibility equations are written in terms of directional differentials along one of the characteristic directions, some of the coefficients will invariably contain derivatives of the dependent variables. Second-order predictor-corrector type integrations schemes, such as the modified Euler scheme, require evaluation of the coefficients at the solution point in terms of the predicted values for the dependent variables. Generally the derivatives are not known at the solution point and thus the coefficients cannot be evaluated. All previous integration schemes which have been developed for three-dimensional steady, supersonic flow have simply not evaluated the terms containing derivatives, and thus the local truncation error is less than third order in the step size.

Butler (12) has developed a general method for achieving second-order accuracy in the integration of hyperbolic systems of equations in three independent variables. Elliott (39) and Richardson (40) have applied the method to two-dimensional unsteady flow. In the present research

the general method of Butler, with certain modifications, is applied to the equations for steady supersonic flow in three dimensions.

In general, the scheme consists of selecting the number and orientation of the bicharacteristic compatibility equations in such a way that the terms containing derivatives at the unknown point appear in two distinct groupings which are common to all the equations. The two common terms, evaluated at the unknown point, are treated as additional unknowns and sufficient independent differential relations are found to enable evaluation, or equivalently, algebraic elimination of these terms. The two additional differential relations are an additional bicharacteristic compatibility relation and an independent noncharacteristic relation which is applied along the streamline direction.

2. PARAMETERIZATION OF THE CHARACTERISTIC SURFACE ENVELOPES

In the numerical scheme it is convenient to use a parametric representation for the bicharacteristic elements of the Mach conoid and the streamline, (i.e., the elements of the wave and stream characteristic surface envelopes). A differential element of a conoid can be represented by the parametric equations

$$dx_i = l_i dt, \qquad (i = 1, 2, 3) \tag{23}$$

where l_i is a vector tangent to an element of the cone and t is a parameter proportional to length along the element, see Figure 6.

The Mach conoid (i.e., the wave surface envelope) is locally a right circular cone whose axis is the flow velocity vector. Thus the tangent vector to an element, l_i, can be represented as the sum of the flow velocity vector, u_i, and a velocity of divergence, c, of the conical surface in a plane normal to the velocity vector, see Figure 6. A plane normal to the velocity vector is defined by two orthogonal unit vectors α_i and β_i which are mutually orthogonal to the velocity vector, u_i. An arbitrary versor in this plane, r_i, is given by

$$r_i = \alpha_i \cos\theta + \beta_i \sin\theta \tag{24}$$

where θ is an angular parameter measured from the α_i direction and has

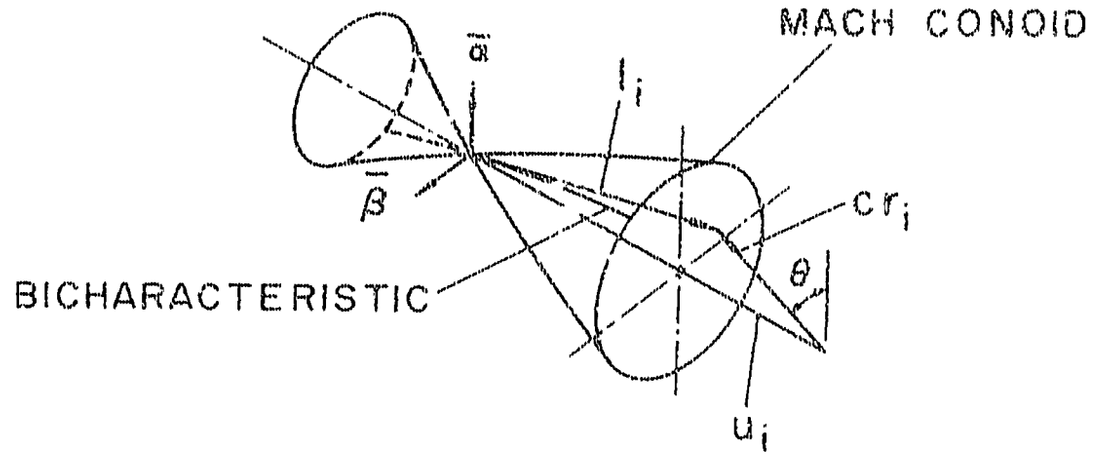

FIGURE 6. BICHARACTERISTIC PARAMETERIZATION

the range $0 \leq \theta < 2\pi$. The velocity of divergence, relative to the flow velocity, of the conical surface along the direction r_i is

$$c = [a^2q^2/(q^2 - a^2)]^{1/2} \tag{25}$$

where q is the magnitude of the flow velocity and a is the local speed of sound. The tangent vector of an element, l_i, corresponding to the direction of r_i has the same direction as the vector obtained by summing the velocity vector u_i and the velocity of divergence vector cr_i. Thus the unnormalized tangent vector is

$$l_i = u_i + c\alpha_i\cos\theta + c\beta_i\sin\theta \tag{26}$$

The parametric equations for a differential bicharacteristic element of the Mach cone are thus

$$dx_i = (u_i + c\alpha_i\cos\theta + c\beta_i\sin\theta)dt, \qquad (i = 1, 2, 3) \tag{27}$$

where the parameter t has the dimension of time and is proportional to length along the bicharacteristic.

A differential element of the streamline (i.e., the stream surface envelope and bicharacteristic) is represented parametrically by Eq. (27) if the velocity of divergence, c, is set equal to zero, thus

$$dx_i = u_i\,dt, \qquad (i = 1, 2, 3) \tag{28}$$

Here the parameter t corresponds to the time of travel of a fluid particle along a streamline.

The form of the parametric equations for the wave surface bicharacteristics, Eq. (27), are the same as those proposed by Butler (12) except that here the remaining degree of freedom in the choice of the reference vectors α_i and β_i is used in such a way that a bicharacteristic curve is obtained for a constant value of θ, see Figure 6. Butler on the other hand held the α_i and β_i reference fixed and allowed θ to vary along a bicharacteristic. The choice of reference used herein results in a significant simplification of the final numerical scheme.

The choice of the vectors u_i, $c\alpha_i$ and $c\beta_i$ as the basis for the parameterization of the Mach conoid also satisfies the quadric equation for the conoid, Eq. (18). The conditions which are necessary for the quadric equation to be satisfied correspond to the general conditions, Eqs. (B-7) and (B-8) of Appendix B, and for the Mach conoid take the form

$$-[u_iu_j - (q^2 - a^2)\delta_{ij}]u_iu_j = c^2[u_iu_j - (q^2 - a^2)\delta_{ij}]\alpha_i\alpha_j$$
$$= c^2[u_iu_j - (q^2 - a^2)\delta_{ij}]\beta_i\beta_j \qquad (29)$$

and

$$c[u_iu_j - (q^2 - a^2)\delta_{ij}]u_i\alpha_j = c[u_iu_j - (q^2 - a^2)\delta_{ij}]u_i\beta_j$$
$$= c^2[u_iu_j - (q^2 - a^2)\delta_{ij}]\alpha_i\beta_j = 0 \qquad (30)$$

These conditions are satisfied for the orthonormal choice for u_i/q, α_i and β_i. Thus the parametric equations for the wave surface bicharacteristics, Eq. (27), satisfy all requirements at a point. However, if the parametric equation is integrated so as to trace out a bicharacteristic, then the reference vector set must be determined such that the more fundamental definition of a bicharacteristic is satisfied, i.e., the curve is a line of contact between the characteristic surface and the conoid. This condition yields the relation (see Eq. (E-1) of Appendix E)

$$[u_iu_j - (q^2 - a^2)\delta_{ij}](u_i + c\alpha_i\cos\theta + c\beta_i\sin\theta)(\partial x_j/\partial\theta) = 0 \qquad (31)$$

which is used to fix the remaining degree of freedom in the choice of the reference vectors α_i and β_i. A numerically useful form of this relation is developed in Appendix E.

3. SYSTEM OF DIFFERENCE EQUATIONS

The system of differential equations, which is the basis of the finite difference integration scheme, consists of the wave surface compatibility relation applied along four particular bicharacteristics,

three of the stream surface compatibility relations and the one non-characteristic relation applied along the streamline. The system of difference equations is obtained by first writing the differential relations in terms of directional differentials along the particular directions to which they apply. These directional differentials are subsequently replaced by first-difference operators.

The wave surface compatibility relation, Eq. (22), can be expressed in terms of the parameters of the bicharacteristic parameterization by developing an expression for the wave surface normal which appears in Eq. (22). The unit normal to the wave surface expressed in terms of the parameters of the wave surface bicharacteristic parameterization is (see Appendix E, Eq. (E-11))

$$n_i = (a/c)[cu_i/q^2 - \alpha_i\cos\theta - \beta_i\sin\theta], \qquad (i = 1, 2, 3)$$

When this expression is used for the components of the normal in terms of the parameter θ, the wave surface compatibility equation, Eq. (22), becomes

$$d_{\xi}p + \rho c(\alpha_i\cos\theta + \beta_i\sin\theta)\, d_{\xi}u_i =$$

$$- \rho c^2(\alpha_j\sin\theta - \beta_j\cos\theta)(\alpha_i\sin\theta - \beta_i\cos\theta)(\partial u_i/\partial x_j)dt \qquad (32)$$

where the operator d_{ξ} denotes a differential along the wave surface bicharacteristic direction.

The stream surface compatibility relations which are used in the numerical scheme, Eqs. (19), (20) and (21), are not affected by the bicharacteristic parameterization, and in terms of the notation for the directional differential operator are

$$d_{\bar{u}}P = 0 \qquad (33)$$

$$d_{\bar{u}}H = 0 \qquad (34)$$

and

$$(\rho/2)\, d_{\bar{u}}(q^2) + d_{\bar{u}}p = 0 \qquad (35)$$

where the subscript $\bar{u}$ on the differential operator denotes the streamline direction (i.e., the stream surface bicharacteristic direction).

The one noncharacteristic differential relation which is used in the numerical scheme, that corresponds to Eq. (B-41) of the general numerical method developed in Appendix B, is obtained in terms of the parameters of the bicharacteristic parameterization by comparison of the general noncharacteristic relation with the general wave surface compatibility relation, Eqs. (B-41) and (B-40) respectively. The coefficients of these two equations are related by Eqs. (B-27) through (B-29). Evaluation of the coefficients by inspection yields

$$d_{\bar{u}}p = -\rho c^2(\alpha_i\alpha_j + \beta_i\beta_j)(\partial u_i/\partial x_j)dt \tag{36}$$

4. DIFFERENCE NETWORK

The local difference network consists of the streamline segment and the four wave surface bicharacteristic segments, see Figure 7. The bicharacteristics are selected in such a way that the terms in the compatibility equation, Eq. (32), and the noncharacteristic relation, Eq. (36), which contain partial derivatives at the unknown point, can be evaluated. Note that for values of θ equal to multiples of $\pi/2$, the terms which contain partial derivatives in the wave surface compatibility relation are of the same form as those which appear in the noncharacteristic relation, Eq. (36), (i.e., two scalar terms $\alpha_i\alpha_j(\partial u_i/\partial x_j)$ and $\beta_i\beta_j(\partial u_i/\partial x_j)$). Thus, all the individual derivatives do not have to be evaluated, only these two summed quantities.

The system of differential relations for $\theta = 0$, $\pi/2$, π and $3\pi/2$ are

$$d_{\bar{I}_1}p + \rho c\alpha_i d_{\bar{I}_1}u_i = -\rho c^2\beta_i\beta_j(\partial u_i/\partial x_j)dt \tag{37}$$

$$d_{\bar{I}_2}p + \rho c\beta_i d_{\bar{I}_2}u_i = -\rho c^2\alpha_i\alpha_j(\partial u_i/\partial x_j)dt \tag{38}$$

$$d_{\bar{I}_3}p - \rho c\alpha_i d_{\bar{I}_3}u_i = -\rho c^2\beta_i\beta_j(\partial u_i/\partial x_j)dt \tag{39}$$

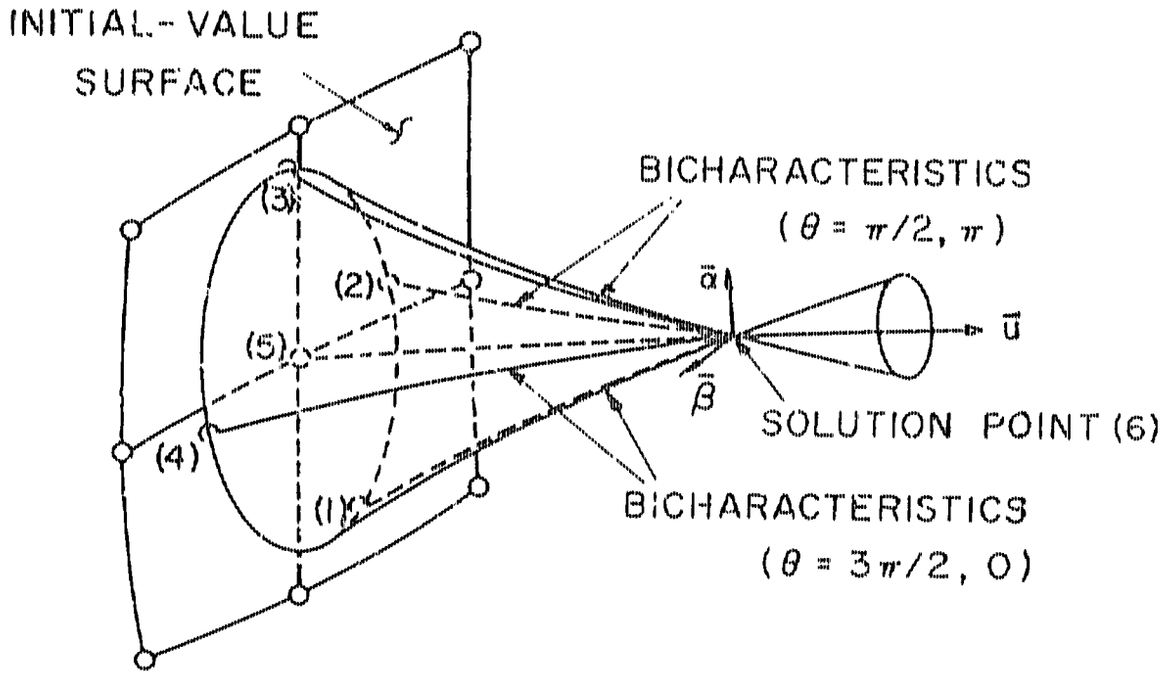

FIGURE 7. INTERIOR POINT COMPUTATIONAL SCHEME

$$d_{\bar{L}_4} p - \rho c \beta_i d_{\bar{L}_4} u_i = - \rho c^2 \alpha_i \alpha_j (\partial u_i / \partial x_j) dt \tag{40}$$

$$d_{\bar{U}} p = -\rho c^2 (\alpha_i \alpha_j + \beta_i \beta_j)(\partial u_i / \partial x_j) dt \tag{41}$$

$$d_{\bar{U}} p = - \rho u_i d_{\bar{U}} u_i \tag{42}$$

$$d_{\bar{U}} P = 0 \tag{43}$$

$$d_{\bar{U}} H = 0 \tag{44}$$

where the subscripts $\bar{L}_1$, $\bar{L}_2$, $\bar{L}_3$ and $\bar{L}_4$ denote the bicharacteristic directions corresponding to values for θ of 0, $\pi/2$, π and $3\pi/2$.

The modified Euler predictor-corrector integration scheme in which arithmetic averages of the coefficients of the differentials are used between the points of the network can now be used to obtain a system of difference equations correct to second order in the step size, see Appendix E, since all the coefficients of the differentials can be evaluated at the unknown point.

The difference network consisting of the four wave surface bicharacteristic segments and the streamline is constructed by means of the parametric differential relations, Eqs. (27) and (28) respectively. The approximate integrals of these relations are also obtained using the modified Euler scheme. The numerical process begins from point (5), the streamline intersection with the initial-value surface, see Figure 8, which is assumed to be a known point and is held fixed. The point of intersection of the streamline passing through point (5) with the solution surface is first found using the streamline parametric equations, Eq. (28). The spatial location of the solution surface is assumed fixed and the three parametric equations are used to solve for two coordinates on the surface and the parameter t along the streamline.

Before the intersections of the four wave surface bicharacteristics can be found, it is necessary to fix the remaining degree of freedom in the specification of the reference vectors α_i and β_i at point (6). An arbitrary selection for the orientation of one of the vectors would be

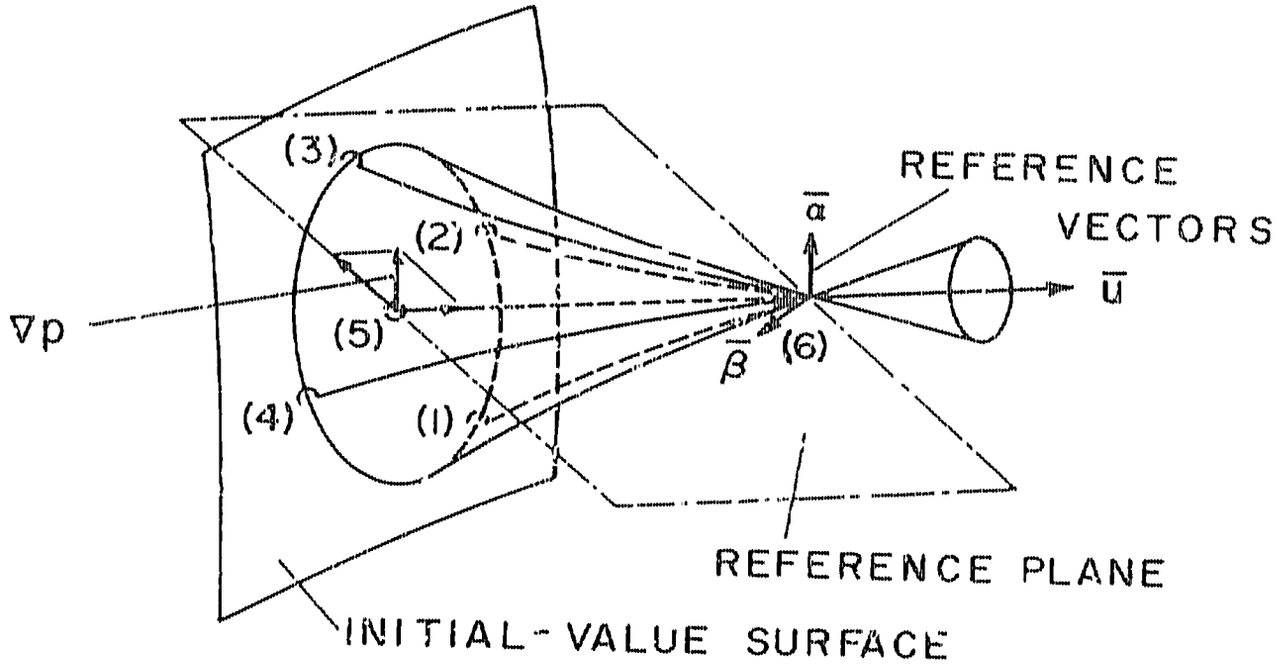

FIGURE 8. METHOD FOR ESTABLISHING REFERENCE VECTORS

satisfactory. However, in the course of numerical studies it was found that slightly better accuracy and more consistent results were obtained by selecting the plane formed by the pressure gradient and the velocity as a reference. In this scheme the vectors α_1 and β_1 were positioned such that the network straddled the reference plane, see Figure 8. Since the pressure gradient at point (6) cannot be determined until an entire solution surface has been generated, the pressure gradient at point (5) is used to establish the reference plane. The four intersections with the initial-value surface of the wave surface bicharacteristics corresponding to $\theta = 0, \pi/2, \pi$ and $3\pi/2$ are next found using the parametric equations for the bicharacteristics, Eq. (27). In each case the intersection is known to lie on the initial-value surface. The three parametric equations are then used to solve for the two coordinates of intersection on the surface and the value of the parameter t.

Once points (1) through (4) are located in this way, the values of the dependent variables at these intersections are found by interpolation. For this purpose second-order polynomials are fit locally to nine neighboring points by the method of least squares (see Appendix F). These nine points consist of the central point, point (5), and the eight nearest surrounding points in the initial-value surface. Note that the values of the dependent variables are known at point (5) and thus interpolation is not necessarily required for these values. However, for reasons of numerical stability it was found necessary to use interpolated values at point (5) for the three velocity components and the pressure.

The reference vectors α_1 and β_1 at points (1) through (4) also are required in the difference equations and thus must be established relative to the selected reference at point (6). The single degree of freedom is established to sufficient accuracy by means of a finite difference form of the tangency condition, Eq. (31) (see Appendix E).

5. ITERATION SCHEME

The modified Euler integration scheme is a predictor-corrector type scheme in which the solution is first approximated by the Euler scheme (i.e., the coefficients of the difference equations are evaluated at the initial-value surface). This approximate solution is then used to evaluate the coefficients of the difference equations at the unknown point

and arithmetic averages of the differer equation coefficients are subsequently used to obtain corrected values for the dependent variables at point (6). This process is repeated until successively obtained values agree to a tolerance consistent with the truncation error. This technique yields a solution in which the local truncation error is third order in step size.

SECTION V

OVERALL NUMERICAL ALGORITHM

1. GENERAL

The global solution for a particular set of initial conditions and boundary conditions is obtained by an algorithm in which the unit integration process is applied repetitively. The scheme consists of integration along a system of streamlines throughout the flow. The particular streamlines which are used are determined by the network of points which are chosen at the initial-value surface. These points are chosen such that a uniform distribution across the flow and on the boundaries is obtained.

The initial-value surface is assumed to be a plane normal to the x_1 coordinate direction and the integration process takes place between a series of planes parallel to the initial-value surface. These planar surfaces are assumed to be everywhere space-like to the flow (i.e., the normals to the surfaces are everywhere interior to the local cone of normals, see Appendix A). These assumptions greatly reduce the complexity of the numerical calculations while not seriously restricting the range of internal flow problems which can be solved if the x_1 coordinate direction is chosen to coincide with the mean flow direction. These assumptions are discussed in greater detail in Appendix G.

As each solution surface is completed, a six component thrust integration and mass flow integration are performed. The mass flow integration provides some indication of the accuracy of the overall process since the total mass flow should remain constant from one solution surface to another.

2. INITIAL-VALUE SURFACE

The values of the six dependent variables, u_1, u_2, u_3, p, P and H, are assumed to be specified by continuous functions on the initial-value

surface such that values may be obtained at any arbitrary point on the surface. If the initial values are only known at a set of points, then continuous data must be generated by interpolation.

A unique scheme was devised for selecting the points on the initial-value surface to be used in the integration process. This scheme not only produces a uniform array of points in the physical space, but also has the very useful property that the points can be ordered in a square logical array. The logical array has the properties that the neighbors of a point in the logical array are, to a close approximation, the neighbors in the physical space and in addition that the points on the perimeter of the logical array are boundary points in the physical space. These properties are used in the selection of points for local interpolation and in the logic for computer programming. The scheme is explained for both circular and noncircular cross sections in Appendix G.

The initial-value surface must adjoin the boundaries and the initial data must satisfy the boundary conditions at the common points. In addition, if the flow geometry is assumed to have one or more planes of symmetry then the initial-value surface and data must also be symmetric about these same planes.

3. BOUNDARY CONDITIONS

The general character of the solution is governed by the boundary conditions as well as by the initial data. The boundary conditions are constraints on the solution which are specified over time-like surfaces which adjoin the initial-value surface (i.e., the normal to the surface is everywhere exterior to the cone of normals, see Appendix A). Boundary conditions which occur in supersonic flow problems are; physical boundaries, planes of symmetry, constant pressure surfaces and shock waves. Except for shock waves the boundary surfaces are stream surfaces of the flow and the interior point integration scheme is easily modified by replacing one of the wave surface bicharacteristic compatibility relations with the boundary condition. These modifications are discussed in Appendix E.

The shock wave boundary condition consists of a discontinuity surface across which the Rankine-Hugoniot conditions apply. The numerical

algorithm required to include shock waves is considerably more complex due to the need to numerically construct the shock surface. This boundary condition is not developed further herein.

The physical boundary condition consists of the requirement that the flow be tangent to the specified boundary, i.e., the velocity vector is orthogonal to the outer normal to the surface. In addition a boundary streamline is constrained to coincide with the boundary. The interior point integration scheme is modified by replacing one of the wave surface bicharacteristic compatibility conditions with the tangency condition, i.e.,

$$u_i n_i = 0 \tag{45}$$

where the u_i are the velocity components and n_i the components of the outer normal to the surface. In addition the remaining three wave surface bicharacteristics are oriented such that the ones corresponding to $\theta = 0$ and π are contained in the tangent plane to the surface and the one corresponding to $\theta = \pi/2$ is interior to the flow. Similar modifications to the basic scheme must be made for the constant pressure boundary, except that the fourth wave surface bicharacteristic compatibility condition is replaced by the condition that the pressure is known. The final numerical algorithm developed in this research does not include this boundary condition. These modifications are further discussed in Appendix E.

The plane of symmetry boundary condition is most easily incorporated into the basic scheme by use of reflection principles to produce image points, see Appendix G. The basic interior point and physical boundary point scheme can then be used without modification. This technique has been used with complete success in the numerical algorithm produced in the course of this research.

4. INTEGRATION STEP REGULATION

The distance between successive solution surfaces must be regulated such that the Courant-Friedrichs-Lewy (CFL) stability criterion is satisfied at all points of the network. The permitted step size is a function

of the local flow parameters and point spacing. This relation is developed in Appendix G and is

$$\Delta x_1 = [u_1^2/(cq)] \quad [1 - (c/q)(q^2/u_1^2 - 1)^{1/2}] \, R_{min} \tag{46}$$

where q is the magnitude of the velocity, c is defined by the relation

$$c = [q^2a^2/(q^2 - a^2)]^{1/2} \tag{47}$$

and R_{min} is the distance from the streamline intersection with the initial-value surface to the nearest point on the convex hull of the points used in the difference scheme, see Appendix S. Equation (46) is used to calculate the step size at each point of the network, and the point which is most restrictive is taken as the point which governs the integration step. As the integration proceeds the governing point is established on each new solution surface. In practice the step size is calculated after the integration has taken place, so that extrapolation of the permitted step is used with a safety factor, which is varied according to whether the extrapolation is too conservative or overly optimistic.

5. OVERALL ALGORITHM

The overall integration process is illustrated in Figure 9. A typical point network for the initial-value surface is shown and the boundary conditions for a physical boundary and a plane of symmetry are illustrated. The algorithm has been programed for both the IBM 7094 and CDC 6500 computers using the Fortran IV language. The program has been used for a variety of accuracy tests and for computation of fully three-dimensional nozzle flows.

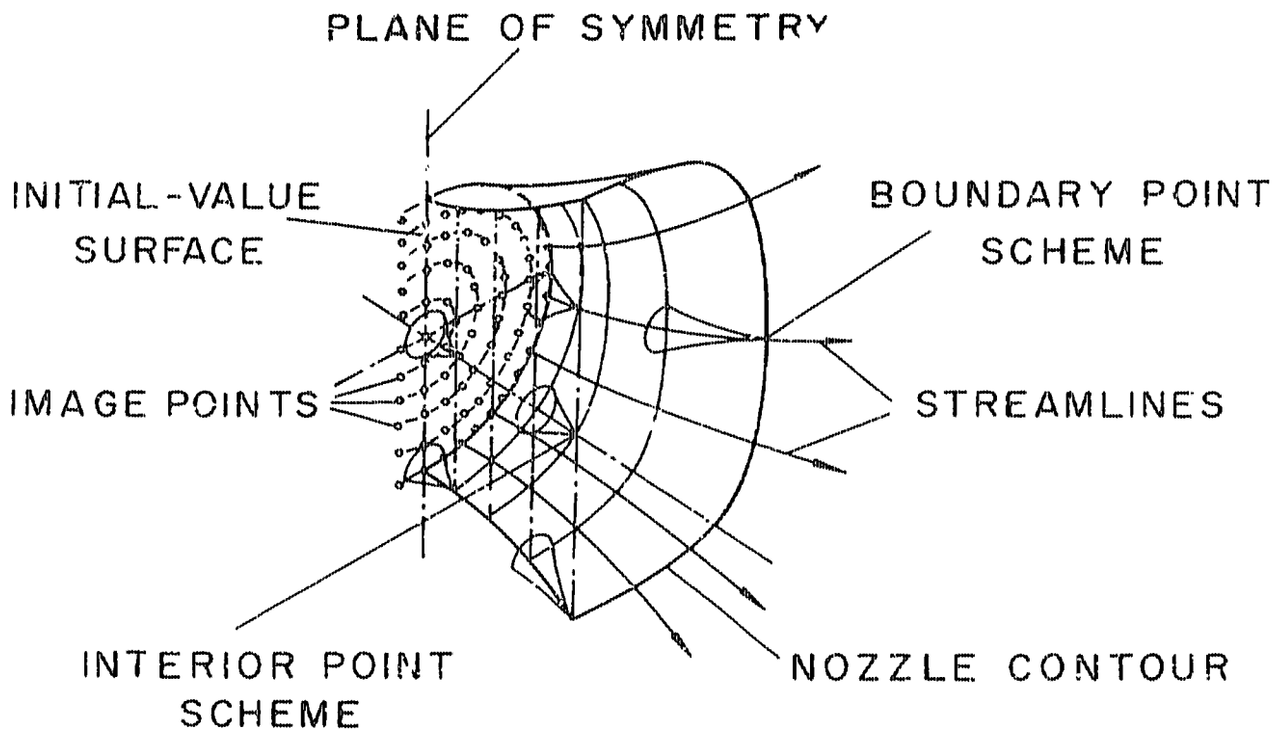

FIGURE 9. OVERALL NUMERICAL ALGORITHM

SECTION VI

NUMERICAL STABILITY

1. STABILITY CRITERIA

The possibility of numerical instability is an ever present danger in any numerical scheme for solution of hyperbolic partial differential equations. Whether or not a scheme is stable is solely a function of the numerical scheme and does not depend upon the differential system that it approximates. Unfortunately, necessary and sufficient criteria for stability exist only for the case of linear equations and analytic initial data. However, although no formal proof exists, experience has shown that these same criteria are appropriate for nonlinear systems when applied locally to the linearized form of the equations, Refs. (5,6). This hypothesis is supported by the results of the present research in which the nonlinear scheme was found to be stable only when the analysis of the linearized system indicated stability.

The two stability criteria which exist are the Courant-Friedrichs-Lewy (CFL) criterion and the von Neumann condition. The CFL criterion is a necessary condition which applies to both linear and nonlinear systems and states that the zone of dependence of the differential system must be embedded within the convex hull of the points in the initial-value surface which are used in the differencing scheme. This condition ensures that the speed of propogation of numerical disturbances, such as round off error, everywhere exceeds the speed of propagation of disturbances in the differential system (i.e., the speed of sound for compressible flow). Thus the numerical disturbances diffuse throughout the network and do not accumulate.

The von Neumann condition states that in order for a numerical scheme to be stable a finite limit must exist for the amplification of any Fourier component of the initial data, Ref. (5). The criterion which must be satisfied in order to ensure this condition is

$$|\lambda_1|_{max} \leq 1 + O(\Delta x_1) \tag{48}$$

where λ_1 is the largest eigenvalue of the amplification matrix for the numerical scheme and $O(\Delta x_1)$ denotes the quantity (Δx_1) multiplied by a finite constant. When the von Neumann criterion is applied to a scheme, the condition, Eq. (48), is usually replaced by the more severe requirement that

$$|\lambda_1|_{max} \leq 1 \tag{49}$$

because of the somewhat arbitrary nature of the term $O(\Delta x_1)$. Note that Eq. (49) is not a stronger condition from the point of view of being sufficient for stability, but it is simply easier to apply.

In the numerical scheme which is developed herein, the CFL condition is used to regulate the integration step size during the numerical integration and is an integral part of the overall algorithm. The von Neumann condition, on the other hand, is used to analyze the effect of various modifications on the numerical stability, but does not play an active role in the actual numerical calculations.

Although the CFL condition was satisfied by an original difference scheme in which interpolation was not used at point (5), it was found in the course of development that this scheme exhibited a neutral stability characteristic. This result prompted a more thorough stability analysis using the von Neumann condition for the basic difference scheme and several permutations, which eventually resulted in the stable scheme in which interpolation was used for the values of the velocity components, u_i, and the pressure, p, at point (5). The details of the analysis are included as Appendix H.

2. LINEAR DIFFERENCE EQUATIONS

A system of linear difference equations is obtained from the system of nonlinear differential equations, Eqs. (37) through (42), by application of small perturbation theory and replacement of the directional differential operators by first difference operators. In doing this the terms containing partial derivatives, in particular $a_i a_j (\partial u_i / \partial x_j)$ and

$\beta_i\beta_j(\partial u_i/\partial x_j)$, are treated as unknown quantities at the point under consideration. Using this approach the resulting six linear equations are just sufficient to evaluate these two terms as well as the four dependent variables.

The form of the two terms containing derivatives in the system of differential equations is a direct result of the scheme for maintaining second-order accuracy and the stability analysis must include consideration of these terms. If these terms were not considered, as is the case in stability analysis for first-order schemes then an overdetermined system of equations would result and either, two equations would have to be eliminated from consideration or the system must be solved in a least squares sense.

The analysis is simplified if the terms containing derivatives are algebraically eliminated to reduce the system to four independent difference equations. The system thus obtained is

$$\Delta_{\bar{I}_1}\tilde{p} + \bar{\rho}\bar{c}\bar{\alpha}_i\Delta_{\bar{I}_1}\tilde{u}_i = (\Delta_{\bar{I}_3}\tilde{p} - \bar{\rho}\bar{c}\bar{\alpha}_i\Delta_{\bar{I}_3}\tilde{u}_i)\,(\Delta_{\bar{I}_1}\tilde{t}/\Delta_{\bar{I}_3}\tilde{t}) \tag{50}$$

$$\Delta_{\bar{I}_2}\tilde{p} + \bar{\rho}\bar{c}\bar{\beta}_i\Delta_{\bar{I}_2}\tilde{u}_i = (\Delta_{\bar{I}_4}\tilde{p} - \bar{\rho}\bar{c}\bar{\beta}_i\Delta_{\bar{I}_4}\tilde{u}_i)\,(\Delta_{\bar{I}_2}\tilde{t}/\Delta_{\bar{I}_4}\tilde{t}) \tag{51}$$

$$\Delta_{\bar{U}}\tilde{p} = (\Delta_{\bar{I}_1}\tilde{p} + \bar{\rho}\bar{c}\bar{\alpha}_i\Delta_{\bar{I}_1}\tilde{u}_i)\,(\Delta_{\bar{U}}\tilde{t}/\Delta_{\bar{I}_1}\tilde{t}) + (\Delta_{\bar{I}_2}\tilde{p} + \bar{\rho}\bar{c}\bar{\beta}_i\Delta_{\bar{I}_2}\tilde{u}_i)\,(\Delta_{\bar{U}}\tilde{t}/\Delta_{\bar{I}_2}\tilde{t}) \tag{52}$$

$$\Delta_{\bar{U}}\tilde{p} = -\bar{\rho}\bar{u}_i\Delta_{\bar{U}}\tilde{u}_i \tag{53}$$

where the bar denotes constant mean values and tilde denotes a small variation. The difference operators apply along the segment of the bicharacteristic network illustrated in Figure 7 and the subscripts $\bar{I}$ and $\bar{U}$ denote the wave surface bicharacteristics and the streamline directions respectively (see Appendix H).

3. APPLICATION OF THE VON NEUMANN CONDITION

The analysis for stability in the von Neumann sense must include consideration of all the numerical operations of the basic integration scheme. In particular, the interpolation process for data in the initial-value surface must be included.

It is assumed that the analytic solution of the system of linear difference equations can be obtained by separation of variables, Ref. (5). Thus the general term of the Fourier representation of the solution is

$$\bar{U} = e^{i\pi Mx_2/L}\, e^{i\pi Nx_3/L}\, \bar{a}(x_1) \tag{54}$$

where $\bar{U}$ is the vector whose elements are the dependent variables of the problem, $\bar{a}(x_1)$ is a corresponding vector function of the direction of integration, x_2 and x_3 are the rectangular cartesian coordinates of the initial-value surface, L is a characteristic dimension and M and N are the frequency factors for an arbitrary component of the solution.

For purposes of the analysis, data on the initial-value surface are assumed to be known at the points of a uniform rectangular grid in an x_2, x_3 plane with spacings Δx_2 and Δx_3 respectively. Thus the independent variables x_2 and x_3 in the general Fourier term are only permitted to have values which are integral multiples, m and n, of the grid spacings, Δx_2 and Δx_3. The values of the dependent variables at these points, given by Eq. (54), are thus

$$\bar{U} = \zeta^m \eta^n\, \bar{a}(x_1) \tag{55}$$

where ζ and η are defined as the complex quantities

$$\zeta = e^{i\pi M\Delta x_2/L} \tag{56}$$

$$\eta = e^{i\pi N\Delta x_3/L} \tag{57}$$

and

$$x_2 = m\Delta x_2, \qquad (m = 0, \pm 1, \pm 2, \cdots) \tag{58}$$

$$x_3 = n\Delta x_3, \qquad (n = 0, \pm 1, \pm 2, \cdots) \tag{59}$$

In the numerical scheme the solution is advanced along the streamlines passing through each of the points of the network. The central streamline point and its eight nearest neighbors are used for local interpolation.

The analysis is simplified, without loss of generality, if the central point of the local mesh is chosen such that $x_2(5) = x_3(5) = 0$. Thus the nine points used for interpolation correspond to values for the integers $m = 0, \pm 1$ and $n = 0, \pm 1$. The second-order bivariate interpolating polynomial is fit to these nine points by the least squares method developed in Appendix F. The resulting polynomial has the general form

$$\tilde{U} = (A_1 + A_2x_2 + A_3x_3 + A_4x_2x_3 + A_5x_2^2 + A_6x_3^2)\,\tilde{a}(x_1) \tag{60}$$

where the coefficients are found to be (see Appendix H)

$$\begin{aligned} A_1 = [&(5/9)(\zeta + \zeta^{-1} + 1)(\eta + \eta^{-1} + 1) \\ &- (1/3)(\zeta + \zeta^{-1})(\eta + \eta^{-1} + 1) \\ &- (1/3)(\zeta + \zeta^{-1} + 1)(\eta + \eta^{-1})] \end{aligned} \tag{61}$$

$$A_2 = [(1/6)(\zeta - \zeta^{-1})(\eta + \eta^{-1} + 1)]/\Delta x_2 \tag{62}$$

$$A_3 = [(1/6)(\zeta + \zeta^{-1} + 1)(\eta - \eta^{-1})]/\Delta x_3 \tag{63}$$

$$A_4 = [(1/4)(\zeta - \zeta^{-1})(\eta - \eta^{-1})]/\Delta x_2\Delta x_3 \tag{64}$$

$$\begin{aligned} A_5 = [&- (1/3)(\zeta + \zeta^{-1} + 1)(\eta + \eta^{-1} + 1) \\ &+ (1/2)(\zeta + \zeta^{-1})(\eta + \eta^{-1} + 1)]/\Delta x_2^2 \end{aligned} \tag{65}$$

$$A_6 = [-(1/3)(\zeta + \zeta^{-1} + 1)(\eta + \eta^{-1} + 1) + (1/2)(\zeta + \zeta^{-1} + 1)(\eta + \eta^{-1})]/\Delta x_3^2 \quad (56)$$

The dependent variables at the intersections of the four wave surface bicharacteristics with the initial-value surface must be evaluated by means of Eq. (60) since these intersections do not generally correspond to points of the initial-value surface network. Even though the streamline intersection coincides with a network point, and thus interpolation is not necessarily required, it was found that interpolation had a significant effect on stability.

The system of difference equations, Eqs. (50) through (53), constitute a recursion relation for the values of the dependent variables at point (6) in terms of values in the initial-value surface. For the case $x_2(5) = x_3(5) = 0$ and the interpolating polynomial, Eq. (60), is used to determine the values of the dependent variables at the points in the initial-value surface, the recursion relation has the following form

$$\bar{U}[x_1(5) + \Delta x_1] = \bar{a}[x_1(5) + \Delta x_1] = A\,\bar{a}[x_1(5)] \quad (67)$$

in which A is called the amplification matrix. Here A is a fourth-order matrix in which the nonzero coefficients are

$$A_{11} = f(5) \quad (68)$$

$$A_{12} = (1/2)[f(3) - f(1)](\bar{c}/\bar{u}_1) \quad (69)$$

$$A_{13} = (1/2)[f(4) - f(2)](\bar{c}/\bar{u}_1) \quad (70)$$

$$A_{14} = \{f(5) - (1/2)[f(1) + f(2) + f(3) + f(4)]\}/(\bar{\rho}\bar{u}_1) \quad (71)$$

$$A_{22} = (1/2)[f(1) + f(3)] \quad (72)$$

$$A_{24} = (1/2)[f(1) - f(3)]/(\bar{\rho}\bar{c}) \quad (73)$$

$$A_{33} = (1/2)[f(2) + f(4)] \tag{74}$$

$$A_{34} = -(1/2)[f(2) - f(4)]/(\bar{\rho}\bar{c}) \tag{75}$$

$$A_{42} = (1/2)[f(1) - f(3)](\bar{\rho}\bar{c}) \tag{76}$$

$$A_{43} = (1/2)[f(2) - f(4)](\bar{\rho}\bar{c}) \tag{77}$$

$$A_{44} = (1/2)[f(1) + f(2) + f(3) + f(4)] - f(5) \tag{78}$$

and the notation f(I) denotes the polynomial portion of Eq. (60) evaluated at the point (I). These results are developed in Appendix H. The recursion relation which results when interpolation at point (5) is not included is also developed in Appendix H.

The von Neumann stability criterion states that the absolute magnitudes of the eigenvalues of the amplification matrix A should not exceed the value $1 + O(1/\Delta x_1)$, where $O(1/\Delta x_1)$ denotes some finite constant times the quantity $(1/\Delta x_1)$. The bound for the eigenvalues of the matrix A was investigated numerically by choosing a characteristic length L and mesh spacings Δx_2 and Δx_3, consistent with physical problems of interest, and subsequently calculating the magnitudes of the eigenvalues for a range of the frequency factors M and N. Values of 10 and 1 were assumed for L and both Δx_2 and Δx_3 respectively. The range of M and N was then selected so that the arguments of the circular functions ranged from 0 to 2π; this results in a range from 0 to 20 for both M and N. The eigenvalue having the maximum magnitude was calculated as a function of a frequency index I wherein all M and N less than or equal to I were searched for the maximum eigenvalue. In the course of the investigation it was found that the results were completely symmetric about the value 10 for I, thus only the results for I less than 10 are reported.

The results of the eigenvalue analysis are shown plotted in Figure 10 for three cases, the basic difference scheme without interpolation, interpolation except at the streamline point and interpolation at all points (see Appendix H for the analytical development for cases without interpolation). When interpolation is not used the scheme is clearly unconditionally unstable since only eigenvalues greater than or equal

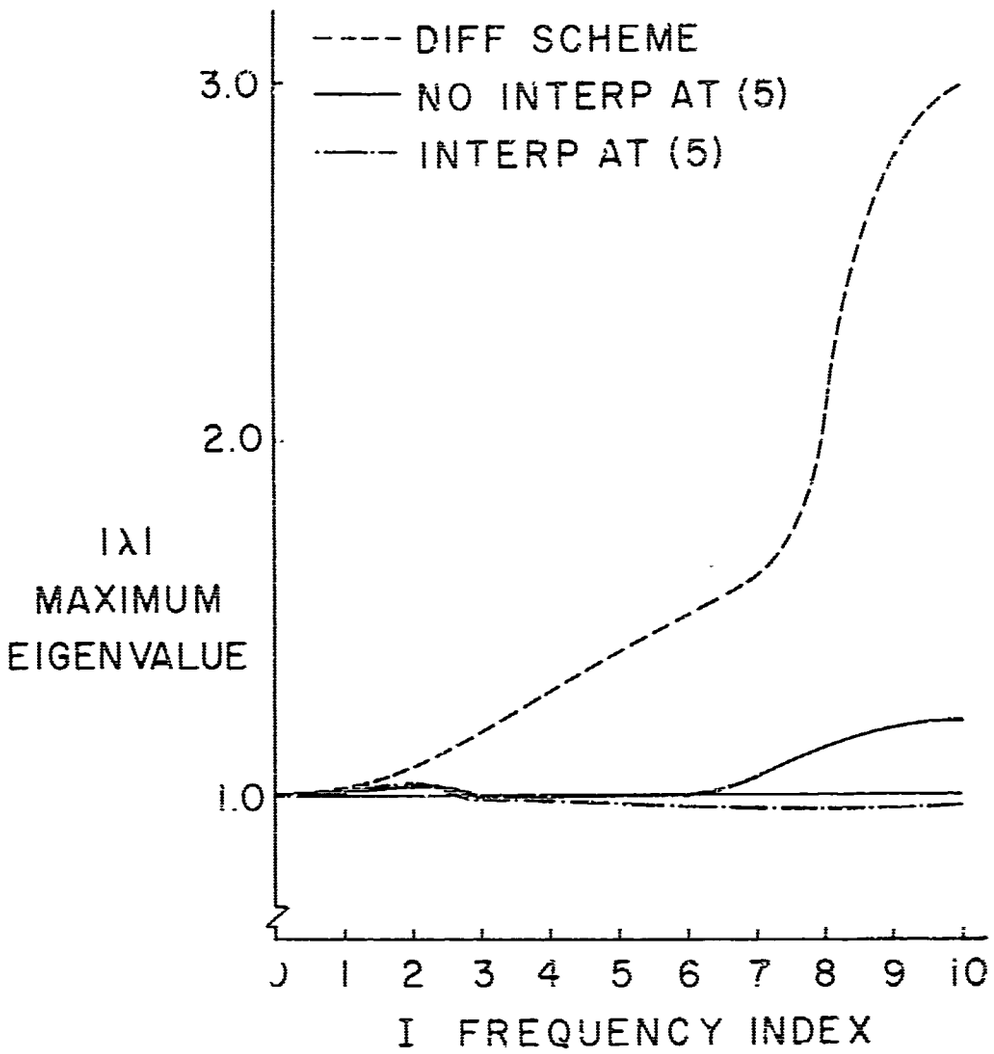

FIGURE 10. STABILITY RESULTS

to unity are obtained. The maximum absolute value of an eigenvalue, approximately 3, occurs for I equal to 10, which corresponds to a Fourier component having a wave length twice the mesh spacing. This result is not surprising since, of the points in the initial-value surface are used (the four wave surface bicharacteristic intersections and the streamline intersection) the convex hull of the four outermost points is a square lying entirely within the circular differential zone of dependence. Thus, the CFL necessary condition for stability is not satisfied.

When interpolation using nine points is used only at the bicharacteristic intersections, a marked improvement in stability characteristic results, but the maximum magnitude of the eigenvalues is still everywhere equal to or exceeds unity, see Figure 10. Numerical tests of this scheme, using the nonlinear second-order algorithm, revealed that numerical instabilities did occur after 20 to 30 integration steps.

When interpolation is used at all five points in the initial-value surface a sufficiently stable scheme results, see Figure 11. In this case eigenvalues greater than unity occur only for low frequency components and even these are only slightly greater than unity. Numerical tests with this scheme have revealed no evidence of instability even after 60 integration steps and in the presence of severe disturbances which would result in shocks in a real flow. Results of the eigenvalue analysis for reductions in the x_1 step size and for rotation of the network are given in Appendix H. Only for the case of zero x_1 step size were all eigenvalues less than or equal to unity. However, the numerical results which have been obtained using the nonlinear scheme clearly indicate that the scheme using interpolation at all points is sufficiently stable if the CFL condition is satisfied.

SECTION VII

ACCURACY STUDIES

1. GENERAL

In order to test the order of the numerical error of the scheme, the numerical solution was compared with the exact solution for a spherical source flow and a Prandtl-Meyer or simple wave flow. Specialized computer programs were written which generated an exact initial-value surface and subsequently generated both the numerical and exact solutions at the points of each subsequent solution surface. The point spacing on the respective initial-value surfaces were successively halved in order to study the error behavior for reductions in step size.

As an additional test of the accuracy, the three-dimensional numerical results for two axisymmetric nozzles were compared with the numerical solution obtained using the two-dimensional method of characteristics. The two nozzles used for comparison were a conical nozzle having a 15 degree half-angle and a contoured axisymmetric nozzle.

2. SOURCE FLOW RESULTS

The local truncation error in the numerical scheme was assumed to be third order in step size; thus, for integration to a fixed point in the flow for which the number of steps is of the order $(1/\Delta x_1)$, the accumulated error is second order in step size. The order of the actual error can be established numerically by successively reducing the step size and comparing the ratio of accumulated errors to the ratio of step sizes raised to the assumed order of the error. This process is illustrated schematically and the results summarized in Figure 11. These results were obtained for a Mach number of four on the initial-value surface and a relatively small source angle. The results verify the assumed second-order error characteristic since the ratios of the errors are in all cases less than the ratios of the step size squared. Similar

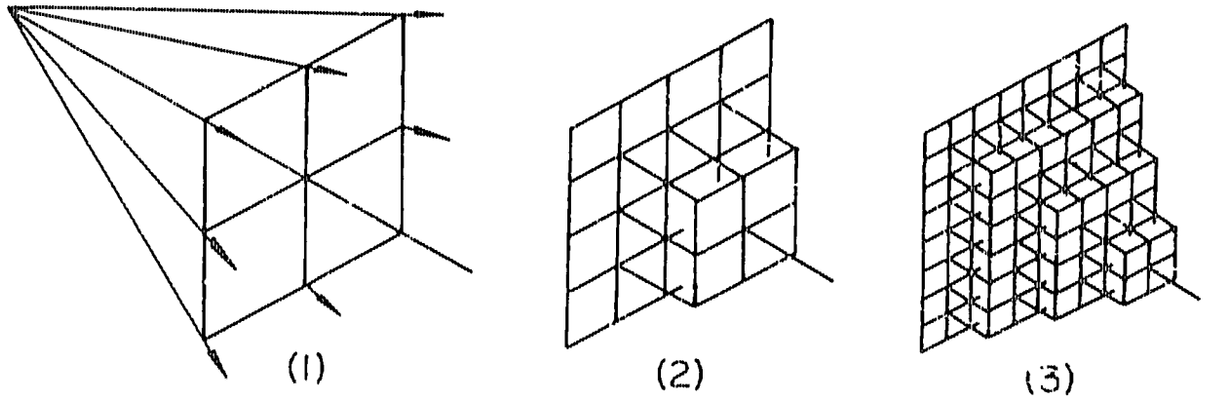

CASE	(1)	(2)	(3)
RELATIVE STEP SIZE	1	1/2	1/4
ACCUMULATED ERROR (%)	0.0104	0.0021	0.0005
RATIO TO CASE (1)	1	1/5	1/21
THEORETICAL RATIO	1	1/4	1/16

FIGURE II. SOURCE FLOW ERROR STUDY, $M_I = 4.0$

results were obtained for circular point networks and for higher gradient flows, i.e., large source angles and Mach numbers near unity, see Appendix I. When a very coarse mesh was used for the higher gradient flows it was found that less than second-order error characteristics resulted. However, as the mesh spacing was reduced the scheme did exhibit the proper second-order characteristic. One possible explanation for this phenomenon is that at large mesh spacing the second-order interpolation scheme is no more accurate than first-order interpolation and thus the accuracy characteristic is reduced. More detailed results of this study are included in Appendix I.

3. PRANDTL-MEYER FLOW RESULTS

Although a Prandtl-Meyer flow is only a one independent variable flow, like the source flow, the flow has a two-dimensional spatial character. Unlike the spherical source flow the streamlines are curved and thus should provide a more severe test for the numerical scheme.

Similar results to those obtained for source flow are presented in Figure 12. Here again a second-order error characteristic is clearly indicated. Error studies similar to those presented in Figure 12 have been made for variations in the initial Mach number and for rotations of the plane of curvature of the streamlines, see Appendix I. Although considerable variation in the absolute accuracy occurs, the second-order characteristic is retained. As a result of the studies for rotation of the plane of curvature, it was decided to use the pressure gradient, which lies in the local plane of curvature, as a reference for orientation of the local difference network. These studies indicated that the local error was a minimum when the system of four bicharacteristic segments just straddled the plane of curvature. It should be emphasized that this effect was small, but was as convenient to employ as a more arbitrary reference, see Appendix I.

4. AXISYMMETRIC RESULTS

As a further test of the general accuracy of the three-dimensional numerical algorithm, two axisymmetric flows were computed and the results were compared to the solutions obtained using a conventional

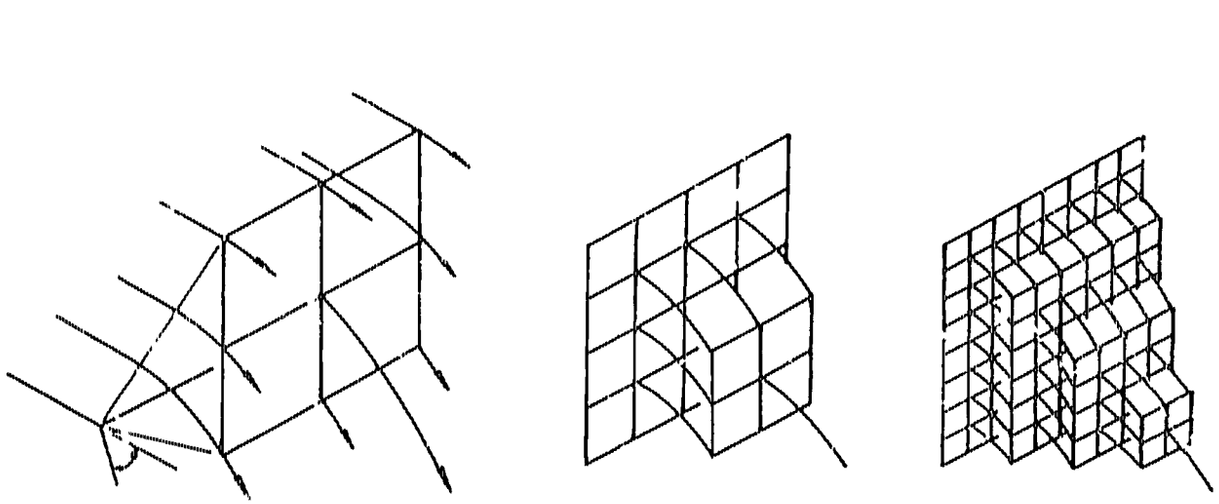

(1) (2) (3)

CASE	(1)	(2)	(3)
RELATIVE STEP SIZE	1	1/2	1/4
ACCUMULATED ERROR (%)	0.00318	0.000827	0.000209
RATIO TO CASE (1)	1	1/4	1/15.5
THEORETICAL RATIO	1	1/4	1/16

FIGURE 12. PRANDTL-MEYER FLOW ERROR STUDY, $M_1 = 4.0$

two-dimensional method of characteristics program. The two cases consisted of a 15 degree half-angle cone and an axisymmetric contoured nozzle having a maximum wall slope downstream of the throat of 35 degrees and an exit half-angle of 13 degrees. In all cases the initial data were generated using a 10 degree spherical source flow. The results of these comparisons are shown in Figures 13 and 14 for the cone and contoured nozzle respectively. Both the nozzle wall and centerline pressures are plotted in each case. The agreement is exceedingly good except at points of discontinuous rates of change in flow properties. The point on the nozzle axis at which the first expansion wave from the wall reaches the axis is such a point. This point is labeled by A in both Figures 13 and 14. The two-dimensional solution, which calculates along characteristics and does not require interpolation, shows the true character of the solution, while the three-dimensional solution smooths out this point. This diffusive characteristic is inherent in any three-dimensional calculation scheme because of the necessity to interpolate and because of the need to satisfy the CFL stability criterion which requires that numerical disturbances be propagated at a velocity greater than the infinitesimal disturbance propagation speed, i.e., the speed of sound.

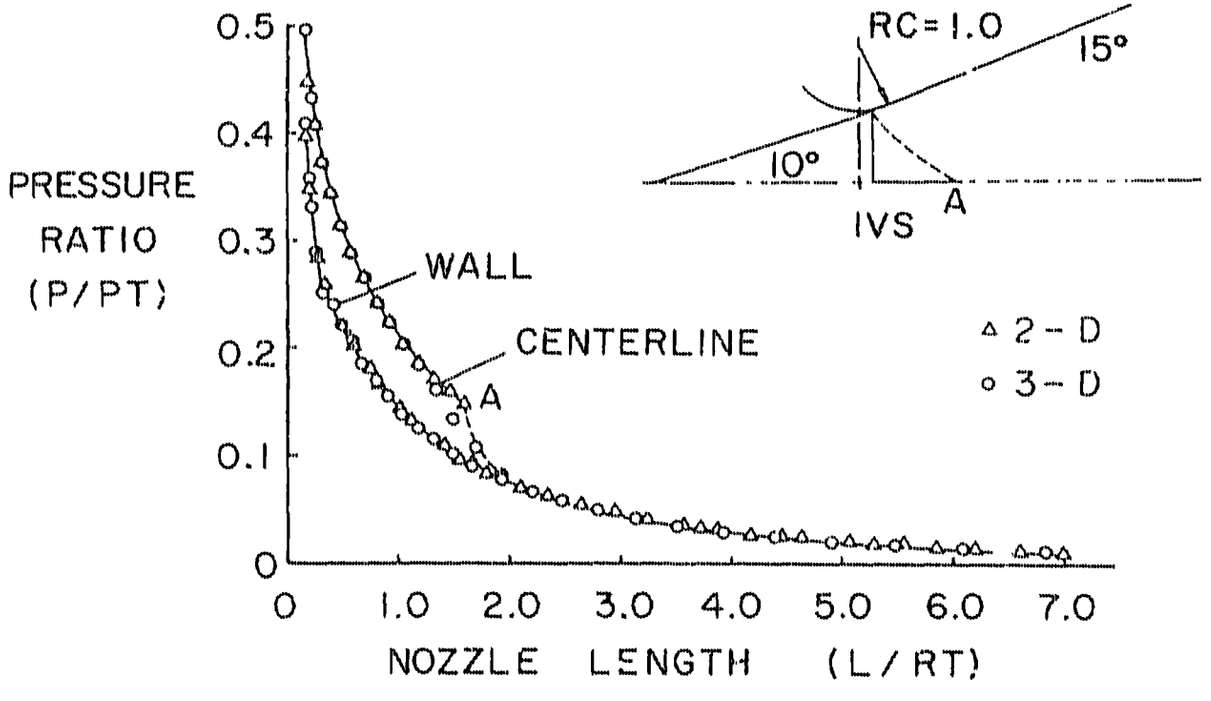

FIGURE 13. SOLUTION FOR CONICAL NOZZLE

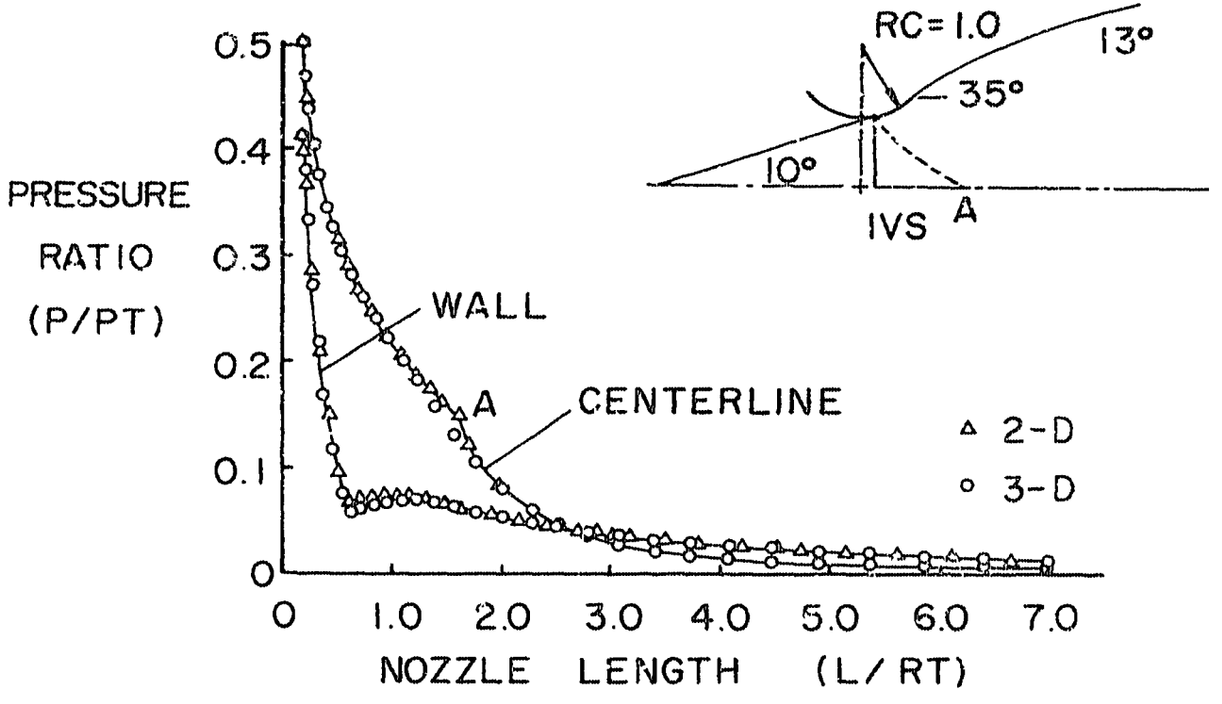

FIGURE 14. SOLUTION FOR CONTOURED NOZZLE

SECTION VIII

THREE-DIMENSIONAL FLOW RESULTS

1. GENERAL

At the present time no exact solutions for three-dimensional supersonic internal flows exist nor does any standard numerical calculation technique; consequently it is not possible to make any comparison with existing results. Several solutions for flows having three-dimensional character are presented here simply to illustrate the general capabilities of the technique. These results were generated using the CDC-6500 version of the computer program which was produced.

The cases presented are not directed toward any specific application, but are typical of the types of nozzles which might, under special constraints, be used as either rocket, ramjet or scramjet nozzles.

2. ELLIPTICAL NOZZLES

These nozzles have ellipitical cross sections normal to the x_1 coordinate axis. The x_2 and x_3 intercepts of the cross sections are functions of the x_1-coordinate such that the contour is initially circular at the throat and elliptical beyond. The intercept variation is described by a circular arc in the throat region which is joined tangentially to a general parabola for the diverging section.

The cross sections and boundary streamlines for one quadrant of the first nozzle are plotted isometrically in Figure 15. In this case the intercept of the contour with the x_1 - x_3 coordinate plane was held fixed while the x_1 - x_2 intercept was allowed to vary. A uniform parallel flow was used to establish flow conditions at the initial-value surface.

The nozzle cross sections and corresponding polar wall pressure contours at each solution surface are shown in Figure 16. The polar pressure plots are constructed such that the pressure is the magnitude of the radius vector to each point on the curve and the polar angle

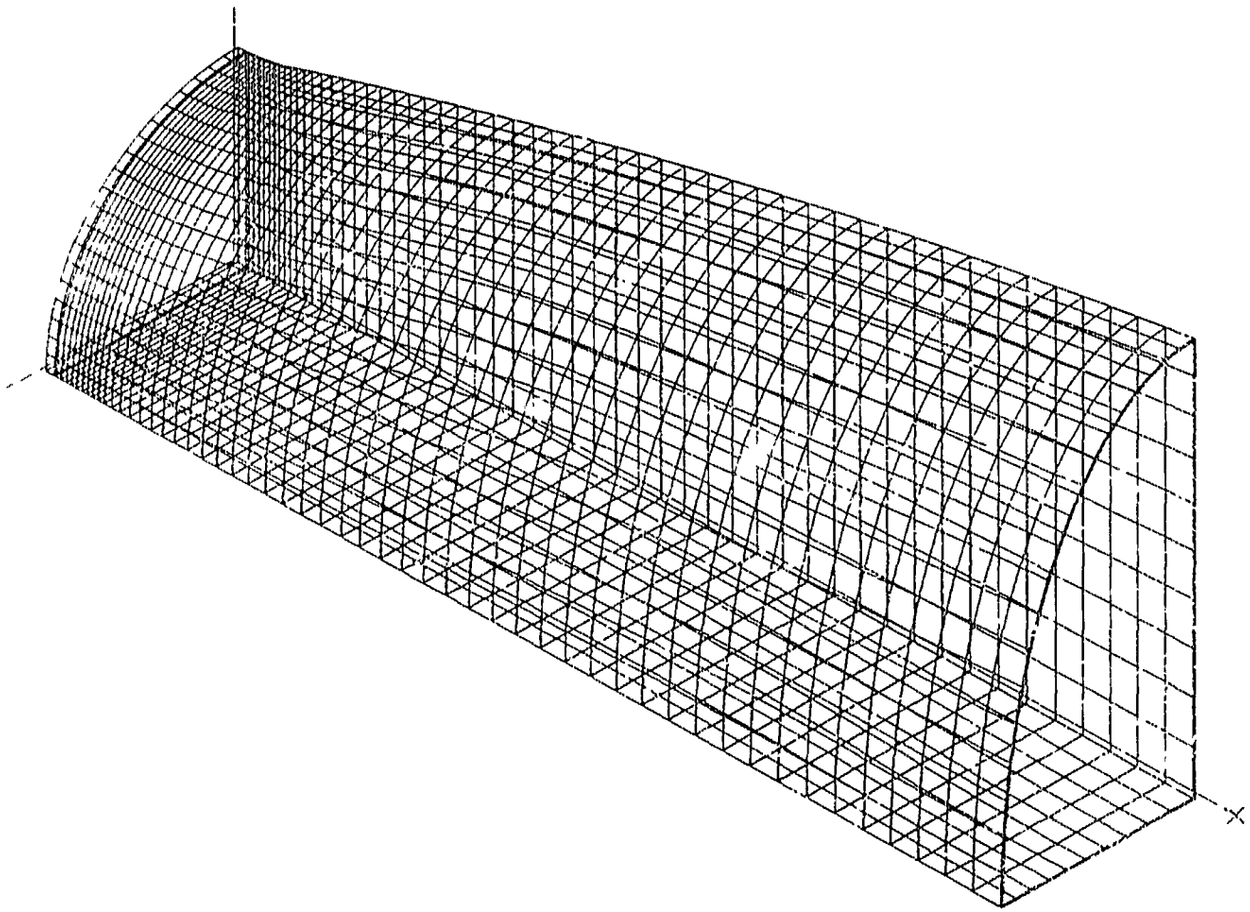

FIGURE 15. ELLIPTICAL NOZZLE I

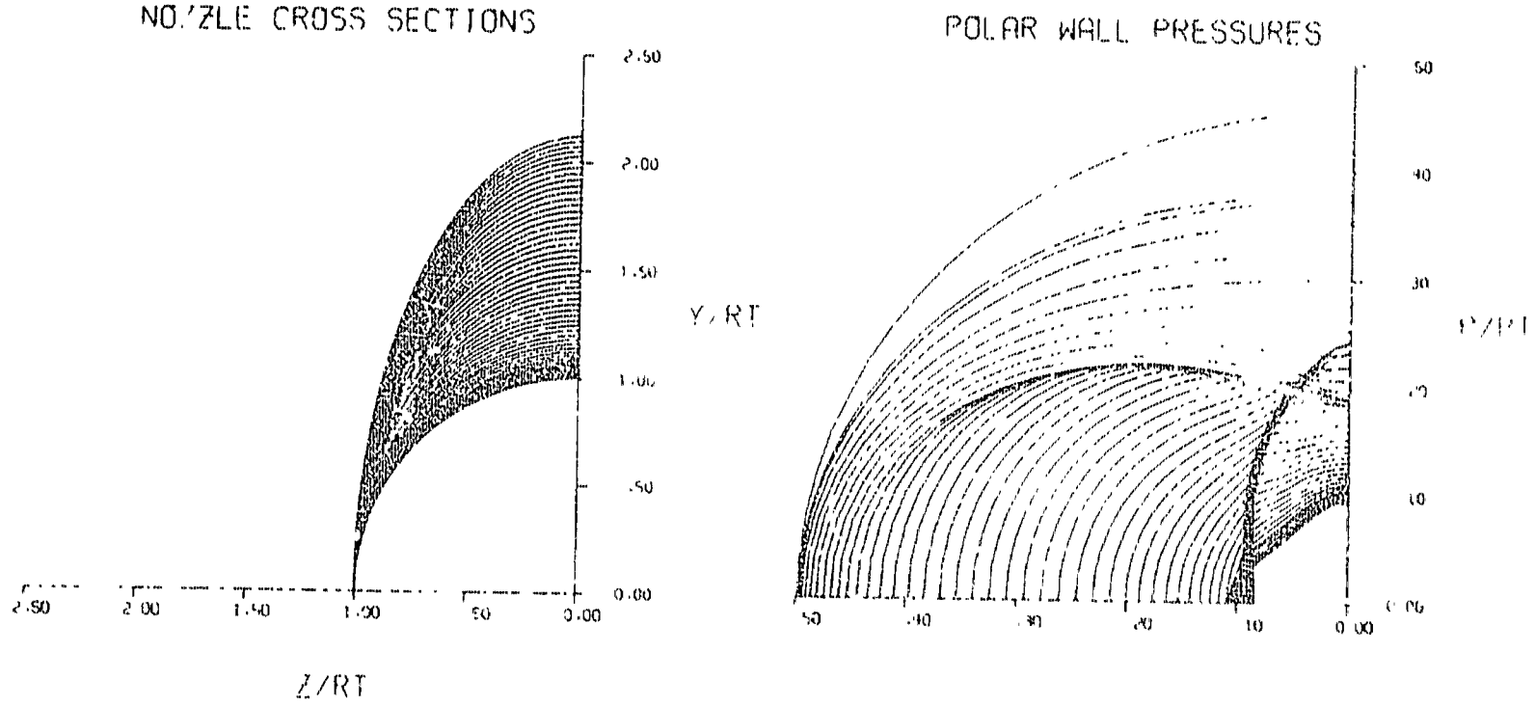

FIGURE 16. WALL PRESSURES FOR ELLIPTICAL NOZZLE I

corresponds to the polar angle of the wall point in the physical plane. Note the pronounced three-dimensional character of the pressure field. Even though the contour is a smooth and relatively gentle transition, significant transverse pressure gradients are present. Clearly a psuedo three-dimensional calculation technique, which neglects cross flow, could not adequately represent such a flow.

The second elliptical nozzle is also circular at the throat, but has variation of both the $x_1 - x_2$ and $x_1 - x_3$ intercepts in the diverging section. An isometric plot of the nozzle cross-sections and the boundary streamlines is shown in Figure 17. The corresponding cross-sections and polar pressure contours are shown in Figure 18. This nozzle has less deviation from axial symmetry than the first nozzle, and consequently, the three-dimensional character is less pronounced.

3. SUPER-ELLIPTICAL NOZZLE

The term super-elliptical is used here to denote a nozzle having cross-sections given by the general equation

$$(x_2/A_2)^{E_2} + (x_3/A_3)^{E_3} = 1 \qquad (79)$$

where x_2 and x_3 are the rectangular cartesian coordinates of the cross-section, A_2 and A_3 are the respective intercepts and E_2 and E_3 are exponents which are greater than or equal to 2.0. The parameters A_2, A_3, E_2 and E_3 are assumed to be differentiable functions of the axial coordinate x_1. As the exponents are given values greater than 2.0 the cross-sections approach a rectangular shape with a smooth fillet at the outer corner.

The super-elliptical nozzle contour used for illustration herein was generated using the same intercepts as for the second elliptical nozzle, but letting the super-elliptical exponents vary from 2.0 at the throat station to 10.0 at the nozzle exit so that the contour is initially circular at the throat and becomes super-elliptical in the diverging section. One quadrant of the resulting contour with boundary streamlines is shown plotted isometrically in Figure 19. The corresponding cross-sections and polar wall pressures are shown in Figure 20. Here again,

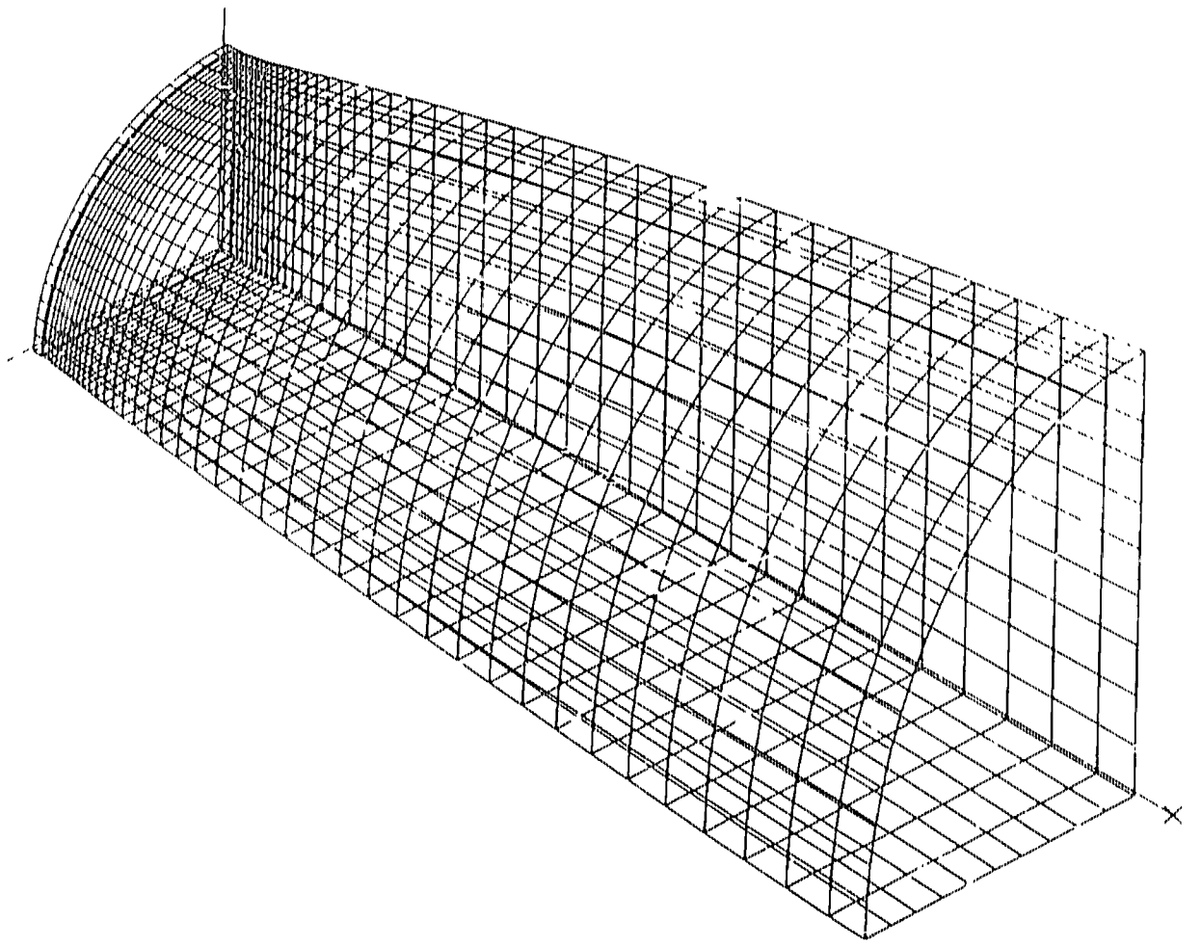

FIGURE 17. ELLIPTICAL NOZZLE 2

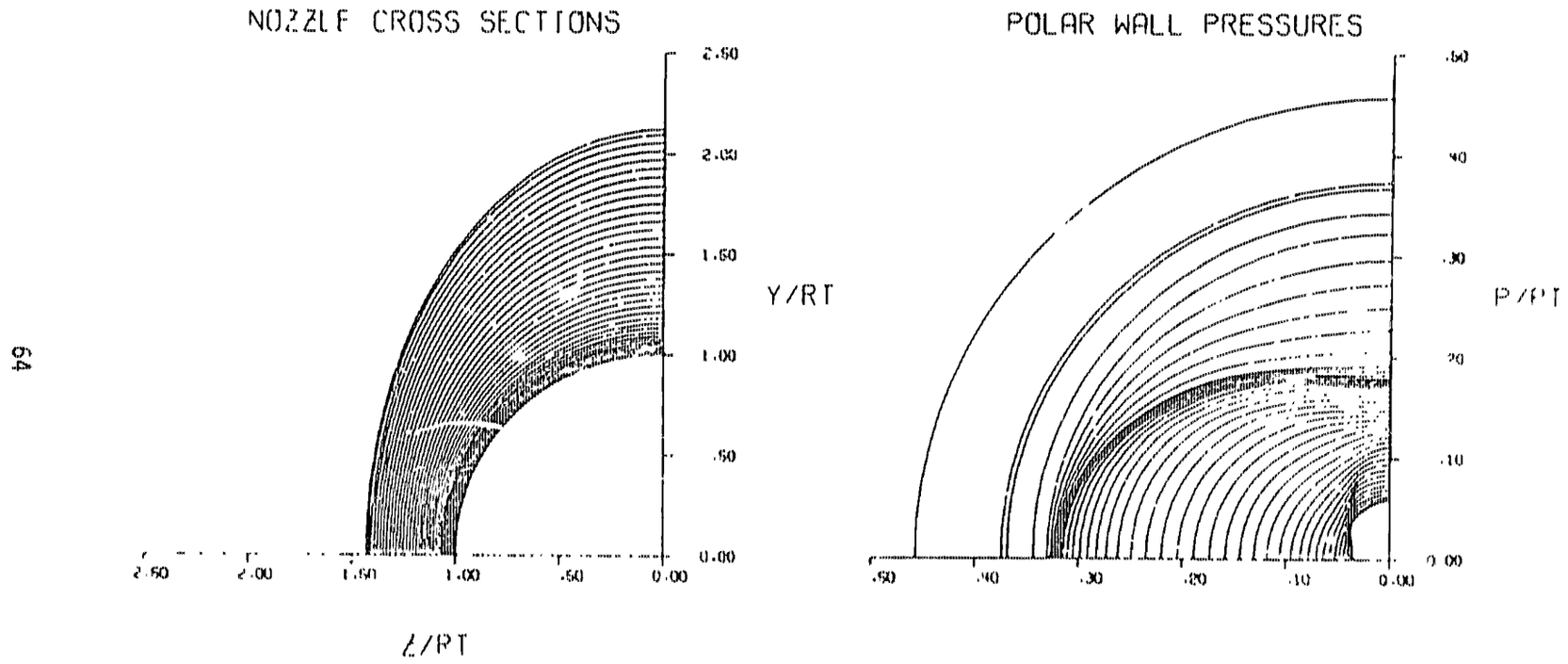

FIGURE 18. WALL PRESSURES FOR ELLIPTICAL NOZZLE 2

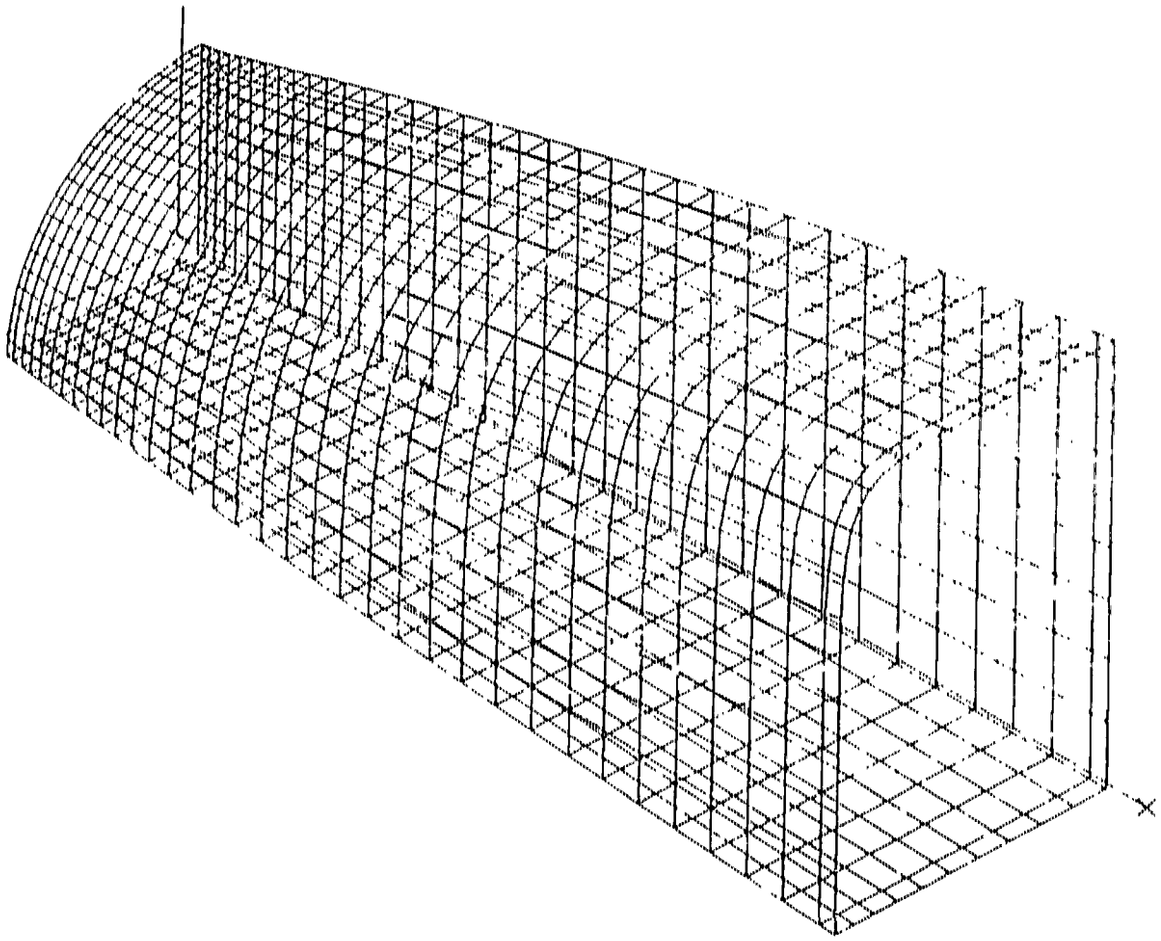

FIGURE 19. SUPER-ELLIPTICAL NOZZLE

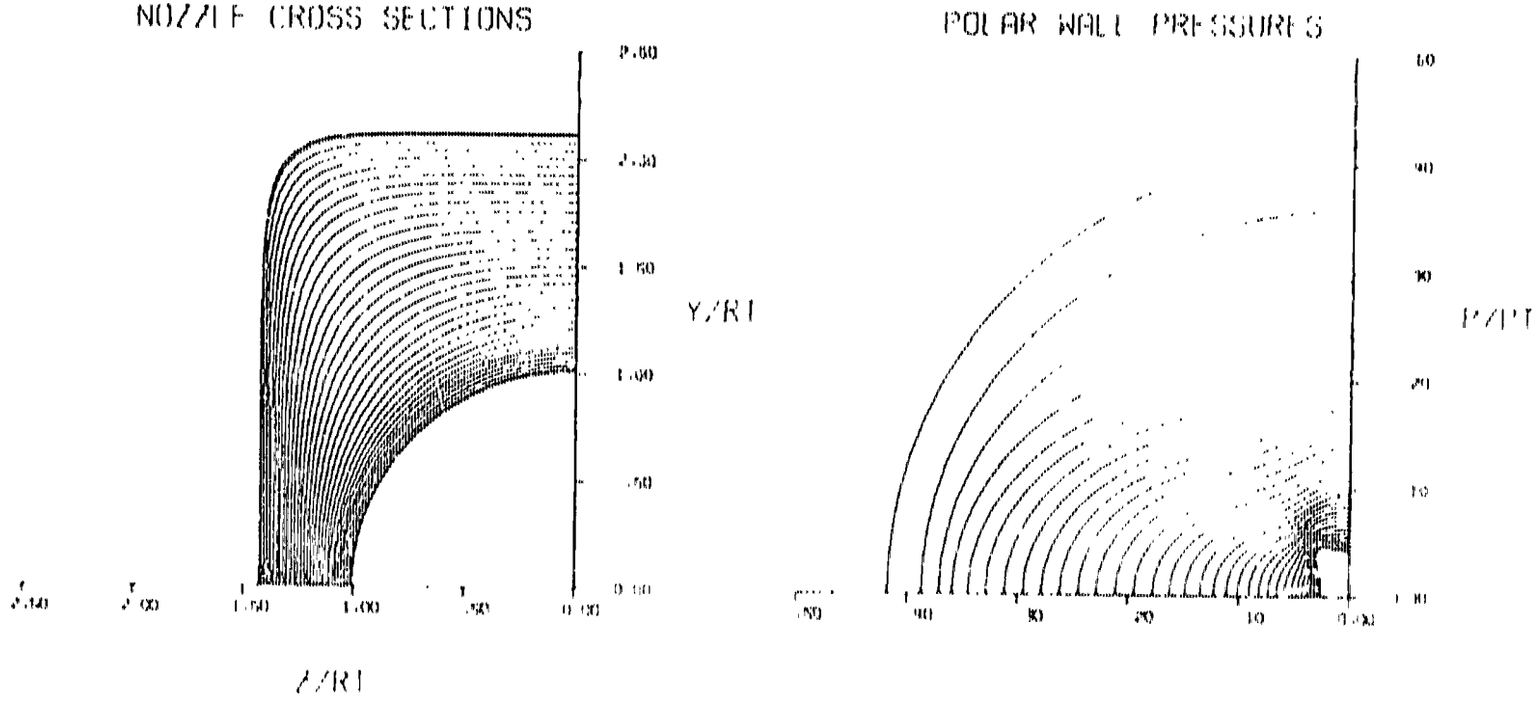

FIGURE 20. WALL PRESSURES FOR SUPER-ELLIPTICAL NOZZLE

pronounced three-dimensional flow effects are present. Note that the highest pressures in the exit plane are in the corner while the lowest pressures occur at the minor axis intercept. A prediction based on a longitudal two-dimensional expansion area ratio would produce just the opposite result. Again the rather complex three-dimensional character of the flow is evident.

4. NONSYMMETRIC INLET FLOW

The case of nonsymmetric inlet flow into an axisymmetric nozzle was investigated in order to illustrate the application of the method to a current engineering problem. Nonsymmetric inlet flow is frequencly encountered in solid rocket motors having asymmetric grain configurations or multiple nozzle aft closures. The asymmetric inlet flow results in misalignment of the thrust axis and is a source of dispersion in unguided rockets.

A nonsymmetric inlet flow was generated, for the purpose of these calculations, by superimposing two one-dimensional source flows, one located symmetrically and the other one offset from the axis. The two source flows were superimposed on the initial-value surface by using periodic weighting functions. The symmetric source was weighted by the factor $\sin^2[(\pi/2)\ (R/R_T)]$ and the asymmetric source was weighted by $\cos^2[(\pi/2)\ (P/R_T)]$, where R is the radial distance from the axis and R_T is the maximum radius, i.e., the radius of the nozzle wall at the initial-value surface. The geometry of the double source model is illustrated in Figure 21. The periodic weighting functions produce the desirable result that the flow is everywhere tangent to the nozzle boundary and has the character of the offset source at the center of the flow.

The Mach number at the center of the initial value surface was 1.05 and the half-angle of the symmetric source was 5 degrees. The offset angle of the second source was also 5 degrees. The total area ratio of the nozzle was 13.3. Figure 22 shows the wall pressure ratios calculated at the upper and lower wall intersections with the plane of symmetry as a function of nozzle length. Note the reversal in relative magnitudes which occurs approximately midway down the nozzle.

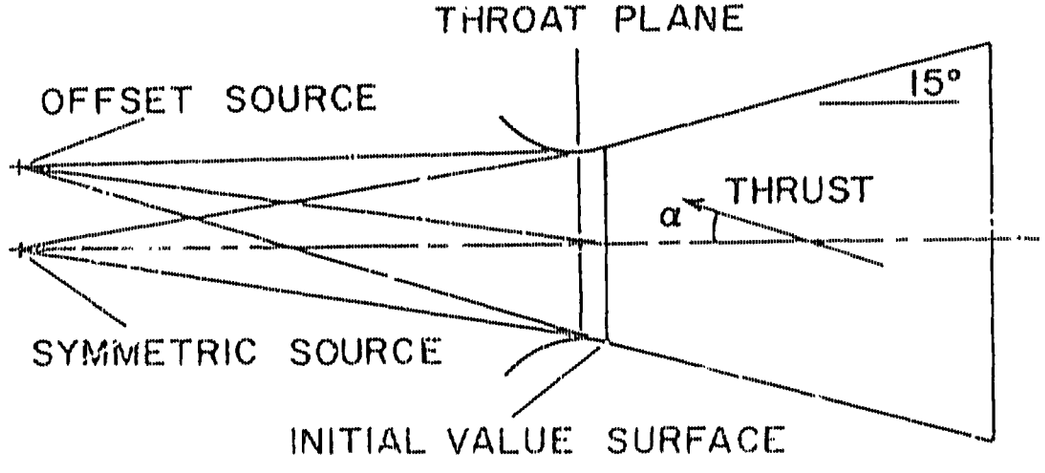

FIGURE 21. DOUBLE SOURCE SKEWED-INLET MODEL

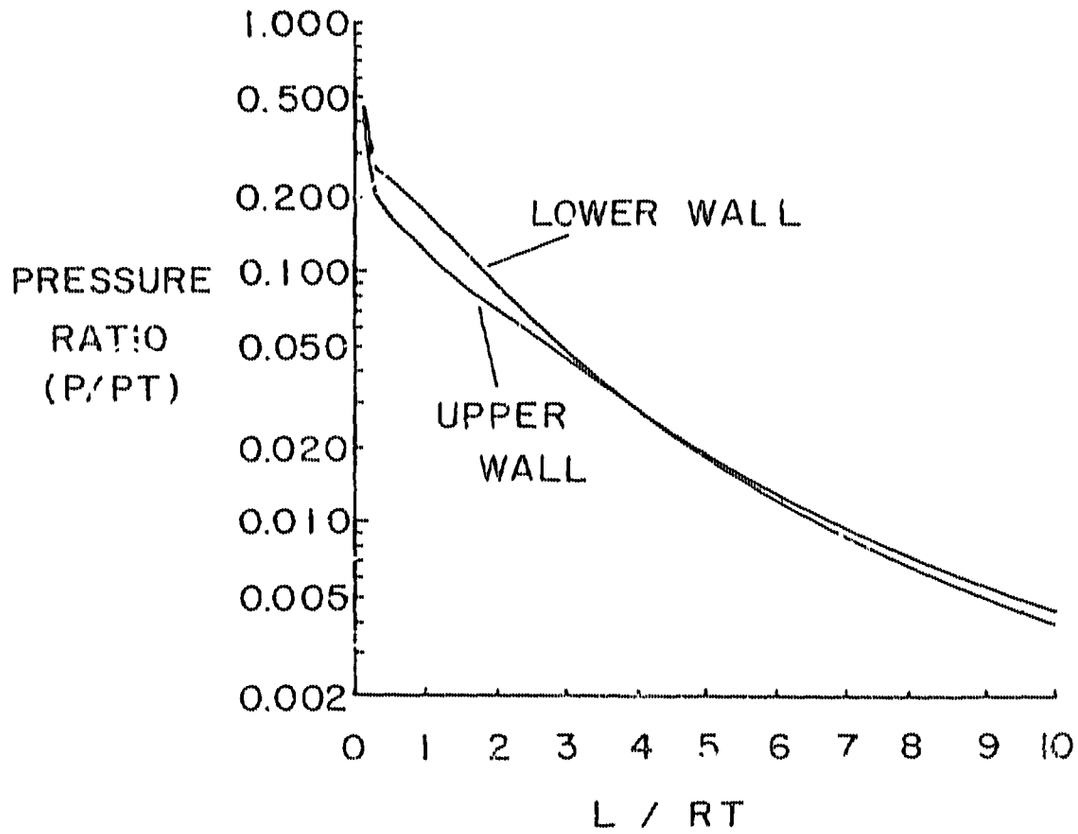

FIGURE 22. SKEWED-INLET WALL PRESSURES

The angle of thrust misalignment, α, is presented in Figure 23 as a function of nozzle length. The results show the damped periodic variation. Although the results show one thrust reversal, the period of such reversals increases greatly with the degree of expansion and a considerably longer nozzle would be required to obtain a null misalignment. The frequency of such reversals is a function of the cone angle or the rate of expansion.

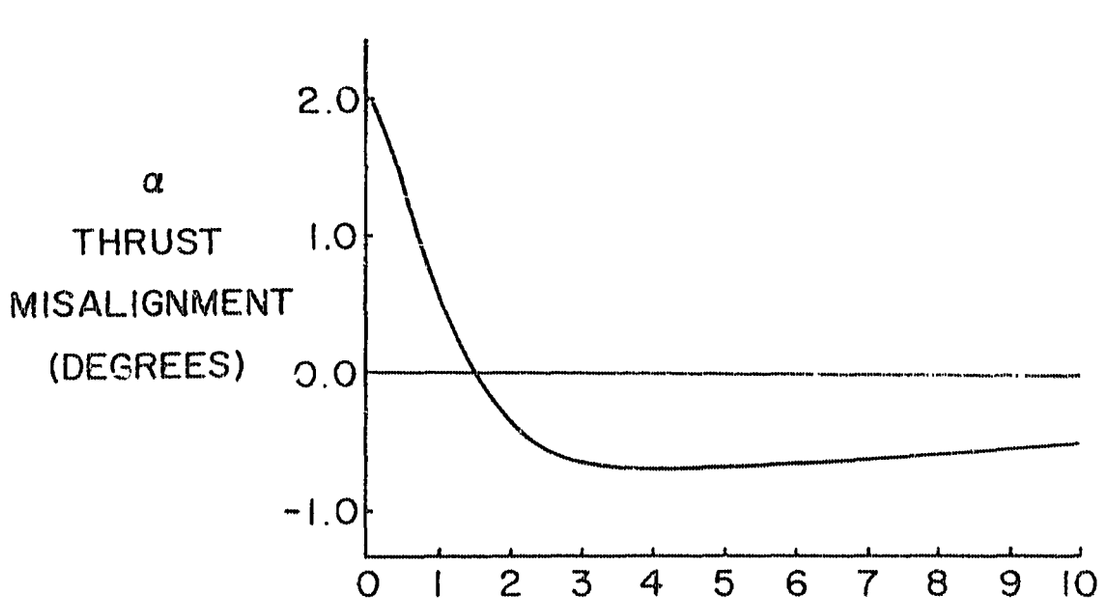

FIGURE 23. SKEWED-INLET THRUST MISALIGNMENT

SECTION IX

CONCLUSIONS

A method of characteristics numerical integration scheme for the governing equations of motion of three-dimensional supersonic flow has been developed and shown to produce results having second-order accuracy. The technique has been applied to several thrust nozzle problems and has produced highly satisfactory results. The culmination of this research (i.e., the theoretical development of the scheme, development of the necessary numerical techniques and the integration of these into an algorithm for internal supersonic flows) is a production type computer program suitable for application to a wide variety of supersonic nozzle problems. The success of the method in this application indicates that the method could be profitably applied to a wide range of other supersonic flow problems, such as supersonic aircraft inlets, supersonic external flow around yawed axisymmetric bodies and supersonic flow around bodies of arbitrary cross-section.

The results of this research indicate that the extra complexity required to maintain second-order accuracy is entirely justified. The ease with which boundary conditions are incorporated into the numerical algorithm is a definite advantage, unique to characteristic methods, over ordinary finite difference schemes. The development of a method of characteristics scheme is certainly more costly in time of development and complexity, but the results justify the efforts.

Although a general study of three-dimensional supersonic flows was not a part of this research per se, the sample cases which were computed permit one general conclusion. The structure of three-dimensional flows, even modestly three-dimensional, is quite complex, and in none of the cases analyzed would a psuedo three-dimensional technique which neglects cross flows have been adequate to predict the true nature of the flow.

REFERENCES

1. Thompson, H. D., Ransom, V. H., Hoffman, Joe D., et al., "An Analytical Study of the Scramjet Exhaust Expansion System, Part I, Final Technical Report for Period 1 September 1966 to 31 August 1967," AFAPL-TR-67-142 Part I, November 1967.

2. Hoffman, Joe D., Thompson, H. D., et al., "An Analytical Study of the Scramjet Exhaust Expansion System, Part II, Final Technical Report for Period 1 September 1967 to 31 August 1968," AFAPL-TR-67-142 Part II, November 1968.

3. Courant, R., Friedrichs, K. O., and Lewy, H., "Uberdie partiellen Differenzialgleichungen der mathematisehen Physik," Math. Ann. 100, 32-74 (1928).

4. Hahn, Susan G., "Stability Criteria for Difference Schemes," Commun. Pure Appl. Math., Vol. XI, 243-255 (1958).

5. Hele, H. and Leigh, D. C., "Stability of the Numerical Solution of Hyperbolic Partial Differential Equations in Three Independent Variables Using the Method of Characteristics," Dept. of Aerospace and Mechanical Sciences Rept. 705, Princeton Univ., October 1964.

6. Hele, H. and Leigh, D. C., "Numerical Stability of Hyperbolic Equations in Three Independent Variables," AIAA J. 3, 1099-1103 (1965).

7. Massau, J., Memorie sur l'integration graphique des equations aux derivees partielles, F. Meyer-VanLou, Ghent (1899).

8. Rusanov, V. V., "The Characteristics of General Equations of Gas Dynamics," LRG-65-T-38 From: Zhurnal Vychislitel'noi matematiki: matematicheskoi fiziki, 3, 3, 508-527 (1963), Translated by Trirogoff, K. N., Literature Research Group, Aerospace Library Services, Aerospace Corp., San Bernardino, Calif.

9. Fowell, L. R., "Flow Field Analysis for Lifting Re-Entry Configurations by the Method of Characteristics," IAS Paper 61-208-1902, June 13-16, 1961.

10. Thompson, H. D., "Analysis of Three-Dimensional Flow in Rocket Motor Nozzles," Report No. TM-54-1, Jet Propulsion Center, Purdue University, February 1964.

11. Strom, C. R., "The Method of Characteristics for Three-Dimensional Steady and Unsteady Reacting Gas Flows," Ph.D. Thesis, University of Illinois, January 1965.

12. Butler, D. S., "The Numerical Solution of Hyperbolic Systems of Partial Differential Equations in Three Independent Variables," Proceedings of the Royal Society of London, 255A, 232 (1960).

13. Chu, C. W., Niemann, A. F., Powers, S. A., "Calculation of Multiple Rocket Engine Exhaust Plumes by the Method of Characteristics," Part I of AIAA Paper No. 66-651, June 1966.

14. Chu, C. W., "Compatibility Relations and a Generalized Finite Difference Approximation for Three-Dimensional Steady Supersonic Flow," AIAA J. 5, 493-500 (1967).

15. Sauerwein, H., "Numerical Calculations of Arbitrary Multidimension and Unsteady Flows by the Method of Characteristics," Aerospace Report No. TR-669 (S6815-71)-2, May 1966 (AD 633-958.).

16. Thornhill, C. K., "The Numerical Method of Characteristics for Hyperbolic Problems in Three Independent Variables," ARC Report and Memorandum No. 2615, September 1948.

17. Sauerwein, H. and Sussman, M., "Numerical Stability of the Three-Dimensional Method of Characteristics," AIAA J. 2, 387-389 (1964).

18. Moeckel, W. E., "Use of Characteristic Surfaces for Unsymmetrical Supersonic Flow Problems," NACA TN 1849, March 1949.

19. Ferrari, C., "Determination of the Pressure Exerted on Solid Bodies of Revolution with Pointed Noses Placed Obliquely in a Stream of Compressible Fluid at Supersonic Velocity," R.T.P. Translation No. 1105, M.A.P.

20. Titt, Edwin W., "An Initial-Value Problem for all Hyperbolic Partial Differential Equations of Second Order with Three Independent Variables," Annals of Mathematics, Vol. 40, No. 4, October 1939.

21. Coburn, N. and Dolph, C. L., "The Method of Characteristics in the Three-Dimensional Stationary Supersonic Flow of a Compressible Gas," Procedures of the First Symposium on Applied Mathematics, American Mathematical Society, 1949.

22. Holt, M., "The Method of Characteristics for Steady Supersonic Rotational Flow in Three Dimensions," Journal of Fluid Mechanics 1, 409 (1956).

23. Sauer, R., "Practical Numerical Methods of Three-Dimensional Supersonic Flow," Technical (Final) Report Contract No. AF61 (052)-377, June 1961 (AD 264817).

24. Sauer, R., "The Method of Finite Differences for the Initial-Value Problem," Numerische Mathematik, 5, 55-67 (1963), (Translation by Trirogoff, K. N., Literature Research Group, Aerospace Library Services, Aerospace Corporation, San Bernardino, California).

25. Holt, M., "Recent Contributions to the Method of Characteristics for Three-Dimensional Problems in Gas Dynamics," Report prepared for Space General Corporation, El Monte, California, Feb. 26, 1963.

26. Holt, M., "The Method of Near Characteristics for Unsteady Flow Problems in Two Space Variables," Institute of Engineering Research, University of California Report No. AS-63-2, June 1963, Contract Nonr -222 (79).

27. Moretti, Gino, "Three-Dimensional Supersonic Flow Computations," AIAA J. 1, 2192-2193 (1963).

28. Moretti, G. et al., "Supersonic Flow About General Three-Dimensional Blunt Bodies," Technical Report No. ASD-TR-61-727 Volumes I, II and III, General Applied Science Laboratory, October 1962, Contract No. AF 33 (616)-7721.

29. Rakich, J., "Three-Dimensional Flow Calculations by the Method of Characteristics," AIAA J. 5, 1906-1908, (1967).

30. Rakich, J., and Cleary, J. W., "Theoretical and Experimental Study of Supersonic Steady Flow Around Inclined Bodies of Revolution," AIAA Paper No. 69-187, January 1969.

31. Sauerwein, H., "The Calculation of Two- and Three-Dimensional Inviscid Unsteady Flows by the Method of Characteristics," Ph.D. Thesis, MIT, June 1964.

32. Sauerwein, H., 'A General Numerical Method of Characteristics," Report No. TDR-469 (S5855-80)-1, Aerospace Corp., Dec. 1964, Contract No. AF 04 (695)-469.

33. Sauerwein, H., "A General Numerical Method of Characteristics," AIAA Paper No. 65-25, January 1965.

34. Tsung, C. C., "Study of Three-Dimensional Supersonic Flow Problems by a Numerical Method Based on the Method of Characteristics," Ph.D. Thesis, University of Illinois, 1961.

35. Reed, V. L., "Characteristic Relations of Compressible Flow with Three Independent Variables," Brown Engineering Company Inc., Technical Note R-40, March 1963.

36. Reed, V. L., "The Numerical Analysis of Three Independent Variable Characteristic Formulations of Compressible Flow Problems," Research Laboratories of Brown Engineering Company, Inc., May 1964, Contract NAS8-5289.

37. Reed, V. L., "Generalized Three Independent Variable Characteristics Computer Program," Brown Engineering Company Inc., TR R-66-2, 3 January 1966.

38. Pridmore Brown, B. N. and Franks, W. J., "A Method of Characteristics Solution in Three Independent Variables," ARL 65-124, June 1965.

39. Elliott, L. A., "Shock Fronts in Two-Dimensional Flow," Proc. Roy. Soc., A 267, 558 (1962).

40. Richardson, D. J., "The Solution of Two-Dimensional Hydrodynamic Equations by the Method of Characteristics," Methods in Computational Physics, Ed. Alder, B, Vol. III, 1964.

41. Hartree, D. R., "Some Practical Methods of Using Characteristics in the Calculation of Nonsteady Compressible Flow," U.S. Atomic Energy Commission Report No. AECU-2713, 1953.

42. Richtmeyer, R. D., Difference Methods for Initial Value Problems, Interscience Publishers, Inc., New York (1957).

43. Forsythe, G. E., and Wasow, W. R., Finite Difference Methods for Partial Differential Equations, Wiley, New York (1960).

44. Thommen, H. U. and D'Attorre, L., "Calculation of Three-Dimensional Supersonic Flowfields by a Finite Difference Method," General Dynamics/Astronautics Report GDA-ERR-AN539, September 1964.

45. Thommen, H. U. and D'Attorre, L., "Calculation of Steady, Three-Dimensional Supersonic Flow Fields by a Finite Difference Method," AIAA Paper No. 65-26, January 1965.

46. D'Attorre, L., Nowak, G., and Thommen, H. U., "An Inviscid Analysis of the Plume Created by Multiple Rocket Engines and a Comparison with Available Schlieren Data, Part II: A Finite Difference Method," AIAA Paper No. 66-651, June 1966.

47. Lax, P. D. and Wendroff, B., "Systems of Conservation Laws," Comm. Pure Appl. Math., Vol. XII, 217-237 (1960).

48. Babenko, K. I., et al., "Three-Dimensional Flow of Ideal Gas Past Smooth Bodies," Science Publishing House, Moscow, 1964. (NASA TT F380) April 1966.

49. Hadamard, J., "Lectures on Cauchy's Problem in Linear Partial Differential Equations," Yale University Press, New Haven (1923).

50. Courant, R. and Hilbert, D., Methods of Mathematical Physics, Volume II, Interscience Publishers, Inc., New York (1962).

51. McConnell, A. J., Applications of Tensor Analysis, Dover Publications Inc., New York (1957).

52. Bulter, D. S., Private Communication, October 1968.

APPENDIX A

GENERAL THEORY OF QUASI-LINEAR HYPERBOLIC PARTIAL DIFFERENTIAL EQUATIONS

1. GENERAL

The problem of obtaining the "general solution," i.e., the totality of all solutions of a system of partial differential equations, hardly every occurs. Usually a specific solution is singled out by imposing further conditions which the solution must satisfy. For three independent variables these conditions usually refer to two-dimensional surfaces on which the solution is further constrained. These constraints can appear as physical boundaries, initial data, or as discontinuity surfaces which bound domains within which the solution is to be found. The initial-value problem is known as a "Cauchy problem" and the theory of such problems has been developed by Hadamard (49), Cauchy and Kowalewsky (50), and more recently by Titt (20).

If a mathematical problem is to correspond to physical reality, the following basic requirements should be met, Ref. (50):

1) The solution must exist.
2) The solution should be uniquely determined.
3) The solution should depend continuously on the initial and boundary data (requirements of stability).

Any problem which satisfies these three requirements is considered properly posed. The problem of obtaining a solution for a system of analytic hyperbolic partial differential equations is properly posed when analytic data are specified over a space-like initial-value surface and appropriate boundary data are specified over time-like surfaces which adjoin the initial-data surface. Uniqueness and existence of the solution are, in general, only guaranteed in the small even under the excessively restrictive condition of analyticity. This is due to the fact that the possible occurrence of discontinuities (shocks) cannot be excluded a priori. However, in the event that discontinuities do appear, it is

possible to use physical arguments to select the proper solution.

The condition of analytic initial data is too restrictive for most problems of physical interest, and less restrictive conditions for a well-posed problem must be sought. The key to establishing the conditions for well-posed problems when the initial data contain discontinuities in the first and higher derivatives of the dependent variables lies in the concept of characteristic surfaces. Hyperbolic systems of partial differential equations have the property that particular linear combinations of the differential equations produce interior differential operators in manifolds of one lower dimension. These manifolds, or surfaces for three independent variables, are called characteristic and the geometry of these manifolds defines the manner in which the solution at a point depends upon the initial and boundary data.

In general, for hyperbolic systems the solution at a point does not depend upon all of the initial or boundary data, but depends upon only a portion of the data within a finite "domain of dependence". The domain of dependence of a point includes that portion of the initial data bounded by all the outermost characteristic surfaces passing through the point. Further, the characteristics are the surfaces along which discontinuities in the initial data or derivatives of the data are propagated. Courant and Hilbert (50) give proofs of existence and uniqueness of the solution in the small for quasi-linear systems with initial data having discontinuous first partial derivatives.

Solutions where the dependent variables are discontinuous in the initial data are known as "weak solutions" and the theory used to prove existence and uniqueness breaks down (50). However, in practice a solution may be obtained by treating the discontinuity surface as a boundary condition across which a jump condition is employed. In summary, the mathematical theory necessary to establish the conditions for well-posed problems is relatively complete and the major difficulties in obtaining a solution are encountered in attempts to devise numerical schemes.

2. CHARACTERISTIC SURFACES

Consider a general system of quasi-linear equations in n dependent variables and three independent variables

$$a_{\mu\nu i}\,(\partial u_\nu/\partial x_i) = b_\mu, \qquad (\mu = 1,2,..n) \tag{A-1}$$

where the $a_{\mu\nu i}$ and the b_μ are known functions of the u_ν and x_i. Here the summation convention is used unless otherwise stated and the Greek subscripts run over the range 1 to n while the Latin subscripts have the range 1 to 3. The system of equations, Eq. (A-1), is a complete set, i.e., n equations having n dependent variables, Ref. (49).

The characteristic property of hyperbolic systems of equations has great significance, not only with respect to determining the conditions for a well-posed problem, but also, with respect to devising a numerical scheme for solution of initial-value problems. Since the system of equations reduces to an interior operator on a characteristic surface, it is not possible to obtain the outer derivatives by means of the system of equations when all derivatives within the surface are known. Thus the solution could not be extended beyond such a surface by power series expansion. In addition, data may not be specified arbitrarily on such a surface but must satisfy a compatibility relation, the interior operator of the system of equations.

These special properties of hyperbolic systems can be shown by a variety of methods, some simpler than others, but all equivalent. A particular approach due to Rusanov (8) will be used here. This approach has the advantage that it yields information concerning the interdependence of the characteristic compatibility relations.

Any arbitrary set of real numbers (a_1, a_2, a_3) can be considered a vector, a_i, in the three-dimensional space under consideration and is denoted by a single Latin subscript. Let f be a function whose first partial derivatives exist. The directional differential of f along a_i, denoted by the operator $d_a f$, in terms of a parameter t is

$$d_a f = a_i(\partial f/\partial x_i)dt \tag{A-2}$$

Let the solution of the system, Eq. (A-1), exist in the neighborhood of a point x_i. These equations can be rewritten using the notation for the directional differential, Eq. (A-2), as follows:

$$d_{\vec{a}_{\mu\nu}} u_\nu = b_\mu dt, \quad (\mu = 1, 2 \ldots n) \tag{A-3}$$

where

$$d_{\vec{a}_{\mu\nu}} u_\nu = a_{\mu\nu i}(\partial u_\nu / \partial x_i) dt \tag{A-4}$$

Consider a linear combination of the n equations which is formed by the scalar product of the left eigenvector, w_μ ($\mu = 1,2 \ldots n$), and the system of equations, Eq. (A-3).

$$w_\mu d_{\vec{a}_{\mu\nu}} u_\nu = w_\mu b_\mu dt \tag{A-5}$$

Again using the notation for the directional differential, Eq. (A-5) may be written

$$d_{\vec{W}_\nu} u_\nu = B dt \tag{A-6}$$

where

$$W_{\nu i} = w_\mu a_{\mu\nu i} \tag{A-7}$$

and

$$B = w_\mu b_\mu \tag{A-8}$$

As before the repeated subscripts are summed over the appropriate range.

Equation (A-6) has the same form as any of the equations, Eq. (A-3). The directions of the vectors $W_{\nu i}$ in the space depend upon the values of w_μ (the case of all w_μ vanishing simultaneously is of no interest and is excluded). The hyperbolic character of the system of equations, Eq. (A-1), is revealed by posing the following problem: is it possible to choose the values for w_μ such that the resulting vectors $W_{\nu i}$ lie in a space of lower dimension than three, or, in other words, such that the vectors $W_{\nu i}$ would be linearly dependent? If such values for w_μ exist, then the surface which contains the vectors $W_{\nu i}$ will have the characteristic property previously discussed and the system of equations, Eq. (A-1), is an interior operator for this surface. In addition, the values of u_ν may not be

specified arbitrarily on such a characteristic surface since they must satisfy Eq. (A-6), which is called a compatibility condition.

Let n_i denote the normal vector to a characteristic surface, then the condition that all the vectors $W_{\nu i}$ lie in this surface is

$$n_i W_{\nu i} = 0, \quad (\nu = 1,2,..n) \tag{A-9}$$

Making use of Eq. (A-7), these equations can be written in terms of the coefficients of the original system of differential equations

$$n_i w_\mu a_{\mu\nu i} = (a_{\mu\nu i} n_i) w_\mu = 0, \quad (\nu = 1,2,..n) \tag{A-10}$$

where n_i and w_μ are to be determined. The equations, Eq. (A-10), are a system of homogeneous linear algebraic equations for the components of the system left eigenvector, w_μ. The condition that a nontrivial solution exists for the w_μ is that the determinant of the coefficients vanish, i.e.,

$$\det [a_{\mu\nu i} n_i] = X(n_i) \equiv 0 \tag{A-11}$$

where $X(n_i)$ is an nth order polynomial in the n_i. Equation (A-11) is called the characteristic equation and it yields a condition which must be satisfied by a normal, n_i, to a characteristic surface. If the length of the normal vector is taken to be unity, then

$$n_i n_i = 1 \tag{A-12}$$

which together with Eq. (, provides two conditions for the three components of the normal. The remaining component of the normal is arbitrary, and Eqs. (A-11) and (A-12) do not uniquely determine a particular normal but rather determine a family, or families, of characteristic normals.

The number of independent solutions for the w_μ in Eq. (A-10) corresponding to a particular normal, n_i, is determined by the rank of the coefficient matrix. In general, the number of independent nontrivial solutions, s, is given by

$$s = n - p \tag{A-13}$$

where n is the order and p the rank of the coefficient matrix. Corresponding to each independent solution for the w_μ there exists a compatibility relation. Thus there exist s independent differential compatibility relationships for each characteristic surface. The differential compatibility relations have the form

$$d\eta_\nu^{(j)} u_\nu = B^{(j)} dt \quad (j = 1, 2, ..s) \tag{A-14}$$

where

$$W_{\nu i}^{(j)} = w_\mu^{(j)} a_{\mu\nu i} \tag{A-15}$$

and

$$w_1^{(j)} .....w_n^{(j)} , \quad (j = 1, 2, ..s) \tag{A-16}$$

are the s linearly independent solutions of Eq. (A-10) for the system of left eigenvectors corresponding to a particular normal, n_i.

Any characteristic compatibility relation is a linear combination of the n original differential equations and thus the number of independent differential relationships corresponding to one or several normals cannot exceed the number of original equations, n. How many and which of the multitude of possible compatibility relations are independent may, in theory at least, be clarified by writing out the matrix of numbers, $w_\mu^{(j)}$, where the range of j is such that all independent solutions for each of the several normals to be considered are included. The rank of the matrix renders the number of independent relationships and the rows of the highest order nonzero determinant show which relationships are independent.

The matrix of numbers $w_\mu^{(j)}$, may pertain to one or several characteristic normals. It may turn out that the same differential compatibility relationship will correspond to two or more normals, and it is also possible that any of the original equations, Eq. (A-1), may be characteristic to begin with (i.e., all $a_{\mu\nu i}$ for some μ lie in one plane).

The two questions which are relevant to the formulation of numerical schemes can be summarized as follows:

1) Can there exist n real and independent compatibility relationships for the system of equations, Eq. (A-1), which can be used to replace the system at a point?

2) Given several characteristic normals, which of the corresponding compatibility relationships are independent?

These questions are investigated for the equations of motion for stationary supersonic flow in Appendix D.

3. CONE OF NORMALS AND CHARACTERISTIC CONOID

The left side of the characteristic equation, Eq. (A-11), is the determinant of an nth order matrix, and thus is an nth order polynomial in the three components of the unit normal, (n_1, n_2, n_3). Equation (A-12) provides one condition for determination of the two degrees of freedom of the normal. One degree of freedom remains such that an nth order family of normals is obtained. The elements of the family of normals so obtained define a conical surface called the cone of normals.

The case in which the cone of normals degenerates into two nonintersecting cones is of particular interest in gas dynamics. The characteristic determinant, Eq. (A-11), in this case factors into the product of a symmetric quadratic factor and a linear factor repeated n-2 times, i.e.,

$$X = A_{ij} n_i n_j (L_k n_k)^{n-2} = 0 \qquad \text{(A-17)}$$

where $A_{ij} = A_{ji}$. Equation (A-17) is satisfied if either of the factors vanish. The first factor yields the equation for a family of normals whose endpoints lie on the surface of a quadratic cone, while the second factor yields the equation for a family of normals whose endpoints all lie in a plane normal to the direction L_k.

In gas dynamics the cone of normals is usually defined as only the quadratic cone generated by the elements corresponding to all the unit normals which satisfy the quadric equation

$$A_{ij} n_i n_j = 0 \qquad \text{(A-18)}$$

The characteristic surfaces which correspond to each of the elements of this cone of normals form a curved conical envelope which is called the

characteristic conoid. The curves of contact between the characteristic surfaces and the conoid are called bicharacteristics. The tangent planes to each of the characteristic surfaces form a conical envelope consisting of straight elements which is called the characteristic cone. The geometric relationship between these conical surfaces is illustrated in Figure A-1.

The equation for the characteristic cone, which is required for development of numerical methods for solution, is the reciprocal cone to the cone of normals. In order to obtain the reciprocal cone, consider the particular unit normal vector, n_i,

$$x_i = x_i^0 + \zeta n_i \,, \qquad (i = 1,2,3) \tag{A-19}$$

where x_i^0 $(i = 1,2,3)$ are the coordinates of the vertex of the cone of normals and ζ is an arbitrary length along the normal. If the components of the unit normal, n_i, are eliminated from Eq. (A-18) by means of Eq. (A-19), the equation for the surface of the cone of normals is obtained

$$A_{ij}(x_i - x_i^0)(x_j - x_j^0) = 0 \tag{A-20}$$

The equation of a plane tangent to the cone of normals at any point x_i^1 lying on the surface of the cone, Ref. (51), is given by

$$A_{ij}(x_i^1 - x_i^0)(x_j - x_j^0) = 0 \tag{A-21}$$

The direction numbers of the normal to the tangent plane, defined by Eq. (A-21), are

$$A_{ij}(x_i^1 - x_i^0), \qquad (j = 1,2,3) \tag{A-22}$$

The reciprocal cone is generated by the normals to all possible planes tangent to the cone of normals at the vertex, x_i^0. An equation for the reciprocal cone can be written in general as

$$a_{ij}\gamma_i\gamma_j = 0 \tag{A-23}$$

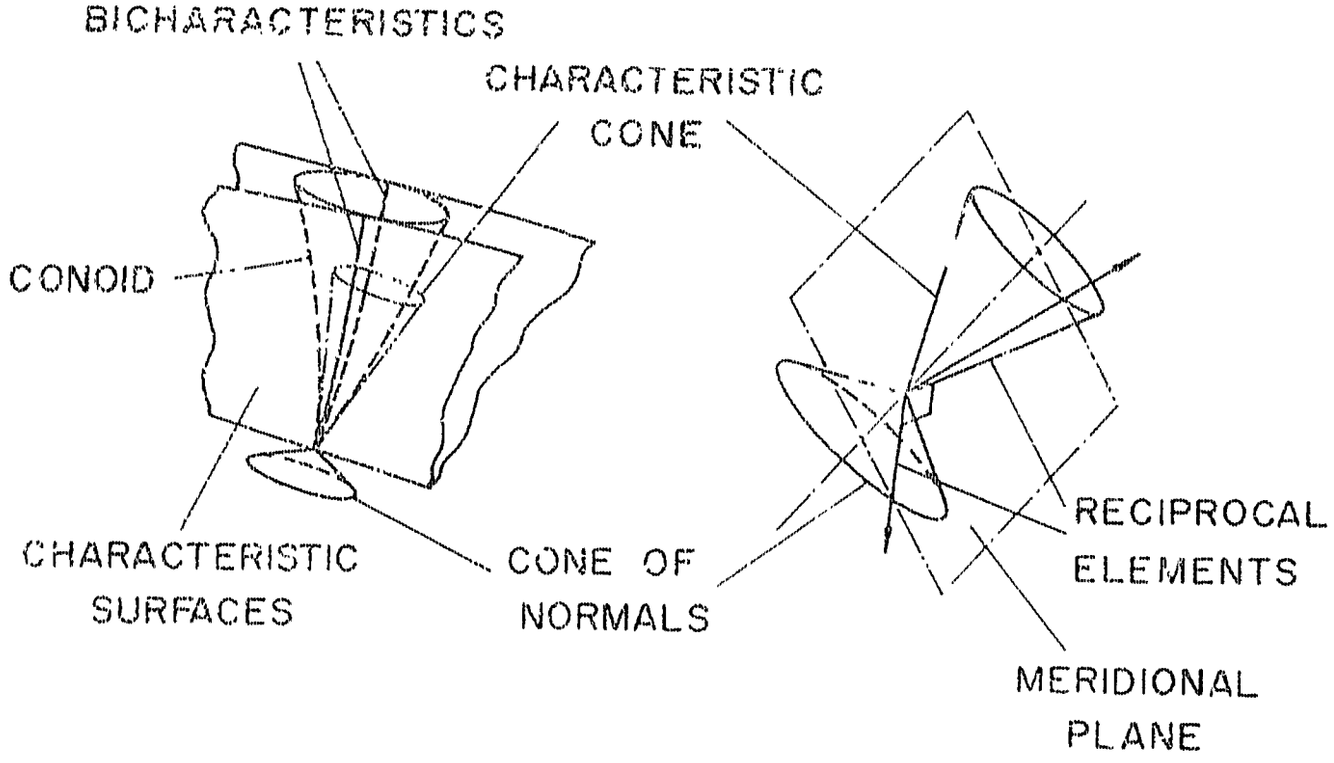

FIGURE A-I. GEOMETRY OF CHARACTERISTIC SURFACES AND CONES

where the v_i (i = 1,2,3) are the components of any versor of the cone. The parametric equations for an element of the cone can be written as

$$(x_i - x_i^0) = \zeta v_i \,, \qquad (i = 1,2,3) \tag{A-24}$$

where ζ is an arbitrary length. Any versor, v_i, of the cone is by definition proportional to the direction ratios of the normal to the corresponding tangent plane of the cone of normals, Eq. (A-22). Thus

$$v_j = \theta A_{ij}(x_i^1 - x_i^0) \tag{A-25}$$

where θ is a constant of proportionality. Substitution of Eq. (A-25) for the v_i into Eq. (A-23) and the fact that the point x_i^1 is an arbitrary point on the surface of the cone of normals yields the result

$$a_{ij}A_{ni}A_{mj}(x_n - x_n^0)(x_m - x_m^0) = 0 \tag{A-26}$$

When this result is compared with the equation for the cone of normals, Eq. (A-20), an identity is obtained

$$a_{ij}A_{ni}A_{mj} = A_{mn} \tag{A-27}$$

This identity is satisfied since the matrix A is symmetric if the matrix a has the values

$$a = \frac{A^+}{|A|} = A^{-1} \tag{A-28}$$

where A^+ denotes the adjoint matrix, and $|A|$ denotes the determinsant of the matrix A. Thus the matrix $[a_{ij}]$ is simply the inverse of the matrix $[A_{ij}]$ and is denoted $[A_{ij}^{-1}]$. The equation for the characteristic cone can now be written

$$A_{ij}^{-1}(x_i - x_i^0)(x_j - x_j^0) = 0 \tag{A-29}$$

A differential element of this cone coincides with the characteristic conoid and has the equation

$$A_{ij}^{-1}\, dx_i dx_j = 0 \qquad \text{(A-30)}$$

This result will be of further use in the development of a numerical technique for solution of the system of equations, Eq. (A-1).

4. GENERAL FORM OF THE COMPATIBILITY RELATION

The system of equations, Eq. (A-1), reducesto an interior differential operator on a characteristic surface. Data may not be prescribed arbitrarily on a characteristic surface since the interior operator, or compatibility condition, must be satisfied. The compatibility relations involve directional differentiation in a space of one lower dimension than the original system of equations and, therefore, are very useful in the development of a numerical scheme.

Consider a transformation of coordinates by simple rotation from the coordinates x_i to a new system x_i' with direction ratios $(\partial x_i'/\partial x_j)$. The x_3' direction will be chosen as the direction normal to a characteristic surface, so that

$$(\partial x_3'/\partial x_i) = n_i$$

The system of equations, Eq. (A-1), under this transformation becomes

$$a_{\mu\nu j}(\partial x_i'/\partial x_j)(\partial u_\nu/\partial x_i') = b_\mu, \quad (\mu = 1,2,..n) \qquad \text{(A-31)}$$

If Eq. (A-31) is multiplied by the left eigenvector, w_μ $(\mu = 1,2,..n)$, defined by Eq. (A-10), then an equivalent form of the compatibility condition, Eq. (A-6), is obtained.

$$w_\mu a_{\mu\nu j}(\partial x_i'/\partial x_j)(\partial u_\nu/\partial x_i') = w_\mu b_\mu \qquad \text{(A-32)}$$

The x_3' direction was chosen as the direction normal to a characteristic surface so that Eq. (A-10) is satisfied, i.e.,

$$w_\mu a_{\mu\nu i}(\partial x_3'/\partial x_i) = w_\mu a_{\mu\nu i} n_i \equiv 0 \qquad \text{(A-33)}$$

Thus Eq. (A-32) is seen to reduce to differentiation with respect to only two independent variables, x_1' and x_2', and can be written

$$w_\mu a'_{\mu\nu 1}(\partial u_\nu/\partial x_1') + w_\mu a'_{\mu\nu 2}(\partial u_\nu/\partial x_2') = w_\mu b_\mu \qquad (A\text{-}34)$$

where

$$a'_{\mu\nu i} = a_{\mu\nu j}(\partial x_i'/\partial x_j) \qquad (A\text{-}35)$$

Equation (A-34) is the general form of the compatibility relation which must be satisfied by the values of the dependent variables, u_ν ($\nu = 1,2,..n$), on a particular characteristic surface having unit normal, n_i, and corresponding left eigenvector w_μ ($\mu = 1,2,..n$). The compatibility relation can be more simply written as

$$E_\nu(\partial u_\nu/\partial x_1') + F_\nu(\partial u_\nu/\partial x_2') = 0 \qquad (A\text{-}36)$$

where the coefficients E_ν and F_ν ($\nu = 1,2,..n$) will depend upon the particular choice for the x_1' and x_2' directions, the only restriction being that they be two independent directions within the characteristic surface corresponding to the unit normal, n_i.

APPENDIX B

THE GENERAL NUMERICAL METHOD

1. REMARKS

D. S. Butler (12) has developed a method having second-order accuracy for integration of special systems of quasi-linear hyperbolic partial differential equations. The method, as developed, is restricted to systems of equations for which the characteristic determinant reduces to a quadratic factor and a repeated linear factor.

The original development by Butler, reported in Ref. (12), is very abbreviated and for this reason the development is repeated here in greater detail. In general, Butler's approach contains several very clever and unique ideas which make it not only academically interesting, but also a very promising numerical scheme.

2. PARAMETERIZATION OF THE BICHARACTERISTICS

It is assumed that the characteristic determinant of the system, Eq. (A-11) of Appendix A, factorizes into a symmetric quadratic factor and a repeated linear factor, i.e.,

$$\det [a_{\nu\nu i} n_i] = (L_k n_k)^{n-2} A_{ij} n_i n_j \qquad (B\text{-}1)$$

where n_i $(i = 1,2,3)$ are the components of the unit normal to a characteristic surface and $A_{ij} = A_{ji}$. Either of the factors of Eq. (B-1) can be required to vanish in order to satisfy the characteristic condition and thus two families of characteristic surfaces result. The first family consists of all surfaces having a unit normal orthogonal to the direction L_i $(i = 1,2,3)$, i.e., all surfaces for which L_i is a tangent vector. The second family of characteristic surfaces consists of all surfaces having unit normals which satisfy the equation for the quadric cone obtained by equating the second factor of Eq. (B-1) to zero, i.e.,

$$A_{ij} n_i n_j = 0 \qquad \text{(B-2)}$$

In Appendix A it was shown that the characteristic surfaces of this second type form a curved conical envelope called a characteristic conoid. The equation for a differential element of the conoid was shown to be

$$A_{ij}^{-1}\, dx_i dx_j = 0 \qquad \text{(B-3)}$$

Bicharacteristics are defined as the lines of contact between the characteristic surfaces and the characteristic conoid (i.e., the elements of the conoid). The family of characteristic surfaces corresponding to the linear factor of Eq. (B-1) can be considered to generate a degenerate conical envelope which simply consists of the line segment having the direction ratios L_i. The bicharacteristics of this family of characteristic surfaces all coincide with this line segment. The bicharacteristics of the family of characteristic surfaces corresponding to the quadratic factor of Eq. (B-1) are the elements of the quadric conoid, Eq. (B-3).

Differential segments of the bicharacteristic curves can be expressed parametrically in terms of the direction ratios of the elements of the respective cones. For the linear factor the degenerate cone has only one distinct element and therefore the parametric equations for all bicharacteristics of this type are

$$dx_i = L_i\, dt\,, \qquad (i = 1,2,3) \qquad \text{(B-4)}$$

where t is a parameter proportional to length along the curve.

The bicharacteristics of the second family, corresponding to the quadratic factor of Eq. (B-1), can be likewise expressed parametrically except that a single infinity of elements of the quadric cone exist. Butler (12) introduced the following bicharacteristic parametization for this family

$$dx_i = (\lambda_i + \mu_i \cos\theta + \nu_i \sin\theta)dt\,, \qquad (i = 1,2,3) \qquad \text{(B-5)}$$

where θ is a parameter corresponding to a particular element of the cone and has the range $0 \leq \theta < 2\pi$. The reference vector set of the

parametization, λ_i, μ_i and ν_i, must satisfy the quadric equation, Eq. (B-3). Substitution of the parametric representation, Eq. (B-5), into Eq. (B-3) yields the result

$$A_{ij}^{-1}\,(\lambda_i\lambda_j + 2\lambda_i\mu_j\cos\theta + 2\lambda_i\nu_j\sin\theta + \mu_i\mu_j\cos^2\theta + 2\mu_i\nu_j\cos\theta\sin\theta + \nu_i\nu_j\sin^2\theta)\,(dt)^2 = 0 \qquad \text{(B-6)}$$

which is satisfied identically if the vectors, λ_i, μ_i and ν_i, are chosen such that

$$-A_{ij}^{-1}\,\lambda_i\lambda_j = A_{ij}^{-1}\,\mu_i\mu_j = A_{ij}^{-1}\,\nu_i\nu_j \qquad \text{(B-7)}$$

and

$$A_{ij}^{-1}\,\lambda_i\mu_j = A_{ij}^{-1}\,\lambda_i\nu_j = A_{ij}^{-1}\,\mu_i\nu_j = 0 \qquad \text{(B-8)}$$

The conditions expressed by Eq. (B-8) produce the result that the reference vector set, λ_i, μ_i and ν_i, are mutual conjugate diameters of the quadric cone, Ref. (51). If λ_i, μ_i and ν_i are chosen as the coordinate axes for a rectilinear transformation of coordinates, then the fact that they are mutual conjugate diameters is sufficient to ensure that the quadric equation for the cone is reduced to canonical form, i.e.,

$$\bar{a}_{11}(d\bar{x}_1)^2 + \bar{a}_{22}(d\bar{x}_2)^2 + \bar{a}_{33}(d\bar{x}_3)^2 = 0 \qquad \text{(B-9)}$$

where the bar denotes values referenced to the transformed coordinates. The equations for a rectilinear transformation having the endpoints of the vectors λ_i, μ_i and ν_i as unit points are

$$dx_i = \lambda_i d\bar{x}_1 + \mu_i d\bar{x}_2 + \nu_i d\bar{x}_3 \qquad (i = 1,2,3) \qquad \text{(B-10)}$$

and the corresponding transformed equation for the quadric cone, Eq. (B-3), is

$$A_{ij}^{-1}\lambda_i\lambda_j(d\bar{x}_1)^2 + A_{ij}^{-1}u_iu_j(d\bar{x}_2)^2 + A_{ij}^{-1}v_iv_j(d\bar{x}_3)^2 = 0 \qquad (B\text{-}11)$$

The normalization conditions, Eq. (B-7), which are assumed for the reference vector set, produce a particularly simple canonical form for the transformed quadric equation

$$-(d\bar{x}_1)^2 + (d\bar{x}_2)^2 + (d\bar{x}_3)^2 = 0 \qquad (B\text{-}12)$$

This is the equation for a real cone completely enclosing the $\bar{x}_1$ axis, i.e., the λ_i direction. Thus the conditions, Eq. (B-7), ensure that the vector λ_i lies interior to the quadric cone. There are an infinity of transformations which will reduce the equation of a quadric cone to canonical form and, therefore, λ_i is permitted to be any vector interior to the cone. This degree of freedom in the choice of λ_i will be required at a latter stage of the numerical development in order to ensure that the compatibility relations for the system of differential equations can be placed in a particular form.

3. GENERAL FORM OF THE COMPATIBILITY RELATIONS

The compatibility relations which exist for characteristic surfaces corresponding to the quadratic factor of the characteristic determinant, Eq. (A-11) of Appendix A, can now be expressed in terms of the parametization for the bicharacteristics, Eq. (B-5). The equation for a differential element of the plane tangent to the quadric cone and corresponding to a particular bicharacteristic direction, Eq. (B-5), is obtained from Eq. (B-3) for the quadric cone, Ref. (51), and has the form

$$A_{ij}^{-1}(\lambda_i + u_i\cos\theta + v_i\sin\theta)dx_j = 0 \qquad (B\text{-}13)$$

The unit normal to this differential tangent plane element coincides with the characteristic normal so that

$$n_i = A_{ij}^{-1}(\lambda_j + u_j\cos\theta + v_j\sin\theta)/N\ , \qquad (i = 1,2,3) \qquad (B\text{-}14)$$

where N is the magnitude of the normal to the differential element

$$N = [A_{ij}^{-1}(\lambda_i + \mu_i\cos\theta + \nu_i\sin\theta)A_{kj}^{-1}(\lambda_k + \mu_k\cos\theta + \nu_k\sin\theta)]^{1/2} \tag{B-15}$$

The bicharacteristic direction, Eq. (B-5), lies in the characteristic surface element and is orthogonal to the unit normal. A second independent direction, which lies within the characteristic surface element, is selected in order to obtain a particular form for the compatibility relation. The second direction is

$$m_i = \nu_i\cos\theta - \mu_i\sin\theta \tag{B-16}$$

The orthogonality of this direction to the unit normal, Eq. (B-14), can be verified by direct calculation and the use of Eqs. (B-7) and (B-8).

The directions x_1' and x_2' in the general compatibility relation, Eq. (A-36) of Appendix A, are any two independent directions in a characteristic surface. Therefore, if the x_1' direction is chosen as the bicharacteristic direction and the x_2' direction as the independent direction defined by Eq. (B-16), then the partial derivatives of the general compatibility relation can be written as directional derivatives in terms of the partial derivatives with respect to the original coordinate system, i.e.,

$$A_\nu(\lambda_i + \mu_i\cos\theta + \nu_i\sin\theta)(\partial u_\nu/\partial x_i) = B + C_\nu(\nu_i\cos\theta - \mu_i\sin\theta)(\partial u_\nu/\partial x_i) \tag{B-17}$$

where the coefficients A_ν, B and C_ν are functions of θ, u_ν and x_i. Butler (52) obtained the functional dependence of the coefficients A_ν, B and C_ν on θ, by first considering the case for n = 3 (i.e., three dependent variables and a system of three equations) and writing out Eq. (B-17) for the values $\theta = 0, \pi/2, \pi$ and $3\pi/2$, i.e.,

$$A_\nu(0)(\lambda_i + \mu_i)(\partial u_\nu/\partial x_i) = B(0) + C_\nu(0)\nu_i(\partial u_\nu/\partial x_i) \tag{B-18}$$

$$A_\nu(\pi/2)(\lambda_i + \nu_i)(\partial u_\nu/\partial x_i) = B(\pi/2) - C_\nu(\pi/2)\mu_i(\partial u_\nu/\partial x_i) \qquad \text{(B-19)}$$

$$A_\nu(\pi)(\lambda_i - \mu_i)(\partial u_\nu/\partial x_i) = B(\pi) - C_\nu(\pi)\nu_i(\partial u_\nu/\partial x_i) \qquad \text{(B-20)}$$

$$A_\nu(3\pi/2)(\lambda_i - \nu_i)(\partial u_\nu/\partial x_i) = B(3\pi/2) + C_\nu(3\pi/2)\mu_i(\partial u_\nu/\partial x_i) \qquad \text{(B-21)}$$

Each of these equations can be considered to be formed by taking linear combinations of the original n equations. Therefore, there exists a linear combination of the four equations which is an identity. Suppose α, β, γ and δ are a set multipliers for Eqs. (B-18), (B-19), (B-20) and (3-21), respectively, which, when the products are summed, yields the identity. Then since the vectors λ_i, μ_i and ν_i are independent, the coefficients of each of the directional derivatives $\lambda_i(\partial u_\nu/\partial x_i)$, $\mu_i(\partial u_\nu/\partial x_i)$ and $\nu_i(\partial u_\nu/\partial x_i)$ and the constant terms in the identity must vanish. This yields the four relations

$$\alpha A_\nu(0) + \beta A_\nu(\pi/2) + \gamma A_\nu(\pi) + \delta A_\nu(3\pi/2) = 0 \qquad \text{(B-22)}$$

$$\alpha A_\nu(0) + \beta C_\nu(\pi/2) - \gamma A_\nu(\pi) - \delta C_\nu(3\pi/2) = 0 \qquad \text{(B-23)}$$

$$-\alpha C_\nu(0) + \beta A_\nu(\pi/2) + \gamma C_\nu(\pi) - \delta A_\nu(3\pi/2) = 0 \qquad \text{(B-24)}$$

$$\alpha B(0) + \beta B(\pi/2) + \gamma B(\pi) + \delta B(3\pi/2) = 0 \qquad \text{(B-25)}$$

In addition, any three of the equations, Eqs. (B-18) through Eq. (B-21), are equivalent to the original system of differential equations and therefore must have the same characteristic surfaces, i.e., the corresponding compatibility relations must have the same directions of differentiation as Eq. (B-17). Therefore, it is necessary that the coefficients of the directional derivatives, $(\lambda_i + \mu_i\cos\theta + \nu_i\sin\theta)(\partial u_\nu/\partial x_i)$ and $(\nu_i\cos\theta - \mu_i\sin\theta)(\partial u_\nu/\partial x_i)$, in the identity obtained by summing Eqs. (B-18) through Eq. (B-21) must also vanish. Equation (B-22) ensures vanishing of the coefficient of the first directional derivative, while the requirement that the coefficient of the second vanish yields the additional

relation

$$\alpha C_\nu(0) + \beta C_\nu(\pi/2) + \gamma C_\nu(\pi) + \delta C_\nu(3\pi/2) = 0 \qquad \text{(B-26)}$$

The relations, Eqs. (B-22) through (B-26), are not only conditions on the multipliers, α, β, γ and δ, but also are conditions on the dependence of A_ν, B and C_ν on the parameter θ.

Since any three of the Eqs. (B-18) through (B-21) are equivalent to the original system of differential equations, then an appropriate combination of these same equations will yield the general compatibility relation, Eq. (B-17). Note that the sine and cose dependence of the directional derivatives in Eq. (B-17) must be produced as a result of the multipliers used in the linear combination of Eqs. (B-18) through (B-21). Butler (52) obtained the general compatibility relation and the functional dependence of A_ν, B and C_ν on θ by using the multipliers, $\alpha(1 + 2\cos\theta)$, $\beta(-1-2\sin\theta)$, $\gamma(1-2\cos\theta)$ and $\delta(-1+2\sin\theta)$, for Eqs. (B-18) through (B-21) respectively. This particular combination has the necessary property that, for $\theta = 0, \pi/2, \pi$ and $3\pi/2$, Eqs. (B-18) through (B-21) are reproduced and the correct θ dependence of the directional derivatives results.

After considerable rearrangement of terms in the summed equation and use of Eqs. (B-22), (B-23), (B-24), (B-25) and (B-26), the general form of Eq. (B-17) is obtained in which the coefficients A_ν, B and C_ν have the following form

$$A_\nu = A_{1\nu} + A_{2\nu}\cos\theta + A_{3\nu}\sin\theta \qquad \text{(B-27)}$$

$$B = B_1 + B_2\cos\theta + B_3\sin\theta \qquad \text{(B-28)}$$

$$C_\nu = C_{1\nu} + C_{2\nu}\cos\theta + C_{3\nu}\sin\theta \qquad \text{(B-29)}$$

where

$$A_{1\nu} = \alpha A_\nu(0) - \beta A_\nu(\pi/2) + \gamma A_\nu(\pi) - \delta A_\nu(3\pi/2) \qquad \text{(B-30)}$$

$$A_{2\nu} = 2[\alpha A_\nu(0) - \gamma A_\nu(\pi)] \qquad \text{(B-31)}$$

$$A_{3\nu} = -2[A_\nu(\pi/2) - \delta A_\nu(3\pi/2)] \tag{B-32}$$

$$C_{1\nu} = 2[\alpha C_\nu(0) + \gamma C_\nu(\pi)] \tag{B-33}$$

$$C_{2\nu} = -f_{3\nu} \tag{B-34}$$

$$C_{3\nu} = A_{2\nu} \tag{B-35}$$

$$B_1 = \alpha B(0) - \beta B(\pi/2) + \gamma B(\pi) - \delta B(3\pi/2) \tag{B-36}$$

$$B_2 = 2[\alpha B(0) - \gamma B(\pi)] \tag{B-37}$$

$$B_3 = -2[\beta B(\pi/2) - \delta B(3\pi/2)] \tag{B-38}$$

4. THE GENERAL FORM OF THE NONCHARACTERISTIC RELATION

In the development of the second-order numerical scheme, Butler (12, 52) employed the parametric form of a particular noncharacteristic linear combination of the system of differential equations. This relation is obtained by the same techniques which were used to obtain the general form for Eq. (B-17). Equations (B-18) through (B-21) are again summed, only this time using the respective multipliers α, $-\beta$, γ and $-\delta$. After rearrangement and use of Eqs. (B-22) through (B-26), the following relation is obtained;

$$A_{1\nu}\,\lambda_i(\partial u_\nu/\partial x_i) = B_1 + C_{2\nu}\,\nu_i(\partial u_\nu/\partial x_i) - C_{3\nu}\,\mu_i(\partial u_\nu/\partial x_i) \tag{B-39}$$

where the coefficients $A_{1\nu}$, B_1, $C_{2\nu}$ and $C_{3\nu}$ are the same as the corresponding coefficients in Eq. (B-17). The reason that this particular differential relation is required will become apparent in the course of development of the numerical integration technique contained in the following section.

5. THE SECOND-ORDER NUMERICAL SCHEME

The two equations, Eqs. (B-17) and (B-39), form the basis for a numerical scheme which can be used to compute the values of u_ν correct to second order at any point $x_i = \alpha_i$ when the u_ν are given on some space-like surface $f(x_i) = 0$ near the point α_i. The solution can then be extended to a family of surfaces of which $f = 0$ is a typical member.

Consider Eqs. (B-17) and (B-39) written in operator notation for the directional differentials along a bicharacteristic direction, ξ_i, and the λ_i direction

$$A_{\nu}\, d_{\tilde{\xi}} u_\nu = [\bar{B} + C_\nu(\nu_1 \cos\theta - u_1 \sin\theta)\,(\partial u_\nu/\partial x_1)]dt \tag{B-40}$$

and

$$A_{1\nu}\, d_{\tilde{\lambda}} u_\nu = [B_1 + [C_{2\nu} u_1 - C_{3\nu} \nu_1]\,(\partial u_\nu/\partial x_1)]dt \tag{B-41}$$

where the subscript $\tilde{\xi}$ denotes the bicharacteristic direction, ξ_i, corresponding to the value of θ at the point under consideration and the subscript $\tilde{\lambda}$ denotes the λ_i direction. The bicharacteristics through the point α_i intersect the space-like surface $f = 0$ at finite values of t, so that the bicharacteristic corresponding to a particular value of θ and starting at $x_i = \alpha_i$ meets $f(x_i) = 0$ at $t = -t(\theta)$. Equation (B-17) written in finite difference form correct to second order in t, using the modified Euler scheme, is

$$\bar{A}_\nu[u_\nu(\alpha) - u_\nu(f)] = \{\bar{B} + \tfrac{1}{2}[S(\alpha) + S(f)]\}\, t(\theta) + O(t^3) \tag{B-42}$$

where

$$S = C_\nu(\nu_1 \cos\theta - u_1 \sin\theta)\,(\partial u_\nu/\partial x_1) \tag{B-43}$$

$$\bar{A}_\nu = (1/2)\,[A_\nu(\alpha) + A_\nu(f)] \tag{B-44}$$

$$\bar{B} = (1/2)\,[B(\alpha) + B(f)] \tag{B-45}$$

The notation $u_\nu(\alpha)$ is used to denote the values of the dependent variables at the point $x_i = \alpha_i$ and $u_\nu(f)$ to denote the values of the dependent

variables at the point at which the bicharacteristic corresponding to e meets the surface $f(x_i) = 0$. The quantities $u_\nu(\alpha)$ and $u_\nu(f)$ appearing in Eq. (B-42) are assumed correct to order $O(t^2)$ while the quantities $\tilde{A}_\nu$, B, $S(\alpha)$ and $S(f)$ need only be correct to order $O(t)$.

The vector λ_i at a point can be any direction interior to the characteristic cone; thus the direction of λ_i is now chosen such that $C_{1\nu} = 0$ throughout the (x_1,x_2,x_3) space.* The vanishing of $C_{1\nu}$ is essential to the procedure used to eliminate the terms containing derivatives at the solution point α_i. In Eq. (B-42), $S(\alpha)$ now becomes

$$S(\alpha) = (C_{2\nu}\cos\theta + C_{3\nu}\sin\theta)\,(\nu_i\cos\theta - \mu_i\sin\theta)\,(\partial u_\nu/\partial x_i) \qquad (B\text{-}46)$$

where $C_{2\nu}$, $C_{3\nu}$, $\nu_i(\partial u_\nu/\partial x_i)$ and $\mu_i(\partial u_\nu/\partial x_i)$ are evaluated at $x_i = \alpha_i$.

One degree of freedom remains in the choice of the reference vector set λ_i, μ_i and ν_i. Butler (12) does not state how this degree of freedom should be fixed in the general case, but arbitrarily uses the base coordinate directions to fix the directions of μ_i and ν_i in the case of two-dimensional, unsteady flow, and for three-dimensional, steady flow states that this degree of freedom "...should be specified so that α_i and β_i and their derivatives vary smoothly along the bicharacteristics and streamline used in the integration." Here the α_i and β_i for the specific cases differ only in magnitude from the μ_i and ν_i in the general case. At this point, the present development deviates from that by Butler and an alternate choice is made for the remaining degree of freedom in μ_i and ν_i. This degree of freedom is used to select an orientation of the reference vector set such that the value of θ is a constant along the length of a bicharacteristic. This approach has the advantage that fewer terms remain in the final form of the difference equations and the numerical scheme for establishing the orientation of the μ_i and ν_i reference vectors is simpler than the corresponding scheme required in Butler's approach to establish the variation of θ along a bicharacteristic.

In order to achieve second-order accuracy, the term $S(\alpha)$ appearing in Eq. (B-42) must be evaluated at the unknown point. Note that the

*It is not clear that this should always be possible and Butler (12, 52) states this without proof. However, this condition can be satisfied for the cases of three-dimensional, steady flow, and two-dimensional, unsteady flow.

equation for S, Eq. (B-43), contains the partial derivatives of the dependent variables at the unknown point α. In any explicit scheme these derivatives cannot be evaluated until after an entire solution surface has been calculated. Therefore, in order to achieve second-order accuracy, the terms containing derivatives at the solution point, α, must be eliminated. The fact that an infinite family of bicharacteristics exist at each point can be used with weighted integration to eliminate the terms containing derivatives.

Consider Eq. (B-42) weighted by the factors $[f(\alpha)\cos\theta]/t(\theta)$ and $[f(\alpha)\sin\theta]/t(\theta)$ and integrated with respect to θ between the limits 0 to 2π to give

$$u_\nu(\alpha)\int_0^{2\pi}\frac{f(\alpha)\,\bar{A}_\nu\cos\theta\,d\theta}{t(\theta)} = \int_0^{2\pi}\frac{f(\alpha)u_\nu(f)\,\bar{A}_\nu\cos\theta\,d\theta}{t(\theta)} + \int_0^{2\pi} f(\alpha)\,\bar{B}\cos\theta\,d\theta + O(f^3(\alpha)) \quad \text{(B-47)}$$

and

$$u_\nu(\alpha)\int_0^{2\pi}\frac{f(\alpha)\,\bar{A}_\nu\sin\theta}{t(\theta)}\,d\theta = \int_c^{2\pi}\frac{f(\alpha)u_\nu(f)\,\bar{A}_\nu\sin\theta}{t(\theta)}\,d\theta + \int_0^{2\pi} f(\alpha)\,\bar{B}\sin\theta\,d\theta + O(f^3(\alpha)) \quad \text{(B-48)}$$

where $f(\alpha)$ denotes the value of the function for the surface $f(x_i) = 0$ evaluated at the point α_i, thus the ratio $f(\alpha)/t = O(1)$. Note that Eqs. (B-47) and (B-48) do not contain any terms involving derivatives of the dependent variables and the integrals are in terms of known quantities on the initial value surface $f(x_i) = 0$.

A third finite difference relation is obtained from the differential noncharacteristic relation, Eq. (B-41) applied along the curve $dx_i = \lambda_i dt$. Suppose that the curve $dx_i = \lambda_i dt$ meets the surface $f(x_i) = 0$ at $t = -h$, and denote the value of u_ν at this point by $u_\nu(h)$. The modified Euler integration scheme is used to obtain a finite difference approximation for Eq. (B-41) which is correct to $O(h^2)$. This gives

$$A^*_{1\nu}[u_\nu(\alpha) - u_\nu(h)] = \{B^*_1 + (1/2)[(C_{2\nu\nu_i} - C_{3\nu\mu_i})(\partial u_\nu/\partial x_i)]_{x_i=\alpha_i}$$

$$+ 1/2[(C_{2\nu\nu_i} - C_{3\nu\mu_i})(\partial u_\nu/\partial x_i)]_{t=-h}\} h + O(h^3) \qquad \text{(B-49)}$$

where

$$A^*_{1\nu} = (1/2)[A_{1\nu}(\alpha) + A_{1\nu}(h)] \qquad \text{(B-50)}$$

$$B^*_1 = (1/2)[B_1(\alpha) + B_1(h)] \qquad \text{(B-51)}$$

Equation (B-42) is weighted by the factor h/t, which is of order O(1), and integrated with respect to θ between the limits $0 \leq \theta \leq 2\pi$. Subsequently, Eq. (B-49) is multiplied by π and subtracted from the resulting integral of Eq. (B-49) to obtain

$$u_\nu(\alpha)\left[\int_0^{2\pi} \frac{h\bar{A}_\nu d\theta}{t} - \pi A^*_{1\nu}\right] = \int_0^{2\pi} \frac{hu_\nu(f)\,\bar{A}_\nu d\theta}{t} - \pi A^*_{1\nu} u_\nu(h)$$

$$- \frac{\pi h}{2}[(C_{2\nu\nu_i} - C_{3\nu\mu_i})(\partial u_\nu/\partial x_i)]_{t=-h}$$

$$+ \int_0^{2\pi} h\bar{B} d\theta - \pi h B^*_1 + O(h^3) \qquad \text{(B-52)}$$

The final three conditions obtained here, Eqs. (B-47), (B-48) and (B-52), differ from those obtained by Butler (12) by the absence of integrals involving S(f). This is a direct result of the choice for the reference vector set λ_i, μ_i, and ν_i such that θ = constant at all points along a bicharacteristic.

Equations (B-47), (B-48) and (B-52) are the necessary three independent equations for the $u_\nu(\alpha)$ when n = 3. If n > 3, it is assumed that the additional n-3 conditions can be obtained from the compatibility relations corresponding to characteristic surfaces containing the curve $dx_i = L_i dt$. None of these conditions involve derivatives of the dependent variables, u_ν, at the unknown point, $x_i = \alpha_i$, so that the modified Euler integration scheme can be used to obtain finite difference relations which can be solved simultaneously with Eqs. (B-47), (B-48) and (B-52) to obtain a solution locally correct to order $O(t^2)$.

6. SYSTEM OF REFERENCE VECTORS

The reference vector set, λ_i, μ_i and ν_i, must be established in order to evaluate the integrals appearing in Eqs. (B-47), (B-48) and (B-52). As stated previously, λ_i is chosen such that the coefficient $C_{1\nu}$ vanishes throughout the (x_1, x_2, x_3) space. In addition the vectors are required to be mutually "orthogonal" in the sense that the "scalar" products $A^{-1}_{ij}\lambda_i\mu_j$, $A^{-1}_{ij}\lambda_i\nu_j$ and $A^{-1}_{ij}\mu_i\nu_j$ vanish, Eq. (B-8). One degree of freedom remains in the choice for μ_i and ν_i and this is used to satisfy the requirement that the integrals

$$x_i - \alpha_i = \int_{0,\theta=\text{constant}}^{t} (\lambda_i + \mu_i\cos\theta + \nu_i\sin\theta)dt, \quad (i = 1,2,3) \tag{B-53}$$

for a constant value of θ define a bicharacteristic curve as a function of the parameter t. The characteristic surface element through the direction $(\lambda_i + \mu_i\cos\theta + \nu_i\sin\theta)$ at any point is given by

$$A^{-1}_{ij}\,(\lambda_j + \mu_j\cos\theta + \nu_j\sin\theta)dx_i = 0 \tag{B-54}$$

which is the equation for an element of the tangent plane in normal form. If the integral of Eq. (B-53) satisfying Eq. (B-54) is $x_i = x_i(t,\theta)$, then a differential element tangent to this surface can also be expressed as

$$dx_i = (\partial x_i/\partial\theta)d\theta + (\partial x_i/\partial t)dt \tag{B-55}$$

Substitution of this expression into Eq. (B-54) must yield an identity since the two elements coincide. Thus,

$$A^{-1}_{ij}(\lambda_j + \mu_j\cos\theta + \nu_j\sin\theta)(\partial x_i/\partial\theta)d\theta$$

$$+ A^{-1}_{ij}(\lambda_j + \mu_j\cos\theta + \nu_j\sin\theta)(\partial x_i/\partial t)dt = 0 \tag{B-56}$$

However, a curve of constant θ is a bicharacteristic so that

$$\partial x_i/\partial t = \lambda_i + \mu_i\cos\theta + \nu_i\sin\theta \tag{B-57}$$

and this, in view of the requirements on λ_i, μ_i and ν_i expressed by Eqs. (B-7) and (B-8), the second term of Eq. (B-56) vanishes identically to yield

$$A_{ij}^{-1}(\lambda_j + \mu_j\cos\theta + \nu_j\sin\theta)(\partial x_i/\partial \xi) = 0 \qquad \text{(B-58)}$$

This relation is sufficient for the determination of the remaining degree of freedom in the reference vectors μ_i and ν_i relative to a fixed reference.

7. SUMMARY

The finite difference relations which have been developed here for the general case can be used in a variety of ways to obtain a numerical algorithm. One method will be outlined here in order to illustrate the application of the equations which have been developed.

The modified Euler integration scheme is a predictor-corrector type scheme in which a system of nonlinear difference relations are solved by iteration. The values of the dependent variables, u_ν, are assumed to be known at discrete points on the initial value surface $f(x_i) = 0$, and the solution is to be extended to a set of corresponding points on a new surface $f'(x_i) = 0$ which is sufficiently close to the initial surface. The integration process is initiated by extending the curve $dx_i = L_i dt$ from a known point on the initial-value surface, $f(x_i) = 0$, to the new solution surface, $f'(x_i) = 0$, the intersection being designated a_i. The system of vectors λ_i, μ_i and ν_i at the point a_i are established so that $C_{1\nu} = 0$, the conditions given by Eqs. (B-7) and (B-8) are satisfied, and by a consistent selection for the one remaining degree of freedom. Next the intersections with the initial-value surface, $f(x_i) = 0$, of the family of bicharacteristics passing through the point a_i are found using Eq. (B-53). The single degree of freedom for the choice of the reference vectors λ_i, μ_i and ν_i along the intersection is chosen to satisfy a finite difference approximation for Eq. (B-58) relative to the vector system orientation at the point a_i. The values of the dependent variables, u_ν, and the vectors λ_i, μ_i and ν_i along the intersection with $f(x_i) = 0$ are used to evaluate the integrals which appear in Eqs. (B-47), (B-48) and (B-52). The resulting three equations along with the additional n-3

equations along the curve $dx_i = L_i dt$ can be used to solve for the n values of $u_\nu(\alpha)$.

The values of $u_\nu(\alpha)$ thus obtained are regarded as the predicted values in the modified Euler integration scheme and these values are subsequently used to repeat the entire process, using averaged coefficients, to obtain the corrected values for $u_\nu(\alpha)$. The iteration process is usually applied successively until the values of the dependent variables, $u_\nu(\alpha)$, obtained on successive iterations agree to within some tolerance consistent with the step size.

APPENDIX C

THERMODYNAMIC RELATIONS FOR A STRIATED FLOW

The working fluid of scramjet and rocket exhaust nozzle expansion systems is produced by combustion of a fuel and an oxidizer stream, each of which is uniform in composition and stagnation enthalpy. The stagnation enthalpy of the combustion products is thus a single valued function of the local oxidizer to fuel ratio. The oxidizer to fuel ratio will in general have spatial variations within the combustor and, therefore, the stagnation enthalpy and composition of the fluid will have spatial variations. However, since the flow is assumed to be inviscid and strictly adiabatic, no diffusion of species or energy occurs and, therefore, both the atomic composition and stagnation enthalpy are constant along each streamline.

In a scramjet combustor the stagnation pressure of the combustion products will in general vary from streamline to streamline due to variations in pressure and velocity of the entering air stream. In rocket systems the stagnation pressure after combustion usually can be assumed to be constant throughout the flow because of the low momentum of the entering propellants and the fact that the combustion occurs at low subsonic velocities.

The general case of combustion products having variations in both stagnation pressure and enthalpy will be considered in the thermodynamic model. The general thermodynamic relation for a mixture of gases in thermal equilibrium, but chemical nonequilibrium, is

$$Tds = dh - \frac{1}{\rho} dp - \sum_{\alpha=1}^{n} \mu_\alpha dc_\alpha \qquad (C\text{-}1)$$

where T is absolute temperature, s, h and μ_α are the intensive properties of entropy, enthalpy and chemical potential of the α species respectively, ρ is the density, p is the pressure and c_α is the mass fraction of the α species.

The system is assumed to exist in a state of "frozen" or equilibrium chemical composition. In the frozen case all the dc_s in Eq. (C-1) are zero, and for the case of chemical equilibrium, no net change in the chemical potential of the system occurs. In both of these cases the last term in Eq. (C-1) is identically zero and the general thermodynamic relation becomes

$$Tds = dh - \frac{1}{\rho} dp \qquad (C-2)$$

Equation (C-2) is the general thermodynamic relation for a simple system and the specification of any two thermodynamic properties is sufficient to determine the state of the system and thus all remaining thermodynamic properties. Equation (C-2) is for a closed system and applies to a particle of fluid as opposed to a fixed point in space. In this sense the velocity of the system is not a thermodynamic variable and cannot be determined from a knowledge of the thermodynamic state. Thus, the stagnation state and corresponding properties cannot be determined unless the system velocity is specified in addition to two thermodynamic variables. It follows that specification of any two thermodynamic variables of the stagnation state, in addition to the system velocity, is sufficient to determine the thermodynamic state of the system.

The stagnation enthalpy of a fluid which is generated by combustion of oxidizer and fuel streams, each having constant enthalpies, is a single valued function of the oxidizer to fuel ratio. If the fluid has spatial variations in the oxidizer to fuel ratio then corresponding variations in the stagnation enthalpy will also be present. For steady flow of an inviscid fluid, no diffusion of energy or mass can occur so that the oxidizer to fuel ratio and, therefore, stagnation enthalpy are constant along the streamlines of the flow. The values of the oxidizer to fuel ratio and the corresponding stagnation enthalpy are assumed to be constant at the values which prevail after completion of the mixing and combustion process. Once expansion of the flow begins the dissipative processes very rapidly die out (i.e., the gradients decrease except in a thin layer near the boundaries) and the inviscid assumption is a good approximation.

The fact that the stagnation properties are constant along the streamlines of a steady and inviscid flow can also be shown by less

heuristic arguments. Consider the mechanical energy equation which is obtained by summing the Euler momentum equations after multiplying each by the corresponding velocity component, i.e.,

$$u_i u_j(\partial u_i/\partial x_j) + (u_i/\rho)(\partial p/\partial x_i) = 0 \qquad (C\text{-}3)$$

or, in terms of the square of the velocity magnitude, $q^2 = u_i u_i$,

$$(u_i/2)(\partial q^2/\partial x_i) + (u_i/\rho)(\partial p/\partial x_i) = 0 \qquad (C\text{-}4)$$

The first law of thermodynamics, applied to a particle of inviscid fluid, yields

$$du = \delta q - pd(1/\rho) \qquad (C\text{-}5)$$

where u is the internal energy and δq the heat transfered to the system. The flow is assumed to be strictly adiabatic so that $\delta q = 0$. Thus,

$$du + pd(1/\rho) = 0 \qquad (C\text{-}6)$$

or in terms of enthalpy

$$dh - (1/\rho)dp = 0 \qquad (C\text{-}7)$$

When the differentials of the dependent variables are expressed in terms of the coordinates for a point fixed in space, Eq. (C-7) becomes

$$u_i(\partial h/\partial x_i) - (u_i/\rho)(\partial p/\partial x_i) = 0 \qquad (C\text{-}8)$$

Addition of Eqs. (C-4) and (C-8) yields the result

$$u_i(\partial h/\partial x_i) + (u_i/2)(\partial q^2/\partial x_i) = 0 \qquad (C\text{-}9)$$

or in terms of the stagnation enthalpy, $H = h + q^2/2$,

$$u_i(\partial H/\partial x_i) = 0 \qquad (C\text{-}10)$$

Although it has not been shown here, this result is also true when discontinuous changes in the flow properties are present (i.e., shocks).

In the absence of discontinuities in the fluid properties, the first law result, Eq. (C-7), can be combined with the general thermodynamic equation, Eq. (C-2), to yield

$$Tds = 0 \tag{C-11}$$

or in terms of the coordinates of a point fixed in space for steady flow

$$u_i(\partial s/\partial x_i) = 0 \tag{C-12}$$

Thus, the entropy is a constant along the streamlines of the flow.

One further property, the stagnation pressure, can also be shown to be conserved along streamlines for continuous property variations. This can be seen by placing Eq. (C-4) in the form of a directional derivative, along a streamline, of a single property.

$$u_i(\partial/\partial x_i)[p + \tfrac{1}{2}\int \rho d(q^2)] = 0 \tag{C-13}$$

If the integral in Eq. (C-13) is taken along a streamline such that the entropy is constant and the limits of integration are from a point on the streamline where the velocity is zero to a point where the velocity is equal to q, then, by definition, the conserved property in Eq. (C-13) is the stagnation pressure, i.e.,

$$P = p + \int_{x_i^1(q=0)}^{x_i^2(q=q)} \rho(\partial \hat{r}/\partial x_i)dx_i \tag{C-14}$$

and Eq. (C-13) becomes

$$u_i(\partial P/\partial x_i) = 0 \tag{C-15}$$

Thus, the steady, inviscid and strictly adiabatic assumptions yield the result that the stagnation enthalpy, entropy and stagnation pressure are all constant along streamlines for continuous property variations.

The fluid generated by combustion at a given oxidizer to fuel ratio forms a simple system in the stagnation state and, therefore, specification of any two stagnation properties is sufficient to determine the stagnation state. The stagnation enthalpy of a fluid generated by combustion of constant property oxidizer and fuel streams is a unique function of the oxidizer to fuel ratio. The remaining properties of the stagnation state depend in addition on the pressure and velocity after combustion. Once the stagnation state is established, the properties along a particular streamline are one-dimensional functions and can be characterized by specification of one additional property such as pressure, density or flow velocity.

For this development of the numerical method of characteristics, the stagnation enthalpy and stagnation pressure were chosen as the two variables necessary to define the stagnation state, and the static pressure was chosen to further define the variation of the system properties with expansion. Thus, the properties density and speed of sound, expressed functionally, are

$$\rho = \rho(p, P, H) \tag{C-16}$$

$$a = a(p, P, H) \tag{C-17}$$

For a thermally and calorically perfect gas the relations for density and speed of sound are analytic expressions. For multi-component systems, having either frozen or equilibrium chemical composition with real gas effects, the density and speed of sound must be obtained by means of thermo-chemical calculations. The relations, Eqs. (C-16) and (C-17), are usually obtained as tabular functions. Continuous functions must be generated either by interpolation or by fitting empirical expressions to the tabular data.

APPENDIX D

CHARACTERISTIC RELATIONS FOR STEADY SUPERSONIC FLOW

1. GENERAL

The general theory for the application of the method of characteristics to systems of hyperbolic partial differential equations is discussed in Appendix A. The application of these methods to the system of equations for a three-dimensional stationary supersonic flow is presented herein. The characteristic compatibility relations corresponding to all families of characteristic surfaces are developed. These include all the characteristic relations required for application of the general numerical method. The possible combinations of independent compatibility relations which are equivalent to the original system of partial differential equations are also investigated.

2. EQUATIONS OF MOTION

The equations of motion for stationary supersonic flow in three-dimensions consist of the three Euler momentum equations, the continuity equation and the conservation equations for stagnation enthalpy and stagnation pressure. This system of equations, when written using the Kronecker delta and matrix notation, are easily recognized as having the same general form as the general system of quasi-linear partial differential equations discussed in Appendix A, Eq. (A-1) Using this notation the equations of motion are

$$\begin{bmatrix} \rho u_i & 0 & 0 & \delta_{1i} & 0 & 0 \\ 0 & \rho u_i & 0 & \delta_{2i} & 0 & 0 \\ 0 & 0 & \rho u_i & \delta_{3i} & 0 & 0 \\ \rho a^2 \delta_{1i} & \rho a^2 \delta_{2i} & \rho a^2 \delta_{3i} & u_i & 0 & 0 \\ 0 & 0 & 0 & 0 & u_i & 0 \\ 0 & 0 & 0 & 0 & 0 & u_i \end{bmatrix} \begin{Bmatrix} \frac{\partial u_1}{\partial x_i} \\ \frac{\partial u_2}{\partial x_i} \\ \frac{\partial u_3}{\partial x_i} \\ \frac{\partial p}{\partial x_i} \\ \frac{\partial P}{\partial x_i} \\ \frac{\partial H}{\partial x_i} \end{Bmatrix} = 0 \qquad \text{(D-1)}$$

where u_1, u_2, u_3 are the three components of velocity, p is the pressure, P the stagnation pressure, H the stagnation enthalpy, ρ the density and a the speed of sound. The three independent variables are the rectangular cartesian coordinates x_1, x_2 and x_3 and the repeated indices imply summation over the range 1 to 3.

3. CHARACTERISTIC SURFACES

The characteristic surfaces of the system, Eq. (D-1), are obtained by solving for the left eigenvector which will reduce the system to an interior operator in a space of one lower dimension, which is called a characteristic surface. Multiplication of Eq. (D-1) by the left eigenvector, $w_\mu (\mu = 1,2,\ldots 6)$, yields the single equation

$$\rho(u_i w_1 + a^2 \delta_{1i} w_4)(\partial u_1/\partial x_i) + \rho(u_i w_2 + a^2 \delta_{2i} w_4)(\partial u_2/\partial x_i)$$

$$+ \rho(u_i w_3 + a^2 \delta_{3i} w_4)(\partial u_3/\partial x_i) + (\delta_{1i} w_1 + \delta_{2i} w_2$$

$$+ \delta_{3i} w_3 + u_i w_4)(\partial p/\partial x_i) + (u_i w_5)(\partial P/\partial x_i) + (u_i w_6)(\partial H/\partial x_i) = 0 \qquad \text{(D-2)}$$

The coefficients of the derivatives in Eq. (D-2) are vectors of directional differentiation and Eq. (D-2) reduces to an interior operator if all the coefficient vectors are coplanar (i.e., if the scalar products of the coefficient vectors and a unit normal to a characteristic surface all vanish). This yields a system of six homogeneous and linear algebraic equations for the six components of the left eignevector, w_μ. The system of equations written in matrix notation is

$$\begin{bmatrix} \rho u_i n_i & 0 & 0 & \rho a^2 \delta_{1i} n_i & 0 & 0 \\ 0 & \rho u_i n_i & 0 & \rho a^2 \delta_{2i} n_i & 0 & 0 \\ 0 & 0 & \rho u_i n_i & \rho a^2 \delta_{3i} n_i & 0 & 0 \\ \delta_{1i} n_i & \delta_{2i} n_i & \delta_{3i} n_i & u_i n_i & 0 & 0 \\ 0 & 0 & 0 & 0 & u_i n_i & 0 \\ 0 & 0 & 0 & 0 & 0 & u_i n_i \end{bmatrix} \begin{Bmatrix} w_1 \\ w_2 \\ w_3 \\ w_4 \\ w_5 \\ w_6 \end{Bmatrix} = 0 \qquad \text{(D-3)}$$

where the n_i are the components of the unit normal to a characteristic surface. A nontrivial solution for the components of w_μ exists if the determinant of the coefficient matrix vanishes. This condition yields the characteristic equation for the system, i.e.,

$$\rho^3 (u_k n_k)^4 \left[u_i u_j - a^2 \delta_{ij} \right] n_i n_j = 0 \qquad \text{(D-4)}$$

Equation (D-4) has the same general form as Eq. (B-1) of Appendix B (i.e., a repeated linear factor and a quadratic factor), and therefore the general numerical method described in Appendix B can be applied to this system.

When each of the two distinct factors of Eq. (D-4) are equated to zero, the equations for two real and nonintersecting cones are obtained. The first factor yields the equation for a degenerate cone formed by all normals to the direction of the velocity, i.e., a plane normal to the

streamline. The reciprocal cone, the corresponding characteristic cone, is also degenerate and consists of the line segment tangent to the streamline.

When the second factor of Eq. (D-4) is equated to zero, a quadric equation for a right circular cone is obtained

$$[u_i u_j - a^2 \delta_{ij}] n_i n_j = 0 \qquad \text{(D-5)}$$

The cone is real for $q > a$, where q is the magnitude of velocity. This cone is called the cone of normals. The characteristic surfaces, which correspond to each of the elements of the cone of normals, form a curved conical envelope which is called the characteristic conoid. The bicharacteristics are the curves of contact between characteristic surfaces and the conoid. The tangent planes to each of these characteristic surfaces form an envelope consisting of straight elements which is called the characteristic cone. The geometric relationship between these conical surfaces is illustrated in Figure D-1.

The characteristic cone is the reciprocal cone to the cone of normals and the corresponding quadric equation is obtained by the inversion process discussed in Appendix A. The resulting quadric equation for a differential element of the characteristic cone is

$$[u_i u_j - (q^2 - a^2) \delta_{ij}] dx_i dx_j = 0 \qquad \text{(D-6)}$$

which also only represents a real cone for $q > a$. The curved cone obtained by integration of Eq. (D-6) is called the characteristic or Mach conoid, and it is the envelope formed by all characteristic surfaces of this second type which pass through each point of the space.

In summary, two families of characteristic surfaces exist. These consist of: first, all surfaces containing the velocity vector at a point, which are called stream surfaces; and second, all surfaces tangent to the characteristic conoid at a point, which are called wave surfaces.

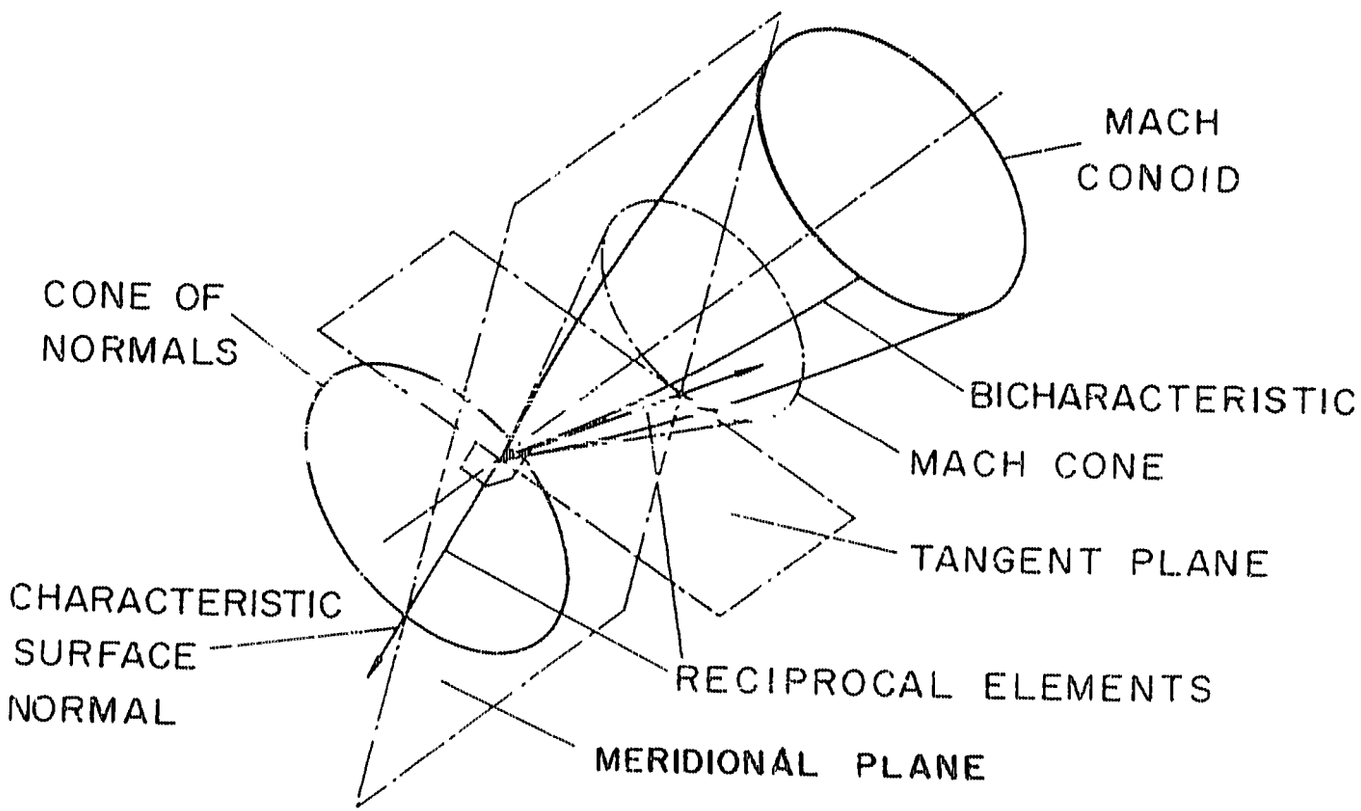

FIGURE D-1. RELATION BETWEEN CONE OF NORMALS AND MACH CONE

4. SOLUTION FOR THE LEFT EIGENVECTOR

The characteristic compatibility relation, Eq. (D-2) is an interior operator for each system left eigenvector, w_μ, obtained by solution of the homogeneous system of equations, Eq. (D-3, The solutions for the w_μ are arbitrary to within some constant factor since the system is homogeneous. Even neglecting this degree of arbitrariness, an infinite number of solutions for the w_μ are possible since two infinite families of normals, n_i, exist and each normal yields a system of equations. However, no more than six of all the possible solutions for the w_μ can be independent, since each independent solution yields a compatibility relation and the total number of independent compatibility relations cannot exceed the number of original differential equations.

The number of independent differential compatibility relations which correspond to one particular normal also is equal to the number of independent solutions for the w_μ. The general form and number of independent solutions for the w_μ corresponding to a particular normal to either of the two types of characteristic surfaces are established by consideration of the system of equations. The fifth and sixth equations of Eq. (D-1) only involve directional derivatives in the streamline direction and thus already appear in characteristic form (i.e., interior operators on stream surfaces). This fact also is evident from an examination of Eq. (D-3), because the variables w_5 and w_6 have only zero coefficients on stream surfaces and their values are thus arbitrary.

First consider the solution for w_μ on the stream surfaces. On any stream surface the normal is ortnogonal to the streamline direction, thus

$$u_i n_i = 0 \tag{D-7}$$

Equation (D-3) for this case reduces to

$$\begin{bmatrix} 0 & 0 & 0 & \rho a^2 n_1 \\ 0 & 0 & 0 & \rho a^2 n_2 \\ 0 & 0 & 0 & \rho a^2 n_3 \\ -n_1 & n_2 & n_3 & 0 \end{bmatrix} \begin{Bmatrix} w_1 \\ w_2 \\ w_3 \\ w_4 \end{Bmatrix} \tag{D-8}$$

The coefficient matrix of Eq. (D-8) is rank two, thus the number of independent solutions for the w_μ, including the variables w_5 and w_6, is four. The most obvious four independent solutions include two solutions for w_5 and/or w_6 nonzero with w_1, w_2, w_3, and w_4 zero (note that $w_4 = 0$ for all solutions), and any two independent solutions having w_4, w_5 and w_6 zero, with the components w_1, w_2 and w_3 orthogonal to the normal n_1.

Next consider the solution of Eq. (D-3) for the wave surfaces which have normals defined by the second factor of Eq. (D-4). The scalar product between the velocity vector and the unit normal to the wave surface is equal to the local speed of sound, i.e.,

$$u_i n_i = a \tag{D-9}$$

The unknown w_5 appears exclusively in the fifth equation and w_6 appears exclusively in the sixth equation of Eq. (D-3). Thus only the trivial solution $w_5 = w_6 = 0$ exists for these two elements. The system of equations for the w_μ, again omitting the equations for w_5 and w_6, is

$$\begin{bmatrix} \rho a & 0 & 0 & \rho a^2 n_1 \\ 0 & \rho a & 0 & \rho a^2 n_2 \\ 0 & 0 & \rho a & \rho a^2 n_3 \\ n_1 & n_2 & n_3 & s \end{bmatrix} \begin{Bmatrix} w_1 \\ w_2 \\ w_3 \\ w_4 \end{Bmatrix} = 0 \tag{D-10}$$

The coefficient matrix is rank three and, therefore, only one independent nontrivial solution for the w_μ exists for each wave surface normal. For the arbitrary choice $w_4 = -1$, the solution for the remaining components yields $w_1 = an_1$, $w_2 = an_2$ and $w_3 = an_3$, where n_1, n_2 and n_3 are the components of a particular wave surface normal.

5. COMPATIBILITY RELATIONS

The general forms of the differential compatibility relations which exist on each of the two families of characteristic surfaces are obtained

by evaluation of Eq. (D-2) for the independent solutions for w_μ. On the family of stream surfaces it has been shown that four independent solutions for the w_μ exist for each independent stream surface normal The two compatibility relations for the solutions w_5 or w_5 not zero with all other components zero, are

$$u_i(\partial P/\partial x_i) = 0 \tag{D-11}$$

and

$$u_i(\partial H/\partial x_i) = 0 \tag{D-12}$$

The remaining two compatibility relations, corresponding to the solutions for the w_μ having w_4, w_5 and w_6 zero and two independent sets of values for w_1, w_2 and w_3 which satisfy the requirement of orthogonality with n_i, are: for $w_1 = u_1$, $w_2 = u_2$ and $w_3 = u_3$

$$u_i u_j(\partial u_j/\partial x_i) + u_i(\partial p/\partial x_i) = 0 \tag{D-13}$$

which is Bernoulli's equation in differential form, and for $w_1 = S_1$, $w_2 = S_2$ and $w_3 = S_3$

$$\rho S_j u_i(\partial u_j/\partial x_i) + S_i(\partial p/\partial x_i) = 0 \tag{D-14}$$

where the S_i are the components of any vector orthogonal to the stream surface normal, n_i (i.e., $S_i n_i = 0$ and is independent of u_i). Equation (D-13) contains a single direction of directional differentiation, u_i, while Eq. (D-14) contains two such directions, u_i and S_i, all of which lie within the stream surface corresponding to the particular normal, n_i.

The compatibility relation for a wave surface is likewise obtained from Eq. (D-2) using the single independent solution for the left eigenvector corresponding to a particular wave surface normal

$$(u_i - an_i)(\partial p/\partial x_i) + \rho a(a\delta_{ij} - n_i u_j)(\partial u_i/\partial x_j) = 0 \tag{D-15}$$

The fact that this equation only involves directional derivatives within the wave surface can be seen by considering the scalar product between

the coefficients of the derivatives and the unit normal vector n_i (recall that the scalar product between the wave surface normal and the velocity vector is the speed of sound, $n_i v_i = a$).

Equation (D-15) contains four directions of directional differentiation, all of which lie within the wave surface having a normal n_i. It is possible to express all four directional derivatives in terms of any two independent directions within the wave surface, and by so doing, to obtain the compatibility relation in a form which by a coordinate system rotation reduces to the form of the general compatibility relation, Eq. (A-36) of Appendix A.

6. EQUIVALENT DIFFERENTIAL SYSTEMS

In the previous sections the number of independent differential compatibility relations, for a particular characteristic surface of the flow was established. However, there exists a doubly infinite number of characteristic surfaces at every point of the flow and, as noted previously, the total number of independent compatibility relations cannot exceed the number of independent differential equations which comprise the original system. Thus it is necessary to further establish which of the possible combinations of six compatibility relations are independent. These questions can be answered by examining the matrix whose rows consist of the independent solutions for the w_μ corresponding to each of the characteristic surface normals being considered. The rows of each sixth-order square matrix of rank six which can be formed from all the solutions for the w_μ will correspond to a system of independent differential compatibility relations. Although a wide variety of combinations will satisfy this requirement, some general conclusions can be drawn.

It was previously shown that on a single stream surface four independent solutions for the w_μ exist. However, w_4 is zero for all solutions and, therefore, any sixth-order matrix formed from solutions for the w_μ on stream surfaces will be at most rank five. Thus no more than five independent compatibility relations exist for any two or more independent stream surface normals.

It was also previously shown that only one independent solution for the w_μ exists for each wave surface normal. In addition w_5 and w_6 are

zero for all wave surface normals. Thus any sixth-order matrix formed from wave surface solutions for the w_μ will be at most rank four and no more than a total of four independent wave surface compatibility relations could possibly exist. However, consider the determinant of the matrix formed by four solutions for the w_μ corresponding to four independent stream surface normals (w_5 and w_6, which are identically zero, are omitted since they have no effect on the resulting rank of the matrix):

$$\begin{bmatrix} an_1^1 & an_2^1 & an_3^1 & -1 \\ an_1^2 & an_2^2 & an_3^2 & -1 \\ an_1^3 & an_2^3 & an_3^3 & -1 \\ an_1^4 & an_2^4 & an_3^4 & -1 \end{bmatrix} \tag{D-16}$$

where the superscripts denote the four independent normals. The four unit normal vectors lie on the surface of a right circular cone and therefore the end-points all lie in a common plane. If one row is subtracted from the remaining three, then the three resulting difference vectors will be coplanar and therefore dependent. The determinant, Eq. (D-16), is thus identically zero and at most only three wave surface compatibility relations are independent.

It is now clear that a complete system of six independent compatibility relations cannot exist for a single family of characteristic surfaces. The remaining question to be investigated then is under what conditions will a combination of relations on the two families of characteristics be independent. For this purpose it is again sufficient to examine the matrix whose rows consist of the w_μ corresponding to each of the characteristic relationships for the system. If all the rows of such a matrix are found to be independent, then any set of six of the w_μ rows of the matrix may be used to form a complete system. Each particular combination of compatibility relations must be examined in this way. Only a few combinations of interest will be listed here, and the interested reader is referred to the work of Rusanov (8). If p is the number of

distinct wave surfaces and q the number of stream surfaces, six independent compatibility relations are obtained for

1) $p = 3, \qquad q = 1,$

2) $p \geq 1, \qquad q = 2,$

3) $p = 2, \qquad q = 1,$

where case 3 is true only if the stream surface normal is not orthogonal to the vector defined by the difference between the two wave surface normals.

It is now clear that the original system of differential equations can be replaced by an equivalent system of equations which all have the characteristic property. In fact, a wide variety of possible choices exist and this, perhaps, helps explain the rather large number of numerical schemes which have been proposed.

The previous discussion of interdependence and equivalence of differential systems pertains only to a point in the solution space. When the differential system is replaced by a difference system, the number of independent relations required for solution will depend upon the order of the approximation. In general, first-order schemes require the same number of independent difference relations as number of independent differential relations. Higher order schemes will require additional independent relations. Some difference schemes have been used in which more than the minimum number of independent first-order difference relations are used and a solution is sought in the least squares sense. These schemes have only first-order accuracy, but may yield improved absolute accuracy and stability characteristics.

APPENDIX E

SECOND-ORDER INTEGRATION SCHEME FOR THREE-DIMENSIONAL STEADY SUPERSONIC FLOW

1. GENERAL

It is initially assumed that the dependent variables, the three velocity components, pressure, stagnation pressure, and stagnation enthalpy, are known to second-order accuracy over a space-like surface $f(x_i) = 0$ (i.e., a surface whose normal vector is everywhere interior to the wave surface cone of normals). A numerical method is required which can be used to compute the values of the dependent variables at any point $x_i(6)$ near $f(x_i) = 0$, see Figure E-1. The global solution can then be generated by successive application of the basic scheme to determine the values of the dependent variables on a family of surfaces of which $f(x_i) = 0$ is a typical member.

In Appendix B a general numerical scheme is developed in which the infinity of bicharacteristics passing through a point are used by weighted integration of the corresponding compatibility equations over all the bicharacteristics. The weighted integration must be performed numerically, which results in an excessively laborious scheme. In addition, the integration over all the bicharacteristics is not necessary in order to maintain second-order accuracy. A simpler scheme results when only the minimum number of bicharacteristics required for second-order accuracy is used. Therefore, the approach which is developed herein uses the wave surface compatibility relation applied along only four particular bicharacteristics, which is the minimum number compatible with second-order accuracy.

2. ORDER OF APPROXIMATION

Before proceeding with the development of the numerical scheme, the meaning of the order of approximation will be reviewed and clarified.

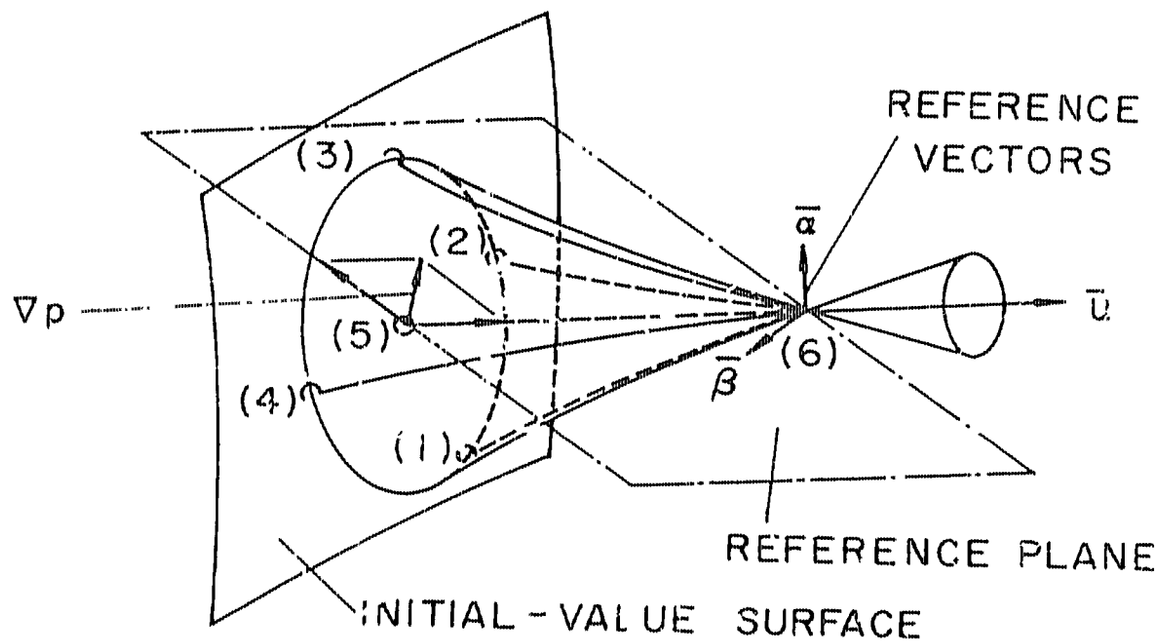

FIGURE E-1. INTERIOR POINT NETWORK

For this purpose consider a power series expansion in one independent variable of some function $p(x)$

$$p(x + \Delta x) = p(x) + (dp/dx)_x \Delta x + (d^2p/dx^2)_x (\Delta x)^2/2!$$
$$+ (d^3p/dx^3)_x (\Delta x)^3/3! \ldots + (d^np/dx^n)_x (\Delta x)^n/n!$$
$$+ (d^{n+1}p/dx^{n+1})_{x+\theta\Delta x} (\Delta x)^{n+1}/(n+1)! \qquad \text{(E-1)}$$

where $0 \leq \theta \leq 1$. If this series is terminated with the nth term, then the error in the approximation of $p(x+\Delta x)$ is defined as the absolute magnitude of the remainder, i.e.,

$$\varepsilon = \left| (d^{n+1}p/dx^{n+1})_{x+\theta\Delta x} (\Delta x^{n+1}/(n+1)!) \right| \qquad \text{(E-2)}$$

The approximation is said to be accurate to order n and the order of the error, ε, is $n + 1$. The order of the error is indicated by the ordering symbol $O(\Delta x^{n+1})$ which implies

$$\lim_{\Delta x \to 0} \left[\frac{\varepsilon}{(\Delta x)^{n+1}} \right] = K \qquad \text{(E-3)}$$

where K is a finite bound for the ratio. Clearly the error can be made as small as desired by reducing Δx if $(n+1) > 0$. However, no information regarding the actual magnitude of the error for a given value of Δx can be deduced from a statement of the order of the approximation. The order only establishes how rapidly the error will be reduced as the step size, Δx, is reduced. Thus it is possible for two different numerical schemes, each having the same order of approximation (i.e., accurate to the same order), to have different errors for equal and finite values of Δx.

The modified Euler predictor-corrector numerical integration scheme, which is used in the numerical method developed in Appendix B, has a local truncation error third order in step size or, equivalently, is accurate to second order. The number of integration steps required to advance to a fixed point in the flow is assumed to be of the order of the reciprocal of the step size (i.e., $O(\Delta x^{-1})$). Thus, the accumulated

truncation error at a fixed point is second order in step size, $O(\Delta x^2)$, and thus the overall scheme is accurate to first order in step size, $O(\Delta x)$.

3. DIFFERENCE NETWORK

The difference network for the integration process consists of segments of four bicharacteristics and the streamline through the solution point. This network is illustrated in Figure E-1 and the points at which the bicharacteristics and the streamline intersect the initial-value surface, $f(x_i) = 0$, are numbered (1) through (5) respectively. The integration process consists of the numerical construction of this network and subsequent integration of the respective differential compatibility and ordinary relations which are applied along these directions.

The family of wave surface bicharacteristic segments through a point in the flow space are represented by the parametric equations

$$dx_i = (u_i + c\alpha_i \cos\theta + c\beta_i \sin\theta)dt, \qquad (i = 1,2,3) \qquad (E\text{-}4)$$

where the u_i are the components of the velocity, α_i and β_i are unit vectors such that u_i, α_i and β_i form a right handed orthogonal system, t is a parameter proportional to length along a bicharacteristic, θ is a parameter which is constant along a bicharacteristic and ranges from 0 to 2π, and c is a velocity defined by the relation

$$c = [q^2a^2/(q^2 - a^2)]^{1/2} \qquad (E\text{-}5)$$

The parameter c can be geometrically interpreted as the velocity of divergence, relative to the flow velocity, of the surface of the Mach conoid away from the streamline.

The form of Eq. (E-4) is identical in form to that proposed by Butler (12). However, here the vectors α_i and β_i and the parameter θ are defined such that θ is a constant along a bicharacteristic. The degree of freedom in the choice of the reference vectors, α_i and β_i, is used to satisfy the requirement that the bicharacteristic be a line of contact between a characteristic surface and the Mach conoid, see Appendix B, Eq. (B-58). This is in contrast to the approach used by Butler

(12) for two-dimensional flow in which the remaining degree of freedom in the choice for α_i and β_i was fixed arbitrarily and θ was allowed to vary in order to satisfy the bicharacteristic condition. The present approach has the advantage that a considerable simplification of the numerical scheme results.

The parametric equation, Eq. (E-4), represents an element of the conoid if the pseudo "normalization" and"orthogonality" conditions, Eqs. (B-7) and (B-8) of Appendix B, are satisfied. These relations for the Mach conoid, defined by Eq. (D-6) of Appendix D, are

$$- [u_i u_j - (q^2 - a^2)\delta_{ij}]\, u_i u_j = c^2 [u_i u_j - (q^2 - a^2)\delta_{ij}]\, \alpha_i \alpha_j$$

$$= c^2 [u_i u_j - (q^2 - a^2)\delta_{ij}]\, \beta_i \beta_j \qquad \text{(E-6)}$$

$$c [u_i u_j - (q^2 - a^2)\delta_{ij}]\, u_i \alpha_j = c [u_i u_j - (q^2 - a^2)\delta_{ij}]\, u_i \beta_j$$

$$= c^2 [u_i u_j - (q^2 - a^2)\delta_{ij}]\, \alpha_i \beta_j = 0 \qquad \text{(E-7)}$$

and are satisfied for the orthonormal choice for the vectors u_i/q, α_i and β_i.

The unit normal to the Mach conoid can be expressed in terms of the parametric representation for the bicharacteristics (i.e., Eq. B-14 of Appendix B for the general case). The equation for a differential element of a plane, which is tangent to the conoid at the apex and corresponds to a particular bicharacteristic denoted by θ, is obtained from the equation for the Mach conoid, Eq. (D-6) of Appendix D, and corresponds to the general result, Eq. (B-13), of Appendix B,

$$[u_i u_j - (q^2 - a^2)\delta_{ij}](u_i + c\alpha_i \cos\theta + c\beta_i \sin\theta)dx_j = 0 \qquad \text{(E-8)}$$

This is the equation for a plane in normal form and therefore the coefficients of the displacements in the plane, dx_j, are the components of a vector normal to the plane. The unit normal vector is thus

$$n_i = [u_i u_j - (q^2 - a^2)\delta_{ij}](u_j + c\alpha_j \cos\theta + c\beta_j \sin\theta)/N \qquad \text{(E-9)}$$

where

$$N = \left\{[u_i u_j - (q^2 - a^2)\delta_{ij}](u_i + c\alpha_i \cos\theta + c\beta_i \sin\theta)x \right.$$
$$\left. [u_j u_k - (q^2 - a^2)\delta_{jk}](u_k + c\alpha_k \cos\theta + c\beta_k \sin\theta)\right\}^{1/2} \qquad \text{(E-10)}$$

When the orthonormal properties of u_i/q, α_i and β_i are employed, Eq. (E-9) for the unit normal can be reduced to the form

$$n_i = (a/c)(cu_i/q^2 - \alpha_i \cos\theta - \beta_i \sin\theta) \qquad \text{(E-11)}$$

The condition for tangency between a characteristic surface and the Mach conoid (i.e., the bicharacteristic condition) was derived for the general case in Appendix B, Eq. (B-58). The form of this relation which corresponds to the parametric form for the wave surface bicharacteristics, Eq. (E-4), and the equation for the Mach conoid, Eq. (D-6) of Appendix D, is

$$[(q^2 - a^2)\delta_{ij} - u_i u_j](u_i + c\alpha_i \cos\theta + c\beta_i \sin\theta)(\partial x_j/\partial s) = 0 \qquad \text{(E-12)}$$

An approximate numerical form of this relation is used to establish the remaining degree of freedom, relative to a fixed reference, in the choice of α_i and β_i. In Butler's proposed approach this same relation is used to determine the variation of θ along the bicharacteristic, the remaining degree of freedom in the vectors α_i and β_i being fixed arbitrarily.

The local difference network is constructed by numerical extension of the streamline from a known point on the initial-value surface to the new solution surface and the subsequent numerical extension of the four bicharacteristics back from the new point to the initial-value surface. The orientation of the reference vector set α_i and β_i is set at the new solution point and the orientation of the reference vectors in the initial-value surface is established relative to the solution point by the use of an approximate form of Eq. (E-12).

The parametric equations for a differential segment of the streamline are

$$dx_i = u_i\, dt\,, \qquad (i = 1, 2, 3) \tag{E-13}$$

where t is a parameter corresponding to time of travel of a fluid particle along the differential segment dx_i. Application of the modified Euler integration scheme yields

$$x_i(6) - x_i(5) = -(1/2)[u_i(6) + u_i(5)]t(5) + 0(t^3) \qquad (i = 1, 2, 3) \tag{E-14}$$

The numbers in parentheses refer to values at the corresponding points of the finite difference network shown in Figure E-1. The value of t(6) has been arbitrarily taken to be zero. Equations (E-14) are used to solve for the values of the two coordinates, $x_2(6)$ and $x_3(6)$, of the new point and the parameter t(5) for a specified value of the remaining coordinate of the new point, $x_1(6)$. Equations (E-14) involve the unknowns $u_i(6)$ and must, therefore, be solved simultaneously with the governing difference equations. Since the resulting equations are nonlinear, the simultaneous solution must be obtained by iteration.

The parametric equations for the bicharacteristics, Eq. (E-4), are next integrated to obtain the intersections of the four bicharacteristics with the initial-value surface. Applying the modified Euler scheme to Eq. (E-4) yields

$$\begin{aligned} x_i(6) - x_i(k) = -(1/2)[&u_i(6) + c(6)a_i(6)\cos\theta(6) + c(6)\beta_i(6)\sin\theta(6) \\ &+ u_i(k) + c(k)a_i(k)\cos\theta(k) \\ &+ c(k)\beta_i(k)\sin\theta(k)]\, t(k), \qquad (i = 1, 2, 3) \end{aligned} \tag{E-15}$$

where the index k is used to denote values at the points (1), (2), (3) and (4) of the network and which correspond to values of $\theta(k)$ equal to 0, $\pi/2$, π and $3\pi/2$ respectively. These choices for $\theta(k)$ result in forms of the compatibility equations in which the derivatives of the dependent variables at the unknown point appear in only two scalar terms. These

two additional terms must be considered as unknowns, since the derivatives cannot be evaluated, and are algebraically eliminated from the finite difference form of the compatibility equations. This permits the modified Euler integration scheme to be used, and hence a solution accurate to second order is obtained.

The components of the reference vector set which appear in Eqs. (E-15) must be established at point (6) and at the four points on the initial-value surface. The orientation of the network is established by the selection of a reference at point (6). In the course of accuracy studies it was determined that the best absolute accuracy resulted if the reference at point (6) was selected so that the vectors α_i and β_i straddle a plane defined by the velocity vector and the pressure gradient. The pressure gradient at point (6) is not known until a complete solution surface is established; consequently, the pressure gradient at point (5) is used to define the reference plane for the orientation of α_i and β_i at point (6). Although the best accuracy was obtained for this choice of reference, it should be stressed that the effect was very minor and the choice of any other reference, such as one of the base coordinate directions, gave essentially as good a result. A primary consideration in the choice of the pressure gradient as a reference was the fact that more symmetric results are obtained for cases having axial symmetry. The additional relations required to establish all the components of the reference vector set at point (6) are the normalization conditions

$$\alpha_i(6)\alpha_i(6) = \beta_i(6)\beta_i(6) = 1 \tag{E-16}$$

and the orthogonality conditions

$$\alpha_i(6)\beta_i(6) = \alpha_i(6)u_i(6) = \beta_i(6)u_i(6) = 0 \tag{E-17}$$

The components of the reference vectors $\alpha_i(k)$ and $\beta_i(k)$, $(k = 1,2,3,4)$, at the intersections of the four bicharacteristics with the initial-value surface are determined relative to the choice of α_i and β_i at point (6) such that the tangency condition, Eq. (E-12), is satisfied to sufficient order of accuracy. For this purpose it is necessary to develop a numerically useful approximation. When Eq. (E-12) is expanded and the

orthonormal property of the vector set α_i, β_i and u_i/q is used, the following identity results

$$[\alpha_i \cos\theta + \beta_i \sin\theta - u_i c/q^2] \, (\partial x_i/\partial\theta) = 0 \qquad \text{(E-18)}$$

The quantities u_i, α_i, β_i and c can be expressed in terms of the parameters t and θ to sufficient order of accuracy, $O(t^2)$, by power series expansions

$$u_i = u_i(6) + u_i(\theta)t + O(t^2) \qquad \text{(E-19)}$$

$$\alpha_i = \alpha_i(6) + \alpha_i(\theta)t + O(t^2) \qquad \text{(E-20)}$$

$$\beta_i = \beta_i(6) + \beta_i(\theta)t + O(t^2) \qquad \text{(E-21)}$$

$$c = c(6) + c(\theta)t + O(t^2) \qquad \text{(E-22)}$$

where numerals in parentheses indicate values at the corresponding network points and parameters in parentheses denote functional dependence of the coefficient of the first-order term of the power series expansion. In order to evaluate the derivative $(\partial x_i/\partial\theta)$ appearing in Eq. (E-18), the equation for the surface of the Mach conoid is used in which the bicharacteristics are the curves for constant values of θ. Such an expression can be obtained by integration of Eq. (E-4).

$$x_i(\theta,t) - x_i(6) = \int_0^t (u_i + c\alpha_i \cos\theta + c\beta_i \sin\theta) \, dt, \quad (i = 1, 2, 3) \qquad \text{(E-23)}$$

The integral, correct to $O(t^2)$, is obtained by substitution of the series approximations, Eqs. (E-19) through (E-22), into Eq. (E-23) and subsequent integration with respect to t. Thus

$$x_i(\theta,t) - x_i(6) = [u_i(6) + c(6)\alpha_i(6)\cos\theta + c(6)\beta_i(6)\sin\theta]t$$
$$+ [u_i(\theta) + c(6)\alpha_i(\theta)\cos\theta + c(\theta)\alpha_i(6)\cos\theta$$
$$+ c(6)\beta_i(\theta)\sin\theta + c(\theta)\beta_i(6)\sin\theta](t^2/2) + O(t^3) \quad \text{(E-24)}$$

An approximate expression for the derivative $(\partial x_i/\partial\theta)$ is obtained by differentiation of Eq. (E-24) with respect to θ

$$\partial x_i/\partial\theta = c(6)[\beta_i(6)\cos\theta - \alpha_i(6)\sin\theta]t$$
$$+ \{u_i'(\theta) - [c(6)\alpha_i(\theta) + c(\theta)\alpha_i(6) - c(6)\beta_i'(\theta)$$
$$- c'(\theta)\beta_i(6)]\sin\theta + [c(6)\alpha_i'(\theta) + c'(\theta)\alpha_i(6)$$
$$+ c(6)\beta_i(\theta) + c(\theta)\beta_i(6)]\cos\theta\}(t^2/2) + O(t^3) \quad \text{(E-25)}$$

where the prime denotes differentiation with respect to θ.

In order to complete the expression of Eq. (E-18) in terms of the power series approximations, an approximation for q^{-2} is required. Recall that $q^2 = u_i u_i$, and introduce the power series approximation for u_i, Eq. (E-19). When the product is expanded and only terms of order less than $O(t^2)$ are retained, the following is obtained

$$q^2 = u_i(6)u_i(6) + 2\,u_i(6)u_i(\theta)\,t + O(t^2) \quad \text{(E-26)}$$

Expanding q^{-2} by the binomial theorem and again retaining only terms of order less than $O(t^2)$ yields

$$q^{-2} = (q^{-2}(6))[1 - 2u_i(6)u_i(\theta)t/q^2(6)] + O(t^2) \quad \text{(E-27)}$$

When the power series approximations for u_i, α_i, β_i, c, q^{-2} and $(\partial x_i/\partial\theta)$ are substituted into Eq. (E-18), the products expanded and the terms collected into powers of t, a power series in t is obtained which must vanish for all arbitrary values of t. Therefore, the coefficients of the series must individually vanish. Sufficient order of accuracy is obtained if the coefficients of the terms up through second order vanish.

The order of accuracy maintained in the power series approximations results in complete coefficients for only the first and second-order terms in t. No zeroth-order terms result since the expression for $(\partial x_f/\partial\theta)$ is homogeneous in t.

The coefficient for the first-order term in t, equated to zero, yields

$$- c(\delta)[\alpha_f(\delta)\cos\theta + \beta_f(\delta)\sin\theta - u_f(\delta)c(\delta)/q^2(\delta)] \times [\alpha_f(\delta)\sin\theta - \beta_f(\delta)\cos\theta] = 0 \qquad \text{(E-28)}$$

Expansion of the product and utilization of the orthonormal properties of α_f, β_f, and u_f/q yields the result

$$- c(\delta)[\alpha_f(\delta)\alpha_f(\delta) - \beta_f(\delta)\beta_f(\delta)]\sin\theta\cos\theta = 0 \qquad \text{(E-29)}$$

which is satisfied identically. Therefore, no condition on the variation of the reference vectors α_f and β_f is obtained or is necessary in order that Eq. (E-18) be satisfied to first order in t.

The coefficient for the second-order term in t, equated to zero, yields

$$\begin{aligned}\Big\{&\alpha_f'(\theta)\cos\theta + \beta_f(\theta)\sin\theta - c(\delta)/q^2(\delta)[u_f(\theta) + u_f(\delta)c(\theta)/c(\delta) \\ &- 2u_f(\delta)u_j(\delta)u_j(\theta)/q^2(\delta)]\Big\}\ [- c(\delta)\alpha_f(\delta)\sin\theta \\ &+ c(\delta)\beta_f(\delta)\cos\theta] + (1/2)[\alpha_f(\delta)\cos\theta + \beta_f(\delta)\sin\theta \\ &- u_f(\delta)c(\delta)/q^2(\delta)]\ \Big\{u_f'(\theta) + [- c(\delta)\alpha_f(\theta) \\ &- c(\theta)\alpha_f(\delta) + c(\delta)\beta_f'(\theta) + c'(\theta)\beta_f(\delta)]\sin\theta \\ &+ [c(\delta)\alpha_f'(\theta) + c'(\theta)\alpha_f(\delta) + c(\delta)\beta_f(\theta) + c(\theta)\beta_f(\delta)]\cos\theta\Big\} = 0\end{aligned} \qquad \text{(E-30)}$$

Expansion of the product terms and use of the orthogonality property of the vector set, α_f, β_f and u_f/q, yields

$$- c(\delta)\alpha_i(\delta)\alpha_i(\theta)\sin\theta\cos\theta + c(\delta)\beta_i(\delta)\alpha_i(\theta)\cos^2\theta - c(\delta)\alpha_i(\delta)\beta_i(\theta)\sin^2\theta$$

$$+ c(\delta)\beta_i(\delta)\beta_i(\theta)\sin\theta\cos\theta + [c^2(\delta)/q^2(\delta)][\alpha_i(\delta)u_i(\theta)\sin\theta$$

$$- \beta_i(\delta)u_i(\theta)\cos\theta] + (1/2)\left\{\alpha_i(\delta)u_i'(\theta)\cos\theta\right.$$

$$- c(\delta)\alpha_i(\delta)\alpha_i(\theta)\sin\theta\cos\theta + c(\delta)\alpha_i(\delta)\beta_i(\theta)\cos^2\theta - c(\theta)\sin\theta\cos\theta$$

$$+ c(\delta)\alpha_i(\delta)\alpha_i'(\theta)\cos^2\theta + c(\delta)\alpha_i(\delta)\beta_i'(\theta)\sin\theta\cos\theta + c'(\theta)\cos^2\theta$$

$$+ \beta_i(\delta)u_i'(\theta)\sin\theta - c(\delta)\beta_i(\delta)\alpha_i(\theta)\sin^2\theta$$

$$+ c(\delta)\beta_i(\delta)\beta_i(\theta)\sin\theta\cos\theta + c(\theta)\sin\theta\cos\theta$$

$$+ c(\delta)\beta_i(\delta)\alpha_i'(\theta)\sin\theta\cos\theta + c(\delta)\beta_i(\delta)\beta_i'(\theta)\sin^2\theta$$

$$+ c'(\theta)\sin^2\theta + [c^2(\delta)u_i(\delta)/q^2(\delta)][-u_i'(\delta)/c(\delta) + \alpha_i(\theta)\sin\theta$$

$$\left. - \beta_i(\theta)\cos\theta - \alpha_i'(\theta)\cos\theta - \beta_i'(\theta)\sin\theta]\right\} = 0 \qquad \text{(E-31)}$$

The power series approximations, Eqs. (E-19) through (E-22), and the orthonormal property of the vector set, u_i/q, α_i and β_i, yield approximate identities which can be used to further simplify Eq. (E-31). These identities need only be accurate to zeroth order in t, since any term $O(t)$ in Eq. (E-31) becomes $O(t^3)$ in Eq. (E-18). Consider the scalar product $\alpha_i\alpha_i$, which has the value unity, and expand the product in terms of the power series approximation for α_i, Eq. (E-20). The resulting zeroth-order identity is

$$\alpha_i(\delta)\ \alpha_i(\theta) = 0 + O(t) \qquad \text{(E-32)}$$

Likewise, for β_i,

$$\beta_i(\delta)\ \beta_i(\theta) = 0 + O(t) \qquad \text{(E-33)}$$

The scalar products $\alpha_i u_i$, $\alpha_i \beta_i$ and $\beta_i u_i$ all vanish due to orthogonality. Thus, expanding the products in terms of the power series approximations, the following additional zeroth-order identities are obtained

$$\alpha_i(6)u_i(\theta) = - u_i(6)\alpha_i(\theta) + 0(t) \tag{E-34}$$

$$\alpha_i(6)\beta_i(\theta) = - \beta_i(6)\alpha_i(\theta) + 0(t) \tag{E-35}$$

$$\beta_i(6)u_i(\theta) = u_i(6)\beta_i(\theta) + 0(t) \tag{E-36}$$

The derivatives with respect to θ of the identities, Eqs. (E-32) - (E-36), are also correct to zeroth order in t. Thus

$$\alpha_i(6)\alpha_i'(\theta) = 0 + 0(t) \tag{E-37}$$

$$\beta_i(6)\beta_i'(\theta) = 0 + 0(t) \tag{E-38}$$

$$\alpha_i(6)u_i'(\theta) = - u_i(6)\alpha_i'(\theta) + 0(t) \tag{E-39}$$

$$\beta_i(6)\beta_i'(\theta) = - \beta_i(6)\alpha_i'(\theta) + 0(t) \tag{E-40}$$

$$\beta_i(6)u_i'(\theta) = - u_i(6)\beta_i'(\theta) + 0(t) \tag{E-41}$$

The identities, Eqs. (E-32) through (E-41), permit great simplification of Eq. (E-31) to obtain

$$\begin{aligned} c(6)\beta_i(6)\alpha_i(\theta) &+ [c^2(6)/q^2(6)]\,[\alpha_i(6)\sin\theta - \beta_i(6)\cos\theta]\,u_i(\theta) \\ &+ [1 + c^2(6)/q^2(6)]\,[\alpha_i(6)\cos\theta + \beta_i(6)\sin\theta]\,u_i'(\theta) \\ &- [c(6)u_i(6)/q^2(6)]u_i'(\theta) + c'(\theta) = 0 + 0(t) \end{aligned} \tag{E-42}$$

The form of Eq. (E-42) is not unique since it is only correct to zeroth order in t and the particular form used here was chosen for convenience since all forms are equivalent.

Before Eq. (E-42) can be used to numerically determine the remaining degree of freedom in the definition of the reference vectors a_i and B_i at the initial-value surface, the quantities $u_i(\theta)$, $u_i'(\theta)$ and $c'(\theta)$ must be evaluated. This is accomplished by again employing the power series approximations for u_i and c, i.e.,

$$u_i = u_i(6) + u_i(\theta)\, t + O(t^2) \tag{E-43}$$

$$c = c(6) + c(\theta)\, t + O(t^2) \tag{E-44}$$

Differentiation with respect to t and θ yields

$$u_i(\theta) = \partial u_i/\partial t + O(t) \tag{E-45}$$

$$c(\theta) = \partial c/\partial t + O(t) \tag{E-46}$$

and

$$u_i'(\theta) = (\partial u_i/\partial \theta)/t + O(t) \tag{E-47}$$

$$c'(\theta) = (\partial c/\partial \theta)/t + O(t) \tag{E-48}$$

Here the derivatives of u_i and c with respect to t and θ may be evaluated at the initial-value surface rather than at point (6) without affecting the accuracy. This is possible because the relations, Eq. (E-45) through (E-48), need only to be correct to zeroth order in t.

The derivatives with respect to the parameters t and θ are expressed in terms of the spatial derivatives by means of the chain rule

$$\partial u_i/\partial t = (\partial u_i/\partial x_j)(\partial x_j/\partial t) \tag{E-49}$$

$$\partial c/\partial t = (\partial c/\partial x_i)(\partial x_i/\partial t) \tag{E-50}$$

$$\partial u_i/\partial \theta = (\partial u_i/\partial x_j)(\partial x_j/\partial \theta) \tag{E-51}$$

$$\partial c/\partial\theta = (\partial c/\partial x_j)(\partial x_j/\partial\theta) \qquad \text{(E-52)}$$

The derivatives of the spatial coordinates with respect to the parameters t and θ are obtained, correct to zeroth order and first order in t respectively, by differentiation of Eq. (E-23) with respect to t and θ and discarding higher-order terms. This yields

$$\partial x_i/\partial t = u_i(6) + c(6)\alpha_i(6)\cos\theta + c(6)\beta_i(6)\sin\theta + O(t) \qquad \text{(E-53)}$$

and

$$\partial x_i/\partial\theta = c(6)\,[-\alpha_i(6)\sin\theta + \beta_i(6)\cos\theta\,]t + O(t^2) \qquad \text{(E-54)}$$

Substituting Eqs. (E-53) and (E-54) into the identities, Eqs. (E-46), (E-47) and (E-48), yields the desired expressions for $u_i(\theta)$, $u_i'(\theta)$ and $c'(\theta)$, i.e.,

$$u_i(\theta) = [u_j(6) + c(6)\alpha_j(6)\cos\theta + c(6)\beta_j(6)\sin\theta](\partial u_i/\partial x_j) + O(t) \qquad \text{(E-55)}$$

$$u_i'(\theta) = c(6)(-\alpha_j(6)\sin\theta + \beta_j(6)\cos\theta)(\partial u_i/\partial x_j) + O(t) \qquad \text{(E-56)}$$

$$c'(\theta) = c(6)(-\alpha_j(6)\sin\theta + \beta_j(6)\cos\theta)(\partial c/\partial x_j) + O(t) \qquad \text{(E-57)}$$

Equations (E-55), (E-56) and (E-57) are used to evaluate the quantities $u_i(\theta)$, $u_i'(\theta)$ and $c'(\theta)$ which appear in Eq. (A-42). Thus one equation is obtained for the quantities $\alpha_i(\theta)$ in terms of quantities at point (6) and the initial-value surface. Two additional independent relations for the components of $\alpha_i(\theta)$ are obtained from the orthonormal identities, Eqs. (E-32) and (E-34). These relations are in terms of the, as yet, unknowns at point (6) and, therefore, must be evaluated on each iteration of the overall scheme.

The equations, Eqs. (E-42), (E-32) and (E-34), are used to evaluate the $\alpha_i(\theta^k)$, where the superscript k is used to denote the four values of

θ (i.e., 0, $\pi/2$, π and $3\pi/2$). Thus the reference vectors α_i and β_i at the intersections of the four bicharacteristics with the initial-value surface, relative to the selected orientation of these vectors at the solution point, can be established to sufficient order of accuracy by a two term power series expansion

$$\alpha_i(k) = \alpha_i(6) + \alpha_i(\theta^k)t(k) + O(t^2) , \qquad i = 1, 2, 3) \qquad (E\text{-}58)$$

Once the components $\alpha_i(k)$ are established, the components of $\beta_i(k)$ are obtained by means of the orthonormal property of the vector set α_i, β_i and u_i/q, since the values of u_i are known on the initial-value surface.

The values of the dependent variables and their derivatives with respect to two independent directions within the initial-value surface are required at the intersections of each of the four bicharacteristics with the initial-value surface. These are obtained by means of second-order polynomials which are fit locally by the method of least squares. Since the initial-value surface is assumed to be space-like, the system of governing partial differential equations can be used along with the derivatives within the initial-value surface to obtain the partial derivatives of all the dependent variables with respect to the three spatial coordinates. The spatial derivatives of the variable c at the intersections of the bicharacteristics with the initial-value surface are also required in Eq. (E-57). These derivatives can be expressed in terms of the spatial derivatives of the six dependent variables. The definition of c, Eq. (E-5), is differentiated to obtain

$$\partial c/\partial x_i = (c^3/a^3)(\partial a/\partial x_i) - (c^3/q^3)(\partial q/\partial x_i) , \quad (i = 1, 2, 3) \quad (E\text{-}59)$$

It is shown in Appendix C that the speed of sound, a, is properly represented as a function of the variables p, P and H, i.e.,

$$\hat{a} = \hat{a}(p,P,H) \qquad (E\text{-}60)$$

where the hat denotes functional dependence on p, P, and H. Thus, the spatial derivative of $\hat{a}$ may be expanded by the chain rule to obtain

$$\partial a/\partial x_i = (\partial \hat{a}/\partial p)(\partial p/\partial x_i) + (\partial \hat{a}/\partial P)(\partial P/\partial x_i) + (\partial \hat{a}/\partial H)(\partial H/\partial x_i) , \quad (i = 1, 2, 3) \tag{E-61}$$

The magnitude of the velocity, q, can be expressed as a scalar product

$$q^2 = u_i u_i \tag{E-62}$$

so that the spatial derivatives of q in terms of the derivatives of the velocity components are

$$\partial q/\partial x_i = (u_j/q)(\partial u_j/\partial x_i), \quad (i = 1, 2, 3) \tag{E-63}$$

Combining Eqs. (E-59), (E-61) and (E-63) to eliminate the derivatives of a and q, yields an expression for $(\partial c/\partial x_i)$ on the initial-value surface in terms of known quantities

$$\partial c/\partial x_i = (c^3/a^3)[\partial \hat{a}/\partial p)(\partial p/\partial x_i) + (\partial \hat{a}/\partial P)(\partial P/\partial x_i) + (\partial \hat{a}/\partial H)(\partial H/\partial x_i)] - (c^3/q^4)u_j(\partial u_j/\partial x_i) \tag{E-64}$$

The parametric equations for the streamline and the bicharacteristics, Eqs. (E-14) and (E-15), the tangency condition, Eq. (E-41), along with the subsidiary relationships, comprise a system of difference equations for the location of the points of the difference network relative to any one fixed point. In this scheme the location of the streamline intersection with the initial-value surface, point (5), is fixed. In addition, the solution point, point (6), is constrained to lie on an a priori selected solution surface. The difference equations are used to establish the locations of the remaining points of the network. Note that the solution for the point locations is expressed implicitly in terms of the values of the dependent variables at the solution point, point (6), as well as in terms of the dependent variables at the as yet undetermined intersections of the bicharacteristics with the initial-value surface. Obviously an iteration scheme is required to solve this system of simultaneous nonlinear equations. Before discussing the relaxation scheme,

however, it is first necessary to develop the finite difference forms of the differential equations which apply along the streamline and the bicharacteristic segments and thus obtain sufficient difference relations to determine all unknown quantities.

4. FINITE DIFFERENCE FORM OF THE DIFFERENTIAL EQUATIONS

The differential relations consist of the wave surface compatibility equation, Eq. (D-15) of Appendix D, applied along the four bicharacteristics of the network, three of the stream surface compatibility equations, Eqs. (D-11), (D-12) and (D-13) of Appendix D, applied along the streamline, and the one noncharacteristic differential equation, corresponding to Eq. (B-41) of Appendix B for the general method.

The wave surface compatibility equation can be expressed in terms of the parameters of the wave surface bicharacteristic parameterization by substitution of the expression for the wave surface normal, Eq. (E-11), into Eq. (D-15) of Appendix D. The orthonormal property of the vector set u_i/q, a_i and s_i yields the following identity

$$a_i a_j + s_i s_j + u_i u_j/q^2 = \delta_{ij} \qquad \text{(E-65)}$$

which can be used to simplify the wave surface compatibility relation to obtain

$$d_{\bar{I}} p + \rho c(a_i \cos\theta + s_i \sin\theta) d_{\bar{I}} u_i = - \rho c^2 (a_i \sin\theta - s_i \cos\theta)(a_j \sin\theta - s_j \cos\theta)(\partial u_i/\partial x_j) dt \qquad \text{(E-66)}$$

where the subscript $\bar{I}$ on the directional differential operator denotes the bicharacteristic direction corresponding to the value for θ.

The one noncharacteristic relation, the equivalent of Eq. (B-41) of the general numerical scheme in Appendix B, can be expressed in terms of the wave surface bicharacteristic parameterization by inspection of the parametric form for the wave surface compatability equation, Eq. (E-66), and use of the relations, Eqs. (B-27), (B-28) and (B-29) of Appendix B, for the form of the general compatibility equation coefficients, see Eq. (B-40) of Appendix B, to establish the respective values for A_{I_v}, B_I,

C_{2v} and C_{3v}. Again the indentity, Eq. (E-65), is used to simplify the resulting expression to obtain

$$d_{\bar{u}}p = -\rho c^2(\alpha_i\alpha_j + \beta_i\beta_j)(\partial u_i/\partial x_j)dt \qquad \text{(E-67)}$$

where the subscript $\bar{u}$ on the directional differential operator denotes the streamline direction.

The wave surface compatibility equation, when placed in finite difference form using the modified Euler integration scheme and applied along the four bicharacteristics yields:
for $\theta = 0$,

$$\begin{aligned} 2[p(6) - p(1)] + [\rho(6)c(6)\alpha_i(6) + \rho(1)c(1)\alpha_i(1)]\,[u_i(6) - u_i(1)] \\ = [\rho(6)c^2(6)\beta_i(6)\beta_j(6)\partial u_i/\partial x_j(6) \\ + \rho(1)c^2(1)\beta_i(1)\beta_j(1)\partial u_i/\partial x_j(1)]\,t(1) + 0(t^3) \end{aligned} \qquad \text{(E-68)}$$

for $\theta = \pi/2$,

$$\begin{aligned} 2[p(6) - p(2)] + [\rho(6)c(6)\beta_i(6) + \rho(2)c(2)\beta_i(2)]\,[u_i(6) - u_i(2)] \\ = [\rho(6)c^2(6)\alpha_i(6)\alpha_j(6)\partial u_i/\partial x_j(6) \\ + \rho(2)c^2(2)\alpha_i(2)\alpha_j(2)\partial u_i/\partial x_j(2)]\,t(2) + 0(t^3) \end{aligned} \qquad \text{(E-69)}$$

for $\theta = \pi$,

$$\begin{aligned} 2[p(6) - p(3)] - [\rho(5)c(6)\alpha_i(5) + \rho(3)c(3)\alpha_i(3)]\,[u_i(6) - u_i(3)] \\ = [\rho(6)c^2(6)\beta_i(6)\beta_j(6)\partial u_i/\partial x_j(6) \\ + \rho(3)c^2(3)\beta_i(3)\beta_j(3)\partial u_i/\partial x_j(3)]\,t(3) + 0(t^3) \end{aligned} \qquad \text{(E-70)}$$

and for $\theta = 3\pi/2$,

$$2[p(6) - p(4)] - [\rho(6)c(6)\beta_i(6) + \rho(4)c(4)\beta_i(4)][u_i(6) - u_i(4)]$$

$$= [\rho(6)c^2(6)\alpha_i(6)\alpha_j(6)\partial u_i/\partial x_j(6)$$

$$+ \rho(4)c^2(4)\alpha_i(4)\alpha_j(4)\partial u_i/\partial x_j(4)]\, t(4) + O(t^3) \qquad \text{(E-71)}$$

where the notation $\partial u_i/\partial x_j(k)$ means the value of the derivative at the point (k), (k = 1, 2, 3, 4, 6) and t(6) has been arbitrarily taken to be zero as before. Bernoulli's equation and the one noncharacteristic relation are applied in finite difference form along the streamline segment from point (5) to point (6) to obtain

$$2[p(6) - p(5)] + [\rho(6)u_i(6)$$

$$+ \rho(5)u_i(5)][u_i(6) - u_i(5)] = 0 + O(t^3) \qquad \text{(E-72)}$$

and

$$2[p(6) - p(5)] - \{\rho(6)c^2(6)[\alpha_i(6)\alpha_j(6)$$

$$+ \beta_i(6)\beta_j(6)]\partial u_i/\partial x_j(6) + \rho(5)c^2(5)[\alpha_i(5)\alpha_j(5)$$

$$+ \beta_i(5)\beta_j(5)]\partial u_i/\partial x_j(5)\}\, t(5) = 0 + O(t^3) \qquad \text{(E-73)}$$

Note that the six finite difference equations, Eqs. (E-68) through (E-73), are nonlinear since the unknown quantities at point (6) also appear in the coefficients of the differences. Also note that none of the equations directly involve either of the dependent variables, the stagnation pressure or the stagnation enthalpy. The two compatibility relations, Eqs. (D-11) and (D-12) of Appendix D, which involve these variables are independent of the remaining system of differential compatibility equations and yield the simple result that both the stagnation pressure and enthalpy are constant along a given streamline and the solution for this case is simply

$$P(6) = P(5) \qquad \text{(E-74)}$$

and

$$H(6) = H(5) \tag{E-75}$$

6. ITERATION SCHEME

The nonlinear nature of the system of difference equations necesitates that an iteration scheme be used to obtain the solution at each point in the flow. The particular iteration scheme employed here is initiated by first estimating values for the dependent variables at the unknown point, point (6). The initial estimate is obtained by either taking a two term power series expansion about the fixed point, point (5), or if this estimate exceeds the theoretical maximum velocity, by assuming the values at point (6) to be the same as those at point (5). The estimated values of the dependant variables at point (6) are then used to calculate the coefficients of the difference equations for the streamline, Eq. (E-14), which can then be solved for the coordinates of the intersection of the streamline with the fixed solution surface.

Next the four bicharacteristics are extended back to the initial-value surface to obtain the coordinates of the intersections, i.e., points (1), (2), (3) and (4), see Figure E-1 . The parametric equations for the bicharacteristics, Eq. (E-15), involve the values of the dependent variables at the respective intersections with the initial-value surface and therefore must also be solved iteratively. This is accomplished initially by assuming the values for the dependent variables at the four points to be the same as those at the fixed point, point (5). Once the four intersections of the bicharacteristics are located, the values of the dependent variables are obtained by interpolation within the initial-value surface. Finally, the values of the dependent variables thus obtained at the intersections of the bicharacteristics with the initial-value surface, points (1), (2), (3) and (4), and the estimated values at point (6) are used to evaluate the coefficients of the six finite difference forms of the differential equations, Eqs. (E-68) through (E-73). These equations are linear and can be solved simultaneously to obtain corrected values of the dependent variables, u_i and p, and the two scalar quantities, $\alpha_i\alpha_j \partial u_i/\partial x_j$ and $\beta_i\beta_j \partial u_i/\partial x_j$, at point (6).

The entire process is successively repeated using the values of the dependent variables at points (1), (2), (3), (4) and (6) which were calculated on the previous iteration as new approximations. This iteration process is continued until the values of the dependent variables obtained on consecutive iterations agree to within a fixed tolerance. Usually less than five iterations are necessary to obtain a fractional difference less than 0.0001.

6. CONDITIONS FOR A DETERMINANT SYSTEM

In describing the relaxation scheme for solving the system of difference equations it was tacitly assumed that the equations were independent and the system was determinant. Unfortunately, no precise test for independence, such as that described in Appendix A for differential equations and linear difference schemes, exists for nonlinear difference equations. Normally one would be tempted to require that the difference relations be independent in the limit as the differences approach zero. However, this is an overly severe requirement since schemes having accuracy higher than first order are meaningless in the limit and the independence of equations comprising such schemes must be considered at finite step sizes. The only conflict between the present scheme and the results for independence of differential compatibility relations obtained in Appendix D is in the number of bicharacteristic compatibility relations which are independent. The results of the analysis of independence for differential systems, which is the same as for linear difference systems, showed that at most only three bicharacteristic compatibility relations are independent. The present scheme uses four such relations. The apparent conflict is resolved by the fact that as a result of the second-order integration scheme the equations used in the present scheme are nonlinear and contain two additional unknowns. The presence of the additional unknowns introduces additional degrees of freedom. It is interesting to note that when the approach using weighted integrations over all bicharacteristics, which is discussed in Appendix B for the general case, is used to eliminate the terms containing derivatives of the dependent variables at the unknown point, then only three independent bicharacteristic relations are found. However, in this case each of the

three relations involves integrals over the entire family of bicharacteristics passing through the unknown point so that in effect all bicharacteristics are used. The scheme using only four particular bicharacteristics can be viewed as an approximation to the integral approach, thus providing further evidence in support of the independence of the system of nonlinear difference equations.

A necessary condition for a determinant system of equations, even for the nonlinear case, is that the number of independent relations must just equal the number of unknowns. That this is true for the present scheme is shown by a count of the number of unknowns and number of equations. At the solution point, point (6), the unknowns consist of the three coordinates of the point, the parameter t along the streamline, the values of the four dependent variables, p and u_i, and the six components of the reference vectors α_i and β_i, for a total of fourteen unknowns. However, the integration step or distance between the initial value surface and the solution surface is assumed known, which eliminates one degree of freedom, thus leaving thirteen unknowns. At the four intersections of the bicharacteristics with the initial value surface there are a total of thirty-six unknowns which consist of the two coordinates on the initial-value surface, the six components of the reference vectors α_i and β_i and the parameter t at each of the four points. These thirty-six additional unknowns, the two unknowns involving the derivatives of the dependent variables at point (6), and the thirteen unknowns at point (6), make a total of fifty-one unknowns.

Next consider the number of available equations. Equation (E-14) yields three conditions along the streamline for the position of point (6). Equations (E-16) and (E-17), the orthonormal conditions for u_i/q, α_i and β_i, and the definition of α_i, provide six conditions for a subtotal of nine equations. The three parametric equations for each of the bicharacteristics, Eq. (E-15), the equation for the α_i variation, Eq. (E-42), and the orthonormal property of u_i/q, α_i and β_i, which yields five conditions, constitute nine equations for each bicharacteristic or a total of thirty-six equations for the four bicharacteristics. The finite difference form of the five compatibility equations and the one noncharacteristic equation, Eqs. (E-68), (E-69), (E-70), (E-71), (E-72)

and (E-73), bring the total number of equations to fifty-one. Thus the number of equations just equals the number of unknowns, and the necessary condition for the system to be determinant is satisfied.

7. BOUNDARY POINT CALCULATIONS

a. General. The properly posed initial-boundary value problem consists of initial data specified on a space-like surface and appropriate boundary data specified on time-like surfaces which adjoin the initial-data surface. The boundary data may take the form of solid boundaries, constant pressure surfaces, planes of symmetry, or shock waves (discontinuity surfaces). The first three boundary conditions share the common property that they are stream surfaces (i.e., surfaces composed of streamlines and, therefore, time-like). The shock wave is a different type of boundary condition since the shock surface is space-like to the upstream flow and time-like to the downstream flow, thus the shape of the shock wave and its position depend on a portion of the downstream flow as well as the upstream conditions. The Rankine-Hugoniot relations are the boundary conditions which must be satisfied across the shock surface. Two type of shocks can generally occur; attached shocks originating at concave discontinuous changes in slope of the boundaries, and imbedded shocks which arise within the flow due to focusing of infinitesmal compressions. The first type of shock is eliminated from the present problem by the initial assumption that the boundaries are smooth (i.e., continuous first derivatives). The presence of imbedded shocks cannot be a priori excluded and in general will be evidenced by steep gradients in flow properties. This type of boundary condition is not explicitly treated in the present research; however, the presence of shock waves will be evidenced by the formation of steep gradients within the flow. The formation of an actual discontinuity is prevented by the smoothing properties of the interpolation scheme. If the gradients become too steep (i.e., a shock too strong to be treated in this manner) the numerical scheme breaks down and the solution cannot be continued further without introducing the shock as a boundary across which discontinuous properties are permitted.

Only the modifications to the basic interior point numerical scheme to incorporate stream surface boundary conditions will be further developed herein.

b. Solid Boundary. The solid boundary condition is simply that the flow be tangent to the boundary. For this purpose it is sufficient to specify the bounding surface, $f(x_i) = 0$, and its first derivatives, $\partial f/\partial x_i$. The tangency condition then replaces one of the conditions normally satisfied at an interior point of the flow. The question of which condition to replace is easily answered since initial data exist only interior to the boundary. Thus it is not possible to find four bicharacteristics through the unknown point on the boundary corresponding to values for θ that are multiples of $\pi/2$, which all intersect the initial-value surface. In the case of concave boundaries, it is generally not possible to have even three bicharacteristics which exactly intersect the initial-value surface, see Figure E-2 . However, the relative curvature of the boundary is assumed to be sufficiently small so that the error caused by extrapolation beyond the boundary to the intersections is of order $O(t^3)$. Thus one of the four bicharacteristic conditions of the interior point scheme is replaced by the tangency condition, i.e.,

$$u_i(6)\, n_i(6) = 0 \qquad \text{(E-76)}$$

where $n_i(6)$ are the components of the outer normal to the boundary at point (6). In addition, the position of point (6) obtained from the streamline integration is adjusted along the direction of the normal so that point (6) lies on the boundary. The reference vectors α_i and β_i are chosen at point (6) such that β_i corresponds to the outer normal, n_i. The vector α_i is subsequently found using the property that the vectors u_i/q, α_i and β_i form an orthonormal set. This selection of the reference vectors has the property that the three bicharacteristics corresponding to $\theta = 0$, $\pi/2$ and π intersect the initial-value surface interior to the boundary for convex boundaries and intersect most closely to the interior in the case of concave boundaries, see Figure E-2 . At point (6) the bicharacteristics corresponding to $\theta = 0$ and π lie in the elemental tangent plane to the boundary.

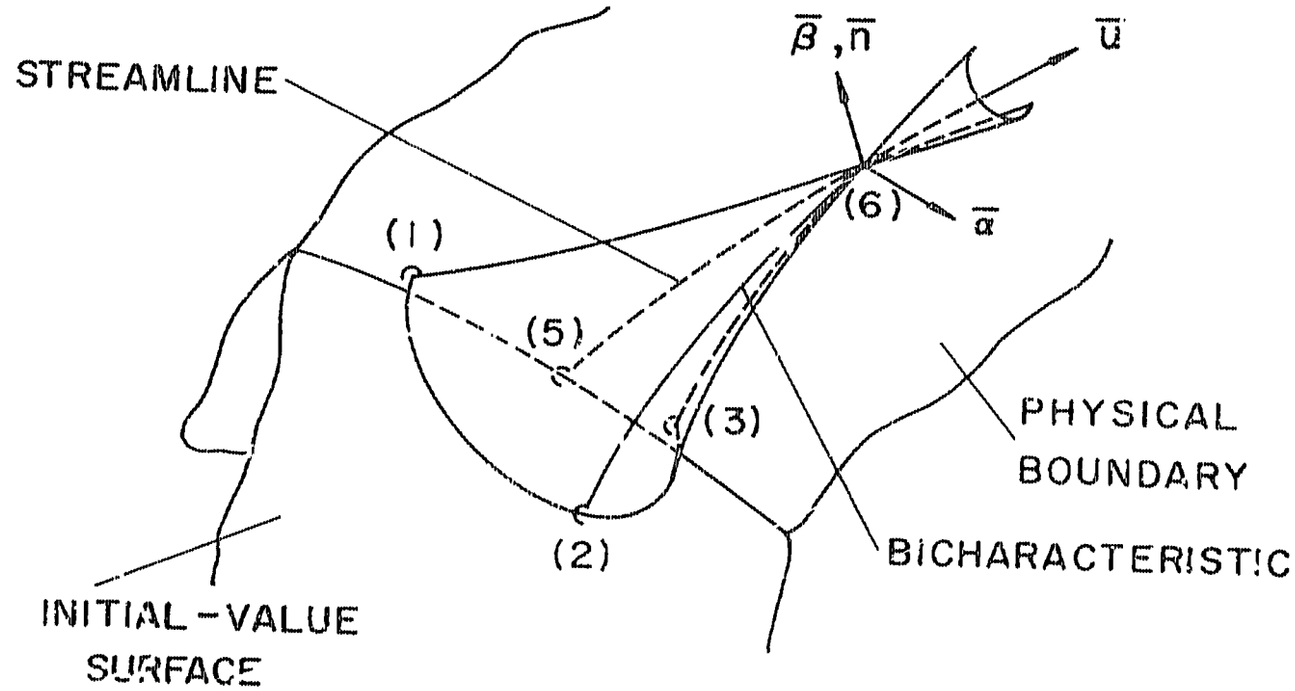

FIGURE E-2. PHYSICAL BOUNDARY POINT NETWORK

The points on the initial-value surface which are used for interpolation are again chosen as a set of nine points which consists of the streamline intersection with the initial-value surface, point (5), and its eight nearest neighbors. The eight nearest neighbors are chosen using an indicial stencil. The stencil is varied slightly with position on the boundary of the array in order to obtain the nearest neighbors uniformly.

The numerical calculations proceed in a manner almost identical to that for the interior point. The only exceptions are that the fourth bicharacteristic is not located and the corresponding compatibility relation is replaced by the tangency condition, Eq. (E-76).

c. Plane of Symmetry. Whenever the boundaries and the initial data possess a common plane of symmetry, the number of point calculations can be greatly reduced, since only one sector of the flow needs to be calculated. The remaining sectors can be found by reflection. This boundary condition is particularly simple since reflection of points about the plane of symmetry can be used to produce a network in which the calculation scheme for an interior point can be used without modification. The nine points of the interpolation scheme are selected such that three points lie on the plane of symmetry (i.e., adjacent boundary points), three are interior points and the remaining three are the image points of the three interior points. This process ensures symmetry in the resulting interpolating polynomials and thus, in the interior point solution. This technique has been demonstrated to give completely satisfactory numerical results. The same logic is also used at the junction between a plane of symmetry and a solid boundary, except that the solid boundary point calculation scheme is used rather than the interior point scheme.

d. Constant Pressure Boundary. In the case of free jets expanding into a quiescent atmosphere without mixing, the boundary of the flow is a stream surface of constant static pressure. The boundary condition is simply that the static pressure on the boundary match the specified value. Along the streamlines the entropy and stagnation enthalpy are constants and, since the static pressure is known, the magnitude of the velocity can be established directly. Thus, the unknown quantities at

the calculated point are the two spatial coordinates, x_2 and x_3, and two components of the velocity (the third component of the velocity is considered known, since the magnitude of the velocity is known).

The reference vector system for the parameterization of the Mach cone is chosen such that e_1 coincides with the unit outer normal to the constant pressure surface. The direction of the outer normal coincides with the direction of the pressure gradient since the gradient is normal to a constant property surface. The pressure gradient is known at point (5) on the initial-value surface and this value is used to construct the reference vectors, see Figure E-3.

Once the system of reference vectors is established, the calculation proceeds in a manner very similar to that for the solid boundary point, the main difference being that Bernoulli's equation along the streamline is not required since the pressure and the velocity at point (6) are known. The three compatibility equations along the three bicharacteristics and the one noncharacteristic relation along the streamline are used. These four relations are sufficient to determine the two remaining velocity components and the two scalar functions of the velocity derivatives at point (6).

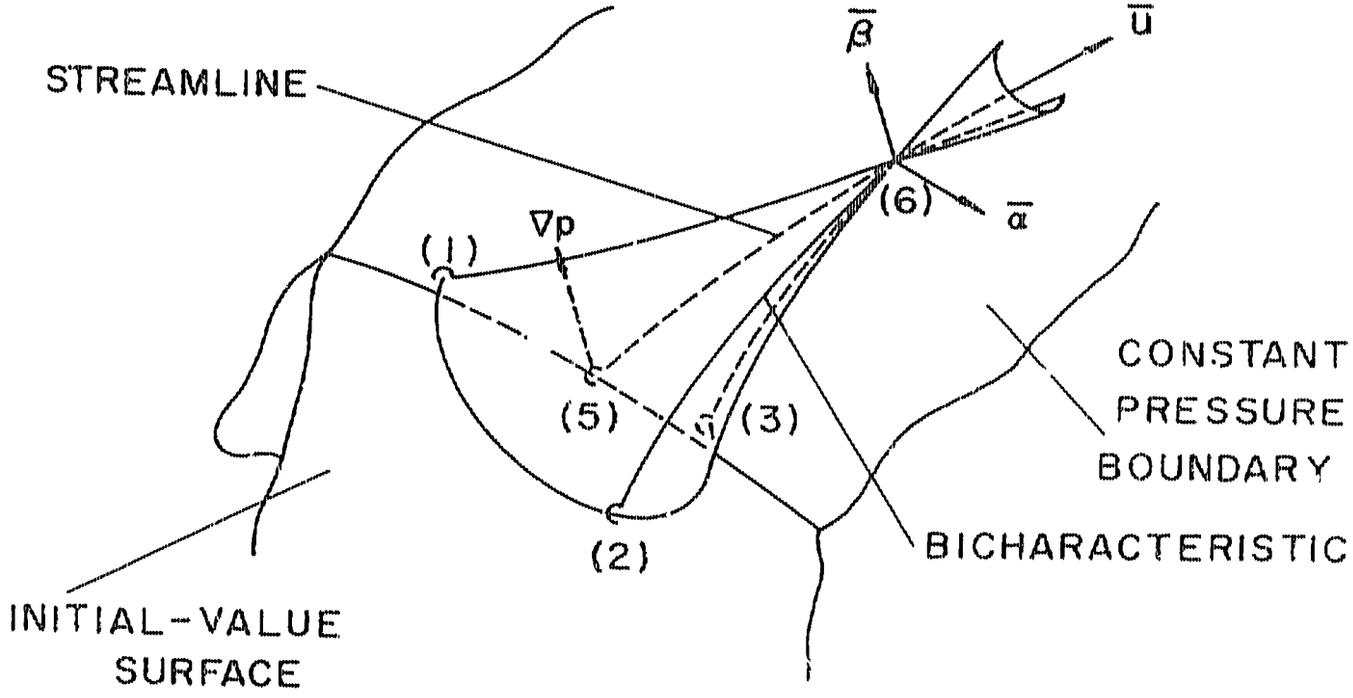

FIGURE E-3. PRESSURE BOUNDARY POINT NETWORK

APPENDIX F

LEAST SQUARES BIVARIATE INTERPOLATION SCHEME

In the numerical integration scheme the values of the six dependent variables, correct to second order in step size, are required at the intersections of the four bicharacteristics and the streamline with the initial-value surface. These intersections do not generally coincide with known points so that interpolation is required. The interpolation process is repeated on each iteration of each point solution in the integration process, and thus speed is of considerable importance. In addition to the requirements of computing speed and accuracy, the interpolation process, in combination with the numerical integration scheme, must be numerically stable.

An interpolation scheme using locally fit second-order least squares polynomials was selected. In this method, second-order bivariate polynomials which have six coefficients are fit to a local group of nine points by the method of least squares. The nine points are selected as the intersection of the streamline, along which the solution is being advanced, with the initial-value surface and the eight nearest neighboring points. The global interpolation process thus consists of the use of a series of overlapping two-dimensional polynomial fits.

This method is relatively fast since a system of six linear symmetric algebraic equations only needs to be solved once for the polynomial coefficients at each point in the numerical integration. Once the coefficients are obtained, interpolations during each iteration are made by simply evaluating the polynomial. Strict second-order accuracy is maintained only if the minimum number of points required to obtain the Lagrange interpolating polynomial, which is six, is used. However, the loss in accuracy due to the redundancy introduced by using nine points is very small and is more than offset by the advantages of computing ease and stabilizing effects.

The least squares interpolation technique has an added advantage in the solution of supersonic flow problems. The occurrence of shock waves, i.e., discontinuities in the solution surfaces, can generally be expected and it is desirable that the numerical method be able to "tolerate" moderate discontinuities without failing. The least squares interpolation scheme has this property since it tends to spread out a discontinuity. This approach results in some loss of accuracy, since in reality the Rankine-Hugoniot jump conditions should be introduced at the discontinuity as an additional boundary condition. The latter approach greatly complicates the numerical calculation and is not warranted for weak shocks. In the case of strong shocks, the shock surface should be introduced as a boundary and located by simultaneous solution for both the upstream and downstream points on the shock. In addition, independent interpolations must be made on each side of the shock intersection with the initial-value surface.

The bivariate polynomial which is fit for the dependent variables has the form

$$u = A_1 + A_2y + A_3z + A_4yz + A_5y^2 + A_6z^2 \qquad (F\text{-}1)$$

where u represents any of the six dependent variables, u_i, p, P and H; A_1, A_2, etc. are the coefficients corresponding to the particular dependent variable, and y and z are rectangular cartesian coordinates on the planar initial-value surface. The nine points, the streamline intersection with the initial-value surface and eight surrounding neighbors, are used to obtain the least squares solution. The mesh points are located in each initial-value surface in such a way that they can be ordered in a two-dimensional array. The eight neighbors of a point in the two-dimensional array are obtained, to close approximation, by a simple system of stored stencils (i.e., lists of coordinates for neighboring points). Thus, the neighboring points used in fitting the interpolating polynomial are readily located without metric information.

Let the values of a particular dependent variable at the known points be designated by u_i, where the subscript ranges from one to nine and is used to designate any group of nine points within the two-dimensional ordering scheme. Likewise, designate the coordinates of each point by

y_i and z_i. The value of the dependent variables calculated from the interpolating polynomial at each of the points, designated by a prime, is

$$u_i' = A_1 + A_2 y_i + A_3 z_i + A_4 y_i z_i + A_5 y_i^2 + A_6 z_i^2 \qquad \text{(F-2)}$$

The sum of the squares of the differences between the exact values and the values obtained from the interpolating polynomials at each point is given by

$$SSQ = \sum_{i=1}^{9} (u_i - u_i')^2$$

$$= \sum_{i=1}^{9} (u_i - A_1 - A_2 y_i - A_3 z_i - A_4 y_i z_i - A_5 y_i^2 - A_6 z_i^2)^2 \qquad \text{(F-3)}$$

Here the repeated indicies do not imply summation. The polynomial coefficients are varied in Eq. (F-3) such that a minimum is obtained for SSQ. The necessary conditions for a minimum are

$$\frac{\partial(SSQ)}{\partial A_1} = \frac{\partial(SSQ)}{\partial A_2} = \frac{\partial(SSQ)}{\partial A_3} = \frac{\partial(SSQ)}{\partial A_4} = \frac{\partial(SSQ)}{\partial A_5} = \frac{\partial(SSQ)}{\partial A_6} = 0 \qquad \text{(F-4)}$$

Written out, these six conditions take the form

$$9A_1 + \Sigma y_i A_2 + \Sigma z_i A_3 + \Sigma y_i z_i A_4 + \Sigma y_i^2 A_5 + \Sigma z_i^2 A_6 = \Sigma u_i \qquad \text{(F-5)}$$

$$\Sigma y_i A_1 + \Sigma y_i^2 A_2 + \Sigma y_i z_i A_3 + \Sigma y_i^2 z_i A_4 + \Sigma y_i^3 A_5 + \Sigma y_i z_i^2 A_6 = \Sigma u_i y_i \qquad \text{(F-6)}$$

$$\Sigma z_i A_1 + \Sigma y_i z_i A_2 + \Sigma z_i^2 A_3 + \Sigma y_i z_i^2 A_4 + \Sigma y_i^2 z_i A_5 + \Sigma z_i^3 A_6 = \Sigma u_i z_i \qquad \text{(F-7)}$$

$$\Sigma y_i z_i A_1 + \Sigma y_i^2 z_i A_2 + \Sigma y_i z_i^2 A_3 + \Sigma y_i^2 z_i^2 A_4 + \Sigma y_i^3 z_i A_5 + \Sigma y_i z_i^3 A_6 = \Sigma u_i y_i z_i \qquad \text{(F-8)}$$

$$\Sigma y_i^2 A_1 + \Sigma y_i^3 A_2 + \Sigma y_i^2 z_i A_3 + \Sigma y_i^3 z_i A_4 + \Sigma y_i^4 A_5 + \Sigma y_i^2 z_i^2 A_6 = \Sigma u_i y_i^2 \qquad \text{(F-9)}$$

$$\Sigma z_i^2 A_1 + \Sigma y_i z_i^2 A_2 + \Sigma z_i^3 A_3 + \Sigma y_i z_i^3 A_4 + \Sigma y_i^2 z_i^2 A_5 + \Sigma z_i^4 A_6 = \Sigma u_i z_i^2 \qquad \text{(F-10)}$$

where Σ implies summation over the same range as in Eq. (F-3). Equations (F-5) through (F-10) are a system of six simultaneous linear algebraic equations for the unknowns A_1 through A_6. The coefficient matrix is symmetric and depends only upon the coordinates of the points used for the least squares fit. Only the nonhomogeneous terms depend upon the values of the dependent variables. Thus, it is only necessary to invert the coefficient matrix once in order to obtain solutions for the polynomial coefficients for all six dependent variables. Each solution may be obtained by multiplication of the respective nonhomogeneous vectors by the inverse of the coefficient matrix. The solution for the polynomial coefficients is obtained using an existing IBM computer library subroutine for solution of systems of symmetric simultaneous linear algebraic equations.

APPENDIX G

THE OVERALL NUMERICAL ALGORITHM

1. GENERAL

The global solution is obtained by an overall numerical algorithm in which the unit processes of interpolation and single point integration are systematically applied to obtain the solution for a particular set of initial values and boundary conditions. The objective of this research is to devise an algorithm suitable for the solution of a wide variety of three-dimensional internal flows, and in particular, flows which are encountered in the design and analysis of thrust nozzles. At the present time very few, if any, three-dimensional thrust nozzles have been employed and so not much experience exists which can be used as a guide for determining the general types of problems to be encountered.

In order to bring the scope of the problem to within practical limits, the following assumptions are made with regard to the geometry of the flow:

(1) The boundaries of the flow space are everywhere smooth such that the outer normal is unique.

(2) The cross section of the flow space is simply connected.

(3) A single direction exists such that the plane normal to this direction is space-like throughout the flow (i.e., the particular direction is everywhere interior to the cone of normals).

(4) When the flow space possesses one plane of symmetry, the normal to the common space-like plane lies within the plane of symmetry.

(5) If the flow has two or more planes of symmetry, the normal to the common space-like plane is parallel to the line of intersection of the planes of symmetry.

Assumption (1) eliminates the possibility of discontinious solutions at the boundary (i.e., attached shocks or Prandtl-Meyer expansions). This assumption is not particularly restrictive in the case of nozzle

flows since other design and construction limitations usually prevent the use of sharp corners on the boundary. Assumption (2) is not a result of any fundamental limitation, but was made in order to simplify the numerical logic (an annular flow is a typical example of a flow having a nonsimply connected cross-section). Assumptions (3), (4) and (5) are again not fundamental limitations, but greatly reduce the numerical complexity of the overall algorithm while not seriously reducing the range of practical problems which can be solved. These assumptions permit the integration to take place between successive planes normal to the x_1 coordinate direction, a condition which was assumed in the development of both the interpolation and integration schemes.

The (x_2, x_3) coordinate plane must be everywhere space-like to the flow, which means that the total angular variation of the streamlines across the flow cannot in the limit exceed the value $2(90-\mu)$, where μ is an average Mach angle. This condition only becomes limiting for Mach numbers near unity where the Mach angle, μ, approaches 90 degrees and the permitted variation in angularity approaches zero. The integration scheme can only be employed at Mach numbers greater than unity so that the limiting case never occurs. High angular variation between streamlines at low Mach numbers does not usually occur in internal flows, since Mach numbers near unity only occur at a minimum in the cross-sectional area and, thus, at a point where the boundaries are nearly parallel. These restrictions are further minimized by choosing the x_1 coordinate direction to be the mean flow direction.

The numerical algorithm could be easily extended to cases in which large variations of the mean flow direction occur along the direction of integration, x_1, by periodically employing a coordinate system rotation as the integration proceeds so that in the transformed system of coordinates the new x_1 direction more nearly coincides with the mean flow direction.

2. INTEGRATION SCHEME

The point computational scheme, which is developed in Appendix E, is used repetitively to obtain the solution at a discrete set of points on planes perpendicular to (x_2, x_3) coordinate planes. When the flow has

or more planes of symmetry as a result of the initial and boundary conditions, the geometry is assumed to be such that the x_1 coordinate direction is parallel to all planes of symmetry (i.e., parallel to the line of intersection of the planes of symmetry).

The point integration scheme establishes the location of the solution point by locating the intersection of the streamline, which passes through a prior computed point on the initial-value surface, with the solution surface. When this process is applied successively, a set of streamlines throughout the flow is generated. The particular streamlines which are generated will depend upon the points which are selected on the first initial-value surface. This technique of constructing streamlines is employed in the numerical process and has the desirable property that the distribution of points, relative to the mass flux distribution, is the same on each new solution surface. An additional benefit of constructing streamlines is that points which are initially on boundaries or in planes of symmetry will remain so throughout the overall integration process. Thus, the boundary calculations are simplified since no interpolation or extrapolation is necessary to obtain the solution at the boundaries.

3. INITIAL-VALUE SURFACE POINT NETWORK

a. Circular Cross Section. The network of points which is generated throughout the flow in the course of obtaining the solution is primarily a function of the selection of points on the initial-value surface. Therefore, a scheme was devised which would select a uniform distribution of points over the flow cross-section. It was also possible to order the points in a two-dimensional square array. The relation of the points to the square array is such that the boundary points of the flow lie on the perimeter of the logical array and the neighboring points in the array are, to a close approximation, neighbors in the physical space. This permits very simple logic to be used for determining the type of point integration scheme to be used and for locating the points to be used in fitting the local interpolating polynomials. The scheme was of further benefit in the computer programming of the algorithm since the points can be stored in two-dimensional arrays and indicial manipulation used to select

points. There is not, to the autnor's knowledge, any way to logically derive the scheme which is used. It was simply invented by a trial and error process and is described, therefore, without any particular attempt at justification, except to point out its virtues. The scheme will first be described for a circular cross-section without planes of symmetry. Subsequently, the extensions to noncircular cross-sections and cross-sections having planes of symmetry will be discussed.

Consider a square array having an odd dimension N_T, expressed in terms of a parameter N_p so that

$$N_T = 2N_p - 1 \qquad \text{(G-1)}$$

The parameter N_p is the number of points on a half side of the array. A typical square array of this type and the corresponding circular array are illustrated in Figure G-1 for $N_p = 11$. In Figure G-1 the rows of points in the square array and the corresponding points in the circular mesh are connected by solid lines while the respective columns of points are connected by dashed curves. In general the square array will have $4(N_T - 1)$ points on the perimeter. If these points are all to correspond to boundary points then the circular array must also have $4(N_T - 1)$ points on the circumference. Further, the number of circular shells are choosen to correspond to the number of inner shells of the square array, see Figure G-1. The radius of each circular perimeter is chosen according to the relation

$$R_K = R_T \sin\left[\frac{\pi}{4}\,\frac{K}{(N_p - 1)}\right], \qquad (K = 1, 2, \cdots N_p - 1) \qquad \text{(G-2)}$$

which produces a sine distribution for the R_K and has the desirable property that the outer shells of the circular mesh are spaced more closely together. This is desirable because one-sided interpolations must be made at the boundaries. The closer spacing of points near the boundaries partially compensates for any loss in accuracy due to one-sided interpolation. Closer spacing of points at the boundary is also desirable because variations in the flow are mostly a result of variations in boundary conditions. Gradients in the flow due to expansions

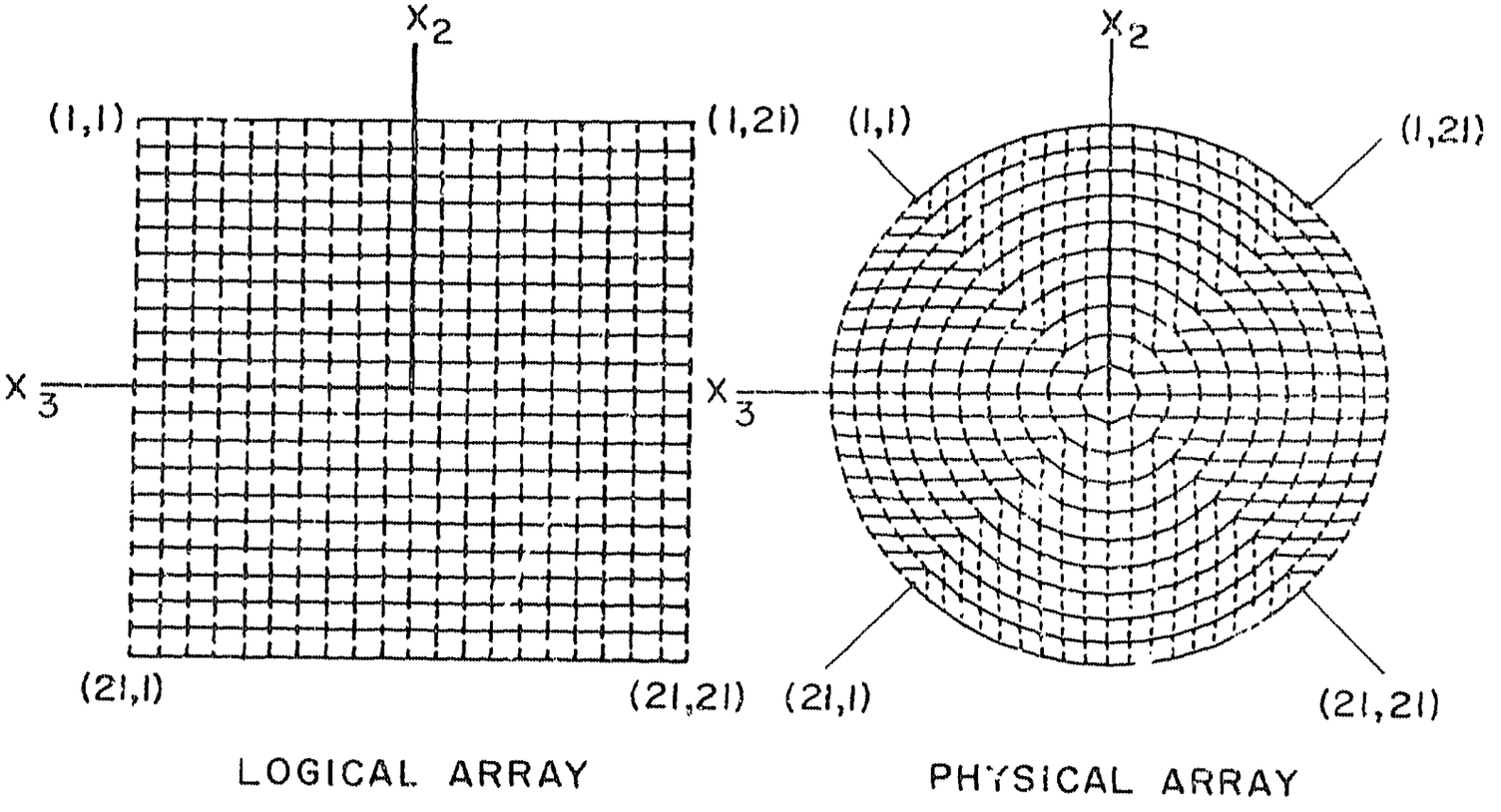

FIGURE G-1. INITIAL-VALUE SURFACE POINT ORDERING SCHEME

at the boundaries are largest in magnitude at the boundaries and become progressively weaker as they are propagated into the flow. The opposite argument can be made for compressions; however, thrust nozzle flows are generally expansive.

b. Planes of Symmetry. The point allocation scheme is easily modified to incorporate the cases of one or more planes of symmetry. When the flow and boundaries have one plane of symmetry, the central point of the mesh is chosen such that it lies on the plane of symmetry. This case is illustrated for a circular mesh in Figure G-2. One-half of the mesh for a complete circle is used and, therefore, only one-half of the square array is required. The dividing line in the mesh corresponds to the plane of symmetry.

When the flow possesses two or more planes of symmetry, the planes are separated by the angle

$$\epsilon = \pi / N , \qquad (N = 2, 3, \cdots) \qquad \text{(G-3)}$$

Each adjoining pair of sectors has a mirror image relation to each other, thus only one sector needs to be calculated since all other sectors can be found by reflection. When the problems possess two planes of symmetry only one-fourth of the grid is used. This case is also illustrated in Figure G-2. For the case of 3 or more planes of symmetry, only one-eighth of the grid is used and the grid is stretched or compressed circumferentially to fit a sector of the flow. The cases of 3, 4, 5, 6 and 7 planes of symmetry are illustrated in Figures G-3 and G-4.

c. Noncircular Cross-Sections. The network illustrated in Figure G-1 for a circular cross-section can be extended to noncircular cross-sections by the following technique. A point in the interior of the cross-section is chosen to correspond to the central point of the two-dimensional array. This point should coincide with the centroid of the area, although other choices may be used. The series of internal shells corresponding to the concentric rings of the circular cross-section are constructed by dividing the radius from the central point to the perimeter into segments according to Eq. (G-1), where the parameter R_T is here defined as the local radius. The resulting shells are illustrated in Figure G-5 for a noncircular cross-section

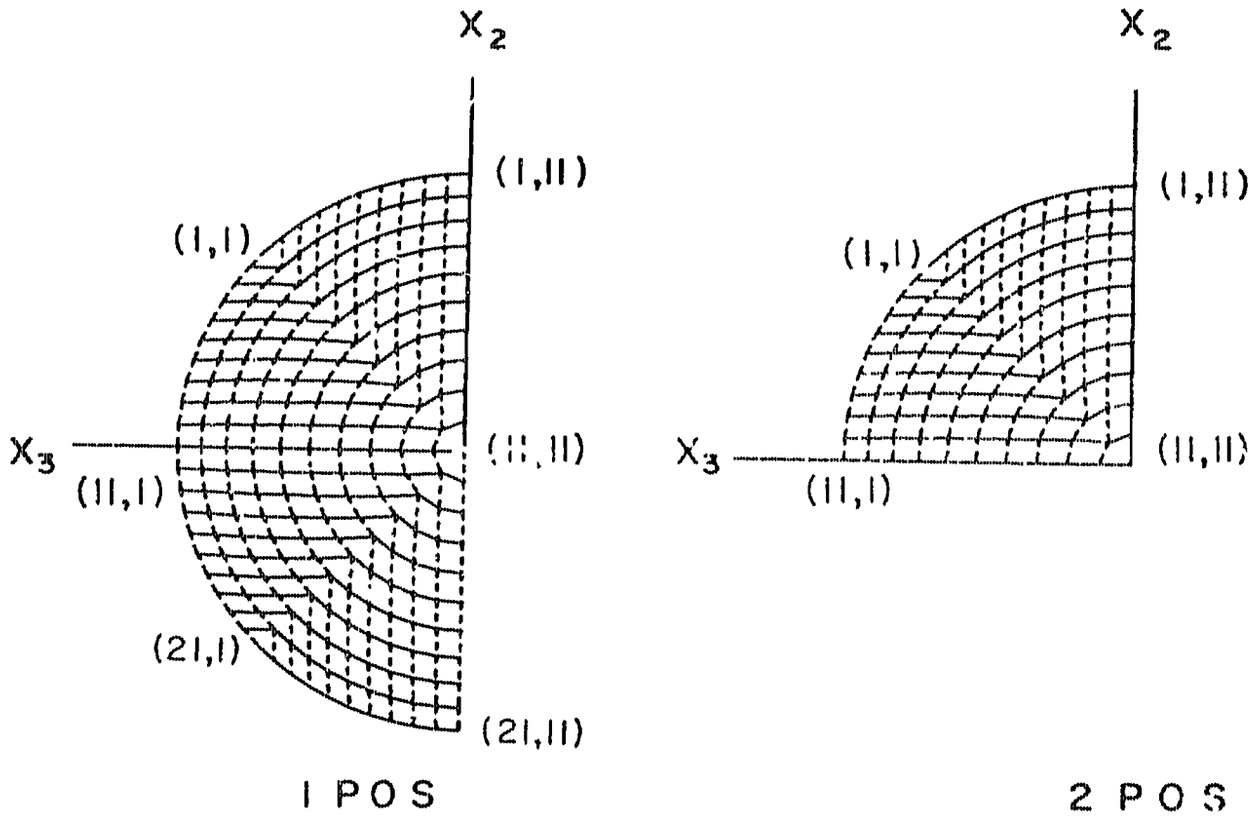

FIGURE G-2. POINT ORDERING SCHEME FOR 1 AND 2 PLANES OF SYMMETRY

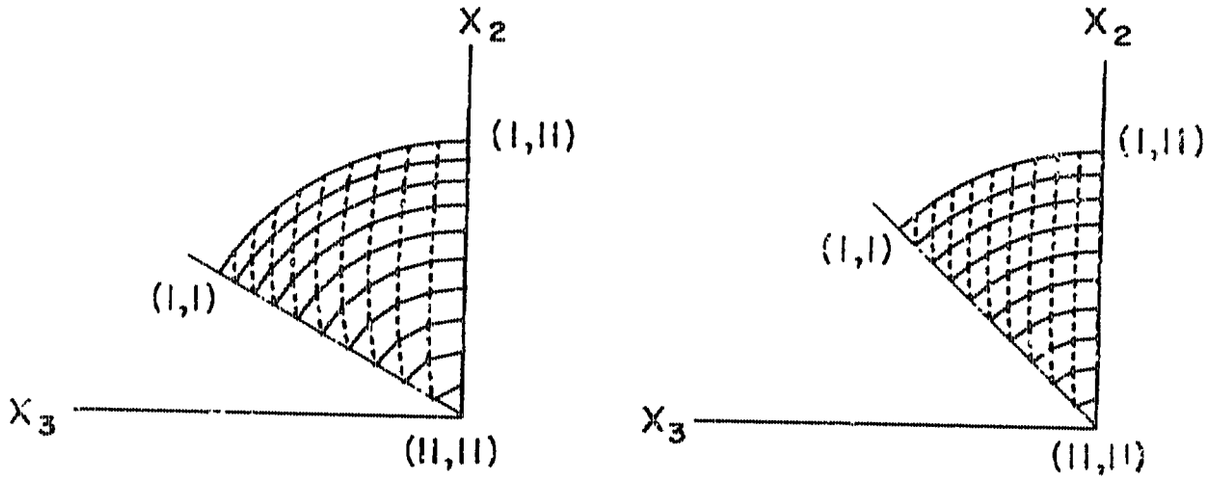

FIGURE G-3. POINT ORDERING SCHEME FOR 3 AND 4 PLANES OF SYMMETRY

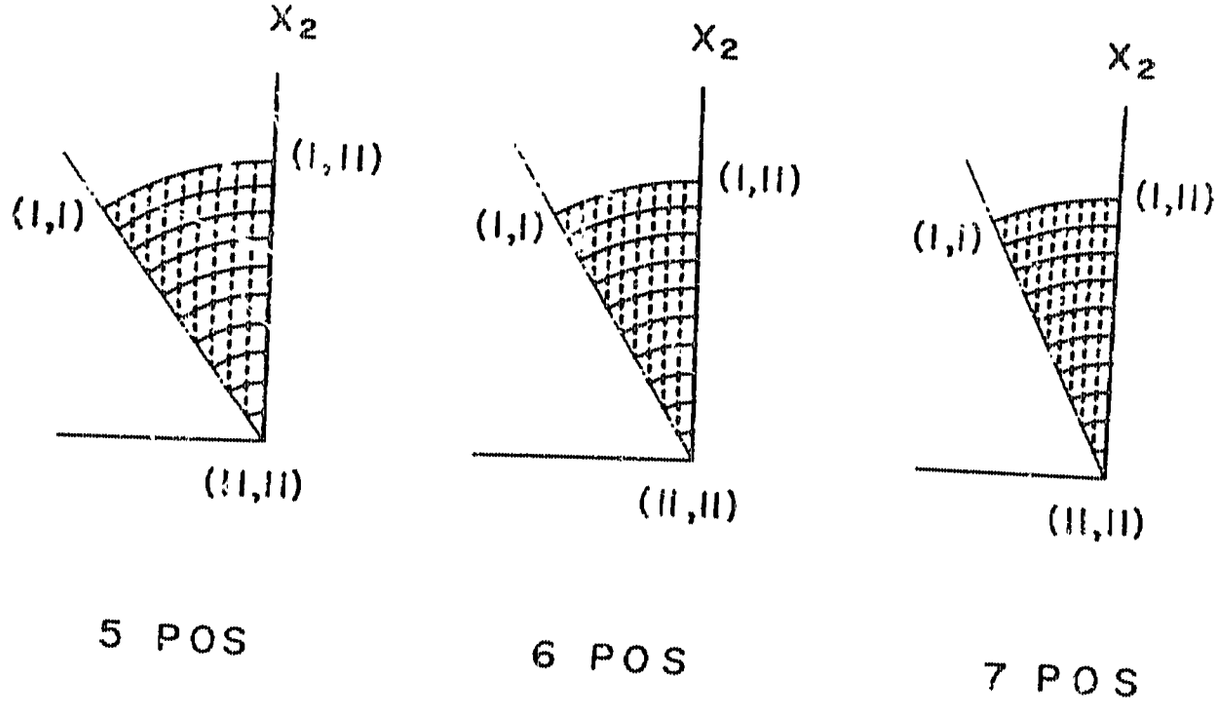

FIGURE G-4. POINT ORDERING SCHEME FOR 5, 6 AND 7 PLANES OF SYMMETRY

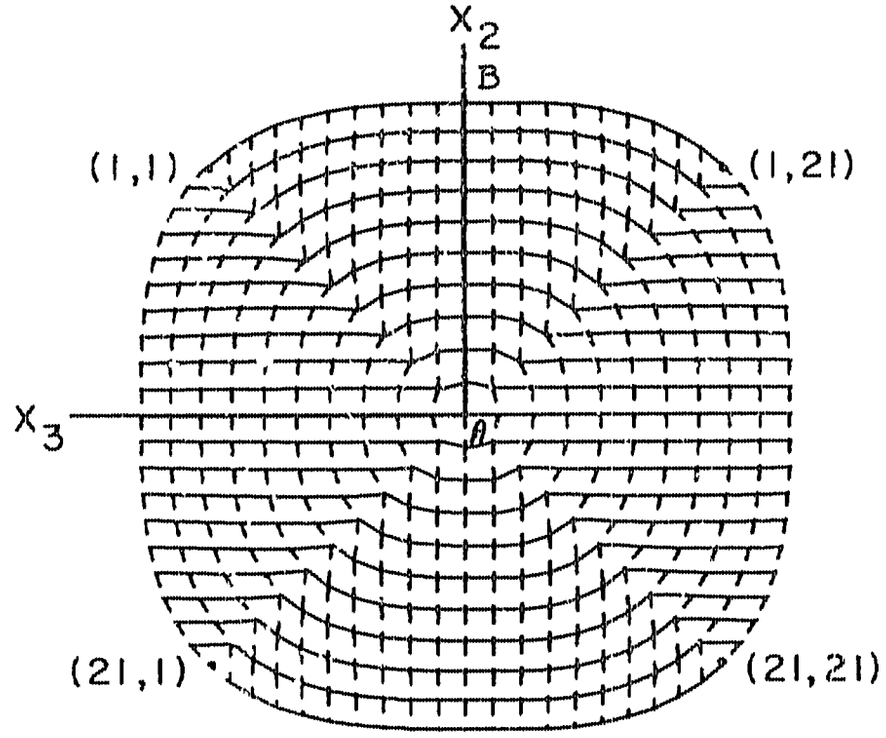

FIGURE G-5. POINT ORDERING SCHEME FOR NONCIRCULAR CROSS-SECTIONS

The locations of the points on each shell are determined by dividing the perimeter into a number of uniform segments of arc equal to the number of points on the shell. A radius parallel to the x_2 coordinate axis is selected as a reference such that the initial point of each shell is placed on the intersection of this reference line and the corresponding shell. The reference is indicated in Figure G-5 by the line A-B. This process produces the same point network as for the circular case when the cross-section is circular and the central point of the network is chosen as the center of the circular section. The extension of the technique to noncircular boundaries with planes of symmetry follows directly from the approach used to extend the circular mesh to noncircular boundaries for no planes of symmetry.

4. INTERPOLATION SCHEME

The point integration scheme requires local interpolation for the values of the dependent variables at the intersections of the bicharacteristics with the initial-value surface. For this purpose second-order least squares polynomials are fit to a group of nine neighboring points in the initial-value surface by the method developed in Appendix F. The nine points are chosen as the intersection of the streamline, along which the solution is being advanced, with the initial-value surface and the eight nearest neighbors. The neighbors of a particular point can be located by means of a stencil or pattern for the indicial coordinates of the points in the square array. The stencil of points must be varied slightly with location in the mesh in order to obtain the best choice of neighbors at all points of the mesh. In the numerical scheme eight different stencils are required to obtain the closest neighbors at all points of the mesh. These eight variations of the stencil are illustrated in Figure G-6. The locations of the corresponding points in a circular flow cross-section are also illustrated.

5. BOUNDARY CONDITIONS

a. General. The character of the solution is governed by the initial conditions and the boundary conditions. The boundary conditions take the form of constraints on the solution which are specified over

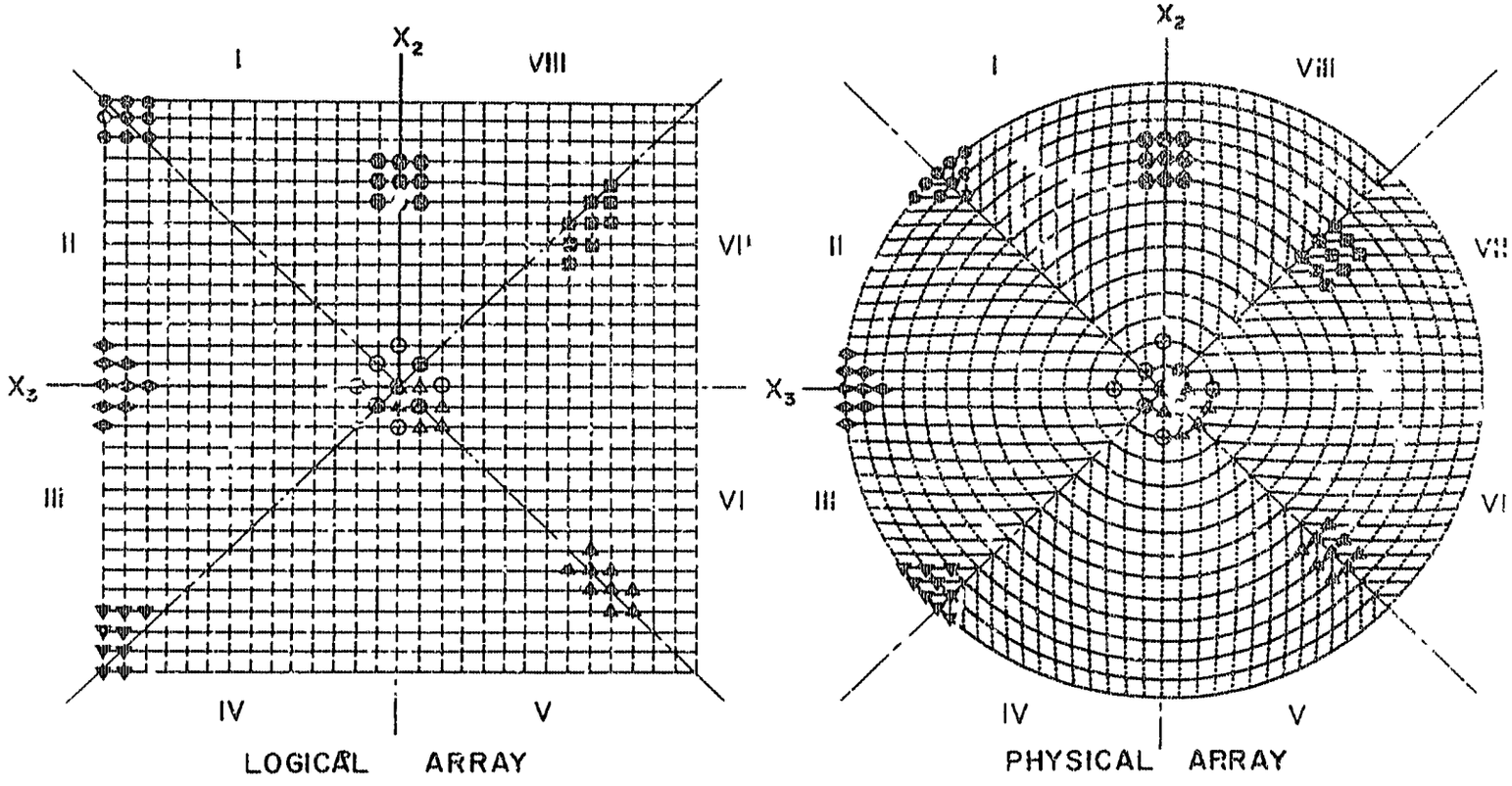

FIGURE G-6. POINT STENCILS FOR INTERPOLATION

time-like surfaces adjoining the initial-value surface. The term time-like is used to denote a surface on which the outer normal is at every point exterior to the local cone of normals. These additional constraints can take the form of a physical boundary (i.e., constrained flow direction), specified pressure, a plane of symmetry or conditions across a discontinuity surface. Only the boundary conditions corresponding to a physical boundary and planes of symmetry are discussed herein.

b. Physical Boundary. The specified physical boundary condition is satisfied by requiring that the flow be tangent to the surface, i.e.,

$$u_i n_i = 0 \qquad \text{(G-4)}$$

where n_i is the unit outer normal to the surface and u_i the flow velocity vector. In addition the outer-most streamlines in the network, which originate from the junction between the initial-value surface and the physical boundary, must at all points lie on the specified boundary surface. Points on the boundary surface are located by obtaining the solution for the intersection of a line with the surface. The line is specified by the coordinates of a point and the direction cosines of the line. More than one intersection with the contour usually will exist and the solution nearest to the known point on the line is assumed to be correct (the direction cosines of the line are chosen to closely approximate the local normal to the surface and the point is chosen in such a way that it is near the boundary of interest so that the correct solution is easily chosen). Once a point on the boundary is located the components of the outer normal are required (i.e., the partial derivatives of the surface function must exist). The boundary surface may be specified as either an analytic function or a tabular function. However, in the case of a tabular function some means for interpolation and numerical differentiation must be provided, since the locations of the boundary solution points are not known a priori. This technique for locating a point on the boundary is used in conjunction with the solid boundary point modification of the basic interior point numerical scheme which is discussed in Appendix E.

c. Planes of Symmetry. The plane of symmetry boundary condition is satisfied by reflection of points with respect to the plane of symmetry and subsequently applying the interior point computational scheme. Although a specialized boundary point scheme, similar to that for the physical boundary, could have been used, the use of reflection is much simpler and it was found to give completely satisfactory numerical results.

A point is reflected at a plane of symmetry such that the plane is the perpendicular bisector of the line joining a point to its image. Any scalar properties at the point have the same magnitude and sense at the image point. Vector quantities, such as the relative position vector and the velocity, are reflected such that components parallel to the plane of symmetry have the same magnitude and sense while components perpendicular are reflected such that they have the same magnitude but opposite sense. The reflection relations for the vector quantities, the relative position vector and the velocity, for an arbitrarily located plane of symmetry are

$$r_i' = r_i - 2(r_j - r_j^0)n_j n_i \tag{G-5}$$

and

$$u_i' = u_i - 2u_j n_j n_i \tag{G-6}$$

where the reflected quantities are denoted by a prime, r_i is the position vector, r_i^0 the position vector for a reference point on the plane of symmetry, n_i the unit outer normal to the plane of symmetry and u_i the velocity vector. These relations reduce to particularly simple forms when the plane of symmetry is parallel to a coordinate plane.

At the point where a plane of symmetry joins a physical boundary, reflection is used to ensure symmetry and the ordinary physical boundary point scheme is used to obtain a solution. Here again specialized routines could be devised, however the logic of the numerical algorithm is greatly simplified by the former approach and completely satisfactory numerical results are obtained.

6. STEP SIZE REGULATION

The distance between each of the successive space-like solution surfaces is regulated such that the Courant-Friedrichs-Lewy (CFL) stability criterion is satisfied at every point of the network. The differential zone of dependence is in general an elliptical region surrounding the streamline intersection with the initial-value surface and is defined as the intersection of the Mach conoid, originating at the solution point, point (6), with the initial value surface. The convex hull of the difference scheme is defined by the positions of the mesh points used for interpolation in the initial-value surface. Both the differential zone of dependence and the convex hull of the difference scheme are illustrated for a typical interior point in Figure G-7. The CFL criterion will always be satisfied if the maximum radius of the differential zone of dependence, R_{max}, is made less than the distance from the streamline intersection with the initial value surface to the nearest mesh point on the convex hull, R_{min}, see Figure G-7.

The relation between the integration step, δx, and the maximum radius of the differential zone of dependence can be expressed as a function of the local flow parameters. The tangent of the angle which the streamline makes with the initial value surface, γ, is simply

$$\tan \gamma = u_1/(u_2^2 + u_3^2)^{1/2} \tag{G-7}$$

where u_1, u_2 and u_3 are the respective velocity components. The tangent of the Mach cone half-angle, μ, with respect to the streamline is simply

$$\tan \mu = (M^2 - 1)^{-1/2} \tag{G-8}$$

where M is the local Mach number. From geometric considerations, see Figure G-8, the ratio of the axial step Δx_1 to R_{max}, called H, is given by

$$H = \Delta x_1/R_{max} = \tan(\gamma-\mu) \tan \gamma/[\tan \gamma-\tan(\gamma-\mu)] \tag{G-9}$$

Application of trigonometric identities and Eqs. (G-7) and (G-8) yields a more useful form of Eq. (G-9), i.e.,

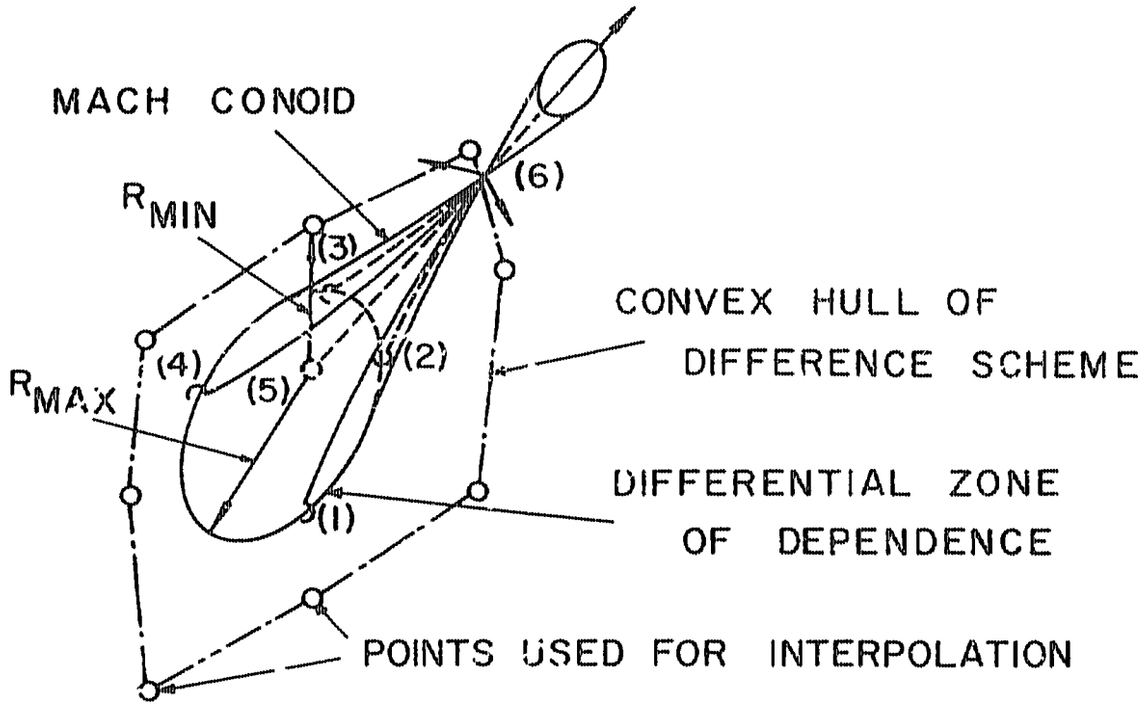

FIGURE G-7. CFL STABILITY CRITERION FOR INTEGRATION SCHEME

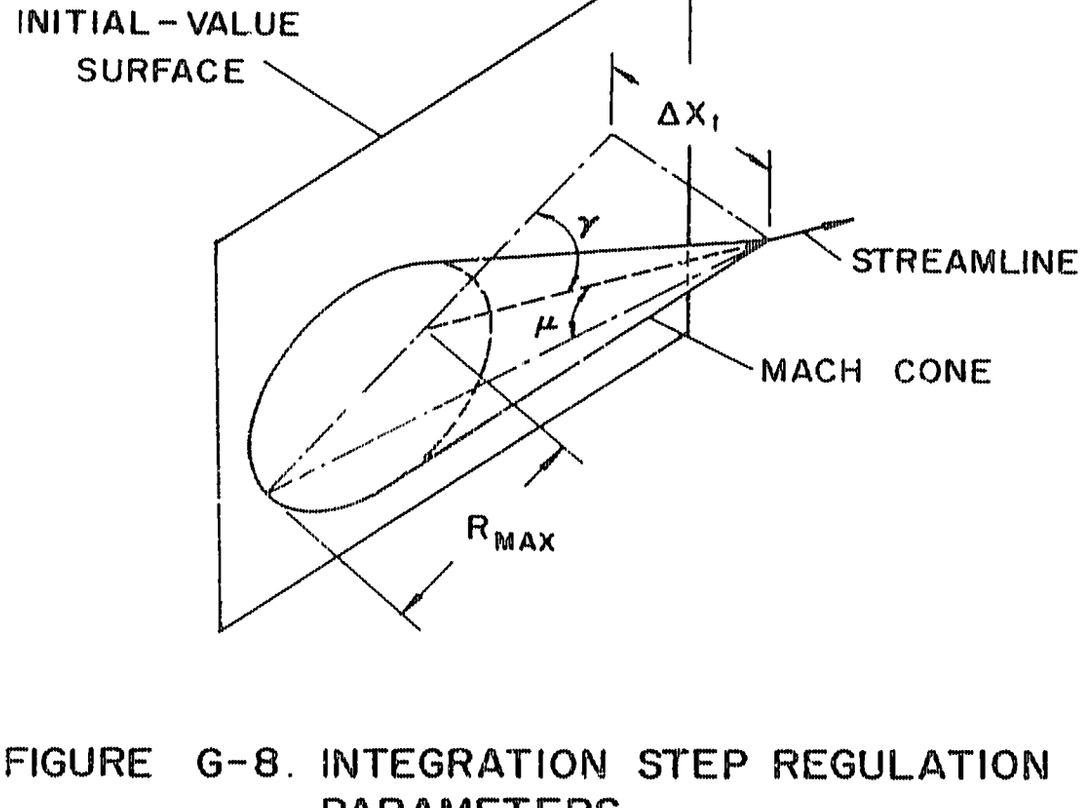

FIGURE G-8. INTEGRATION STEP REGULATION PARAMETERS

$$H = [u_1^2/(cq)][1 - (c/q)(q^2/u_1^2 - 1)^{1/2}] \qquad \text{(G-10)}$$

where q is the magnitude of the velocity

$$q = (u_1^2 + u_2^2 + u_3^2)^{1/2} \qquad \text{(G-11)}$$

c is defined by the relation

$$c = [q^2a^2/(q^2 - a^2)]^{1/2} \qquad \text{(G-12)}$$

and a is the local speed of sound.

The actual Mach conoid is curved, whereas the relation, Eq. (G-10), has been derived assuming a linear cone. The curvature effects can be compensated for to some degree by using mean properties in Eq. (G-10). An appropriate mean is the arithmetic average of the values between points (5) and (6) of the overall network, Figure G-7.

The minimum distance from the streamline intersection with the initial-value surface to the closest point on the convex hull is determined by a search of the eight neighboring points of the difference scheme. The permitted step size is then computed from the relation

$$\Delta x_1 = H R_{min} \qquad \text{(G-13)}$$

Note that the permitted step size given by Eq. (G-13) will be a conservative estimate since in general the direction of the distance R_{max} will not coincide with the direction of the distance R_{min}. In addition this criterion is applied at the most restrictive point of the network at each solution surface. However, numerical experience has shown this criterion to be very close to the maximum value permitted from numerical stability considerations. The use of arbitrary factors of 1.25 and 1.50 times the predicted step in numerical calculations resulted in some evidence of neutral stability and unstable behavior, respectively.

7. OVERALL ALGORITHM

The overall numerical integration process is illustrated in Figures G-9 and G-10. Figure G-9 shows typical boundary and interior point computations for a flow having no planes of symmetry while Figure G-10 shows the corresponding operations for a flow having two planes of symmetry. After completion of the calculations on each solution surface the thrust and mass flow are calculated by numerical integration over the solution surface.

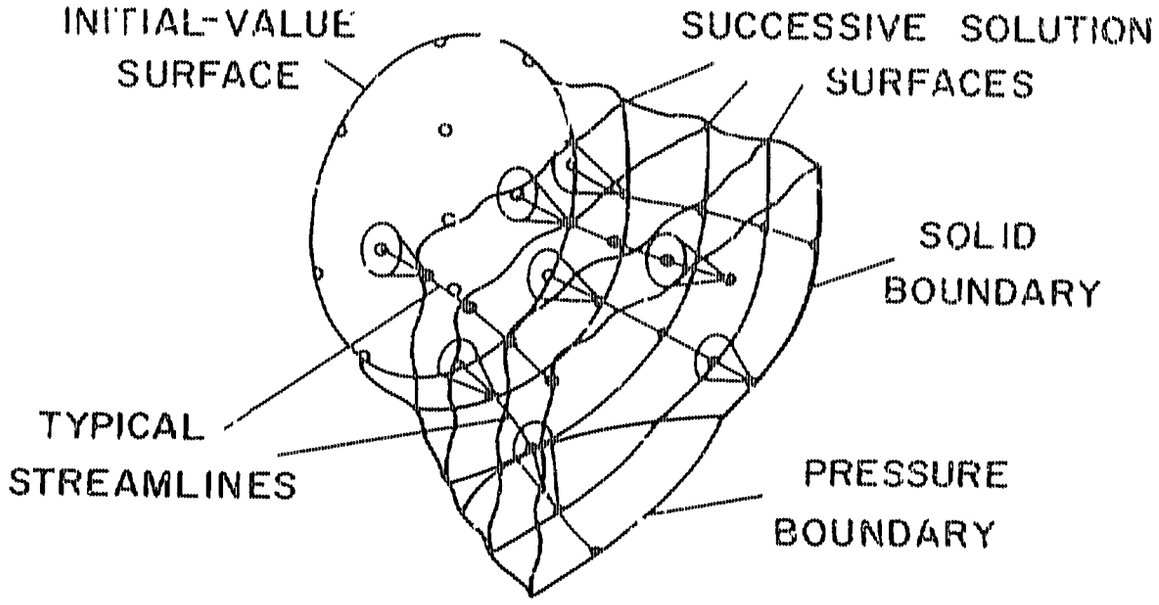

FIGURE G-9. OVERALL SCHEME, NO PLANES OF SYMMETRY

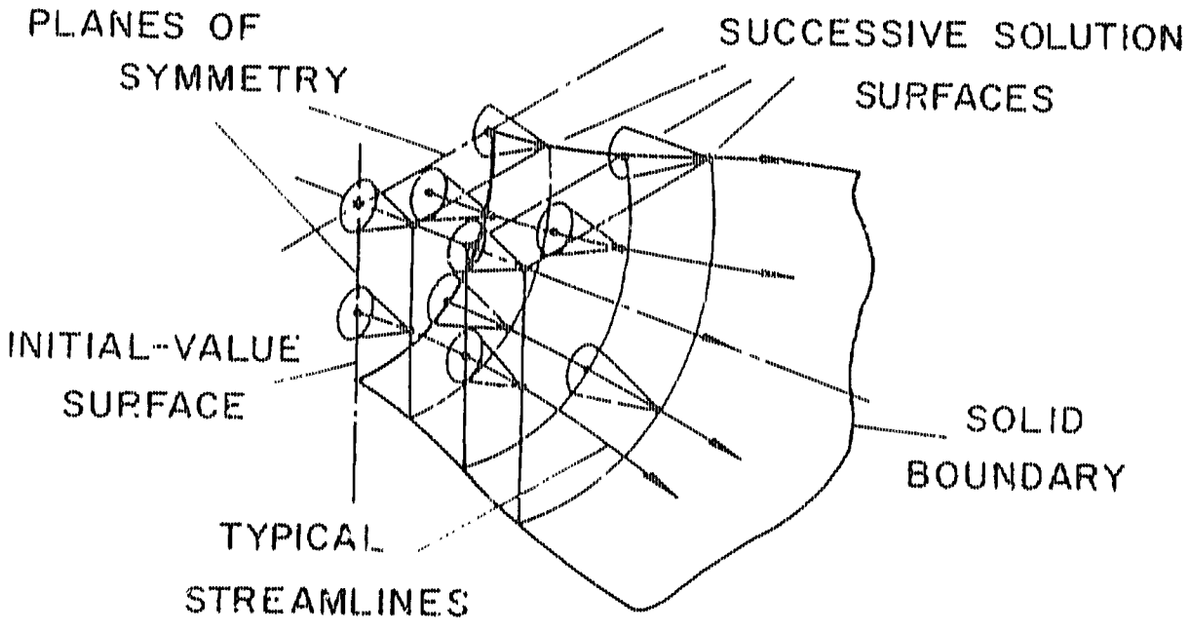

FIGURE G-10. OVERALL SCHEME, 2 PLANES OF SYMMETRY

APPENDIX H

STABILITY ANALYSIS

1. GENERAL

This analysis was motivated by the occurrence of numerical instability in the original numerical scheme. Numerical tests for stability using initial-value problems failed to reveal the unstable character of the scheme, thus the instability was not discovered until the solution of initial-boundary value problems were attempted in which larger numbers of integration steps could be taken.

The stability analysis showed the original scheme to be only moderately unstable, which is the reason that the unstable character did not become apparent until after a rather large number of integration steps. In addition, the analysis showed that the scheme could be made sufficiently stable by a very simple modification.

2. STABILITY OF LINEAR DIFFERENCE EQUATIONS

Numerical stability is a property which does not depend upon the nature of the system of differential equations, but is solely a function of the difference equations which are used as approximations to the differential equations. The stability of linear difference schemes has been studied extensively by a number of investigators and a good summary of this work as well as applications of the stability criteria to several difference schemes for three-dimensional steady flow are given by Hefe and Leigh (5, 6). Stability criteria have only been developed for linear difference equations having constant coefficients and for analytic initial data. For linear difference schemes having variable coefficients, the same stability criteria as for constant coefficients are applied locally. If the governing difference equations are nonlinear, as is the case for steady flow in three dimensions, then generally the corresponding system of difference equations will also be nonlinear and no exact test for

stability presently exists. The usual approach consists of locally applying the same criteria as for linear equations to the linearized form of the nonlinear system and regarding these criteria as necessary conditions. In all cases which are known to have been investigated, including the present work, this approach has been sufficient to ensure stability.

Two stability criteria have been developed for systems of linear difference equations. These are the Courant-Friedrichs-Lewy (CFL) stability criterion and the von Neumann condition. The CFL stability criterion states that the domain of dependence of the difference equations, defined as the convex hull of the points in the initial-value surface, which are used in the difference scheme, must contain the domain of dependence of the differential system, see Figure H-1. The CFL criterion is regarded as a necessary condition for all difference schemes, both linear and nonlinear, and has been shown to be both necessary and sufficient for simplicial linear difference schemes, Ref. (5).

The von Neumann condition states that a difference scheme is stable only if there is a limit to the extent that every Fourier component of the initial data can be amplified by successive application of the difference scheme. The von Neumann condition is sufficient for stability of linear difference schemes only for the case of analytic initial data. However, the von Neumann condition has turned out to be sufficient for all nonlinear, as well as linear, schemes which are known to have been investigated, Ref. (5).

In the present analysis the CFL criterion is regarded as a necessary condition and it is satisfied in the nonlinear difference scheme by regulating the integration step size such that the Mach conoid intersection with the initial-value surface is contained within the convex hull of the initial-value surface points of the difference scheme. The difference scheme, with the CFL condition satisfied, is then tested for stability in the von Neumann sense.

3. LINEAR DIFFERENCE EQUATIONS FOR STEADY SUPERSONIC FLOW

The system of differential equations for steady supersonic flow in three dimensions consists of the wave surface characteristic compatibility

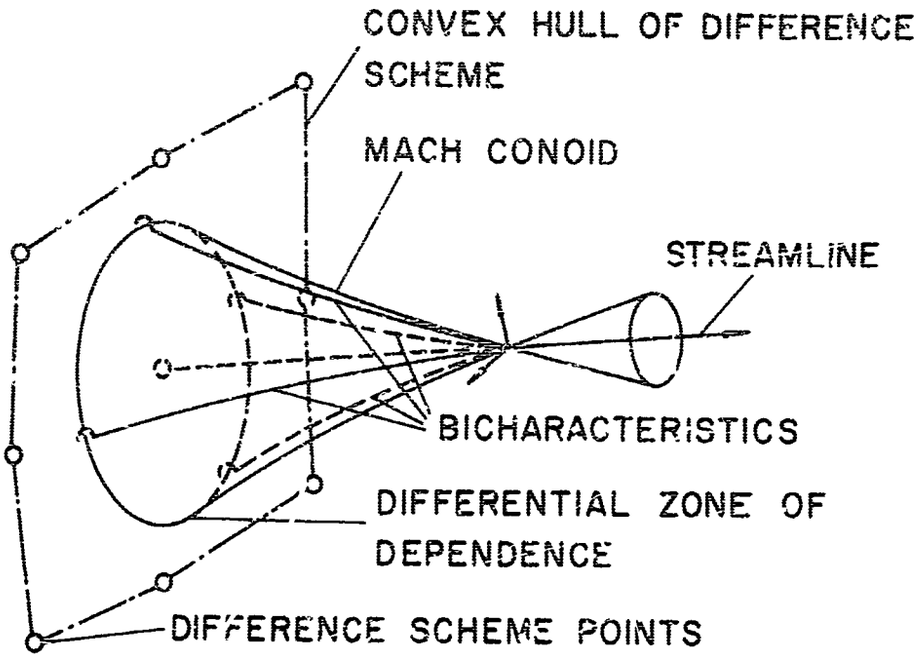

FIGURE H-1. CFL STABITITY CRITERION

relation applied along four orthogonal bicharacteristics, a stream surface characteristic compatibility relation applir along the streamline direction and one noncharacteristic relation applied along the streamline direction. These six equations written in terms of the operator for the directional differential are:

$$d_{\tilde{\ell}_1} p + \rho c \alpha_i \, d_{\tilde{\ell}_1} u_i = - \rho c^2 \beta_i \beta_j (\partial u_i / \partial x_j) \, dt \qquad \text{(H-1)}$$

$$d_{\tilde{\ell}_2} p + \rho c \beta_i \, d_{\tilde{\ell}_2} u_i = - \rho c^2 \alpha_i \alpha_j (\partial u_i / \partial x_j) \, dt \qquad \text{(H-2)}$$

$$d_{\tilde{\ell}_3} p - \rho c \alpha_i \, d_{\tilde{\ell}_3} u_i = - \rho c^2 \beta_i \beta_j (\partial u_i / \partial x_j) \, dt \qquad \text{(H-3)}$$

$$d_{\tilde{\ell}_4} p - \rho c \beta_i \, d_{\tilde{\ell}_4} u_i = - \rho c^2 \alpha_i \alpha_j (\partial u_i / \partial x_j) \, dt \qquad \text{(H-4)}$$

$$d_{\bar{u}} p = - \rho c^2 (\alpha_i \alpha_j + \beta_i \beta_j) \, (\partial u_i / \partial x_j) \, dt \qquad \text{(H-5)}$$

$$d_{\bar{u}} p = - \rho u_i d_{\bar{u}} u_i \qquad \text{(H-6)}$$

where the subscripts $\tilde{\ell}_i$, $(i = 1, 2, 3, 4)$ and $\bar{u}$, denote the four bicharacteristic directions and the streamline direction respectively. The network of bicharacteristics and the streamline along which the system of equations apply is illustrated in Figure H-1.

Normally the system of linear differential equations for use in stability analysis is obtained directly from the system of nonlinear differential equations. However, in the present case two difficulties are encountered which require some judicious consideration. First, the nonlinear system consists of six equations which would yield six linear differential equations for only four dependent variables. Second, the two unusual terms, $\alpha_i \alpha_j \, (\partial u_i / \partial x_j)$ and $\beta_i \beta_j \, (\partial u_i / \partial x_j)$, that appear in some of the coefficients involve partial derivatives and cannot be evaluated in terms of simple differences along the bicharacteristic network.

These differences are a direct result of the scheme for maintaining second-order accuracy in the nonlinear numerical algorithm and consequently may have a significant effect on the numerical stability of the scheme. The approach used herein is to consider the quantities $\alpha_i\alpha_j(\partial u_i/\partial x_j)$ and $\beta_i\beta_j(\partial u_i/\partial x_j)$ as unknown quantities of the differential system, Eqs. (H-1) through (H-6), at a point, and to eliminate these quantities by simultaneous solution. The remaining four independent differential relations are subsequently linearized.

In the linearization process the dependent variables are assumed to be adequately represented as the sum of a constant quantity plus a small variation, i.e.,

$$u = \bar{u} + \tilde{u} \tag{H-7}$$

where the quantity u represents any of the dependent variables, $\bar{u}$ is a constant and $\tilde{u}$ is a small perturbation. The constant value, $\bar{u}$, can be interpreted as a mean value about which perturbations occur. When second-order terms are discarded and differentials replaced by finite difference operators, the following linear system of difference equations is obtained

$$\Delta_{\bar{\ell}_1}\tilde{p} + \bar{\rho}\bar{c}\bar{\alpha}_i\Delta_{\bar{\ell}_1}\tilde{u}_i = (\Delta_{\bar{\ell}_3}\tilde{p} - \bar{\rho}\bar{c}\bar{\alpha}_i\Delta_{\bar{\ell}_3}\tilde{u}_i)\,(\Delta_{\bar{\ell}_1}\tilde{t}/\Delta_{\bar{\ell}_3}\tilde{t}) \tag{H-8}$$

$$\Delta_{\bar{\ell}_2}\tilde{p} + \bar{\rho}\bar{c}\bar{\beta}_i\Delta_{\bar{\ell}_2}\tilde{u}_i = (\Delta_{\bar{\ell}_4}\tilde{p} - \bar{\rho}\bar{c}\bar{\beta}_i\Delta_{\bar{\ell}_4}\tilde{u}_i)\,(\Delta_{\bar{\ell}_2}\tilde{t}/\Delta_{\bar{\ell}_4}\tilde{t}) \tag{H-9}$$

$$\Delta_{\bar{U}}\tilde{p} = (\Delta_{\bar{\ell}_1}\tilde{p} + \bar{\rho}\bar{c}\Delta_{\bar{\ell}_1}\tilde{u}_i)\,(\Delta_{\bar{U}}\tilde{t}/\Delta_{\bar{\ell}_1}\tilde{t}) + (\Delta_{\bar{\ell}_2}\tilde{p} + \bar{\rho}\bar{c}\bar{\beta}_i\Delta_{\bar{\ell}_2}\tilde{u}_i)\,(\Delta_{\bar{U}}\tilde{t}/\Delta_{\bar{\ell}_2}\tilde{t}) \tag{H-10}$$

$$\Delta_{\bar{U}}\tilde{p} = -\bar{\rho}\bar{u}_i\Delta_{\bar{U}}\tilde{v}_i \tag{H-11}$$

where the difference operators are defined by

$$\Delta_{\tilde{\ell}_i}\tilde{f} = \tilde{f}(6) - \tilde{f}(i), \quad (i = 1, 2, 3, 4) \tag{H-12}$$

$$\Delta_{\tilde{u}}\tilde{f} = \tilde{f}(6) - \tilde{f}(5) \tag{H-13}$$

The stability of the system oflinear difference equations is not a function of the coordinate orientation and an orientation which simplifies the system of equations can be used without loss of generality. Thus, a uniform difference network is used in which $\Delta_{\tilde{\ell}}\tilde{t} = 0$, so that $\Delta_{\tilde{\ell}_2}\tilde{t} = \Delta_{\tilde{\ell}_3}\tilde{t} = \Delta_{\tilde{\ell}_4}\tilde{t} = \Delta_{\tilde{u}}\tilde{t}$. That this is true may be seen by considering the linearized parametric equations for a wave surface bicharacteristic

$$\Delta_{\tilde{\ell}}\tilde{x}_i = (\bar{u}_i + \bar{c}\bar{\alpha}_i\cos\theta + \bar{c}\bar{\beta}_i\sin\theta)\,\Delta_{\tilde{\ell}}\tilde{t}, \quad (i = 1, 2, 3, 4) \tag{H-14}$$

and for the streamline

$$\Delta_{\tilde{u}}\tilde{x}_i = \bar{u}_i\Delta_{\tilde{u}}\tilde{t}, \quad (i = 1, 2, 3) \tag{H-15}$$

The reference vectors, $\bar{\alpha}_i$ and $\bar{\beta}_i$, form an orthonormal system with $\bar{u}_i/\bar{q}$, where $\bar{q}$ is the magnitude of the constant components of the velocity. Thus for $\bar{u}_2 = \bar{u}_3 = 0$, $\bar{\alpha}_1$ and $\bar{\beta}_1$ are identically zero and Eq. (H-14) for $\Delta_{\tilde{\ell}}\tilde{x}_1$ along the bicharacteristics reduces to

$$\Delta_{\tilde{\ell}}\tilde{x}_1 = \bar{u}_1\,\Delta_{\tilde{\ell}}\tilde{t} \tag{H-16}$$

which is identical to Eq. (H-15) for $\Delta_{\tilde{u}}\tilde{x}_1$ along the streamline direction. The reference vectors, $\bar{\alpha}_i$ and $\bar{\beta}_i$, have one remaining degree of freedom which may be fixed arbitrarily. A convenient choice is $\bar{\alpha}_2 = \bar{\beta}_3 = 1$ and $\bar{\alpha}_3 = \bar{\beta}_2 = 0$. The initial-value surface is assumed to be normal to the x_1 direction so that, see Figure H-2,

$$\Delta_{\tilde{\ell}_1}x_1 = \Delta_{\tilde{\ell}_2}x_1 = \Delta_{\tilde{\ell}_3}x_1 = \Delta_{\tilde{\ell}_4}x_1 \tag{H-17}$$

Thus it is clear that the Δt's along all bicharacteristics and the streamline are equal, and thus that the difference ratios involving the

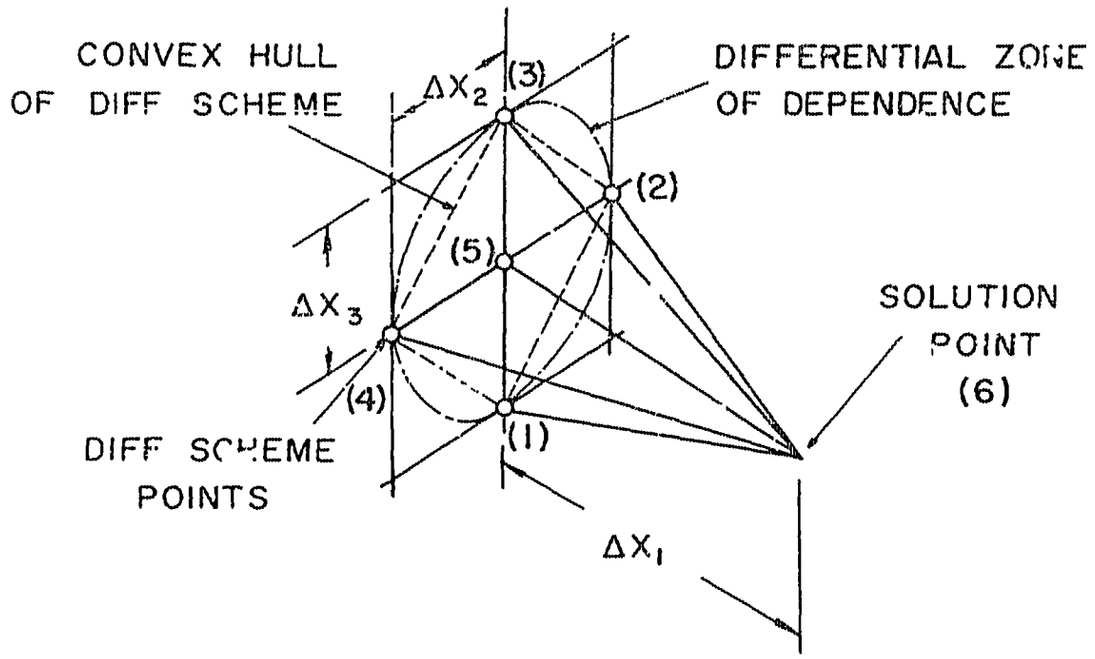

FIGURE H-2. BASIC DIFFERENCE SCHEME

parameter t in Eqs. (H-8) through (H-10) are all unity.

The final difference equations for the selected network and coordinate orientation are

$$\tilde{p}(6) - \tilde{p}(1) + \bar{\rho}\bar{c}[\tilde{u}_2(6) - \tilde{u}_2(1)] = \tilde{p}(6) - \tilde{p}(3) - \bar{\rho}\bar{c}[\tilde{u}_2(6) - \tilde{u}_2(3)] \quad \text{(H-18)}$$

$$\tilde{p}(6) - \tilde{p}(2) + \bar{\rho}\bar{c}[\tilde{u}_3(6) - \tilde{u}_3(2)] = \tilde{p}(6) - \tilde{p}(4) - \bar{\rho}\bar{c}[\tilde{u}_3(6) - \tilde{u}_3(4)] \quad \text{(H-19)}$$

$$\tilde{p}(6) - \tilde{p}(5) = \tilde{p}(6) - \tilde{p}(1) + \tilde{p}(6) - \tilde{p}(2) + \bar{\rho}\bar{c}[\tilde{u}_2(6) - \tilde{u}_2(1) + \tilde{u}_3(6) - \tilde{u}_3(2)] \quad \text{(H-20)}$$

$$\tilde{p}(6) - \tilde{p}(5) = -\bar{\rho}\bar{u}_1[\tilde{u}_1(6) - \tilde{u}_1(5)] \quad \text{(H-21)}$$

4. STABILITY OF THE BASIC DIFFERENCE SCHEME

The stability analysis must include all operations of the overall numerical algorithm (i.e., interpolation, difference equations, etc.). However, in order to more fully illustrate the stability characteristics of the individual processes of the overall numerical algorithm, the basic difference scheme will first be analyzed as though interpolation was not required. Next the interpolation scheme will be analyzed. Then the combination of the difference scheme and the original method of interpolation, and finally the modifications which resulted in a stable scheme, will be analyzed.

Before beginning an analysis of the basic difference scheme without interpolation, note that the CFL stability criterion is not satisfied, see Figure H-2, since the differential zone of dependence is not imbedded within the convex hull of the difference scheme. Thus, when the scheme is analyzed for stability in the von Neumann sense an unstable result is anticipated.

It is assumed that the analytic solution of the system of linear difference equations can be obtained by separation of variables, Ref. (5). For the purpose of stability analysis it is sufficient to examine the solution for only one arbitrary component of the half range Fourier series representation of the initial data. The complete solution could be obtained by superposition of all such terms necessary to completely represent the initial data. The form for a general term of the solution is thus assumed to be

$$\bar{U} = e^{iM\pi x_2/L}\, e^{iN\pi x_3/L}\, \bar{a}(x_1) \qquad \text{(H-22)}$$

where $\bar{U}$ is a vector whose components are the dependent variables $\tilde{u}_1$, $\tilde{u}_2$, $\tilde{u}_3$ and $\tilde{p}$, i is the complex quantity $\sqrt{-1}$, M and N are frequency factors for the particular Fourier component of the initial data, L is a characteristic dimension such that x_2 and x_3 have the range $-L$ to L, and $\bar{a}$ is a vector function of the integration direction, x_1, which has four components corresponding to the four components of $\bar{U}$. The coordinates of the points in the difference network can be represented relative to the coordinates of point (5) in terms of increments of the respective coordinate directions, see Figure H-2. Thus

$$x_1(1) = x_1(2) = x_1(3) = x_1(4) = x_1(5)$$

Point (1): $x_2(1) = x_2(5) - \Delta x_2$

$$x_3(1) = x_3(5)$$

Point (2): $x_2(2) = x_2(5)$

$$x_3(2) = x_3(5) - \Delta x_3$$

Point (3): $x_2(3) = x_2(5) + \Delta x_2$

$$x_3(3) = x_3(5)$$

Point (4): $x_2(4) = x_2(5)$

$$x_3(4) = x_3(5) + \Delta x_3$$

Point (6): $x_1(6) = x_1(5) + \Delta x_1$

$$x_2(6) = x_2(5)$$

$$x_3(6) = x_3(5)$$

where $\Delta x_2 = \Delta x_3$ for the particular choice of coordinate orientation, and they are related to the value of Δx_1 by the parametric equations for a bicharacteristic, Eq. (H-14). The assumed form of the solution, Eq. (H-22), evaluated at each of the network points yields

$$\tilde{U}(6) = e^{i\pi Mx_2(5)/L}\, e^{i\pi Nx_3(5)/L}\, \tilde{a}(x_1(5) + \Delta x_1) \qquad \text{(H-23)}$$

$$\tilde{U}(5) = e^{i\pi Mx_2(5)/L}\, e^{i\pi Nx_3(5)/L}\, \tilde{a}(x_1(5)) \qquad \text{(H-24)}$$

$$\tilde{U}(4) = e^{i\pi Mx_2(5)/L}\, e^{i\pi N(x_3(5) + \Delta x_3)/L}\, \tilde{a}(x_1(5)) \qquad \text{(H-25)}$$

$$\tilde{U}(3) = e^{i\pi M(x_2(5) - \Delta x_2)/L}\, e^{i\pi Nx_3(5)/L}\, \tilde{a}(x_1(5)) \qquad \text{(H-26)}$$

$$\tilde{U}(2) = e^{i\pi Mx_2(5)/L}\, e^{i\pi N(x_3(5) - \Delta x_3)/L}\, \tilde{a}(x_1(5)) \qquad \text{(H-27)}$$

$$\tilde{U}(1) = e^{i\pi M(x_2(5) - \Delta x_2)/L}\, e^{i\pi Nx_3(5)/L}\, \tilde{a}(x_1(5)) \qquad \text{(H-28)}$$

Equations (H-23) through (H-28) all contain the common factor

$$e^{i\pi Mx_2(5)/L}\, e^{i\pi Nx_3(5)/L}$$

and the difference equations, Eqs. (H-18) through (H-21), are homogeneous in the dependent variables; thus the common factor may be eliminated. Substituting the respective values for the dependent variables into the difference equations, writing the system in matrix notation, and substituting the exponential definitions for the circular functions yields

$$\begin{bmatrix} 0 & 1 & 0 & 0 \\ 0 & 0 & 1 & 0 \\ 0 & -1 & -1 & -1/\bar{\rho}\bar{c} \\ \bar{\rho}\bar{u}_1 & 0 & 0 & 1 \end{bmatrix} \tilde{a}[x_1(5) + \Delta x_1]$$

$$+ \begin{bmatrix} 0 & B_{12} & 0 & B_{14} \\ 0 & 0 & B_{23} & B_{24} \\ 0 & B_{32} & B_{33} & B_{34} \\ B_{41} & 0 & 0 & B_{44} \end{bmatrix} \tilde{a}[x_1(5)] = 0 \qquad \text{(H-29)}$$

where

$$B_{12} = -\cos(\pi M \Delta x_2/L) \qquad \text{(H-30)}$$

$$B_{14} = (1/\bar{\rho}\bar{c})\sin(\pi M \Delta x_2/L) \qquad \text{(H-31)}$$

$$B_{23} = -\cos(\pi N \Delta x_3/L) \qquad \text{(H-32)}$$

$$B_{24} = (1/\bar{\rho}\bar{c})\sin(\pi N \Delta x_3/L) \qquad \text{(H-33)}$$

$$B_{32} = \cos(\pi M \Delta x_2/L) - (1)\sin(\pi M \Delta x_2/L) \qquad \text{(H-34)}$$

$$B_{33} = \cos(\pm N\Delta x_3/L) - (i)\sin(\pm N\Delta x_3/L) \tag{H-35}$$

$$B_{34} = (1/\bar{\rho}\bar{c})\left\{[\cos(\pm M\Delta x_2/L) + \cos(\pm N\Delta x_3/L) - (i)[\sin(\pm M\Delta x_2/L) + \sin(\pm N\Delta x_3/L)] - 1\right\} \tag{H-36}$$

$$B_{41} = -\bar{\rho}\bar{u}_1 \tag{H-37}$$

$$B_{44} = -1 \tag{H-38}$$

If Eq (H-35) is premultiplied by the inverse of the leading coefficient matrix, a recursion relation for the x_1 dependence of the dependent variables is obtained which has the general form

$$\bar{a}(x_1(5) + \Delta x_1) = A\ \bar{a}(x_1(5)) \tag{H-39}$$

The matrix A is defined as the amplification matrix for the system of difference equations. The particular form of A is found to be

$$A = \begin{bmatrix} 1 & (i\bar{c}/\bar{u}_1)\sin\phi_2 & (i\bar{c}/\bar{u}_1)\sin\phi_3 & (1/\bar{\rho}\bar{u}_1)(1-\cos\phi_2-\cos\phi_3) \\ 0 & -\cos\phi_2 & 0 & (i/\bar{\rho}\bar{c})\sin\phi_2 \\ 0 & 0 & \cos\phi_3 & (i/\bar{\rho}\bar{c})\sin\phi_3 \\ 0 & (-i\bar{\rho}\bar{c})\sin\phi_2 & (-i\bar{\rho}\bar{c})\sin\phi_3 & (\cos\phi_2 + \cos\phi_3 - 1) \end{bmatrix} \tag{H-40}$$

where $\phi_2 = \pm M\Delta x_2/L$ and $\phi_3 = \pm N\Delta x_3/L$.

The von Neumann necessary condition for stability of linear difference equations requires that the eigenvalues of the amplification matrix, A, satisfy the inequality

$$|\lambda_i| \leq 1 + O(\Delta x_1) \qquad \text{(H-41)}$$

where λ_i denotes any of the four eigenvalues of A, i.e., solutions of the determinantal equation

$$|A - I\lambda| = 0 \qquad \text{(H-42)}$$

Expansion of Eq. (H-42) yields a fourth-order polynomial in λ

$$(1 - \lambda)[(\cos\phi_2 - \lambda)(\cos\phi_3 - \lambda)(\cos\phi_2 + \cos\phi_3 - 1 - \lambda) + (\cos\phi_2 - \lambda)\sin^2\phi_3 + (\cos\phi_3 - \lambda)\sin^2\phi_2] = 0 \qquad \text{(H-43)}$$

Note that the determinant is not a function of the coefficients of the system of difference equations and, thus, that the stability characteristics are independent of the local values of the dependent variables.

The eigenvalues of the amplification matrix were calculated for all combinations of Fourier components, corresponding to the independent variables x_2 and x_3, over a range of frequency factors M and N. The range of M and N was selected such that the arguments ϕ_2 and ϕ_3 range from 0 to 2π, thus covering one complete period of the circular functions. Values of 10 and 1 were assumed for the characteristic length L and the mesh spacings Δx_2 and Δx_3 respectively. These values generally correspond to the mesh densities of interest in the solution of three-dimensional nozzle flow problems. Using these values a range of frequency factors, M and N, from 0 to 20 results. This range includes Fourier components having wave lengths from one mesh length to infinity. The eigenvalues of the amplification matrix were calculated for all combinations of the frequency factors M and N. The results of the eigenvalue calculations are shown plotted in Figure H-3. The plot is constructed by plotting the maximum absolute value of the eigenvalues for all combinations of frequency factors $M \leq I$ and $N \leq I$. Thus a discrete set of maximums as a function of I results. Although the index I was varied from 0 to 20, it was found that the results were symmetric about the value 10 so that only the results for $0 \leq I \leq 10$ are shown in Figure H-3.

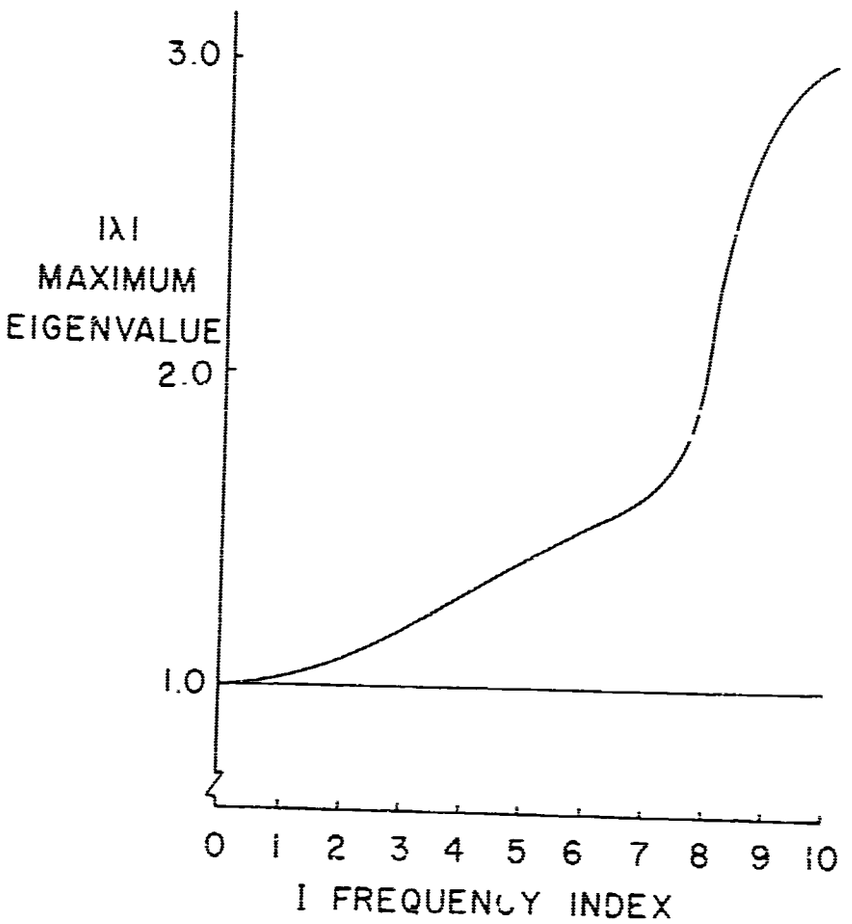

FIGURE H-3. AMPLIFICATION FACTORS FOR DIFFERENCE SCHEME ONLY

As expected, the basic difference scheme is highly unstable for all values of the frequency index J. This is due to the violation of the CFL stability criterion when the points at which the bicharacteristics intersect the initial-value surface are prior computed points, as in the case of these calculations.

5. STABILITY OF INTERPOLATION SCHEME

In the general numerical algorithm the bicharacteristic intersections will not coincide with prior computed points so that interpolation is necessitated. However, the streamline intersection with the initial-value surface, point (5) in Figure H-4, is always a prior computed point. Thus interpolation is not necessarily required to obtain the values of the dependent variables at this point, although interpolation could be used for purposes of providing additional damping. It will be shown in the course of this analysis that interpolation at point (5) is not only desirable, but necessary for stability.

The interpolation technique using least-square, bivariate, second-order polynomials, which was developed in Appendix F, must be considered in the overall stability investigation. The approach taken here will be to first consider the interpolation scheme as a recursive smoothing operation and analyze the stability of such a scheme. These results are subsequently incorporated with the difference scheme to obtain the stability characteristics of the overall numerical algorithm, both with and without interpolation at point (5).

The analysis of the interpolation scheme is simplified, without loss of generality, if the central point of the network, point (5) of the overall numerical scheme, is taken at the origin of the coordinate system (i.e., any arbitrary point of the network can be brought to the origin by a simple translation of of coordinates). A rectangular cartesian grid is assumed on which an arbitrary Fourier component of the values to be interpolated is represented by

$$\bar{U} = e^{i\pi Mx_2/L}\, e^{i\pi Nx_3/L}\, \bar{a}(x_1) \qquad \text{(H-44)}$$

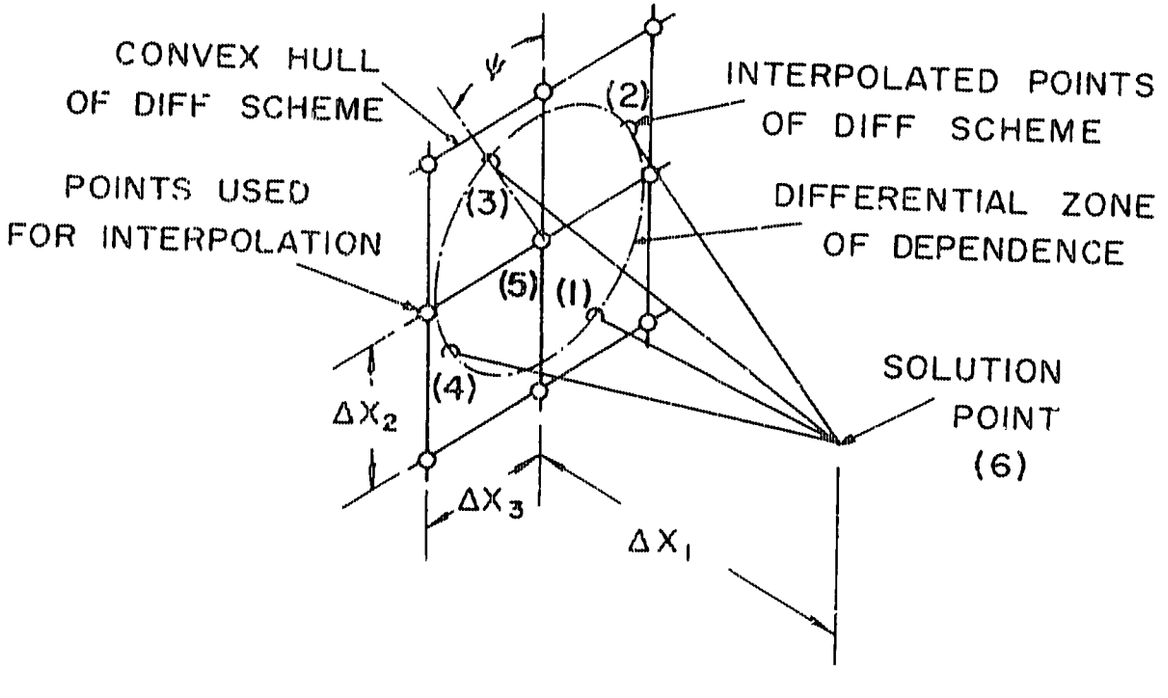

FIGURE H-4. DIFFERENCE NETWORK WITH INTERPOLATION

where

$$x_2 = m\Delta x_2, \qquad (m = 0, \pm 1, \pm 2, \cdots) \tag{H-45}$$

and

$$x_3 = n\Delta x_3, \qquad (n = 0, \pm 1, \pm 2, \cdots) \tag{H-46}$$

The complex quantities ζ and η are defined as

$$\zeta = e^{i\pi M\Delta x_2/L} \tag{H-47}$$

$$\eta = e^{i\pi N\Delta x_3/L} \tag{H-48}$$

so that the general Fourier component, Eq. (H-43), becomes

$$\bar{U} = \zeta^m \eta^n \bar{a}(x_1) \tag{H-49}$$

The interpolation technique developed in Appendix F uses the central point and the eight nearest neighbors to fit the bivariate second-order polynomials. These nine points are indicated on Figure H-4, and the corresponding values for the dependent variables at each of the nine points are

$$\bar{U}(1,1) = \bar{a}\zeta\eta \tag{H-50}$$

$$\bar{U}(1,0) = \bar{a}\zeta \tag{H-51}$$

$$\bar{U}(1,-1) = \bar{a}\zeta\eta^{-1} \tag{H-52}$$

$$\bar{U}(0,1) = \bar{a}\eta \tag{H-53}$$

$$\bar{U}(0,0) = \bar{a} \tag{H-54}$$

$$\bar{U}(0,-1) = \bar{a}\eta^{-1} \tag{H-55}$$

$$\bar{U}(-1,1) = \bar{a}\zeta^{-1}\eta \tag{H-56}$$

$$\bar{U}(-1,0) = \bar{a}\zeta^{-1} \tag{H-57}$$

$$\bar{U}(-1,-1) = \bar{a}\zeta^{-1}\eta^{-1} \tag{H-58}$$

The least squares system of equations in Appendix F, evaluated for this system of points, is

$$\begin{bmatrix} 9 & 0 & 0 & 0 & 6\Delta x_2^2 & 6\Delta x_3^2 \\ 0 & 6\Delta x_2^2 & 0 & 0 & 0 & 0 \\ 0 & 0 & 6\Delta x_3^2 & 0 & 0 & 0 \\ 0 & 0 & 0 & 4\Delta x_2^2\Delta x_3^2 & 0 & 0 \\ 6\Delta x_2^2 & 0 & 0 & 0 & 6\Delta x_2^4 & 4\Delta x_2^2\Delta x_3^2 \\ 6\Delta x_3^2 & 0 & 0 & 0 & 4\Delta x_2^2\Delta x_3^2 & 6\Delta x_3^4 \end{bmatrix} \begin{Bmatrix} A_1 \\ A_2 \\ A_3 \\ A_4 \\ A_5 \\ A_6 \end{Bmatrix} =$$

$$= \begin{Bmatrix} (\zeta + \zeta^{-1} + 1)(\eta + \eta^{-1} + 1) \\ (\zeta - \zeta^{-1})(\eta + \eta^{-1} + 1)\Delta x_2 \\ (\zeta + \zeta^{-1} + 1)(\eta - \eta^{-1})\Delta x_3 \\ (\zeta - \zeta^{-1})(\eta - \eta^{-1})\Delta x_2\Delta x_3 \\ (\zeta + \zeta^{-1} + 1)(\eta + \eta^{-1})\Delta x_2^2 \\ (\zeta + \zeta^{-1})(\eta + \eta^{-1} + 1)\Delta x_3^2 \end{Bmatrix} \qquad \text{(H-59)}$$

Solving for the coefficients A_i, $(i = 1, 2, \cdots, 6)$ yields

$$A_1 = [(5/9)(\zeta + \zeta^{-1} + 1)(\eta + \eta^{-1} + 1) - (1/3)(\zeta + \zeta^{-1})(\eta + \eta^{-1} + 1) - (1/3)(\zeta + \zeta^{-1} + 1)(\eta + \eta^{-1})] \qquad \text{(H-60)}$$

$$A_2 = [(1/6)(\zeta - \zeta^{-1})(\eta + \eta^{-1} + 1)]/\Delta x_2 \qquad \text{(H-61)}$$

$$A_3 = [(1/6)(\zeta + \zeta^{-1} + 1)(\eta - \eta^{-1})]/\Delta x_3 \qquad \text{(H-62)}$$

$$A_4 = [(1/4)(\zeta - \zeta^{-1})(\eta - \eta^{-1})]/\Delta x_2 \Delta x_3 \qquad \text{(H-63)}$$

$$A_5 = [-(1/3)(\zeta + \zeta^{-1} + 1)(\eta + \eta^{-1} + 1) + (1/2)(\zeta + \zeta^{-1})(\eta + \eta^{-1} + 1)]/\Delta x_2^2 \qquad \text{(H-64)}$$

$$A_6 = [-(1/3)(\zeta + \zeta^{-1} + 1)(\eta + \eta^{-1} + 1) + (1/2)(\zeta + \zeta^{-1} + 1)(\eta + \eta^{-1})]/\Delta x_3^2 \qquad \text{(H-65)}$$

The values of the dependent variables, $\bar{U}$, can now be expressed at any point of the initial-value surface contained within the convex hull of the system of points used to obtain the polynomial coefficients (the CFL stability criterion requires that the interpolated points lie far enough within the convex hull so that the differential zone of dependence is also imbedded within the convex hull, see Figure H-4). The least squares second-order polynomial for $\bar{U}$ is thus

$$\bar{U} = (A_1 + A_2 x_2 + A_3 x_3 + A_4 x_2 x_3 + A_5 x_2^2 + A_6 x_3^2)\, \bar{a}(x_1) = f(x_2, x_3)\, \bar{a}(x_1) \qquad \text{(H-66)}$$

where the coordinates x_2 and x_3 are relative to point (5).

In order to examine the stability characteristics of the interpolation scheme, consider a recursive process in which new values of the dependent variables, $\bar{U}$, are calculated at point (5) using the polynomial, Eq. (H-66) For this case $x_2 = 0$, $x_3 = 0$ and

$$\bar{U}(5) = \bar{a}(x_1(5))\, A_1 = \bar{a}(x_1(5))\, [(5/9)(\zeta + \zeta^{-1} + 1)(\eta + \eta^{-1} + 1) - (1/3)(\zeta + \zeta^{-1})(\eta + \eta^{-1} + 1) - (1/3)(\zeta + \zeta^{-1} + 1)(\eta + \eta^{-1},] \qquad \text{(H-57)}$$

The previous values of the dependent variables at point (5) are given by Eq. (H-49) with m = n = 0, i.e.,

$$\tilde{U}(5) = \tilde{a}(x_1(5)) \tag{H-68}$$

Thus, since no change in the x_1 coordinate occurs in the process, the recursion relation is simply Eq. (H-67), and only one eigenvalue or amplification factor results.

$$\begin{aligned}\lambda = [&(5/9)(\zeta + \zeta^{-1} + 1)(\eta + \eta^{-1} + 1) \\ &- (1/3)(\zeta + \zeta^{-1})(\eta + \eta^{-1} + 1) \\ &- (1/3)(\zeta + \zeta^{-1} + 1)(\eta + \eta^{-1})]\end{aligned} \tag{H-69}$$

The absolute value of the amplification factor is shown plotted on Figure H-5 along with the previous results for the basic difference scheme and for the same range of the frequency index. The amplification is everywhere less than one, thus the process is unconditionally stable for all Fourier components. Note that the damping of the components is relatively modest at all frequencies, reaching a maximum at I = 10 where the amplification factor has a minimum value of 0.956. Because of the modest alteration characteristic, yet unconditional stability, of this recursion process, it could well be used as a smoothing process for two-dimensional data.

6. STABILITY OF THE DIFFERENCE SCHEME WITH INTERPOLATION

A numerical scheme in which the values of the dependent variables at points (1) through (4) of the difference scheme are obtained by the interpolation process was first used and found to be numerically unstable. For the purpose of gaining further insight into the cause of the instability, a linear stability analysis for this case is made below. Points (1) through (4) of the difference scheme are equally spaced along the circumference of a circle of radius r and centered about point (5), see Figure H-4. The CFL stability criterion is satisfied if r is less than Δx_2 (only the case of equal Δx_2 and Δx_3 is considered in this analysis). The coordinates of the points (1) through (4) are located by specification

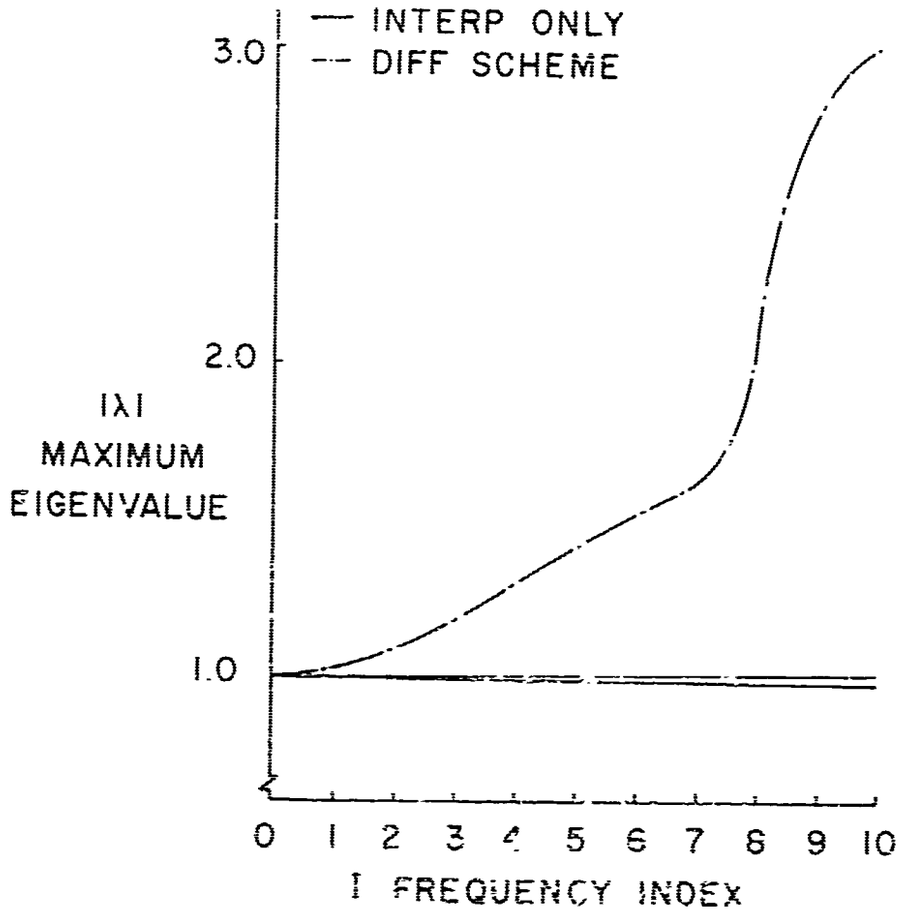

FIGURE H-5. AMPLIFICATION FACTORS FOR INTERPOLATION SCHEME

of the angle ψ and the value for r (the single degree of freedom in choice for α_1 and β_1 is specified by a value of ψ). The values of the dependent variables, $\bar{U}$, are subsequently obtained by evaluating the interpolating polynomial, Eq. (H-66), at each of the intersection points. The values of the dependent variables at point (5) are assumed known since point (5) always coincides with a point in the network of initial-value surface points. The values of the dependent variables at points (5) and (6) are expressed in terms of the assumed exponential form of the solution (i.e., Eqs. (H-23) and (H-24) evaluated for $x_2(5) = x_3(5) = 0$), which yields

$$\bar{U}(6) = \bar{a}(x_1 + \Delta x_1) \tag{H-70}$$

$$\bar{U}(5) = \bar{a}(x_1) \tag{H-71}$$

$$\bar{U}(I) = f(I)\, \bar{a}(x_1), \qquad (I = 1, 2, 3, 4) \tag{H-72}$$

where f(I) denotes the polynomial function, Eq. (H-66), evaluated at the designated point of the difference network. The system of difference equations in matrix form for this case is the same as Eq. (H-29) for the basic difference scheme, but with the nonzero elements of the coefficient matrix of $\bar{a}(x_1(5))$ replaced by the expressions

$$B_{12} = -(1/2)[f(3) + f(1)] \tag{H-73}$$

$$B_{14} = (1/2)[f(3) - f(1)]/(\bar{c}\bar{c}) \tag{H-74}$$

$$B_{23} = -(1/2)[f(4) + f(2)] \tag{H-75}$$

$$B_{24} = (1/2)[f(4) - f(2)]/(\bar{c}\bar{c}) \tag{H-76}$$

$$B_{32} = f(1) \tag{H-77}$$

$$B_{33} = f(2) \tag{H-78}$$

$$B_{34} = [f(1) + f(2) - 2]/(\bar{c}\bar{c}) \tag{H-79}$$

$$B_{41} = - \bar{\rho}\bar{u}_1 \tag{H-80}$$

$$B_{44} = - 1 \tag{H-81}$$

The system amplification matrix is obtained by premultiplication by the inverse of the leading coefficient matrix to obtain

$$A = \begin{bmatrix} A_{11} & A_{12} & A_{13} & A_{14} \\ 0 & A_{22} & 0 & A_{24} \\ 0 & 0 & A_{33} & A_{34} \\ 0 & A_{42} & A_{43} & A_{44} \end{bmatrix} \tag{H-82}$$

where the nonzero elements are

$$A_{11} = 1 \tag{H-83}$$

$$A_{12} = (1/2)[f(3) - f(1)](\bar{c}/\bar{u}_1) \tag{H-84}$$

$$A_{13} = 1/2\ [f(4) - f(2)](\bar{c}/\bar{u}_1) \tag{H-85}$$

$$A_{14} = \{1 - (1/2)[f(1) + f(2) + f(3) + f(4)]\}(\bar{c}/\bar{u}_1) \tag{H-86}$$

$$A_{22} = (1/2)[f(1) + f(3)] \tag{H-87}$$

$$A_{24} = (1/2)[f(1) - f(3)]/(\bar{\rho}\bar{c}) \tag{H-88}$$

$$A_{33} = (1/2)[f(2) + f(4)] \tag{H-89}$$

$$A_{34} = - (1/2)[f(2) - f(4)]/(\bar{\rho}\bar{c}) \tag{H-90}$$

$$A_{42} = (1/2)[f(1) - f(3)](\bar{\rho}\bar{c}) \tag{H-91}$$

$$A_{43} = (1/2)[f(2) - f(4)](\bar{\rho}\bar{c}) \tag{H-92}$$

$$A_{44} = (1/2)[f(1) + f(2) + f(3) + f(4)] - 1 \tag{H-93}$$

The results of the eigenvalue analysis for the range of frequency factors from 0 to 10 are plotted on Figure H-6. The previous results for the basic difference scheme and the interpolation scheme are also shown for comparison. The scheme is clearly unstable since the maximum absolute value of the eigenvalues are greater than or equal to 1.0 for all values of the frequency index. The largest amplification, $\lambda = 1.2$, occurs at I = 10 which corresponds to a Fourier component having a wave length equal to twice the network spacing. The relatively small value of the maximum amplification factor accounts for the fact that, in the numerical calculations, the instability did not show up until 20 to 30 integration steps were taken.

In an effort to stabilize the numerical scheme a modification in which interpolated values of the dependent variables are also used at point (5) was analyzed for stability. In this case the coefficients B_{34}, B_{41} and B_{44} of the system of difference equations become

$$B_{34} = [f(1) + f(2) - f(5)]/(\bar{\rho}\bar{c}) \tag{H-94}$$

$$B_{41} = - \bar{\rho}\bar{u}_1 f(5) \tag{H-95}$$

$$B_{44} = - f(5) \tag{H-96}$$

all other coefficients remaining the same. These changes result in a system amplification matrix, A, in which only the elements A_{11}, A_{14} and A_{44} are changed, the new values being

$$A_{11} = f(5) \tag{H-97}$$

$$A_{14} = \{f(5) - (1/2)[f(1) + f(2) + f(3) + f(4)]\}/(\bar{\rho}\bar{u}_1) \tag{H-98}$$

$$A_{44} = (1/2)[f(1) + f(2) + f(3) + f(4)] - f(5) \tag{H-99}$$

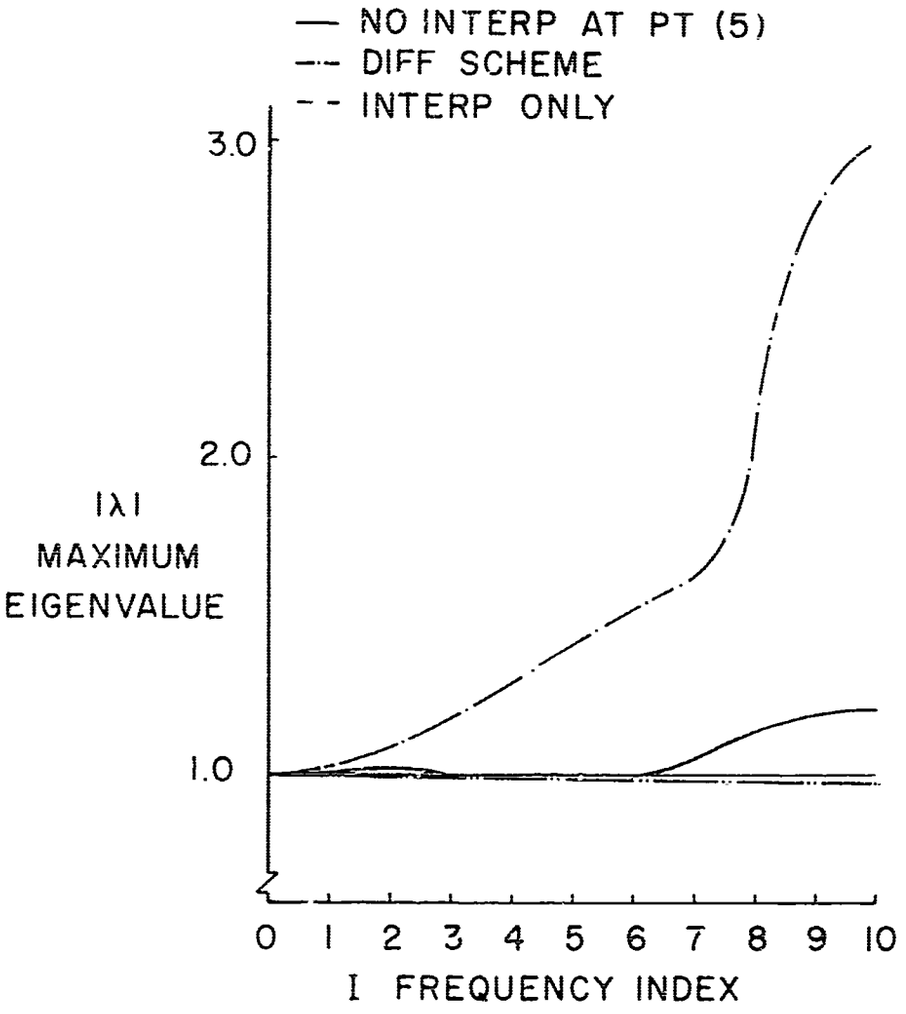

FIGURE H-6. AMPLIFICATION FACTORS FOR INTERPOLATION EXCEPT AT POINT(5)

The results of the eigenvalue analysis using the revised elements, Eq. (H-97) through (H-99), are shown on Figure H-7, along with the previous results, for comparison. The revised scheme is clearly stable at the higher frequency factors, but has amplification factors slightly greater than one at values for the frequency index of 1, 2, and 3, which correspond to Fourier components having wave lengths of 20, 10 and 7 times the grid spacing. Although the scheme cannot be judged unconditionally stable because of the amplification factors slightly greater than one, experience with the scheme has shown it to be highly stable. The result could be due to the fact that the von Neumann condition permits amplification factors somewhat greater than one (i.e., $|\lambda| \leq 1 + O(\Delta x)$), or due to the stabilizing effect of the nonlinearities of the numerical scheme.

When interpolation is used, the possibility exists of rotating the mesh and changing the axial step size, Δx_1. The effect of varying these parameters, on the stability, are shown in Figure H-8. Here the maximum amplification factor is plotted as a function of the frequency index I. A 45 degree rotation of the finite difference network relative to the initial-value surface grid produced a shift of the point of maximum amplification from I = 2 to I = 3 with no appreciable change in magnitude. Reductions in axial step size to 0.9 and 0.5 produced corresponding reductions in the maximum amplification; however in each case amplifications greater than unity were present.

7. SUMMARY

The results of the stability study did not indicate that any of the schemes investigated were unconditionally stable. However, the results dramatically illustrated the effect of the various modifications on the numerical stability. In particular the results showed the final scheme to be stable at the fundamental frequency (i.e., the frequency corresponding to a wave length twice the mesh spacing). The Fourier components corresponding to the fundamental frequency are the ones which are normally most amplified by an unstable scheme.

The results of this analysis, and subsequent numerical experience with the difference scheme, seem to support the general finding that the von Neumann condition is sufficient for stability of nonlinear schemes.

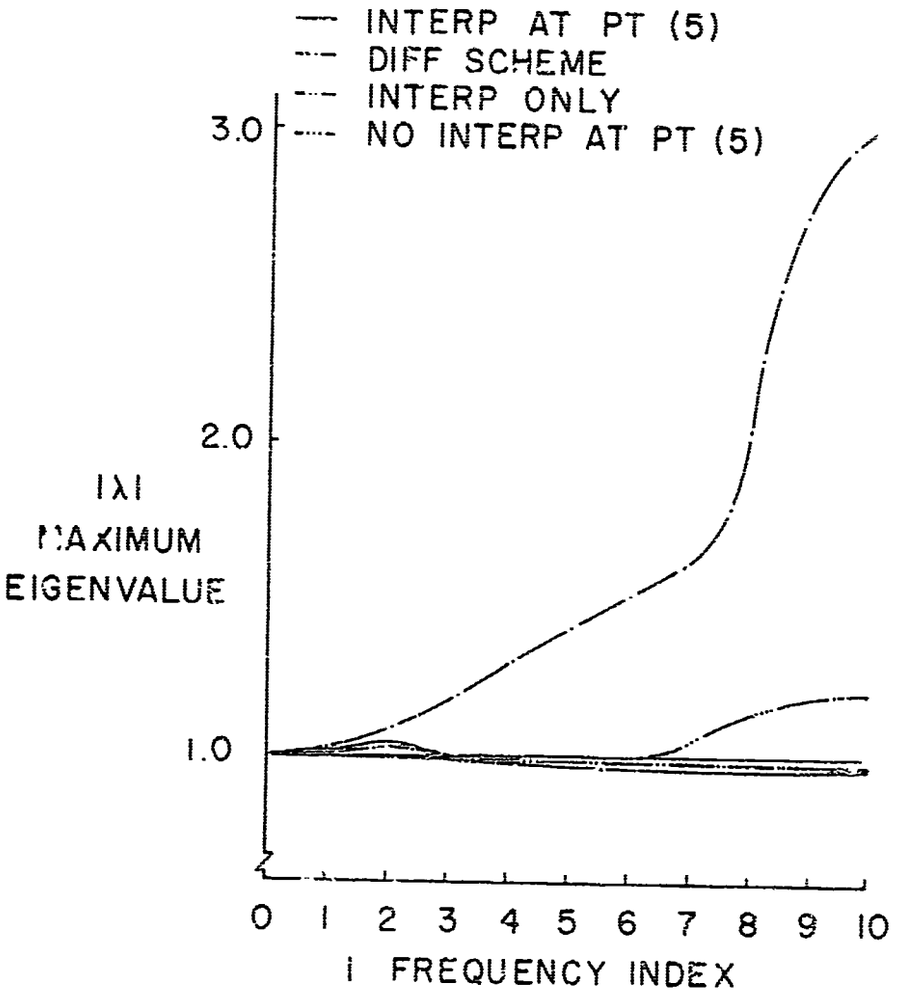

FIGURE H-7. AMPLIFICATION FACTORS FOR INTERPOLATION AT ALL POINTS

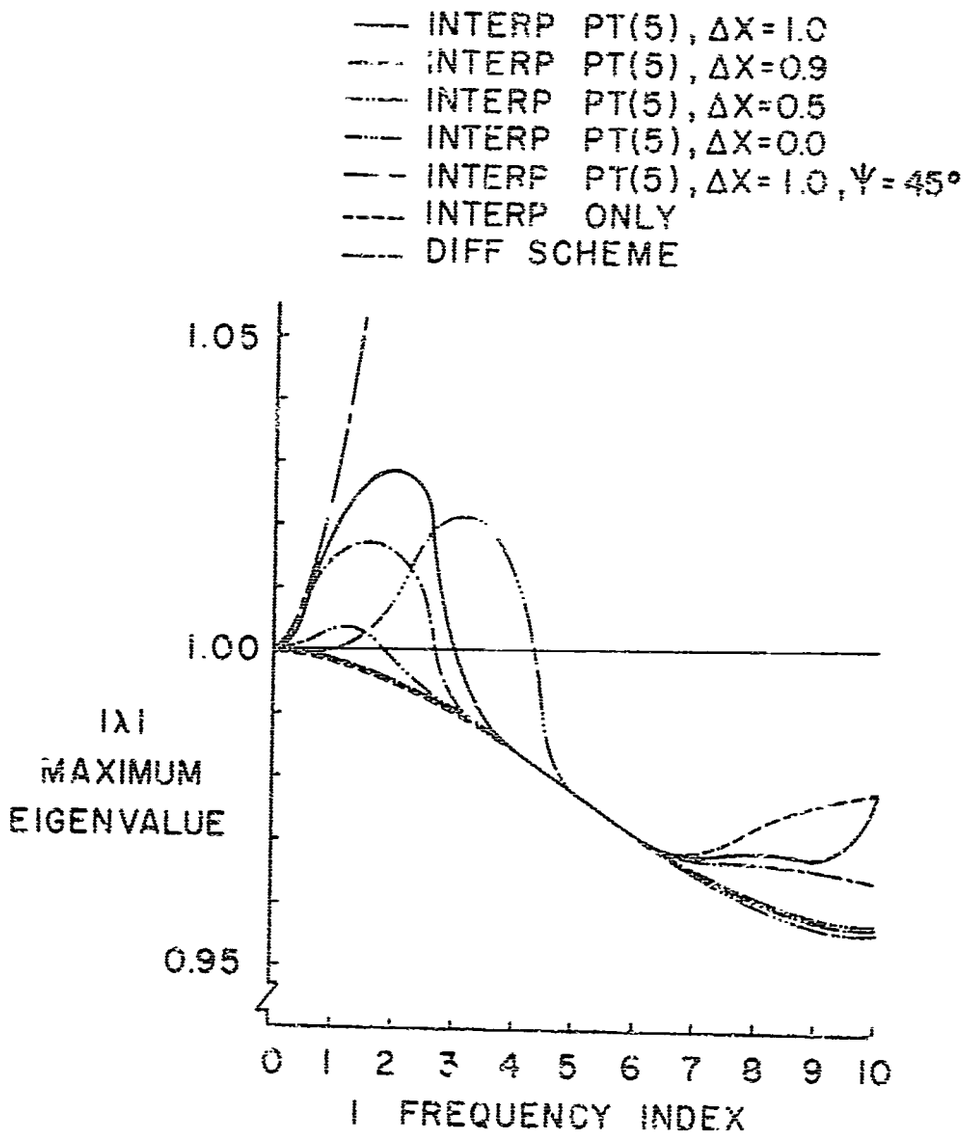

FIGURE H-8. AMPLIFICATION FACTORS FOR NETWORK VARIATIONS

APPENDIX I

ACCURACY STUDIES USING SOURCE AND PRANDTL-MEYER FLOWS

1. GENERAL

The accuracy of a numerical scheme is most easily checked by numerically obtaining the solution to problems for which an exact solution exists. No exact three-dimensional supersonic flow solutions are known to exist, but exact solutions do exist for several one independent variable flows which have three-dimensional spatial character. Source flows and Prandtl-Meyer, or simple wave, flows are two examples of such flows. Numerical solutions for these two cases using the three-dimensional algorithm were compared to the exact solution in order to determine the absolute accuracy of the scheme and also to study the error behavior with reduction in step size. Throughout the development of the integration scheme only numeric elations accurate to at least second-order were used, and consequentl the accuracy tests provided a means for experimentally verifying the order of the error for the resultant algorithm.

When an exact solution exists the order of the error for a scheme is easily determined by running two cases at different step sizes and comparing the ratio of the errors to the ratio of the step sizes raised to a power equal to the assumed order of the error. If the ratio of the errors is greater than the ratio of the step sizes raised to a power equal to the assumed order, then the scheme is accurate at least to the order assumed.

In addition to providing tests to determine the order of accuracy for the scheme, the comparisons with the exact solutions provided a quantitative way to readily evaluate the effect of new numerical innovations on the accuracy of the scheme.

2. SOURCE FLOW

A spherical source flow was used because of its three-dimensional geometric character. In such a flow the properties are only a function of the distance from the source point, and hence, result in only a one independent variable flow in which the streamlines are straight lines. In order to test the numerical scheme a planar initial-value surface, for starting the numerical integration, was generated using the exact source flow solution. Successive solution surfaces were generated numerically.

The initial investigations used a rectangular point network and the flow was only calculated within the zone of determinacy of the initial-value surface. Later, circular networks with a conical boundary were used so that a greater number of integration steps could be taken. At each solution point the exact source flow solution was also generated so that the absolute error could be calculated.

Throughout the theoretical development of the numerical scheme the local truncation error was assumed to be third-order in step size and, since the number of steps required to integrate to a fixed point in the solution space is the order of the reciprocal of the step size, the accumulated truncation error at a fixed point in the solution space was assumed to be second-order in step size. The actual order of the error in the integration scheme was determined by successively halving the step size and integrating to the same fixed point in space. In the limit as the step size approaches zero the theoretical ratio of the accumulated errors, for a scheme locally accurate to second order, is the square of the step size ratio.

The static pressure was found to be the dependent variable which is computed least accurately and thus is the most sensitive error indicator. The error in pressure at a fixed point in space for three step sizes is shown, along with illustrations of the process, in Figure 1-1. These results are for an initial Mach number of 4.0 and a rectangular point network, as illustrated. The results clearly confirm the second-order accuracy of the scheme for these initial conditions, since the ratios of the errors are in each case less than the ratio of the step sizes squared.

The error along the central streamline is shown plotted versus the

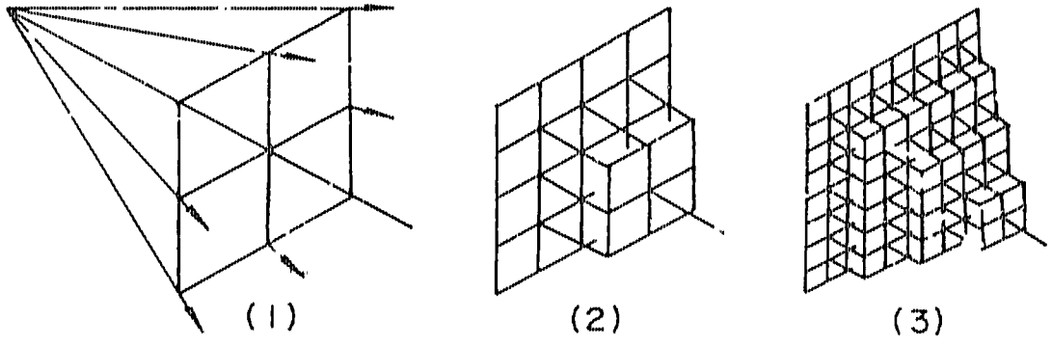

CASE	(1)	(2)	(3)
RELATIVE STEP SIZE	1	1/2	1/4
ACCUMULATED ERROR (%)	0.0104	0.0021	0.0005
RATIO TO CASE (1)	1	1/5	1/21
THEORETICAL RATIO	1	1/4	1/16

FIGURE 1-1. SOURCE FLOW ACCURACY STUDY, RECTANGULAR NETWORK

number of integration steps in Figure I-2. Note that the rate of error increase monotonically decreases with the number of steps, thus indicating a bounded error characteristic

The effect of the local Mach number on the error in a source flow was also investigated using the rectangular network and the results are presented in Figure I-3. The reason that high inaccuracies are encountered at a Mach number near unity is due, at least in part, to the fact that the equations approach a parabolic character, the family of wave surfaces degenerate to a single surface, and the numerical scheme degenerates. In addition, the gradients in velocity and pressure are greatest near a Mach number of unity which, undoubtedly, also contributes to the increase in error.

A conical boundary and a circular network of points on the initial-value surface were used with source flow initial data in order to test the accuracy of the overall scheme. In addition, this approach permits the solution to be calculated beyond the zone of determinacy of the initial data. This approach is illustrated in Figure I-4. The results of this type of error study for an initial Mach number equal to 1.05, a 10 degree source angle, and for three step sizes are shown plotted as a function of axial length from the initial-value surface in Figures I-5 and I-6 for the central streamline and a streamline at the boundary respectively. The combination of a 10 degree source angle and a Mach number of 1.05 produces a flow having a gradient comparable to that which exists at the throat of a rocket nozzle. The results in both Figures I-5 and I-6 do not show the expected error reduction between the two largest step sizes, cases (1) and (2). However, the reduction in error between the two smaller step sizes, cases (2) and (3), does have the proper second-order characteristic. These results indicate that the scheme does have second-order accuracy but that the nonlinear aspects of the scheme lead to increased relative error at large step size. These results are not in conflict since a statement with respect to the order of accuracy of a scheme only applies in the limit as step size becomes small such that the coefficient of the error term in the power series representation of the solution approaches a constant value.

The high relative error on the centerline, shown in Figure I-5 near

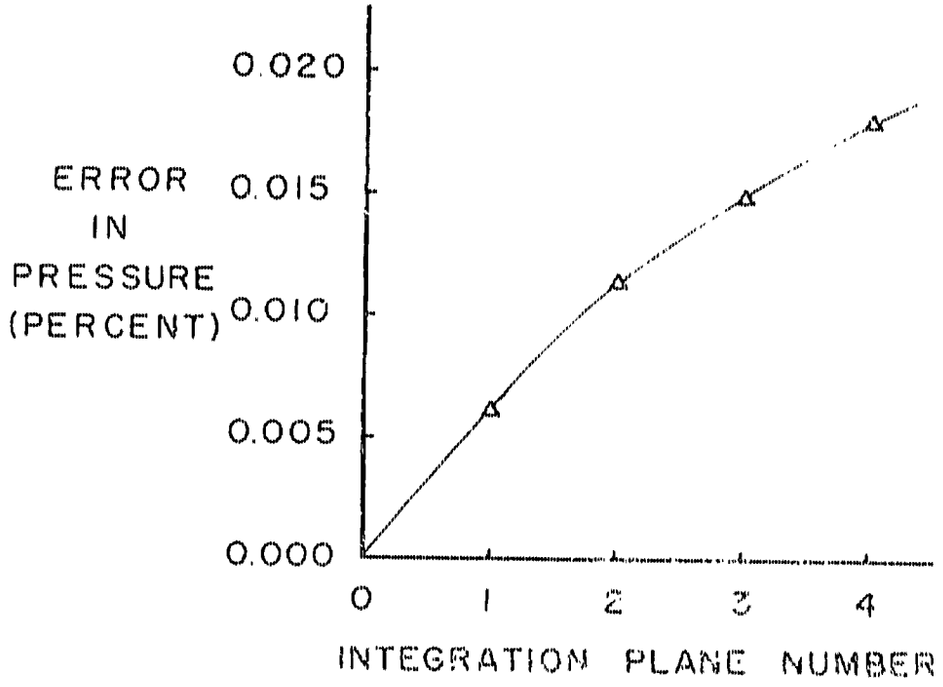

FIGURE I-2. SOURCE FLOW ERROR ACCUMULATION

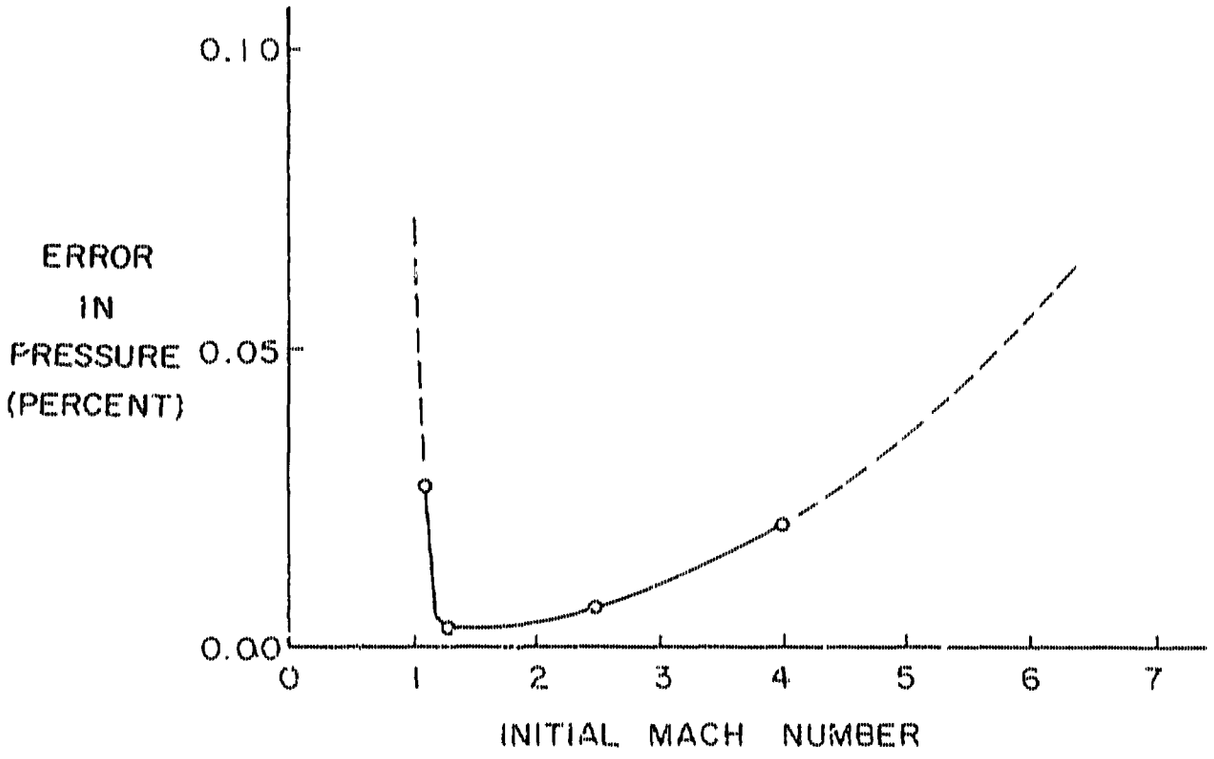

FIGURE 1-3. SOURCE FLOW ACCUMULATED ERROR VS. INITIAL MACH NUMBER

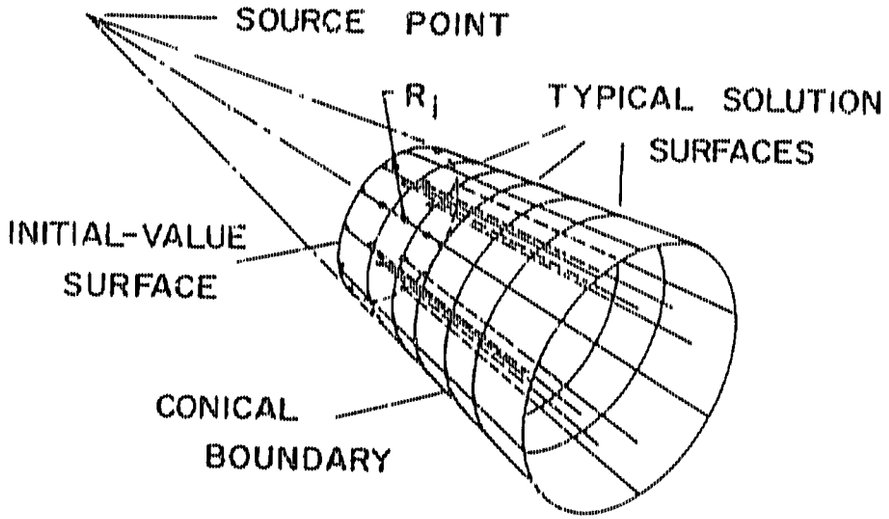

FIGURE I-4. SOURCE FLOW CIRCULAR NETWORK

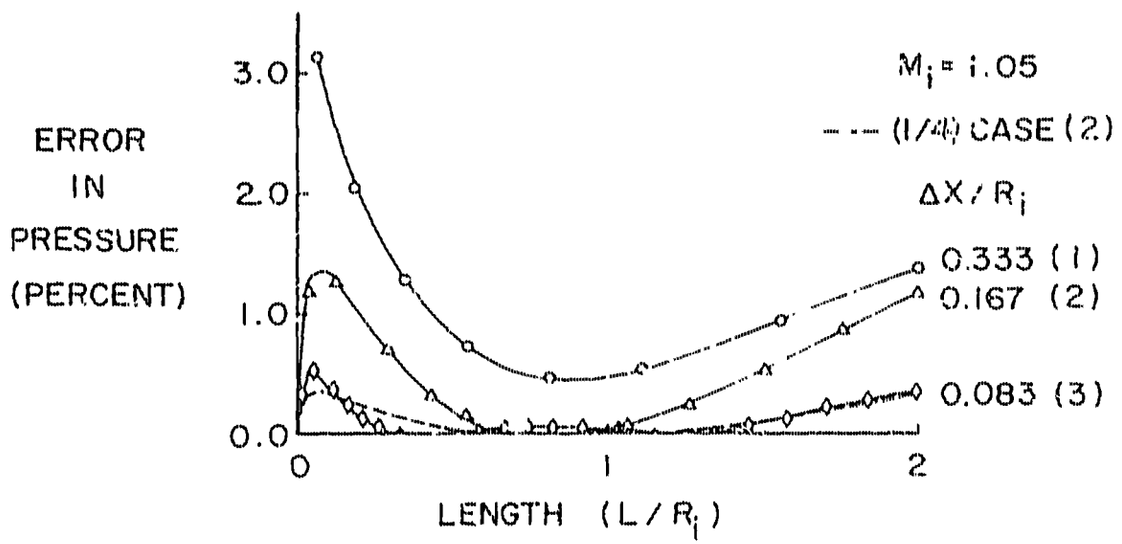

FIGURE 1-5. SOURCE FLOW CIRCULAR NETWORK CENTERLINE ERRORS

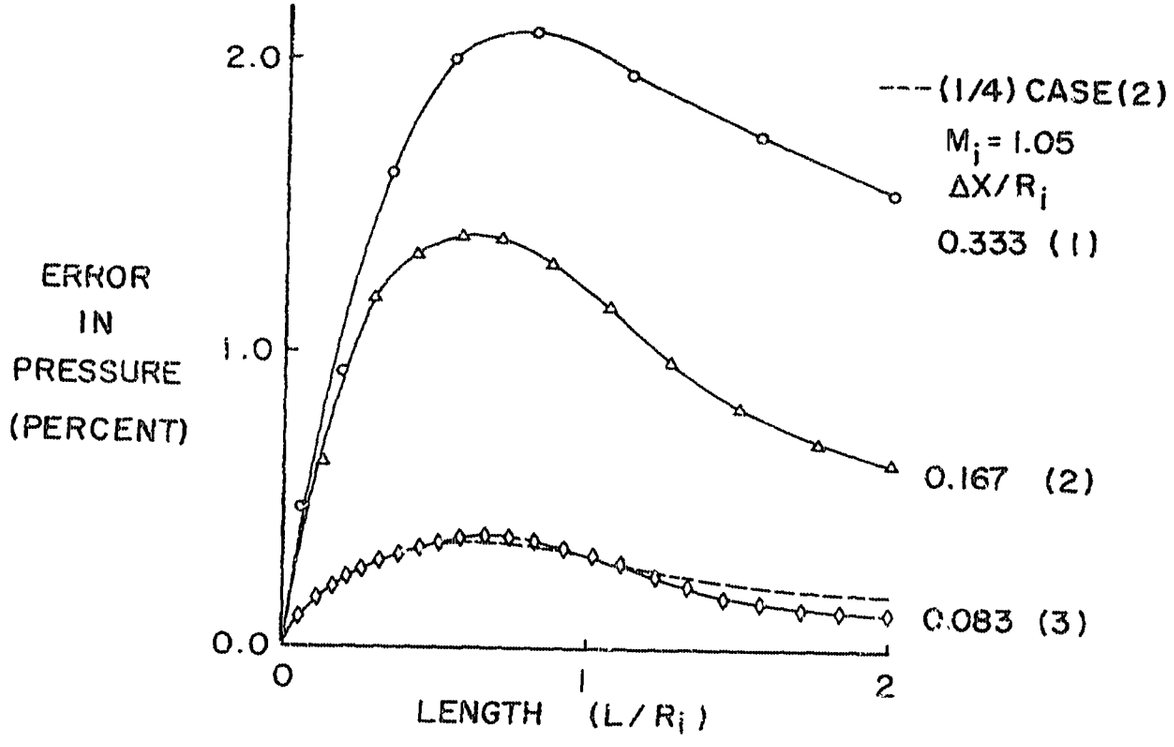

FIGURE I-6. SOURCE FLOW CIRCULAR NETWORK WALL ERRORS

the initial-value surface is partially explained by the large effect of Mach number shown in Figure I-3. However, no explanation can be offered for the fact that the accumulated error actually decreases in the direction of integration. Normally the accumulated error would be expected to continually increase in magnitude with the number of integration steps as was the case for the higher Mach number results (see Figure I-2).

3. PRANDTL-MEYER FLOW

Essentially the same error studies, which were made using a source flow, were repeated for a Prandtl-Meyer flow. A Prandtl-Meyer flow is also a one independent variable flow (i.e., the properties of the flow are functions of the turning angle only). However, the Prandtl-Meyer flow differs from the source flow by the fact that the streamlines are curved, whereas the streamlines of a source flow are straight. In such a flow the streamlines are plane curves and, as a further test of the numerical method, a coordinate rotation was used such that the planes of curvature could be arbitrarily oriented with respect to the reference vectors of the numerical network.

Here again a computer program was written in which an exact initial-value surface was generated to start the integration and the exact solution was calculated at each solution point in order to obtain the absolute error. In the region of simple wave flow the streamlines are curved and boundary point calculations could not be conveniently included as was done in the source flow. Thus calculations could only be made within the numerical domain of determinacy.

The networks for successive halving of the grid spacing and the accumulated errors are shown in Figure I-7. These results were generated for an initial Mach number of 4.0 and a turning angle of 10 degrees. These results also confirm the second-order error characteristic of the scheme (i.e., the ratios of the errors agree with the ratios of the step sizes squared). The accumulated error versus number of integration steps is shown in Figure I-8 and the accumulated error at a fixed point versus the initial Mach number is shown in Figure I-9. These results are essentially the same as the corresponding results for the source flow.

The studies in which the plane of curvature of the streamlines was

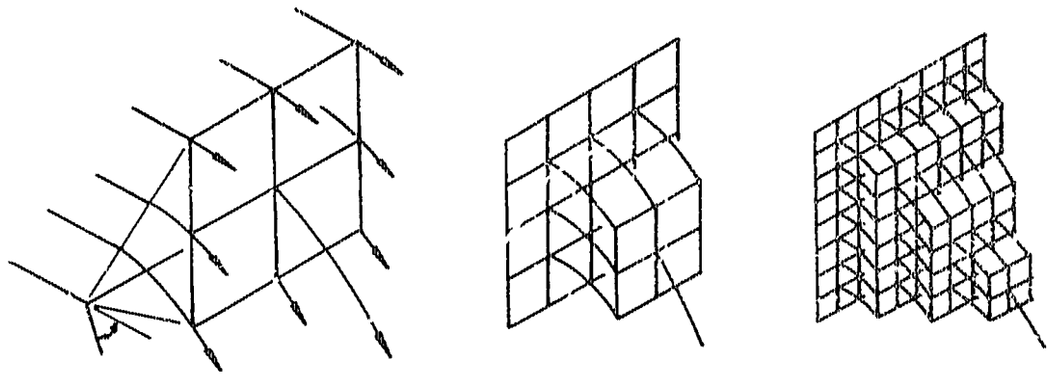

(1) (2) (3)

CASE	(1)	(2)	(3)
RELATIVE STEP SIZE	1	1/2	1/4
ACCUMULATED ERROR (%)	0.00318	0.000827	0.000209
RATIO TO CASE (1)	1	1/4	1/15.5
THEORETICAL RATIO	1	1/4	1/16

FIGURE I-7. PRANDTL-MEYER FLOW ACCURACY STUDY

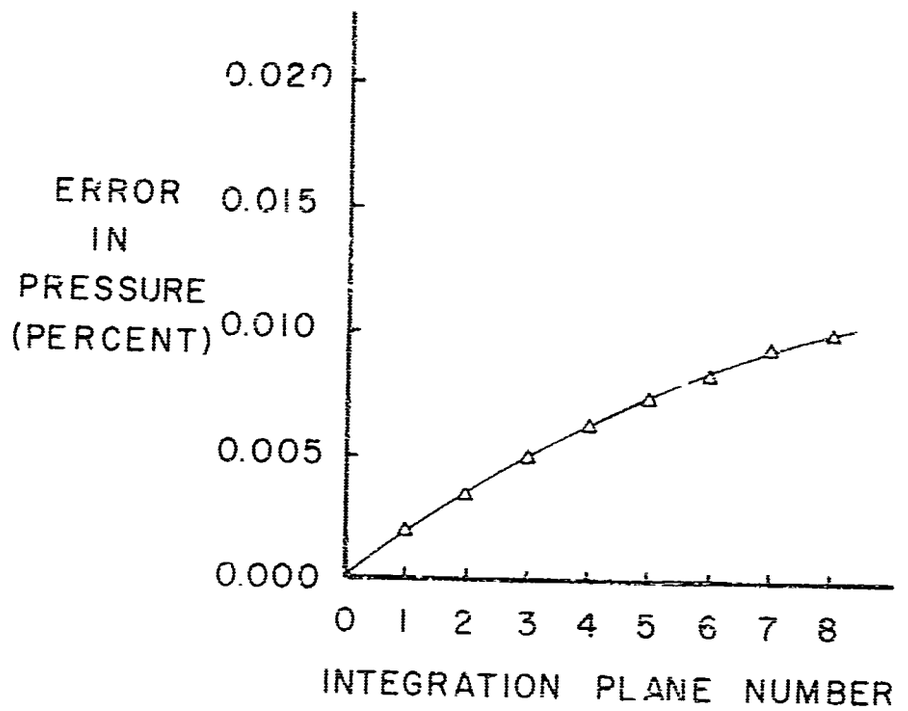

FIGURE I-8. PRANDTL-MEYER FLOW ERROR ACCUMULATION

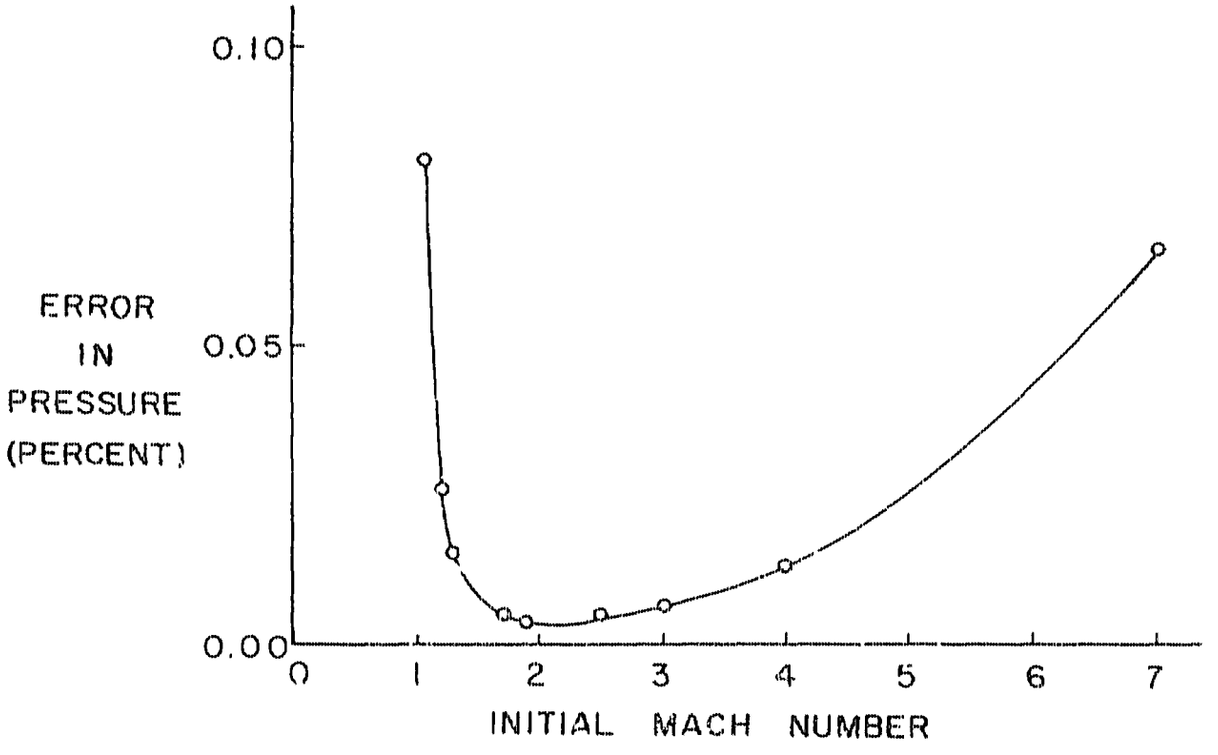

FIGURE I-9. PRANDTL-MEYER FLOW ACCUMULATED ERROR VS. INITIAL MACH NUMBER

rotated with respect to the base coordinate system produced the results shown in Figure I-10. The error was minimum when the flow was rotated 45 degrees and the bicharacteristic network just straddled the plane of curvature of the streamlines. In view of this result, it was decided to use the plane defined by the pressure gradient and a velocity vector as the reference with which to fix the single degree of freedom in the orientation of the bicharacteristic network. The network was oriented so that it symmetrically straddled the reference plane. It should be noted that the effect of rotation on the accuracy was very small, see Figure I-10, and referencing the network to the pressure gradient was not essential.

The accuracy studies for Prandtl-Meyer flow revealed an additional phenomenon of some significance. When the initial-value surface included a portion of the uniform flow which preceeds the region of simple wave flow, significant increases in error were noted at the junction of the two regions. This is due to the fact that the derivatives of the fluid properties are discontinuous at that point. The interpolation scheme using second-order polynomials assumes continuity in derivatives up to second order and as a result the accuracy of interpolation drops to first order in the neighborhood of the discontinuity. The accuracy of the numerical scheme at such points could only be improved by locating the discontinuity surface throughout the flow and using one sided interpolation formulas on each side of the discontinuity surface. Fortunately, flows having discontinuous derivatives are seldom encountered in practice since sharp corners, in the mathematical sense, do not physically exist. In addition, the flow boundaries are usually required to be smooth as a result of structural considerations.

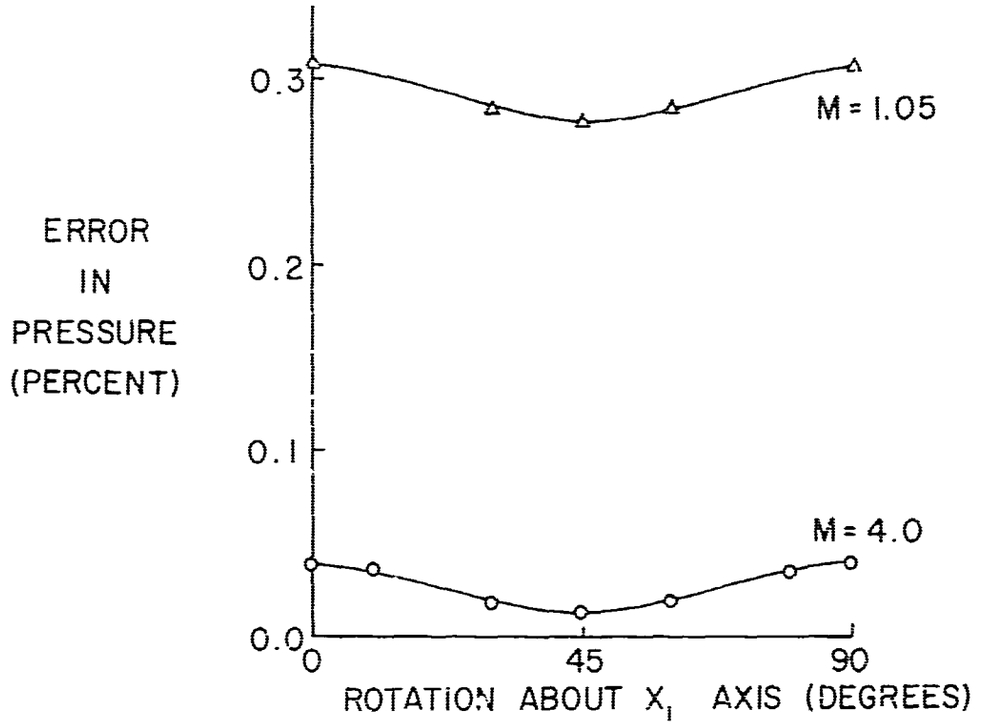

FIGURE 1-10. PRANDTL-MEYER FLOW ERROR FOR NETWORK ROTATION

UNCLASSIFIED

DOCUMENT CONTROL DATA - R & D

Purdue University
Lafayette, Ind. 47907

UNCLASSIFIED

A SECOND-ORDER NUMERICAL METHOD OF CHARACTERISTICS FOR THREE-DIMENSIONAL SUPERSONIC FLOW, Vol. I, THEORETICAL DEVELOPMENT AND RESULTS

Technical Report 1 September 1966 to 31 August 1969

Victor H. Ransom, Joe D. Hoffman, and H. Doyle Thompson

October 1969 | 228 | 52

Air Force F33615-67-C-1068

BPSN: 7(63 301206 6205214)

AFAPL-TR-69-98 , Vol. I

This document is subject to special export controls and each transmittal to foreign governments or foreign nationals may be made only with prior approval of AFAPL, Wright-Patterson AFB, Ohio

Air Force Aero Propulsion Laboratory
Wright-Patterson Air Force Base, Ohio

A new method of characteristics numerical scheme for three-dimensional steady flow has been developed which has second-order accuracy. Heretofore all such schemes for three-dimensional flow have had accuracies less than second-order. A complete numerical algorithim for computing internal supersonic flows of the type encountered in ramjet, scramjet or rocket propulsion systems has been developed and programmed for both the IBM 7094 and CDC 6500 computers. The method has been tested for order of accuracy using the exact solution for source flow and Prandtl-Meyer flow. The results of these tests have verified the second-order accuracy of the scheme. Additional accuracy tests using existing methods for solution of two-dimensional axisymmetric flows have shown that the scheme produces accuracies comparable to that of the two-dimensional method of characteristics.

The computer program has been used to generate the flow field for several three-dimensional nozzle contours and for nonsymmetric flow into an axisymmetric nozzle. These results reveal the complex nature of three-dimensional flows and the general inadequacy of quasi-three-dimensional analyses which neglect crossflow.

An operationally convenient computer program was produced. The program has the capability to analyze nonisoenergetic and nonhomentropic flows of a calorically perfect gas or homentropic flows of a real gas in chemical equilibrium. The initial-value surface options include uniform flow, source flow or axisymmetric tabular data. The nozzle boundary options include conical nozzles, axisymmetric contoured nozzles and super-elliptical nozzles

DD FORM 1473 (PAGE 1)

UNCLASSIFIED

Scramjet Technology
Exhaust Nozzles
Method of Characteristics
Three-Dimensional Flow